Sustainable Process Development for Olefin Carbonylation Reactions

Zur Erlangung des akademischen Grades eines

Dr. rer. nat.

von der Fakultät Bio- und Chemieingenieurwesen

der Technischen Universität Dortmund

genehmigte Dissertation

vorgelegt von

Tom Gaide, M.Sc.

aus

Mesum

Tag der mündlichen Prüfung: 23.10.2017

1. Gutachter: Prof. Dr. Arno Behr
2. Gutachter: Prof. Dr. Stefan Mecking

Dortmund 2017

Veröffentlichung als Dissertation in der Fakultät Bio- und Chemieingenieurwesen der Technischen Universität Dortmund, Dortmund.

Danksagung

Die vorliegende Dissertation wurde im Zeitraum Februar 2014 – Mai 2017 am Lehrstuhl für Technische Chemie an der TU Dortmund angefertigt. Ohne die Hilfe vieler Personen wäre das nicht möglich gewesen. Aus diesem Grund möchte ich diesen Personen danken.

Zunächst möchte ich Prof. Dr. rer. nat. Arno Behr und Dr. rer. nat. Andreas J. Vorholt für die Möglichkeit danken, meine Doktorarbeit mit einer spannenden Themenstellung am Lehrstuhl TC durchführen zu können. Die großen Freiheiten, die ich in der Bearbeitung der Themenstellung genossen habe, haben mich stets stark motiviert. Außerdem möchte ich beiden für die ausgezeichnete Betreuung sowie die hervorragenden Arbeitsbedingungen danken.

Des Weiteren möchte ich Prof. Dr. rer. nat. Stefan Mecking für die Übernahme des Zweitgutachtens danken.

Diese Arbeit wurde im Rahmen des Transregio TRR63 (Inprompt, Projekt A1) angefertigt. Der Deutschen Forschungsgemeinschaft danke ich für die Finanzierung des Projektes. Außerdem möchte ich allen Mitgliedern des Projektes für den fachlichen Austausch danken.

Ein riesiges Dankeschön geht auch an meine Studenten (Francesco, Michael, Jonas, Arnela, Christoph, Lisa, Sven, Stefan, Alexander, Kim, Vedat und Norman), die ich im Rahmen meiner Doktorarbeit betreuen durfte. Ohne euch hätte ich diese Arbeit niemals anfertigen können. Mit euch zu Arbeiten war ein großer Spaß und es war spannend, eure wissenschaftliche Entwicklung zu verfolgen.

Für die tolle Arbeitsatmosphäre möchte ich dem gesamten Lehrstuhl TC danken. Ihr seid super! Besonders hervorheben möchte ich hier Jens, der sich sowohl das Projekt, als auch das Büro mit mir geteilt hat. Außerdem möchte ich Andreas Stadler und Iris Henkel für die tatkräftige Unterstützung meiner Vorhaben danken.

Großer Dank gilt auch meinem ehemaligem Betreuer Peter Neubert.

Natürlich möchte ich auch meinen Freunden danken, die mir immer ein großer Rückhalt waren und für das nötige Kontrastprogramm zum Forschungsalltag gesorgt haben. Hervorheben möchte ich hier Susi, Philipp, Sören, Thomas, Stefan, Ann Katrin, Patrick, Mathias, Julius und Michael.

Zum Schluss möchte ich meinen Eltern und meinem Bruder von ganzem Herzen danken! Danke für euren Rückhalt und eure Unterstützung, insbesondere in schwierigen Zeiten. Danke, dass ihr mir all das ermöglicht habt!

Contents

CONTENTS I

LIST OF SYMBOLS AND ABBREVIATIONS V

ABSTRACT VIII

KURZZUSAMMENFASSUNG IX

1. PREFACE 1

2. THEORETICAL BACKGROUND 3

2.1. Process Design for Olefin Carbonylation Reactions in the Context of Green Chemistry 3

2.2. Catalyst Recycling in Homogeneous Catalysis 5

2.2.1. Thermomorphic Multicomponent Solvent Systems (TMS Systems) 10

2.3. Sequential Reactions/Tandem Catalysis 16

2.4. Carbonylation reactions 17

2.4.1. Hydroformylation 19

2.4.2. Hydroesterification 27

3. AIMS OF THE PRESENT WORK 31

4. PUBLICATIONS 33

4.1. Thermomorphic Solvent Selection for Homogeneous Catalyst Recovery based on COSMO-RS 33

4.1.1. Abstract 34

4.1.2. Introduction 34

4.1.3. Background and Motivation 35

4.1.4. Framework 38

4.1.5. Screening Results 46

4.1.6. Experimental Validation 48

4.1.7. Conclusion 53

4.1.8. Acknowledgments 55

4.2. Isomerization/Hydroformylation Tandem Reaction of a Decene Isomeric Mixture with Subsequent Catalyst Recycling in Thermomorphic Solvent Systems 56
4.2.1. Abstract 57
4.2.2. Introduction 57
4.2.3. Materials and Methods 60
4.2.4. Results and Discussion 62
4.2.5. Acknowledgments 71
4.3. Overcoming Phase Transfer Limitations in the Conversion of Lipophilic Oleocompounds in Aqueous Media - A Thermomorphic Approach 72
4.3.1. Abstract 73
4.3.2. Communication 73
4.3.3. Acknowledgements 81
4.4. Hydroesterification of Methyl 10-Undecenoate in Thermomorphic Multicomponent Solvent Systems - Process Development for the Synthesis of Sustainable Polymer Precursors 83
4.4.1. Abstract 84
4.4.2. Introduction 84
4.4.3. Materials and Methods 86
4.4.4. Results and Discussion 88
4.4.5. Conclusion 98
4.4.6. Acknowledgements 99
4.5. Catalyst Comparison in the Hydroesterification Methyl 10-undecenoate in Thermomorphic Solvent Systems 100
4.5.1. Abstract 101
4.5.2. Einleitung 101
4.5.3. Experimenteller Teil 104
4.5.4. Ergebnisse und Diskussion 105
4.5.5. Zusammenfassung und Schlussfolgerungen 114
4.5.6. Danksagung 115
4.6. Tandem Reductive Hydroformylation of Castor Oil Derived Substrates and Catalyst Recycling by Selective Product Crystallisation 116
4.6.1. Abstract 117
4.6.2. Communication 117
4.6.3. Conclusions 124
4.6.4. Acknowledgements 124
4.7. Renewable Surfactants *via* Hydroaminomethylation of Terpenes 125

4.7.1. Abstract....126
4.7.2. Communication....126
4.7.3. Acknowledgements....133
4.8. Linear Selective Isomerization/Hydroformylation of Unsaturated Fatty Acid Methyl Esters – A Bimetallic Approach....134
4.8.1. Abstract....135
4.8.2. Introduction....135
4.8.3. Results and Discussion....138
4.8.4. Conclusions....149
4.8.5. Experimental....150
4.8.6. Acknowledgments....150

5. SUMMARY, CONCLUSIONS AND OUTLOOK....151
5.1. Catalyst Recovery *via* Thermomorphic Multicomponent Solvent Systems (TMS Systems)....151
5.1.1. Development of a New Solvent Selection Strategy for TMS Systems....152
5.1.2. Application of TMS Systems in the Conversion of Technical Grade Feedstocks....152
5.1.3. Application of TMS Systemsin the Conversion of Renewable Feedstocks....153
5.1.4. Application of TMS systems in Reactions with Inherently Limited Degrees of Freedom in the Solvent Choice....154
5.1.5. Guide for the Application of TMS Systems....155
5.2. Design of New Catalytic Systems for Tandem Reactions with Renewables....161
5.2.1. Catalyst Development for the Reductive Hydroformylation of Castor Oil Derived Substrates....161
5.2.2. Catalyst Development for the Hydroaminomethylation of 1,3-Dienic Substrates....162
5.2.3. Catalyst Development for the Tandem Isomerisation/Hydroformylation of Fatty Acid Methyl Esters (FAMEs)....163
5.3. This Work in the Context of Sustainable Chemistry and Industrial Relevance....165

6. REFERENCES....167

7. APPENDIX....X
7.1 Supporting Information to Chapter 4.3....X

7.1.1. Experimental Procedure for the Continuously-Operated Miniplant X
7.1.2. Gas Chromatography X
7.1.3. ICP-OES X
7.1.4. Process Chart XI
7.1.5. Product Isolation XII
7.1.6. Additional Investigations on the Influence of the Substrate Concentration on the Reaction Rates and Catalyst Preforming (not published) XIII
7.2. Supporting Information to Chapter 4.6 XIV
7.2.1. Preparation of Methyl 12-hydroxydodecanoate XIV
7.2.2. Methodology for the Recycling Experiment XIV
7.2.3. Methodology for an Optimised Crystallisation: XVI
7.2.4. Conversion *vs* Time Experiments: Methodology XVI
7.2.5. NMRs of Methyl 12-hydroxydodecanoate and Methyl 12-oxododecanoate XX
7.2.6. Recycling Experiments: FIDs and ICPs Analyses XXI
7.3. Supporting Information to Chapter 4.7 XXV
7.4. Supporting Information to Chapter 4.8 XXV
7.5. List of Figures XXXVII
7.6. List of tables XLI
7.7. Publications XLIII
7.8. Posters and Lectures XLIV
7.9. Supervised Thesis XLVI

8. CURRICULUM VITAE XLVIII

List of Symbols and Abbreviations

Symbol/Abbreviation	Expression
1,2-DTBPMB	1,2-Bis(di-tert-butylphosphinomethyl)benzene
acac	Acetylacetonato
b	Branched
Biphephos	6,6′-[(3,3′-Di-tert-butyl-5,5′-dimethoxy-1,1′-biphenyl-2,2′-diyl)bis(oxy)]bis(dibenzo[d,f][1,3,2]dioxaphosphepin)
BISBI	2,2'-Bis(diphenylphosphinomethyl)-1,1'-biphenyl
DMF	*N,N*-Dimethylformamide
DPPB	1,2-Bis(diphenylphosphino)butan
DPPE	1,2-Bis(diphenylphosphino)ethan
DPPP	1,2-Bis(diphenylphosphino)propan
e.g.	exempli gratia
EI	Electron impact
et al.	et alii

etc.	et cetera
eV	Electron Volt
FAME	Fatty acid methyl ester
FID	Flame ionisation detector
GC	Gas chromatography
HSP	Hansen solubility parameter
ICP-OES	Inductively coupled plasma optical emission spectrometry
l	Linear
l/b	Linear/branched
MeOH	Methanol
MMA	Methyl methacrylate
MS	Mass spectroscopy
MSA	Methanesulfonic acid
NMR	Nuclear magnetic resonance
PCP-SAFT	Perturbed chain polar statistical associating fluid theory
Pd_2dba_3	Tris(dibenzylideneacetone)dipalladium(0)

PhD	Philosophiæ Doctor
PPh_3	Triphenylphosphine
$Rh(CO)_2acac$	(Acetylacetonato)dicarbonylrhodium(I)
S	Selectivity
SHOP	Shell higher olefin process
SI	Supporting Information
SulfoXantphos	4,5-Bis(diphenylphosphino)-9,9-dimethyl-2,7-disulfoxanthene disodium salt; 4,5-Bis(diphenylphosphino)-9,9-dimethylxanthene-2,7-disulfonic acid disodium salt
P^tBu_3	Tri-*tert*-butylphosphine
THF	Tetrahydrofuran
TMS	Thermomorphic multicomponent solvent
TPPTS	Tri-(natrium-meta-sulfonatophenyl)-phosphine
UCST	Upper critical solution temperature
X	Conversion
Xantphos	4,5-Bis(diphenylphosphino)-9,9-dimethylxanthene
Y	Yield

Abstract

The development of sustainable processes and the implementation of renewable raw materials are increasingly important for the chemical industry. In particular, homogeneous catalysis is a key technology in this context since it allows for atom economic and selective syntheses under mild reaction conditions. In this work, two important tasks in process development for homogeneously catalysed carbonylation reactions were investigated:

- Recycling of known homogeneous transition metal catalysts
- Development of new catalytic systems for the conversion of substrates based on renewable raw materials in tandem reactions

As a recycling strategy for homogeneous transition metal catalysts, the use of thermomorphic multicomponent solvent (TMS) systems was systematically investigated in four steps:

1. *Development of a new solvent selection strategy for TMS systems*
2. *Application of TMS systems in the conversion of technical grade feedstocks*
3. *Application of TMS systems in the conversion of renewable feedstocks*
4. *Application of TMS systems in reactions with inherently limited degrees of freedom in the solvent choice*

The results of these investigations led to the development of a guideline for process development for homogeneously catalyzed reactions in thermomorphic multicomponent solvent systems.

Three new catalytic systems were developed for the conversion of substrates based on renewable raw materials in tandem hydroformylations. In the hydroaminomethylation and the reductive hydroformylation, two of the novel catalyst systems allow for a direct conversion of the intermediately formed aldehydes. This makes their purification superfluous, which is of great advantage from an economic and ecologic point of view. The newly developed catalyst system for the isomerising hydroformylation of unsaturated fatty acid methyl esters opens a new way for the synthesis of valuable products from renewable raw materials.

Kurzzusammenfassung

Die Entwicklung nachhaltiger Prozesse sowie die Implementierung nachwachsender Rohstoffe gewinnen zunehmend an Bedeutung für die chemische Industrie. Insbesondere die homogene Katalyse stellt in diesem Zusammenhang eine Schlüsseltechnologie dar, da sie atomökonomische, selektive Synthesen unter milden Reaktionsbedingungen ermöglicht. In dieser Arbeit wurden zwei wichtige Aufgabestellungen der Prozessentwicklung für homogenkatalysierte Carbonylierungsreaktionen untersucht:

- Das Recycling bekannter, homogener Übergangsmetallkatalysatoren
- Die Entwicklung neuer Katalysatorsysteme für die Umsetzung von Substraten auf Basis nachwachsender Rohstoffe in Tandemreaktionen

Als Recyclingstrategie für homogene Übergangsmetallkatalysatoren wurde die Anwendung von thermomorphen Mehrkomponenten-Lösungsmittelsystemen (TMS Systeme) systematisch anhand der folgenden vier Schritte untersucht:

1. *Entwicklung neuer Strategien zur Lösungsmittelauswahl*
2. *Anwendung der TMS Systeme in der Umwandlung von Substratmischungen mit technischer Reinheit*
3. *Anwendung der TMS Systeme in der Umwandlung von nachwachsenden Substraten*
4. *Anwendung der TMS Systeme in Reaktionen, die intrinsisch die Freiheitsgrade in der Lösungsmittelauswahl limitieren*

Die Ergebnisse dieser Untersuchungen führten zur Erarbeitung eines Leitfadens zur Prozessentwicklung homogenkatalysierter Reaktionen in TMS Systemen. Für die Umsetzung von Substraten auf Basis nachwachsender Rohstoffe in Tandem-Hydroformylierungen wurden drei neue Katalysatorsysteme entwickelt. In der Hydroaminomethylierung und der reduktiven Hydroformylierung ermöglichen zwei der neuen Katalysatorsysteme die direkte Folgereaktion der intermediär gebildeten Aldehyde. Dadurch entfällt deren Aufreinigung, was aus ökonomischen sowie ökologischen Gesichtspunkten von großem Vorteil ist. Das neu entwickelte Katalysatorsystem zur isomerisierenden Hydroformylierung ungesättigter Fettsäuremethylester eröffnet einen neuen Weg zur Synthese von Wertprodukten ausgehend von nachwachsenden Rohstoffen.

1. Preface

Sustainability is one of the most important global megatrends in our society.[1] Today, mankind is consuming the resources of about 1.6 planets.[2] As a result we have to deal with crucial environmental issues such as climatic change, loss of biodiversity, decreasing availability of water and fossil fuels or environmental pollution.

Sustainability of course also affects the chemical industry. The global demand for chemicals is expected to be more than doubled until the year 2030.[3] Consequently, there is a strong driving force for the development of more sustainable chemical processes and the implementation of renewable feedstocks in the chemical industry.

In terms of sustainable process development and value creation catalysis plays a decisive role. Catalysts are applied in approximately 85% of all chemical processes.[4]

Basically, a chemical reaction can be catalysed in a homogeneous or a heterogeneous manner. Especially in view of sustainable process development, homogeneous catalysis provides some pivotal advantages compared to its heterogeneous counterpart such as high selectivities and mild process conditions. This helps to safe energy and resources as well as to prevent waste production.

In this context, olefin carbonylation catalysed by homogeneous transition metal complexes is of outstanding potential. This type of reaction allows for a highly atom economic introduction of carbon monoxide into readily available starting materials. This leads to the formation of valuable intermediates and products without having to activate or to protect the substrate prior reaction. Additionally, many catalysts have a high tolerance against functional groups. This enables not only the implementation of simple olefins but also of starting materials derived from renewable feedstocks.

Olefin carbonylations can also beneficially be merged with other reactions in one preparative step. These so called tandem reactions are extremely efficient from both an economical and an ecological point of view. No intermediate purification or work up is required between several reaction steps. Synergetic effects in tandem reactions also enable new catalytic pathways and therefore, the implementation of alternative feedstocks in the value-added chain of the chemical industry.

The main drawbacks of olefin carbonylation reactions in view of designing chemical processes are the separation and the subsequent recycling of the homogeneous transition

metal catalysts. These complexes mostly consist of a precious metal centre and tailored ligands, which often makes them expensive.

Consequently, an olefin carbonylation process using those catalysts can only be economically feasible, if an efficient catalyst recycling strategy is applied. Unluckily, the sensitivity of homogeneous transition metal catalysts against high temperature, air or other chemicals makes their recovery challenging. This is particularly the case if renewable starting materials are applied. These compounds often have high boiling points. Additionally, they contain functional groups, which make them comparably polar and difficult to extract. Also, impurities in the substrate feed can cause problems in catalyst separation or catalyst stability.

This work covers two important aspects in the field of process development for olefin carbonylation reactions:

1. Advancement and evaluation of innovative catalyst recycling concepts for known homogeneous transition metal catalysts.

2. Design of new catalytic systems for tandem carbonylation reactions

The core reactions investigated in this work are the hydroformylation and the hydroesterification.

The guidelines for the developments in this thesis are sustainability and industrial relevance. While industrial relevance is given by the conversion of readily available starting materials into products with high potential in technical applications, sustainability is considered by the 12 principles of green chemistry, especially by designing processes for the conversion of renewable resources.

2. Theoretical background

Parts of this chapter were published in the book Homogeneous Catalysis with Renewables.[5]

2.1. Process Design for Olefin Carbonylation Reactions in the Context of Green Chemistry

The term green chemistry describes a different way of thinking about how chemistry can be done. The guideline of green chemistry is to design chemical reactions and products by increasing sustainability, safety and lowering the environmental impact. In 1998, Paul Anastas and John Warner postulated the “Twelve Principles of Green Chemistry”. This framework helps to design chemical reactions in the sense of green chemistry. The “Twelve Principles of Green Chemistry” are the following:[6]

1 Prevention

“It is better to prevent waste than to treat or clean up waste after it has been created.”

2 Atom Economy

“Synthetic methods should be designed to maximize the incorporation of all materials used in the process into the final product.“

3 Less Hazardous Chemical Syntheses

“Wherever practicable, synthetic methods should be designed to use and generate substances that possess little or no toxicity to human health and the environment.“

4 Designing Safer Chemicals

“Chemical products should be designed to affect their desired function while minimizing their toxicity.“

5 Safer Solvents and Auxiliaries

“The use of auxiliary substances (e.g., solvents, separation agents, etc.) should be made unnecessary wherever possible and innocuous when used.“

6 Design for Energy Efficiency

“Energy requirements of chemical processes should be recognized for their environmental and economic impacts and should be minimized. If possible, synthetic methods should be conducted at ambient temperature and pressure. “

7 Use of Renewable Feedstocks

“A raw material or feedstock should be renewable rather than depleting whenever technically and economically practicable. “

8 Reduce Derivatives

“Unnecessary derivatization (use of blocking groups, protection/deprotection, temporary modification of physical/chemical processes) should be minimized or avoided if possible, because such steps require additional reagents and can generate waste. “

9 Catalysis

“Catalytic reagents (as selective as possible) are superior to stoichiometric reagents. “

10 Design for Degradation

“Chemical products should be designed so that at the end of their function they break down into innocuous degradation products and do not persist in the environment. “

11 Real-time Analysis for Pollution Prevention

“Analytical methodologies need to be further developed to allow for real-time, in-process monitoring and control prior to the formation of hazardous substances.“

12 Inherently Safer Chemistry for Accident Prevention

“Substances and the form of a substance used in a chemical process should be chosen to minimize the potential for chemical accidents, including releases, explosions, and fires.“

Catalysis (principle 9) is one of the key technologies in this context. It allows for atom economic synthesis under mild reaction conditions without preliminary derivatisation (principles 1, 2, 6, 8). It also paves the way for the implementation of renewable resources in chemical synthesis (principle 7).

This is especially the case for homogeneously catalysed olefin carbonylation reactions. Additionally, olefin carbonylations are perfectly suited for merging them together with other reactions in so-called tandem reactions. The resulting carbonyl compounds are reactive intermediates, which can easily be converted into further valuable products.

The concept of tandem catalysis itself also strongly contributes to sustainable chemical synthesis, since no intermediate purification between several reaction steps is necessary.

For this reason, the application of tandem catalysis safes waste production, energy and auxiliaries (principles 1, 2, 6). Additionally, some reactions can only be carried out in a tandem catalytic manner, which e.g. enables the usage of renewable starting material in chemical reactions (principle 7).

However, it is important to notice that green chemistry is not a self-purpose. It will only have high impact on the society, if developments made in the context of green chemistry are applicable on industrial scale. Therefore, it is important to design economically feasible processes for the synthesis of products with potential technical application areas.

In homogeneous catalysis, economical feasibility is strongly linked to the recycling of the valuable transition metal catalyst complexes. This important topic will be discussed in the next chapter 2.2.

2.2. Catalyst Recycling in Homogeneous Catalysis

In homogeneous catalysis catalysts have to be separated from the product, unless they are applicable in very small traces.

On the one hand, transition metal complexes are often of high toxicity and therefore, letting them remain in the product is not an option. On the other hand, homogeneous catalysts often consist of precious noble metals and tailored ligands, which make them very expensive. This is especially the case for olefin carbonylation reactions. In this case, solely separating of the catalyst from the product is often insufficient and the catalyst has to be recycled into the reactor in its active form to achieve an economically feasible process. An overview over the different separation techniques is given in this chapter.

Precipitation/Crystallisation

The underlying principle of this separation technique is the different solubility of the catalyst and the product in one liquid phase. Crystallisation can be induced by cooling or evaporation of the reaction mixture. Resulting solid has a crystalline structure. Precipitation is induced by adding a further substance to the reaction mixture. The origin of the precipitation can be a chemical modification or displacement of the precipitate. If precipitation results in formation of crystals, this is called precipitation crystallisation.[7]

A promising strategy for keeping the catalyst active after separation is the crystallisation of the products from the reaction mixture.[8]

Distillation/Rectification

Distillation and rectification are the most important separation techniques in industrial organic chemistry. These processes utilise the different volatility of compounds in a mixture. They are well suited for the separation of low boiling products from homogeneous catalysts. Unfortunately, it is mostly not suitable for high boiling products since homogeneous catalysts often are very sensitive against higher temperatures.[9] On industrial scale, catalyst separation *via* distillation is e.g. realised in the propene hydroformylation[10] or in acetic acid synthesis via the BP Cativa process.[11]

Membrane Processes

Membranes can be applied to separate molecules of different sizes. This technique has some crucial advantages compared to other techniques such as a low energy demand or the retention of the catalyst in its active form. This technique was already shown to be very promising e.g. in the hydroformylation of 1-dodecene in a continuously operated miniplant process.[12] One important factor to achieve an efficient separation and a stable process is the choice of a suitable membrane material. Also, a big difference in the size of the catalyst and the product is highly desirable.[13] This can be achieved by enlargement of ligands.[14]

Catalyst Immobilisation

Homogeneous catalysts can in principle be immobilised on a solid carrier or in a liquid phase. The immobilisation on a solid carrier can be achieved by physisorption (reversible) or chemisorption (irreversible). This heterogenisation transforms the homogeneous catalyst into a heterogeneous one. Ideally, advantages of homogeneous catalysis (e.g. high selectivity, mild reaction conditions) are combined with the easy separability of a heterogeneous catalyst. Today, there is no application of such catalysts on industrial scale since they often suffer from lower reactivity and/or selectivity compared to their homogeneous counterparts. Low stability, high catalyst leaching, higher costs and higher complexity of a process often are additional limitations.[15] Recently, Evonik Industries reported about an efficient supported ionic liquid phase hydroformylation catalyst enabling high activity and selectivity in the hydroformylation of a technical grade C4-feed. The catalyst was applied in a continuously operated miniplant for more than 2000 h on stream, which is sufficient for industrial application.[16]

Catalyst immobilisation in liquid phase, which is also called liquid-liquid biphasic catalysis (LLBC), is often advantageous in terms of the catalytic performance compared to immobilisation on a solid carrier. Connecting a catalyst to a solid carrier leads to a restricted mo-

bility and causes changes in the catalytic behaviour. This is not the case in a liquid-liquid biphasic system.[9]

The most straightforward way for catalyst separation *via* liquid-liquid biphasic technique is shown in Figure 2.1. The catalyst is dissolved in a solvent and the substrates can react under product formation. If these products have a substantially different polarity compared to the solvent, they will separate after reaction. Important industrial examples for this technique are the Ruhrchemie/Rhône-Poulenc process (RCh - RP)[9,17,18,18] and the Shell Higher Olefin Process (SHOP)[9,19,20]. The catalysts are dissolved in water (RCh - RCP) or 1,4-butanediol (SHOP). The products form a second liquid phase after reaction and can be separated *via* simple decantation. Although this elegant process concept is of high value for industrial homogeneous catalysis, it is limited in scope. Many products are soluble in organic solvents and do not form a second phase.

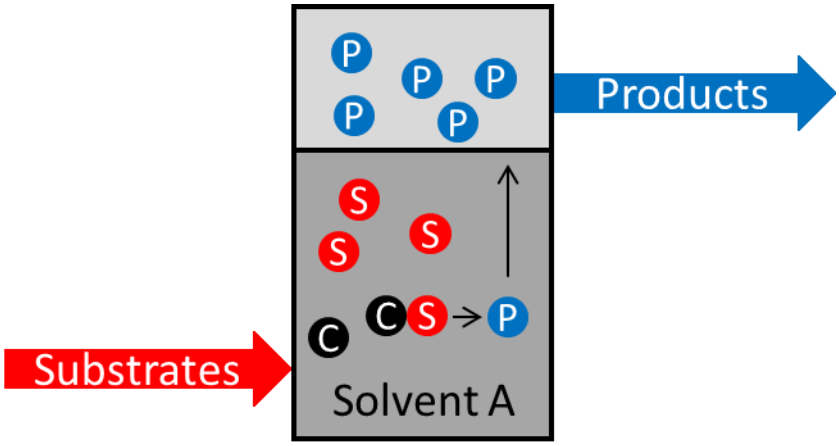

Figure 2.1: LLBC principle.
(C = catalyst; S = substrates; P = products)

These limitations can be overcome by addition of a second solvent either during the reaction (*in-situ* extraction) or after reaction as consecutive extraction in an additional separation unit (Figure 2.2).[9]

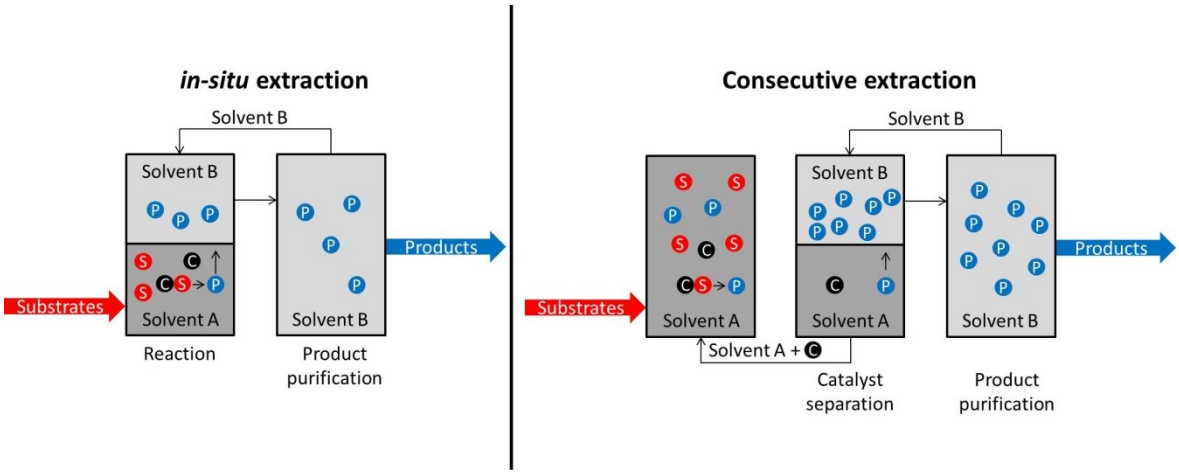

Figure 2.2: Principles of *in-situ* (left) and consecutive (right) extraction.
(C = catalyst; S = substrates; P = products)

In both cases, the catalyst must have a high solubility in one solvent and the product a high solubility in the other solvent. Additionally, both solvents must have a low solubility in each other to enable the phase separation after reaction.

Catalyst recycling after the reaction is, for example, realised in the Kuraray process for the telomerisation of butadiene with water. The catalyst is immobilised in a water/sulfolane mixture. Product extraction after reaction is done with hexane.[9]

However, liquid-liquid biphasic reaction strategies often suffer from mass transfer and solubility limitations between the liquid phases. As a consequence, parts of the catalyst cannot interact with the substrate leading to poor reaction results. Temperature-controlled multiphase systems are a promising approach to overcome these limitations.

Temperature-controlled Multiphase Systems

The different concepts in temperature-controlled multiphase catalysis are discussed in this chapter.

In the **temperature-controlled phase transfer catalysis**, ligands are modified in a way that their phase-behaviour (and therefore the catalysts phase-behaviour) changes with temperature (Figure 2.3). This can be achieved by tagging phosphorous ligands with polyethylene glycol chains. These ligands are soluble in water at low temperatures due to the formation of OH-bridges between water and the polyethylene glycol chain. Higher temperatures disturb this interaction and the catalyst gets soluble in organic solvents.[21,22] One disadvantage of this technique is that the ligand synthesis is effortful and therefore makes the catalyst expensive.

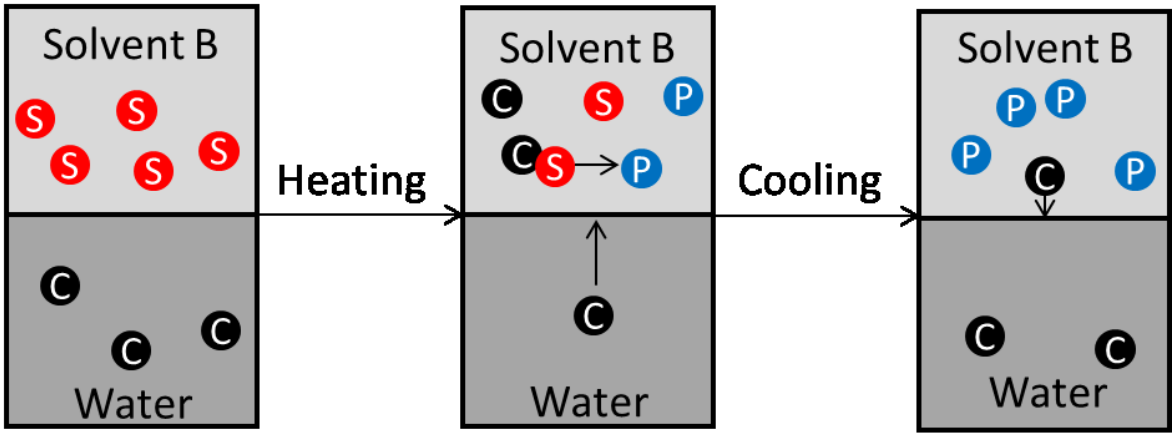

Figure 2.3: Principle of temperature-controlled phase transfer catalysis.
(C = catalyst; S = substrates; P = products)

Addition of surfactants to a biphasic mixture of water and oil can lead to the formation of **microemulsions** with temperature-controlled phase behaviour.[23,24] Depending on the temperature and surfactant concentration, these systems can form a water in oil microemulsion, an oil in water microemulsion, a three-phasic microemulsion containing an aqueous phase, an oil phase and one bicontinuous phase, or a bicontinous microemulsion (Figure 2.4).[24] This behaviour can be described by the so-called "Kahlweit's-fish"-diagram.[25] If a water soluble catalyst is used for the transformation of hydrophobic substrates, the most promising phase behaviour for the reaction as well as for the separation can be adjusted. Challenging in this process strategy is the phase separation after reaction.The different states of the microemulsion systems are often only stable over a small temperature or surfactant concentration range.[23]

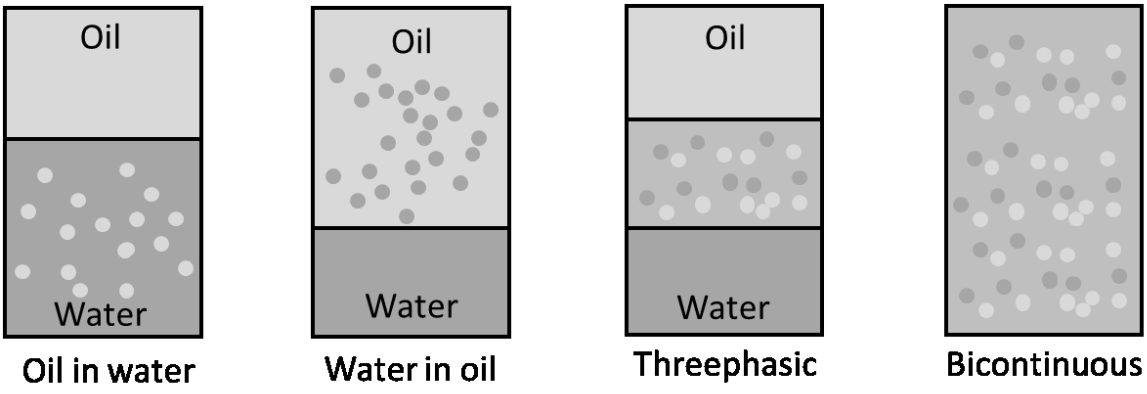

Figure 2.4: Four states of a temperature-controlled microemulsion system.[23,24,26]

One approach leading to a completely homogeneous reaction mixture is the application of **temperature-controlled fluorinated solvent systems**. In these systems, fluorinated solvents are combined with organic solvents or water in order to form a biphasic reaction

mixture. The catalyst is immobilised in the fluorinated solvent *via* fluor-containing ligands. At higher temperatures (upper critical solution temperature; UCST), these mixtures become homogeneous and the reaction can take place without mass transfer– or solubility limitations (Figure 2.5).[27,28] Unfortunately, fluorinated solvents and ligands are comparably expensive and critical from an green chemistry point of view.

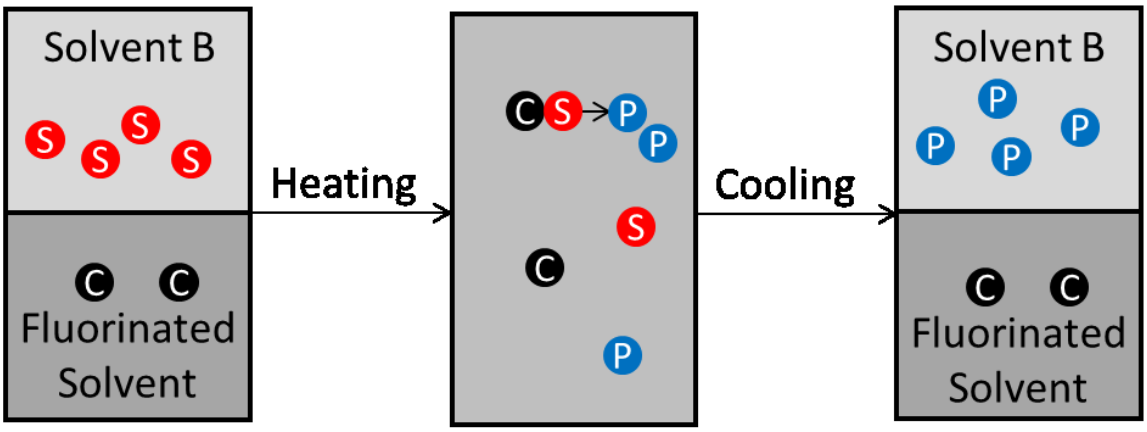

Figure 2.5: Principle of temperature-controlled fluorinated solvents.
(C = catalyst; S = substrates; P = products)

The same temperature-dependent phase behaviour of a reaction mixture can also be achieved by adding a **soluble polymer** to certain liquid-liquid biphasic systems. The catalyst can also be connected to the polymer. This technique allows for monophasic conditions without the usage of fluorinated solvents as well as for tuning the catalysts phase behaviour and therefore, offers interesting possibilities for application in homogeneously catalysed reactions.[9,29]

However, all these approaches presented above have in common, that they require modifications on the catalysts, addition of surfactants or the usage of fluorinated solvents. Additionally, not all of them allow for a complete homogeneous reaction or an easy separation of the catalyst.

These drawbacks do not occur by the application of thermomorphic multicomponent solvent systems (TMS systems). They are discussed in detail in Chapter 2.2.1.

2.2.1. Thermomorphic Multicomponent Solvent Systems (TMS Systems)

General

The concept of TMS systems (Figure 2.6) is based on the idea to utilise the temperature dependency of the miscibility gap of a polar and a non-polar solvent. At low temperatures, these mixtures form two phases. Increasing the temperature leads to a smaller miscibility

gap and therefore, a higher solubility of both solvents into each other. If the upper critical solution temperature (UCST) is reached the mixture is completely homogeneous. Since this phase behaviour is reversible, lowering the temperature leads to the formation of two phases again. The operating point for a process is chosen in a way that the mixture is homogeneous at reaction temperature and biphasic at separation temperature. The phase behaviour can further be tuned by addition of a third mediator solvent. These switchable solvent mixtures are of high potential for the process development in homogeneous catalysis, if the catalyst is predominately soluble in the one and the product of the reaction predominately soluble in the other solvent.[9]

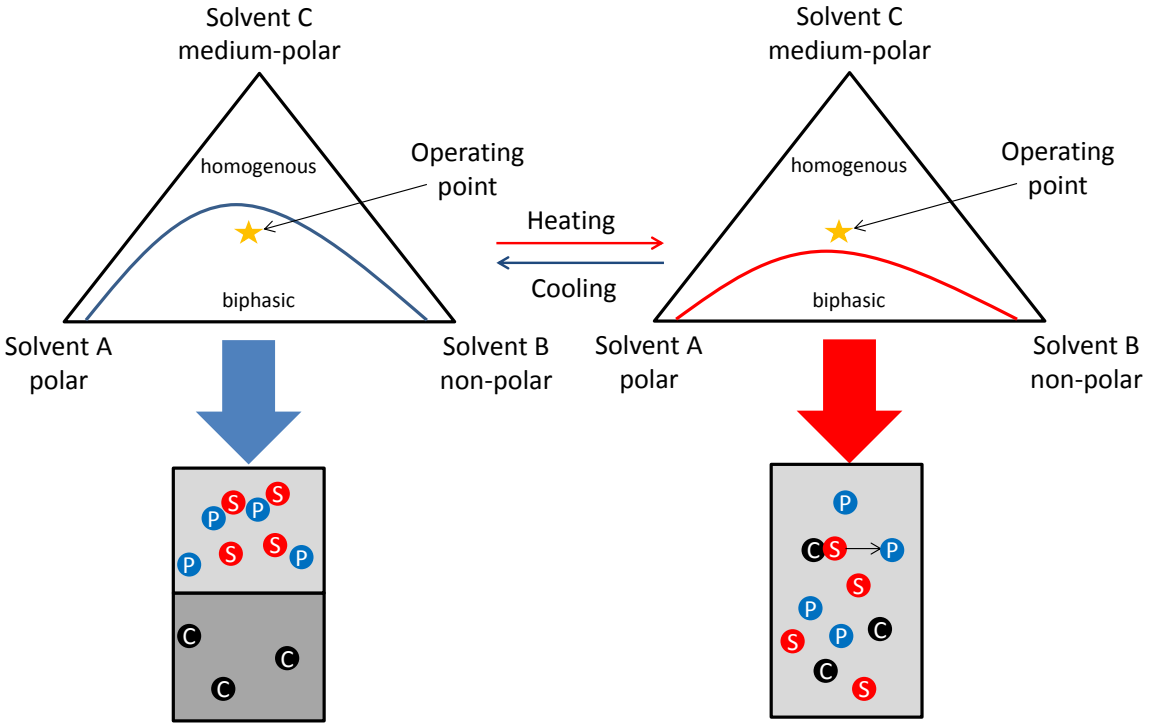

Figure 2.6 Principle of a thermomorphic multicomponent solvent (TMS) system.
(C = catalyst; S = substrates; P = products).

In principle, also mixtures with a lower critical solution temperature (LCST) such as water/triethylamine[30] can be used for process development, but no examples for this are described in literature yet.

The TMS system concept provides some crucial advantages compared to other temperature-controlled approaches discussed above:

- Use of commercially available solvents
- Use of commercially available catalysts
- No mass transport or solubility limitations between the liquid phases during the reaction

- Straightforward catalyst separation *via* decantation after reaction

One drawback of this technique is that the concentration of the substrate is often limited. Additionally, conditions have to be found, which lead to satisfying results in the reaction as well as in the separation. This leads to limitations in the degrees of freedom for the design of a chemical reaction and therefore, to compromises.

Pioneering work in the application of this technique in process development for homogeneous catalysis was done by Arno Behr from the Technische Universität Dortmund. In the following, the classification of TMS systems, different methods for solvent selection and examples for applications are presented.

Classification

According to the literature, TMS systems can be divided into three types. **Type I TMS systems** consist of three different solvents, one polar catalyst solvent (e.g. acetonitrile), one mediator solvent (e.g. morpholine) and one non-polar solvent for the product (e.g. octane). They have a closed miscibility gap at separation as well as at reaction temperature. For an efficient catalyst separation, the miscibility gap at low temperatures should be as large as possible. Figure 2.7 shows several ternary diagrams of type I TMS systems at room temperature.[31]

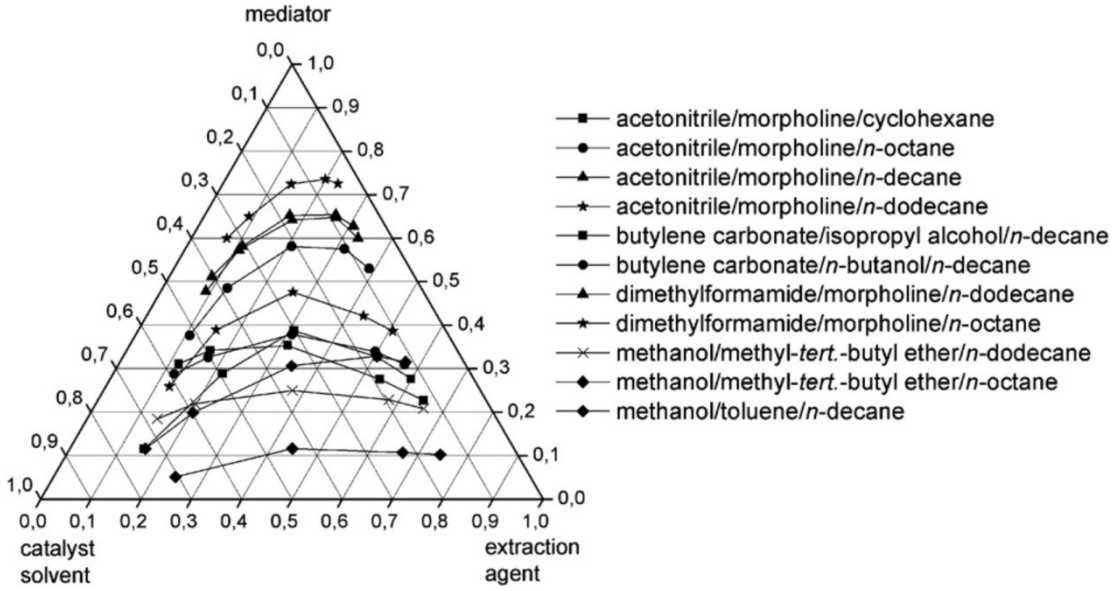

Figure 2.7**:** Miscibility gap of type I TMS systems at room temperature.[31]

Type II TMS systems also consist of three solvent components. In contrast to type I TMS systems, they show an open miscibility gap at room temperature and a closed one at higher temperatures. This can be achieved by choosing a mediator with a polarity similar to the catalyst solvent. Compared to type I TMS systems, they have the advantage that

the product phase does contain only traces of the catalyst solvent. Therefore, the separation of the catalyst from the product is expected to be more efficient. Figure 2.8 shows some exemplary ternary diagrams of type II TMS systems at room temperature.[31]

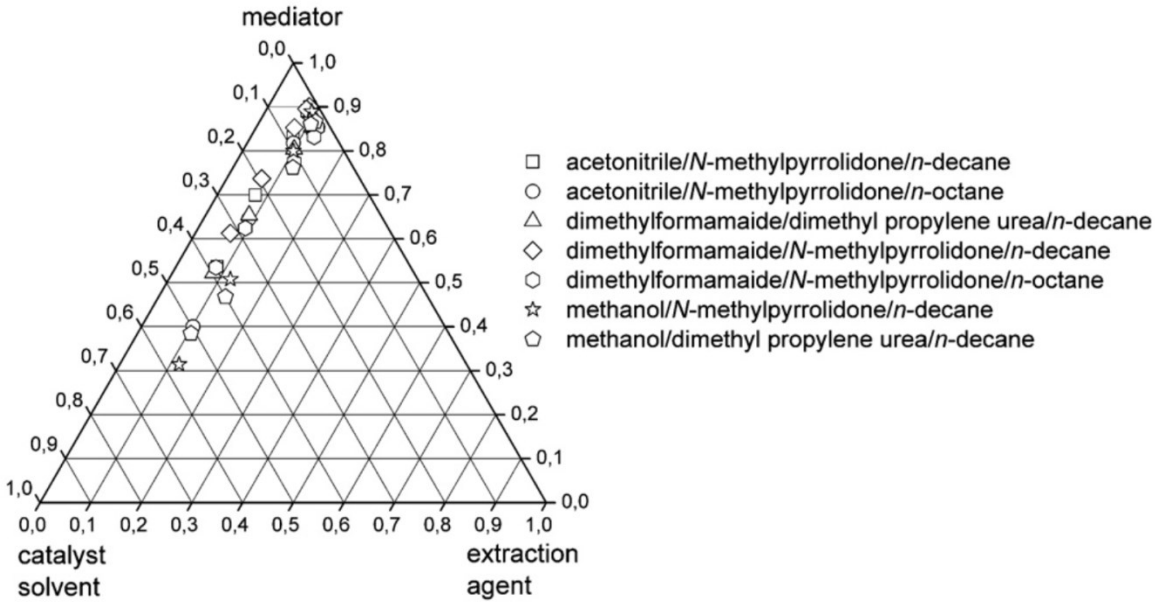

Figure 2.8: Ternary diagrams of type II TMS systems at room temperature.[31]

Type III TMS systems consist of only two solvent components (one polar catalyst solvent and one non-polar product solvent). They can further be divided into TMS systems, which only show a higher miscibility at increased temperatures (type IIIa), and those, which are completely mixable at higher temperatures (type IIIb). These type III TMS Systems are beneficial from a process development point of view due to their lower complexity compared to type I or type II TMS systems.

However, it is important to mention that the presence of a substrate or a product strongly influences the phase behaviour of every type of TMS system. For example, if the polarity of the substrate in a type III TMS system is in between the polarities of the catalyst solvent and the product solvent, it can act as a mediator shifting the UCST towards lower values. These effects are not considered in the current classification of TMS systems, but have to be taken into account in the solvent selection process.

Solvent Selection

Choosing the right solvent or solvent mixture for a chemical reaction is an important task from a process development point of view. The ideal solvent is inert under reaction conditions, non-toxic with low impact on its environment and inexpensive. Despite that, a solvent can have crucial impact on a chemical reaction due to its polarity or its coordination ability.

Solvent selection for TMS systems is even more complex, since the phase behaviour of the solvent mixture has to meet the criteria of the desired process.

One strategy for choosing the right combination of solvents for TMS systems with suitable phase behaviour is to utilise the Hansen solubility parameter (HSP, Equation. 1).[32–34] This three-component solubility parameter considers dispersive (d), polar (p) and hydrogen bonding interactions (h).[31,35]

(Equation 1) $$\delta_0 = \sqrt{\delta_d^2 + \delta_p^2 + \delta_h^2}$$

In principle, solvents with similar HSP values show a high solubility in each other. Therefore, the phase behaviour of potential type I, type II or type III TMS systems can be evaluated and tuned by selecting solvents with suitable HSP values. These values are collected in several databases.[36,37]

Instead of the HSP, other concepts quantifying the polarity of different solvents (e.g. the Kauri-butanol Value[38]) or computational methods can be used for solvent selection. The phase behaviour of a TMS system can also be modelled, e.g. by application of the perturbed chain polar statistical associating fluid theory (PCP-SAFT).[39] Products and substrate can be considered by this method.

Applications

TMS systems have successfully been applied in numerous homogeneously catalysed reactions. The first example was the Pt-catalysed hydrosilylation of methyl 10-undecenoate with triethoxysilane in a TMS system consisting of toluene/cyclohexane/propylene carbonate described by Behr et al. in 1999.[40,41]

In the following, many different transition metal catalysed reactions have been investigated in TMS systems, namely tandem isomerisation/cooligomerisations[42,43], hydroaminations[44–46]; telomerisations[47], hydroetherifications[48], hydroaminomethylations[34,49], hydrogenations[31], codimerisations[50], hydroacylations[51], metathesis[52,53], hydroesterifications[54], cross-couplings[55] and hydroformylations[35,56–59].

Application of TMS systems is also described in organocatalysis[60], enzymatic reactions[61], oligosaccharide-[62] and peptide synthesis[63].

The applicability of TMS systems in continuously operated processes has also been reported in literature. Behr et al. described the rhodium-catalysed isomerising cooligomerisation of linoleic acid with ethene for the synthesis of branched fatty acid derivatives in a TMS system consisting of propylene carbonate and 1,4-dioxane (Figure 2.9).[64] The major challenge in this reaction was the high leaching of the rhodium catalyst caused by the

coordination of the conjugated products to the rhodium. Addition of triphenylphosphine leads to a significant reduction of the rhodium leaching. Unfortunately, the reaction rate was also strongly decreased by triphenylphosphine. However, a stable yield was obtained over a period of 100 h. In a later publication, the problem of the catalyst loss was tackled by subsequent hydrogenation of the branched fatty acid derivatives.[65]

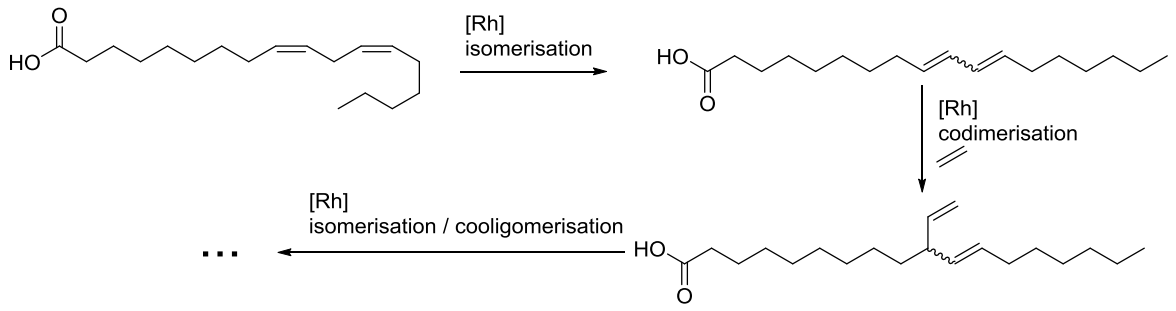

Figure 2.9: Isomerising cooligomerisations of linoleic acid with ethene.

Another interesting example for an application of a TMS system in a continuously operated process is the Pd-catalysed hydroamination of myrcene with morpholine (Figure 2.10).

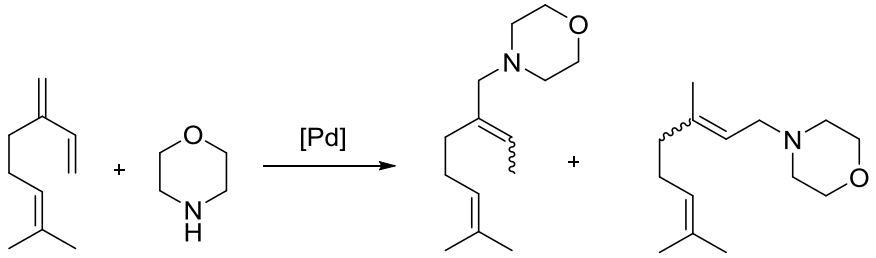

Figure 2.10: Hydroamination of myrcene with morpholine.

The reaction was carried out in a TMS system consisting of *N,N*-dimethylformamide (DMF) and *n*-heptane over 24 h. Although the leaching of the catalyst was low (6% after 24 h) the yields of the terpenyl amines were not stable due to catalyst decomposition.

From special interest is the hydroformylation of long chained olefins in TMS systems. The collaborative research project “Integrated chemical processes in liquid multiphase systems” (InPROMPT) investigated the hydroformylation of 1-dodecene as a model substrate (Figure 2.11). High yields of the desired linear tridecanal (80%) and an excellent regioselectivity in the hydroformylation (99%) were obtained by using a Rh/Biphephos catalyst in a DMF/decane TMS system. The separation of the catalyst was very effective (leaching <1%). The catalyst can successfully be recycled over 30 runs, if the ligand is refreshed after each reaction.[39] Based on these results, several thermodynamic[66,67], mechanistic[68] and kinetic[69] investigations were carried out, resulting in the development of a continu-

ously operated process in miniplant scale. Stable yields and selectivities were achieved for more than 200 h runtime.[70–72] Moreover, further downstreaming of the product phase was investigated resulting in an efficient recycling of the decane and the not converted substrate into the reactor.[73]

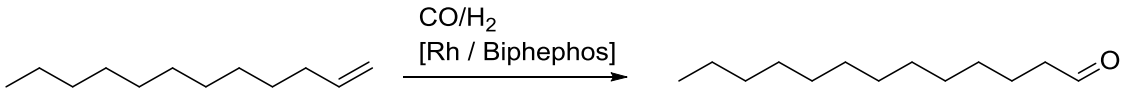

Figure 2.11: Hydroformylation of 1-dodecene to tridecanal.

However, the applicability of known TMS systems reaches its limits in the synthesis of products of relatively high polarity. Carpentier et al. attempts to apply the TMS system technique for recovering the catalyst in the hydroformylation of 10-undecenenitrile failed. The catalyst and the product remained in the same (polar) phase after phase separation.[74]

2.3. Sequential Reactions/Tandem Catalysis

Sequential reactions involve a wide range of chemical reactions in which more than two components participate in the reaction, more than one catalyst is involved in the reaction and/or more than one reaction takes place the reactor.

If a sequence of consecutive reactions can be conducted in one reactor in an efficient manner, it is obviously beneficial in terms of economy and sustainability. For example, no intermediate purification of products is required. This safes energy, chemicals, time and effort.

Additionally, sequential reactions enable transformations, which are not feasible *via* a “classical” synthesis. One important example for this is the synthesis of long chained linear aldehydes *via* isomerisation/hydroformylation of internal olefins.

A classification of different sequential reactions was done by Fogg and dos Santos in 2004 (Figure 2.12).[75] This classification of the different kinds of sequential reactions is exclusively based on the catalyst.

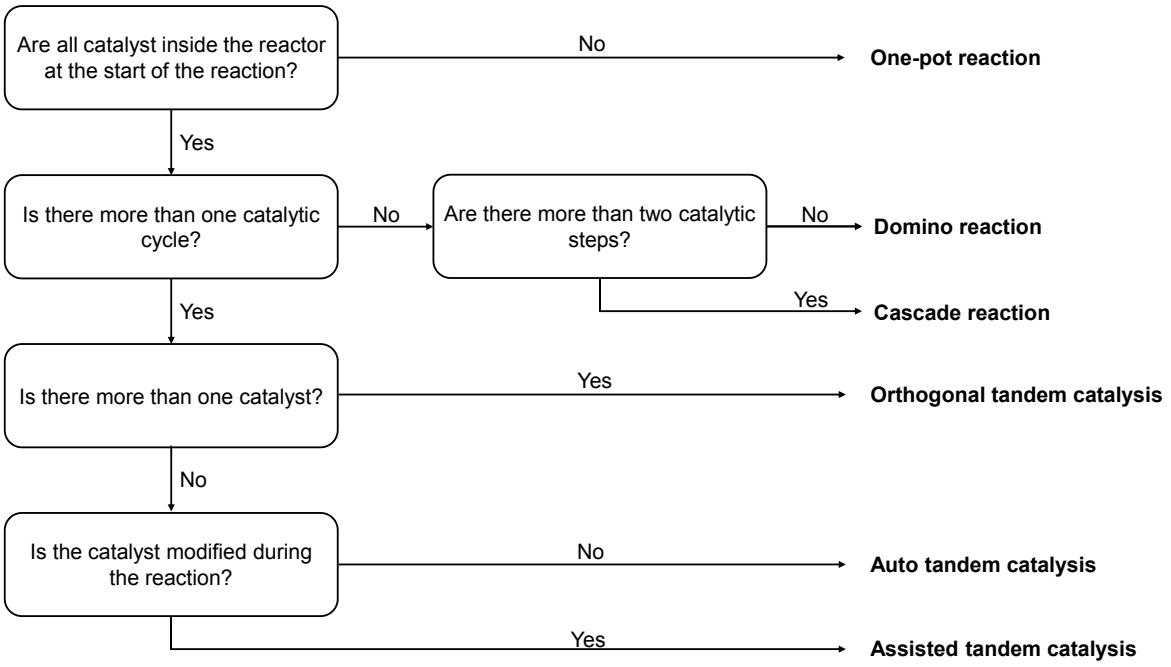

Figure 2.12**:** Definition of sequential reactions.[75]

A reaction is called “one-pot reaction”, if one or more catalyst precursors are added after a certain reaction time. If all catalyst precursors are in the reactor from the beginning of the reaction and there is only one catalytic cycle it is either a domino or a cascade reaction.

If more catalytic cycles are involved in the reaction sequence, this is called “tandem catalysis” Tandem catalysis are further subdivided into “orthogonal tandem catalysis” (two or more catalyst precursors), “auto tandem catalysis” (one catalyst precursor which is not manually modified during the reaction) and assisted tandem catalysis (catalyst is manually modified during the reaction).

In the context of tandem catalysis, olefin carbonylation is of outstanding potential. This transformation allows for introduction of carbon monoxide into easily available unsaturated substrates. This is in particular the case for tandem hydroformylation reactions, since the resulting reactive aldehydes can be converted (e.g. by reduction, condensation or oxidation) into further products in a straightforward way. Some examples for tandem catalysis using olefin carbonylation as a key transformation are given in chapters 2.4.1 and 2.4.2. The concept of sequential reactions in the context of green chemistry is further discussed in chapter 2.1.

2.4. Carbonylation reactions

Insertion reactions of carbon monoxide (CO) into organic molecules are widely known as carbonylation reactions. This type of chemistry was discovered in the 1930s by Otto Roe-

len and Walter Reppe, who can be described as the pioneers in the field of carbonylation reactions.[9] Otto Roelen discovered the hydroformylation ("Roelen reaction") for the conversion of olefins and synthesis gas into aldehydes during his research regarding the Fischer-Tropsch synthesis in the laboratories of Ruhrchemie (Oberhausen, Germany).[18] This reaction is discussed in detail in chapter 2.4.1. Walter Julius Reppe substantially investigated different carbonylation reactions ("Reppe chemistry") at the BASF laboratories (Ludwigshafen, Germany).[76,77] As the first examples for transition metal catalysed homogeneous catalysis, these revolutionary findings initiated a lot of new developments in the field of catalysis.

However, due to the large substrate scope and the availability of CO as an inexpensive and versatile C1 building block, carbonylations are the most important class of homogeneous transition metal catalysed reactions today. The most relevant industrial applications for carbonylation reactions are the acetic acid synthesis *via* methanol carbonylation (14 mio. t/a)[78] and the hydroformylation of unsaturated compounds (12 mio t/a)[18]. An overview over different substrates and products of carbonylation reactions is given in Table 2.1.

Table 2.1: Overview over carbonylation reactions.[9]

Substrate	Products
alkenes	carboxylic acids, esters, aldehydes, alcohols
dienes	Unsaturated carboxylic acids/esters, dicarboxylic acids/diesters, unsaturated aldehydes,
alkynes	acrylic acid/ esters (and derivatives)
alcohols	carboxylic acids
diols	dicarboxylic acids
halogen compounds	carboxylic acids/esters, ketoacids
ether	esters
esters	anhydrides
amines	amides

In the following chapters, the hydroformylation and the hydroesterification are discussed in greater detail.

2.4.1. Hydroformylation

The formal addition of a hydrogen atom and a formyl group to a double bond in presence of a transition metal catalyst is called hydroformylation or oxo synthesis. This reaction is one of the most important industrial applications of homogeneous catalysis.[79] In the year 2012 more than 12 million tons of hydroformylation products have been synthesised.[80] A schematic hydroformylation of a terminal olefin is shown in Figure 2.13.

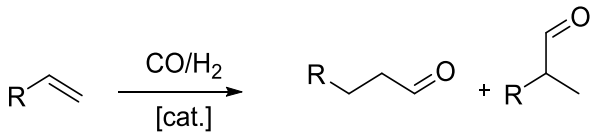

Figure 2.13: Hydroformylation of a terminal olefin.

The formyl group can be added to each of the double bond's carbon atoms, yielding either in a linear (*l*-) or in a branched (*b*-) aldehyde. Due to the rule of Keulemans, the formyl group is preferably added to the lower substituted carbon atom, thus formation of the *l*-aldehyde is favoured.[81]

Phosphine modified complexes of cobalt and rhodium are the only catalysts applied on industrial scale today.[17] Rhodium catalysts are the most active catalysts in hydroformylations and enable the application of mild reaction conditions (e.g. 15 bar synthesis gas pressure and 100 °C). They are mainly applied in the hydroformylation of short chained olefins. Cobalt catalysts are predominately used for the hydroformylation of long chained alkenes (>C10) due to their higher robustness. They require harsh reaction conditions (up to 300 bar synthesis gas pressure and 180 °C).

However, there is some promising research in the development of hydroformylation catalysts using alternative catalyst metals (see the section "Recent Trends in Academic Research" in this chapter).

A detailed overview about the hydroformylation was recently published by Franke and Börner.[82]

Mechanisms and Side Reactions

A mechanism for cobalt-catalysed hydroformylation of olefins was developed by Heck and Breslow in the 1960s (Figure 2.14).[83]

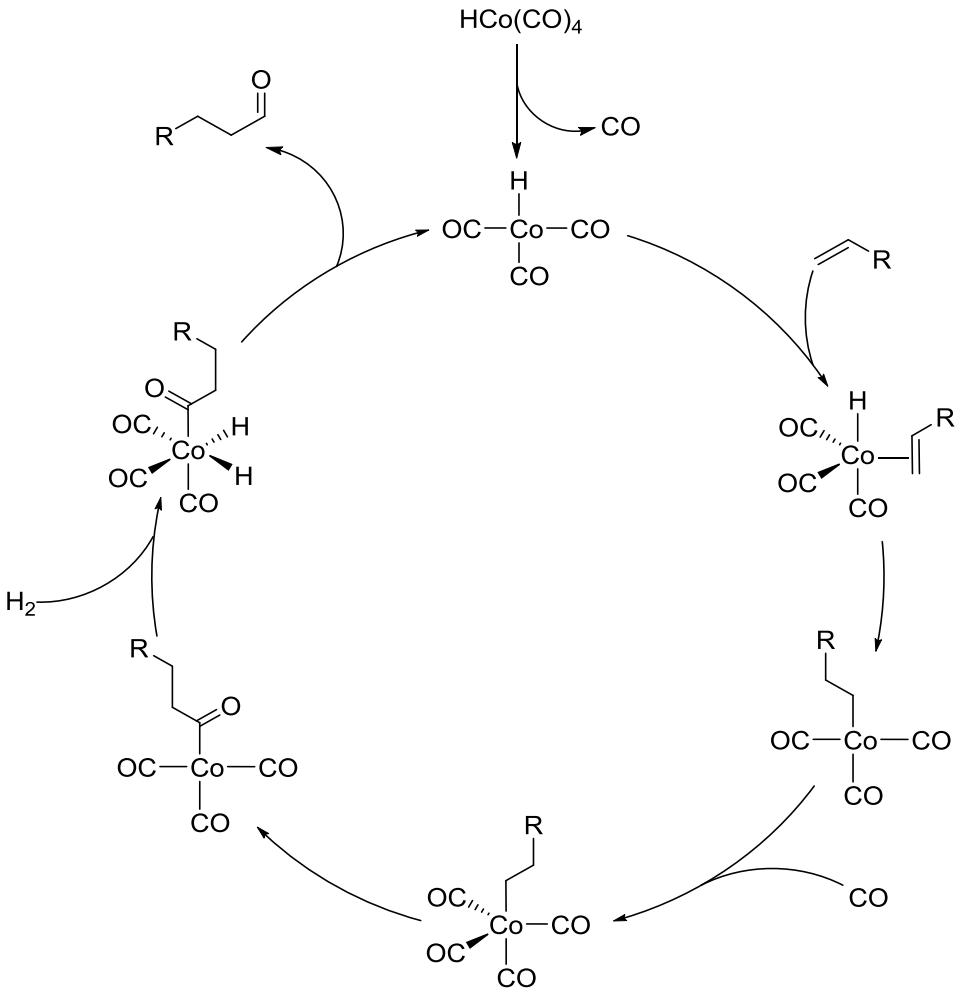

Figure 2.14: Mechanism of the cobalt-catalysed hydroformylation (under formation of the linear aldehyde).

Starting from the cobalt (I) precursor tetracarbonylhydridocobalt, the active catalyst is formed by loss of one molecule carbon monoxide. The resulting tricarbonylhydridocobalt is able to associate an olefin, which undergoes insertion into the Co-H bond. This step determines whether the *l*-aldehyde or the *iso*-aldehyde (or *b*-aldehyde) is formed. After insertion in the Co-H bond, the complex associates a carbon monoxide molecule and insertion of carbon monoxide into the Co-Alkyl bond occurs. Finally, the oxidative addition of dihydrogen followed by reductive elimination of the free aldehyde under recovery of the active catalyst takes place.

G. Wilkinson made a suggestion for a mechanism of the alkene hydroformylation by use of rhodium-phosphine complex catalysts (Figure 2.15).[84]

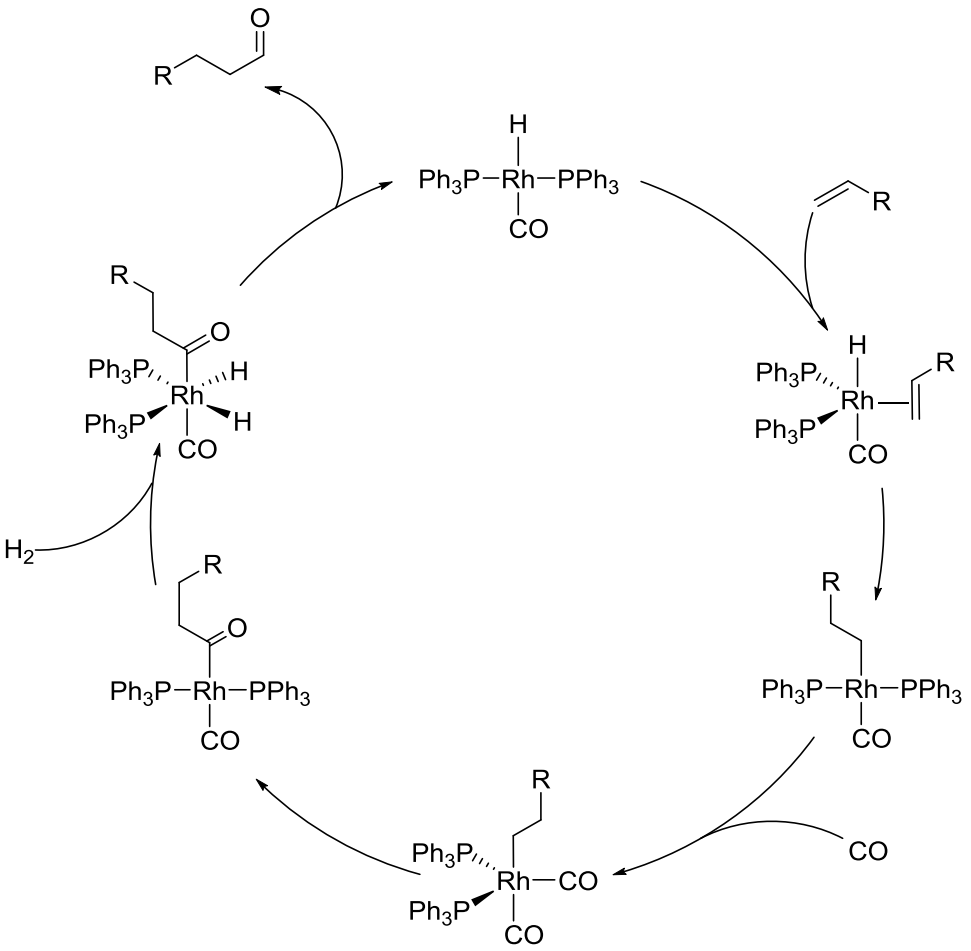

Figure 2.15: Mechanism of the rhodium-catalysed hydroformylation (under formation of the linear aldeyhde).

The reaction steps proceed in the same sequence compared to the mechanism of the cobalt catalysed hydroformylation but by use of an additional phosphine ligand, there are many possible intermediates involving different number of phosphine ligands bonding to the rhodium or different geometric arrangements.[85,86]

In presence of a transition metal catalyst and synthesis gas, several side- and consecutive reactions can occur. The most prominent side reactions are the hydrogenation and the isomerisation of the C=C double bond. Consecutively, resulting aldehydes can be reduced to the corresponding alcohols or undergo a condensation reaction (Figure 2.16).[9]

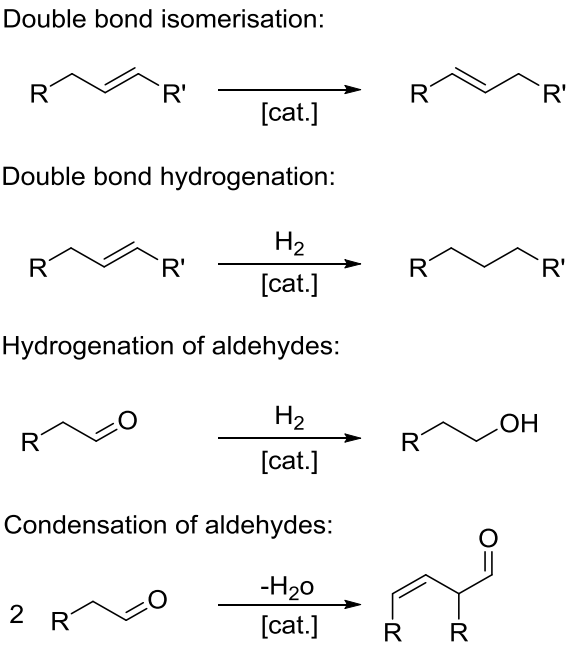

Figure 2.16: Common side reactions of the hydroformylation.

Double bond isomerisation constitutes an interesting side reaction in hydroformylations. In respect of formation of linear aldehydes, isomerisation is boon and bane depending on the starting material. Starting from substrates with internal double bonds, linear aldehydes are available through double bond isomerisation to the end of the carbon chain and subsequent hydroformylation. If the starting material already contains a terminal double bond, isomerisation is disadvantageous and leads to formation of internal aldehydes or decelerates the reaction rate.[87]

The hydrogenation of double bonds is an undesired side reaction, leading to loss of substrate to low value chemicals and lower selectivity in hydroformylation.

Hydrogenation of nascent aldehydes can be used to synthesize corresponding alcohols in a tandem reaction.[88] This reaction can either be desired or not. On the one hand, alcohols are an important class of chemical intermediates and a tandem reaction consisting of hydroformylation and consecutive aldehyde reduction (reductive hydroformylation) offers an easy access for them. Consequently, this reaction is implemented on industrial scale *via* the Shell process in which a phosphine-modified cobalt catalyst is used. On the other hand, aldehydes are straightforward convertible into further classes of chemical intermediates (e.g. carboxylic acids, amines etc.). In this case, formation of alcohols is undesired.

Condensation of two aldehydes is also described in literature. Again, this can be an interesting consecutive reaction for the synthesis of chemical intermediates. For example, condensation of two molecules *n*-butanal to 2-ethylhex-2-enal (Figure 2.17) is a crucial

reaction step for the synthesis of 2-ethylhexanol, which is an important intermediate in the syntheses of PVC-plasticizers.[89,90]

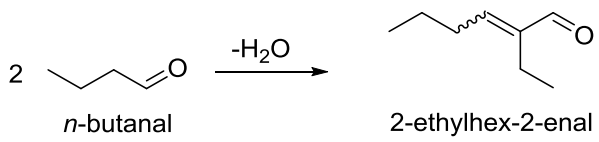

Figure 2.17: Condensation of *n*-butanal.

Catalyst Development in Industrial Hydroformylation Processes

Several transition metal complexes are suitable catalysts for the hydroformylation reaction, e.g., rhodium, cobalt, ruthenium, iridium and platinum-tin.[91] However, only cobalt and rhodium catalysts have gained industrial importance until today. The first hydroformylation, discovered by Otto Roelen, was realised with a cobalt catalyst as side product of Fischer-Tropsch experiments.[2] Cobalt catalysts require relative high pressures and temperatures for satisfying yields in the hydroformylation. Rhodium, as the most active catalyst metal, enables hydroformylation under milder conditions compared to cobalt.[9]

The industrial implementation of the hydroformylation ensues in four steps. **The first catalyst generation** consists of unmodified cobalt carbonyl hydride complexes. Corresponding processes were developed by BASF and Exxon in the 1950s. In this processes high pressures (200-300 bar) and temperatures between 110 °C and 180 °C are required. The cobalt catalyst was separated *via* chemical precipitation.

The second hydroformylation catalyst generation consists of phosphine modified cobalt catalysts and is applied in the Shell process. Corresponding alcohols are obtained as main products and a reduced synthesis gas pressure compared to the first catalyst generation (50-100 bar) is applicable. Separation of the catalyst is realised *via* product distillation after reaction.

In the 1970s, Union Carbide Corporation designed the low-pressure oxo (LPO) process applying a rhodium-phosphine catalyst, which is referred to as **the third catalyst generation**, for hydroformylation under mild conditions (15-20 bar, 85-115 °C). The rhodium-catalyst in the LPO-process can either be recycled *via* gas or liquid recycle. In the gas recycle process, the products are evaporated under process conditions. In the liquid recycle process, both the catalyst and the products leave the reactor as a liquid and the hydroformylation products are separated from the catalysts *via* distillation.

The Ruhrchemie/Rhône-Poulenc process uses water soluble phosphine-modified rhodium catalysts (**fourth catalyst generation**) in the hydroformylation of short chain olefins, enabling a straightforward catalyst recycling *via* phase separation after reaction. Hydro-

formylation with this technique is limited to short chain olefins due to poor solubility of higher olefins in water.[10,78]

Recent Trends in Academic Research

One important field of research in hydroformylation reactions is developing new catalysts aiming for higher selectivity and activity. Improving catalyst stability and lowering catalyst prices are also attractive aims in catalyst development. The catalytic performance of a transition metal complex in hydroformylations is influenced by the catalyst metal and its ligands. Consequently, both are subject of academic research today.

In terms of the catalyst metal, rhodium complexes are the most active ones and as a result also the most important ones from an industrial point of view. About 80% of all industrial hydroformylation processes are based on rhodium.[17] Due to their outstanding potential, large research effort has been put in improving rhodium based hydroformylation catalysts. The major drawback of rhodium is its high price and the high volatility of this price. While today, one ounce of rhodium costs between 600 – 700 $, one ounce of rhodium in 2008 has cost 10000 $ (Figure 2.18).[92] For the rhodium production in 2017 a surplus is predicted.[93]

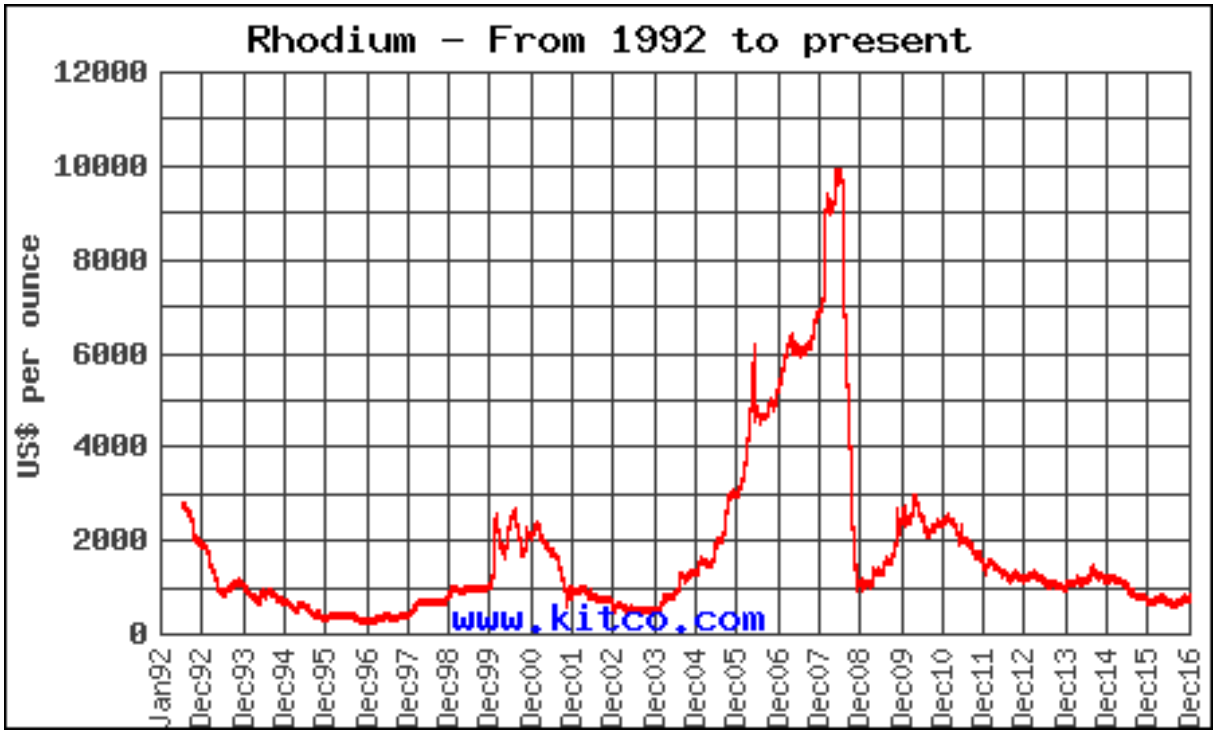

Figure 2.18: Price development of rhodium.[92]

However, due to the problems discussed above, the substitution of rhodium by other transition metals is desirable. Besides by use of Co, which is also implemented on industrial scale, promising results are obtained e.g. by application of Ir[94–97], Pd[98–100], Ru[101–104] or

Pt[105–107]. Ru-[108] and Ir-catalysts[97] have already been applied on continuously operated miniplant scale. A detailed overview over hydroformylation with alternative catalyst metals was published by Beller et al in 2013.[91]

Ligand design is another important field of research, which targets different aspects of hydroformylation catalyst development. Especially the selectivity is strongly influenced by ligands. For example, in many hydroformylation applications a high regioselectivity towards the linear aldehyde is desired. In particular, the application of chelating phosphorous ligands enables excellent control of the regioselectivity. Some examples for these ligands are shown in Figure 2.19.

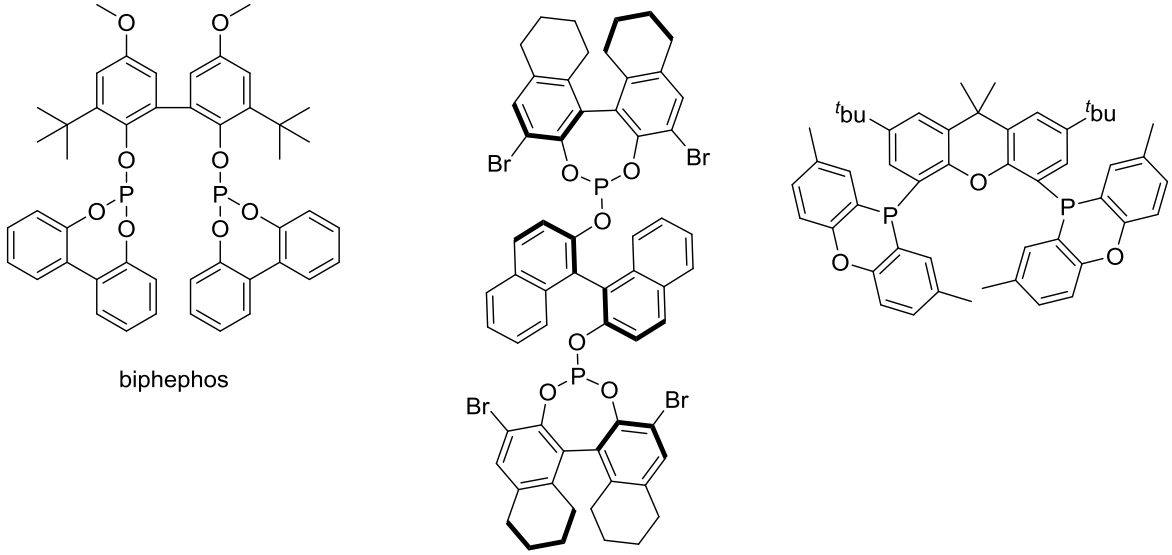

Figure 2.19: Examples for ligands enabling high linear selectivity in hydroformylations.[109–111]

Not only regioselectivity but also stereoselectivity can be controlled, if chiral ligands are applied.[112–114] This is of high value in fine chemical and pharmaceutical synthesis.

Ligands can not only control the catalytic performance of a transition metal complex in the hydroformylation, but can also be utilised to enable an efficient catalyst recovery after reaction. For example, ligands can be modified to control the phase behaviour of transition metal complexes in hydroformylation reactions. One effective example is ligand sulfonation to make the catalyst soluble in water.[115–117] These aqueous catalyst phases can easily be separated from hydroformylation products by decantation. Ligand enlargement (e.g. with polyhedral oligomeric silsesquioxanes) enables the possibility for a highly efficient separation *via* membranes.[14] Also heterogenisation of the hydroformylation catalysts can be achieved, e.g. by connecting ligands to a solid carrier.[118]

These efforts in designing ligands for separation clearly underline that catalyst recovery is also an important field of research in hydroformylation. There are several strategies for

separation of catalyst and product. As mentioned above, one of them is catalyst immobilisation in water. The major challenge using this strategy is to bring the substrate in contact with the catalyst. This is particularly the case if long chained olefins with low solubility in water are converted. There are several strategies to overcome these limitations such as addition of a co-solvent [119], surfactants [120], particles [121] or cyclodextrines.[122] Procedural approaches also lead to promising results in this context.[123] Also „switchable systems“ with tuneable phase behaviour of the catalyst have been shown to be successful. For example, the phase behaviour of complexes containing ligands bearing a nitrogen atom can be changed by adding CO_2 after reaction.[124] An overview of different chemical approaches to overcome phase transfer and solubility limitations in hydroformylation in aqueous media was published by Obrecht et al..[117]

Another promising strategy for catalyst separation is the use of thermomorphic multicomponent solvent systems (TMS systems).[35,39,58,71] This strategy is discussed in detail in chapter 2.2.1.

As discussed in chapter 2.3, tandem reactions are a very promising strategy for designing an efficient process. In this context, the hydroformylation is of outstanding potential. On the one hand, resulting aldehydes are reactive intermediates and can easily undergo consecutive reactions such as reductions, oxidations or condensation reactions. On the other hand, the hydroformylation is one of the most investigated homogeneous transition metal catalysed reactions and a variety of different catalysts is available. These catalysts offer different selectivities, tolerances against other chemicals and cause different side reactions which can be utilised for tandem reactions. That is why tandem hydroformylation is also a “hot topic” in academic research.

One very important example for a tandem hydroformylation is the isomerising hydroformylation.[125] This tandem reaction enables the synthesis of linear aldehydes from internal olefins or even mixtures of internal olefins and therefore opens the reaction pathway for the implementation of new alternative feedstocks. This topic was reviewed by Börner et al. in 2014.[126]

Further interesting examples are hydroaminomethylations[8,127,128], hydroformylations in combination with consecutive aldehyde reduction[129] or acyloin reactions.[130,131]

The implementation of renewable feedstocks is also an important trend in hydroformylation research. Hydroformylation of fatty compounds for example, leads to bifunctional molecules with interesting scope of application (e.g. lubricants, polyamides, plasticizers polyurethanes).[132] While the synthesis of branched hydroformylated fatty compounds itself is not a great challenge, recycling of the catalyst is a great issue tackled by actual

research projects. Promising results are obtained e.g. in aqueous solvent systems[122,133] or ionic liquids[134]. Tandem hydroformylation reactions with fatty compounds are also of great interest. Isomerisation/hydroformylation of unsaturated fatty compounds leads to asymmetric α,ω-functionalised molecules. These are very valuable intermediates for the synthesis of bio-based polymers.[135] Unfortunately, there is no catalyst known today which can catalyse this reaction in an effective way. Highest yield of the linear aldehyde in the isomerisation/hydroformylation of methyl oleate is 26% with a regioselectivity of 75%.[87,125] Besides formation of branched aldehydes, double bond hydrogenation is a main issue. If not the aldehyde itself is targeted, but the alcohol, a yield of 52% can be achieved.[136]

Also the hydroaminomethylation of fatty acid methyl esters is an interesting conversion aiming e.g. the synthesis of polyamide monomers.[137]

Other interesting renewable starting materials for the hydroformylations are terpenes and naturally occurring allyl benzenes. Resulting products are fragrance compounds.[138,139] Hydroformylation (tandem reactions) of terpenes containing a 1,3-diene moiety (e.g. myrcene) is more challenging regarding the catalytic activity and the selectivity of the reaction.

Also the replacement of CO with CO_2 is possible, if a reverse water-gas-shift reaction is done prior to the hydroformylation.[140]

However, it is important to notice that new developments in all of these research areas are influencing each other. For example, the development in ligand design can cause new possibilities for the application of alternative metals, catalyst recycling concepts or tandem reactions. These developments can facilitate the implementation of renewable starting materials in hydroformylation.

2.4.2. Hydroesterification

The addition of carbon monoxide and an alcohol to an unsaturated substrate under formation of an ester moiety is called hydroesterification or alkoxycarbonylation (Figure 2.20). This reaction, discovered by Walter Reppe[76], is a straightforward and 100% atom economic way for ester synthesis from cheap bulk chemicals. The most important catalyst metal in this reaction is palladium, but also cobalt or nickel can be applied.[77]

On industrial scale, the hydroesterification is realised in Lucite's two-step Alpha process for producing methyl methacrylate (MMA). The first step in this process is the palladium-catalysed hydroesterification of ethene with methanol and carbon monoxide under formation of methyl propionate, which reacts subsequently in a second reaction with formaldehyde under MMA formation. 120.000 tons of MMA per year are produced by this tech-

nology. In 2017, a second Alpha plant with a capacity of 250.000 tons per year will go on stream.[141,142]

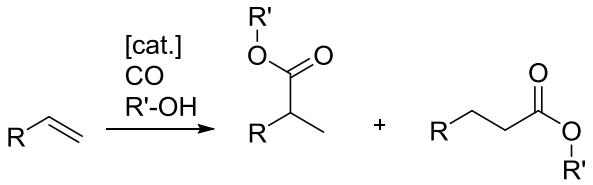

Figure 2.20: Hydroesterification of a terminal olefin.

Mechanisms

There are two different mechanistic pathways described in the literature for the palladium-catalysed hydroesterification.[77] The hydride mechanism (Figure 2.21) starts from a Pd-hydride species. After insertion of the alkene into the Pd-H-bond, an acyl-complex is formed *via* CO-insertion. This acyl-complex is converted into the ester *via* alcoholysis under reformation of the active Pd-hydride catalyst.

The alkoxy mechanism (Figure 2.22) starts from Pd-alkoxy species. After CO-insertion into the Pd-O-bond, alkyl insertion takes place under formation of an ester moiety at the end of the carbon chain. Subsequent alcoholysis leads to the formation of the product under regeneration of the catalyst.

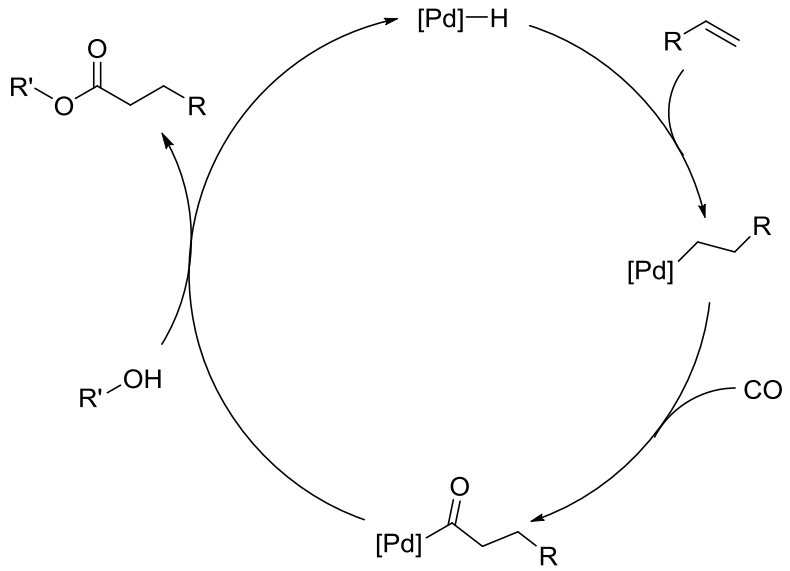

Figure 2.21: Pd-catalysed hydroesterification *via* hydride mechanism.

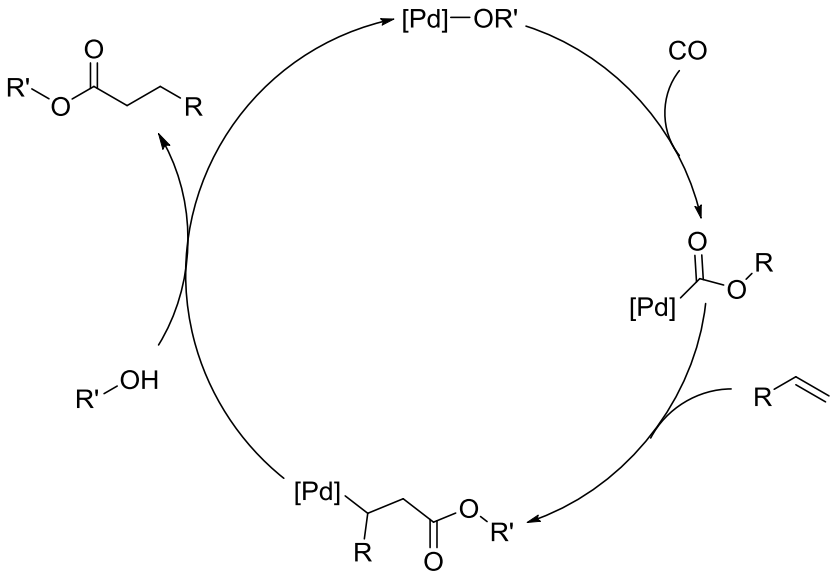

Figure 2.22: Pd-catalysed hydroesterification *via* alkoxy mechanism.

Recent Trends in Academic Research

In the past ten years, the isomerising hydroesterification was probably the most important research topic in the field of hydroesterification. In 2004, Cole-Hamilton's group reported about the high efficiency of a palladium complex bearing the 1,2-DTBPMB ligand (which is also applied in the Lucite Alpha process, Figure 2.23) in the *n*-selective hydroesterification of terminal and internal unsaturated olefins and oleo chemicals. Independently from the position of the double bond, regioselectivities of 93% and higher towards the linear products are achieved using this catalyst.[143,144] Due to this catalysts outstanding potential, it was used to convert many different unsaturated substrates derived from renewables into corresponding esters.[144–151] From special interest for new bio-based polymers is the synthesis of α,ω-bifunctional molecules (e.g. *via* hydroesterification of methyl oleate, Figure 2.23).[152–155]

Instead of methanol also water can be used as a nucleophile (hydroxycarbonylation or hydrocarboxylation) under formation of the free carboxylic acids by use of this catalyst.[156]

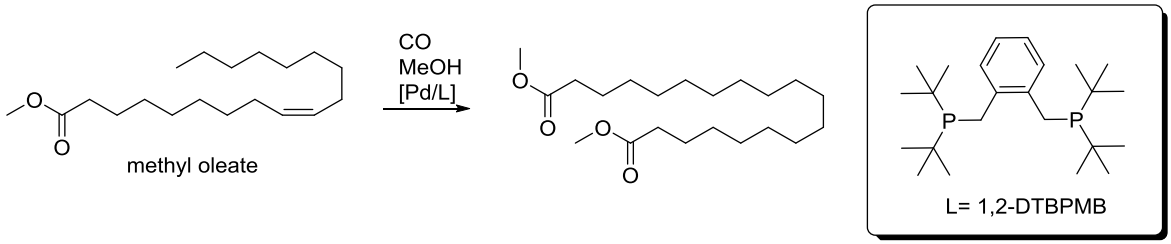

Figure 2.23: Tandem isomerisation/hydroesterification of methyl oleate and the 1,2 -DTBPMB ligand.

Several studies were done regarding the activity for this type of hydroesterification catalyst. [157–160] Detailed mechanistic studies on the tandem isomerization/hydroesterification were made by Mecking et. al.[161,162] and Köckritz et. al.[163].

Very recently, the group of Beller developed a hydroesterification catalyst (a palladium complex bearing ligand L1, Figure 2.24) showing the contrary selectivity enabling for the selective synthesis of branched esters.[164] This group also developed a new hydroesterification catalyst (a palladium complex bearing ligand L2, Figure 2.24) allowing for the hydroesterification of tri- and tetra substituted alkenes. This new catalyst also shows an extremely high activity in the hydroesterification of ethene (Lucite's Alpha process), even at room temperature. Its catalytic performance is superior compared to the state-of-the-art industrial catalysts.[165]

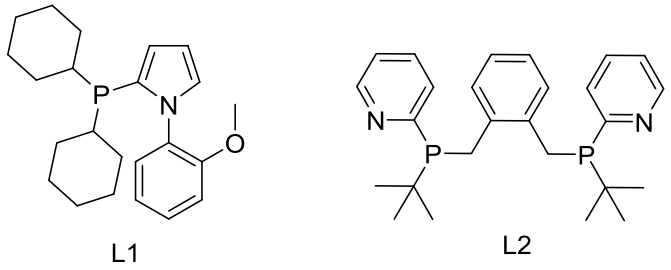

L1 L2

Figure 2.24: Ligands for new hydroesterification catalysts.

3. Aims of the Present Work

The aim of this work is to enhance the knowledge in developing new sustainable processes for homogeneously catalysed olefin carbonylation reactions. Two main aspects with crucial impact on the process design are tackled within this thesis:

Recycling of known homogeneous transition metal catalysts

The recovery of valuable transition metal catalysts is essential for the development of economic feasible processes in homogeneous catalysis. The concept of thermomorphic multicomponent solvent (TMS) systems is of high potential in this context.

Although TMS systems have been applied in several reactions as catalyst recycling strategy, a systematic evaluation of their potential is missing. The first important target of this PhD thesis is the development of a general guide for the application of TMS systems. This task will be tackled by a systematic evaluation and expansion of their scope in 4 steps:

1. Development of a new solvent selection strategy for TMS systems

Solvent selection is important when designing new TMS systems. The methods described in literature deal solely with phase behaviour of the applied solvents. Developing a method, which takes into account thermodynamic properties of catalyst and product in the initial stage of solvent selection would lead to an improvement in prediction of the TMS systems performance and therefore, reduce the required experimental effort.

2. *Application of TMS systems in the conversion of technical grade feedstocks*

The selective conversion of technical grade feedstocks into value-added products places high demands on both the catalyst and the TMS system. Impurities can cause issues in terms of catalyst stability and phase behaviour.

3. Application of TMS systems in the conversion of renewable feedstocks

In contrast to non-functionalised long chained olefins, renewable substrates like unsaturated oleo compounds already contain a functional group. Introducing an additional moiety further increases their polarity. This essentially complicates the separation process and was rarely shown to be solved in an efficient manner *via* TMS systems in literature.

4. Application of TMS systems in reactions with inherently limited degrees of freedom in the solvent choice

The efficiency of TMS system can strongly decrease, if the reaction limits the choice of solvents, e.g. in the hydroesterification. An alcohol is required as a second liquid substrate in this reaction. The concentration of the alcohol can have crucial impact on the reaction performance. The fact, that the alcohol is consumed during reaction (and therefore changes phase behaviour) is potentially problematic. Both phenomena have to be considered in designing TMS systems.

Development of new catalytic systems for the conversion of substrates based on renewable raw materials in tandem reactions

Designing new catalysts or catalytic systems is an important task in order to increase the efficiency of known reactions and to enable new reaction pathways. The second focus of this thesis aims for developing new catalytic systems for tandem reactions with renewables. The core element of these investigations is the hydroformylation. In principle, the hydroformylation can be the initial or the terminal part of a tandem reaction sequence. Both cases are investigated in within this thesis. All transformations aim for the synthesis of products with potential technical application from renewable starting materials.

Hydroformylation as initial step in tandem reactions

For catalysing the *n*-selective synthesis of alcohols *via* reductive hydroformylation (hydroformylation/hydrogenation tandem reaction) of terminal unsaturated substrates, bimetallic catalytic systems have proven to be very efficient. Simplifying these systems *via in situ* generation of the catalytic active species would be of high value from an economic point of view.

The application of 1,3-dienic substrates in the hydroaminomethylation is very challenging compared to the utilisation of substrates with isolated double bonds. Today, no catalyst combining high reaction rates and high selectivities for this conversion is described in literature, although this transformation is of high potential for the chemical industry.

Hydroformylation as terminal step in tandem reactions

The selective synthesis of asymmetric α,ω-functionalised molecules *via* tandem isomerisation/hydroformylation of fatty acid methyl esters lead to products with a broad application area. No catalyst allowing for this valuable transformation in an efficient manner is known today.

The results of these investigations are presented in eight publications. Afterwards, a guide for the application of TMS systems derived from the results will be presented and the new catalyst systems will be evaluated. Finally, this work will be discussed in the context of industrial relevance and sustainable chemistry.

4. Publications

4.1. Thermomorphic Solvent Selection for Homogeneous Catalyst Recovery based on COSMO-RS

Kevin McBride, Tom Gaide, Andreas J. Vorholt, Arno Behr, Kai Sundmacher, *Chem. Eng. Process.* **2016**, *99*, 97–106.

Contributions:

The concept and ideas leading to this publication were contributed by Kevin McBride. Calculations *via* COSMO-RS were done by Kevin McBride. Experimental data for validation was provided by me. Art-work and literature search were search were done by Kevin McBride. Preparation of the manuscript was done by Kevin McBride and me. Kai Sundmacher, Andreas J. Vorholt and Arno Behr supervised this project and corrected the manuscript.

4.1.1. Abstract

One method that has shown much promise due to its simplicity and effectiveness in homogeneous catalyst recovery is the use of thermomorphic solvent systems (TMS). In this contribution, a novel method for TMS solvent selection based on quantum chemical predictions of catalyst solubility and phase equilibrium is presented. This allows for solvent effects on the catalyst to be incorporated directly into the solvent screening process. A framework for TMS design is developed and implemented using the hydroformylation of 1-dodecene and the rhodium-Biphephos catalyst as an example reaction system. In this way, several promising TMS systems were identified. Experiments were then performed to validate the model based on catalyst partitioning and phase equilibrium. This was followed by conducting a series of reactions to investigate feasibility of the new TMS systems in the actual hydroformylation. In the end it was shown that although some problems arise from inconsistencies in phase equilibrium predictions, the method does provide a functioning *a priori* basis for TMS development.

4.1.2. Introduction

Although homogeneous catalysis can deliver many benefits to a process such as high activity, good selectivity, robust catalyst systems, etc., separation and recycling of the catalyst can be quite cumbersome.[9] Additionally, the loss of expensive transition metals often used in homogeneous catalyst complexes may lead to economically infeasible processes if not recovered satisfactorily. One important yet simple method for recovering homogeneous catalysts from a post-reaction mixture is temperature controlled liquid phase separation through the use of thermomorphic solvent systems (TMS).[166] Composed of solvents with varying degrees of polarity, these tunable mixtures form a homogeneous phase at reaction temperature and separate into two phases when cooled, ideally recovering the catalyst in one phase and the product in the other. TMS systems are investigated in several homogeneously catalyzed reactions including hydroaminomethylation[49], hydroformylation[31,35] and cooligomerization[42,167] where low levels of catalyst loss were realized. More specifically, the hydroformylation of 1-dodecene in a TMS composed of *n*-decane and dimethylformamide (DMF) has been the topic of much research in recent years in the areas of reaction kinetics[69] and reactor and process optimizations[168–170]. Thus the importance and practicality of TMS usage for catalyst recovery is well established.

Choosing which solvents to include in the TMS is an important task. Solvent selection methods developed have been so far successfully based on the liquid phase separation behavior of two or three solvents and their respective polarities as measured using Han-

sen parameters.[31,35] A framework for selecting a mediator solvent in the hydroaminomethylation of 1-octene was recently presented that more rigorously dealt with the pros and cons of using solvent descriptors and predictive thermodynamic models in selecting suitable solvent candidates.[34] Although such methods for solvent selection often lead to good candidate solvents, predictions of phase behavior or solubility are not always accurate enough to be considered completely reliable. This is something the authors experience with some of the predicted solubilities compared to those found experimentally. Thus the authors advise, as is often the case in solvent selection, that experimental validation is still very much necessary. Although some issues are found in predictive methods for phase equilibrium, still no aspect of catalyst solubility is discussed at this point.

These methods for solvent selection rely on the fact that the usually polar catalyst will be recovered in the polar phase while the less polar product is recovered in the non-polar phase. In principle the design of the TMS system should ideally include some aspects of the thermodynamic behavior of the catalyst into the initial stage of solvent selection. This would ensure, at least at some fundamental level, that the TMS will function as intended. It is proposed that by predicting the thermodynamic properties of the catalyst ligand, a TMS effective at minimizing catalyst loss can be designed from the ground up. Since thermodynamic and experimental data regarding the solvent effects on the catalyst are limited or non-existent, the *ab initio* COSMO-RS model[171], is used as the basis for thermodynamic predictions. Solvents are to be chosen as TMS components based on catalyst complex solubilities, as represented by the catalyst ligand, and phase equilibrium characteristics. A framework is developed to systematically screen solvents and to generate a list of candidate TMS systems. These potential solvent mixtures are then investigated experimentally in order to validate the model's ability to accurately predict functioning TMS systems. In this way, several identified TMS systems are evaluated in an example reaction to ensure process feasibility.

4.1.3. Background and Motivation

4.1.3.1. Thermomorphic Solvent Systems

The model reaction considered in this contribution is the hydroformylation of 1-dodecene, a reaction that has garnered much attention in recent years. It is desirable to convert the terminal alkene, 1-dodecene, with synthesis gas (CO, H_2) to the terminal aldehyde tridecanal. However, the reaction is not that simple and many side products are also produced. In order to achieve high selectivity and conversion, many different catalyst formulations are investigated by Brunsch[172] who finds that a catalyst based on rhodium (Rh) and 6,6-

[(3,3-di-tert-butyl-5,5-dimethoxy-1,1-biphenyl-2,2-diyl)bis(oxy)]bis(dibenzo[d,f][1,3,2]dioxaphosphepine), (or Biphephos) shown in Figure 4.3, delivers the best performance with respect to conversion, selectivity, and reaction rate. The downside to using this catalyst is the high cost of both Rh and Biphephos. Even low levels of leaching can lead to inordinately high process costs.[173]

The primary method to recover the Rh-Biphephos catalyst complex is by using the previously mentioned thermomorphic solvent system (TMS). These special mixtures are composed of solvents with varying degrees of polarity allowing for simple temperature induced phase switching. In Figure 4.1, the basic principle of the TMS is outlined. At a certain reaction temperature, T1, the mixture of solvents should form a homogeneous phase that allows the reaction to proceed unhindered by mass transfer limiting effects. Once the reaction is complete, the resulting mixture should form two phases upon cooling to the desired separation temperature, T2. Ideally the catalyst is recovered in the polar phase while the product and unconverted reactant are recovered in the non-polar phase. Several TMS compositions are investigated for the hydroformylation of 1-dodecene.[31] One of the better performing systems uses a TMS composed of the polar solvent dimethylformamide and non-polar solvent *n*-decane. These solvents are able to provide good recovery through single-stage phase splitting of the Rh-Biphephos catalyst while still separating out modest amounts of the tridecanal product. Reaction conditions and solvent compositions used with this TMS are investigated in more detail and result in process conditions leading to lower levels of catalyst leaching.[58] A continuous miniplant is also designed[174] and operated[71] using this DMF and *n*-decane TMS in equal weight percentages. Since this TMS system is well analyzed and still the target of current, ongoing research, it will serve as a good benchmark for other TMS systems.

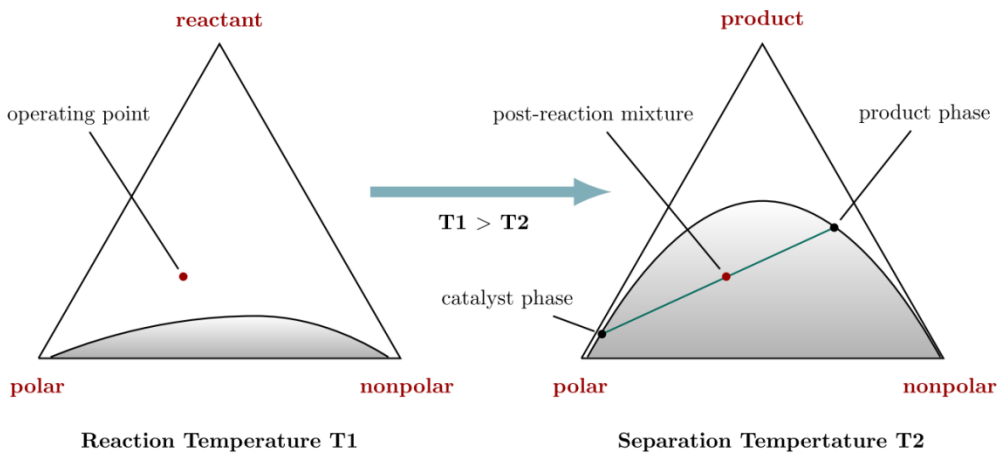

Figure 4.1: TMS functionality.

A TMS of this nature, consisting of only a pair of polar and non-polar solvents, was labeled as a Type III TMS.[31] In the present contribution, a method is proposed to identify an optimal Type III TMS system, exemplified on the hydroformylation of 1-dodecene. The goal is to find two solvents that produce the appropriate TMS characteristics: a polar, catalyst solvent in which the ligand Biphephos has a high affinity and a non-polar, product solvent in which catalyst solubility is low and product solubility is high. Proper miscibility at the operating point (homogeneous) and post-reaction mixture (heterogeneous) are also required.

4.1.3.2. Thermodynamic Model: COSMO-RS

The primary method of solvent screening will be to estimate the solubility of the Biphephos ligand in various candidate solvents. Many methods exist for predicting thermodynamic properties of a molecule for which experimental data is lacking, UNIFAC for example[175], but due to the complexity and size of Biphephos, many of these methods are unsuitable for the proposed purpose. For this reason, thermodynamic properties of the catalyst ligand in solution are predicted using the COSMO-RS method[171] as implemented in the commercial software package COSMOtherm.[176] All calculations are made using the BP TZVP C30,1401 parameterization. The Conductor-like Screening Model for Real Solvents (COSMO-RS) is a method for predicting thermodynamic properties based on interacting molecular surfaces of pure component liquids or liquid mixtures. Each desired molecule is modeled in a perfect conductor in order to define the screening charge of the molecule. This is done using the efficient continuum solvation model COSMO.[177] In the “Real Solvent” extension, the three dimensional surface information is condensed into a histogram, the σ-profile, detailing the amount of surface segment type within a certain polarity interval. COSMO-RS then combines the σ-profile data with a statistical thermodynamics approach where the chemical potentials of pair-wise interactions of surface segments are calculated using important molecular interactions such as electrostatic misfit and hydrogen bonding energies. Therefore, only the energetically optimized molecular structure of each molecule is necessary to make predictions of phase behavior or solubility.

The alluring feature of using COSMO-RS for solvent screening is the absence of required experimental data. Many papers in the literature, such as those by Tung et al.[178] Hahnenkamp et al.[179] and Pozarska et al.[180] detail the use of COSMO-RS theory in predicting solubilities of pharmaceuticals as part of a priori solvent screening. Bouillot et al.[181] compare several thermodynamic models including COSMO-RS on their ability to predict pharmaceutical solubilities. Another important article written relative to this topic is by Wichmann and Klamt[182], who give a detailed description of the COSMO-RS method as

used in solvent screening. The conclusion in these articles is that COSMO-RS can qualitatively predict the solubility of large and complex molecules in various solvents. Therefore, the application of this method appears to be suitable for the task of qualitatively predicting catalyst ligand solubility in various solvents uniquely applied to TMS design.

4.1.4. Framework

The procedure used to screen for component solvents in the Type III TMS is outlined in Figure 4.2. The framework consists of two major components: the computational solvent screening of TMS systems and the empirical investigation of candidate solvent mixtures. In the solvent screening section several steps are presented in order to come to feasible TMS compositions. The first step is to generate the COSMO file of the catalyst ligand. The next step is concerned with simple pre-screening of molecules included in a database to reduce the search space. Remaining steps are primarily concerned with the solvent behaviors related to predicted solubility of Biphephos in each solvent, product recovery, miscibility, and feasibility of use. After the solvent screening procedure is concluded, promising solvents are then experimentally validated in part two of the framework. Here predictions made about partition coefficients based on catalyst ligand solubilities are investigated as well as performing the hydroformylation of 1-dodecene in each chosen mixture. Each step is explained in more detail in the following sections.

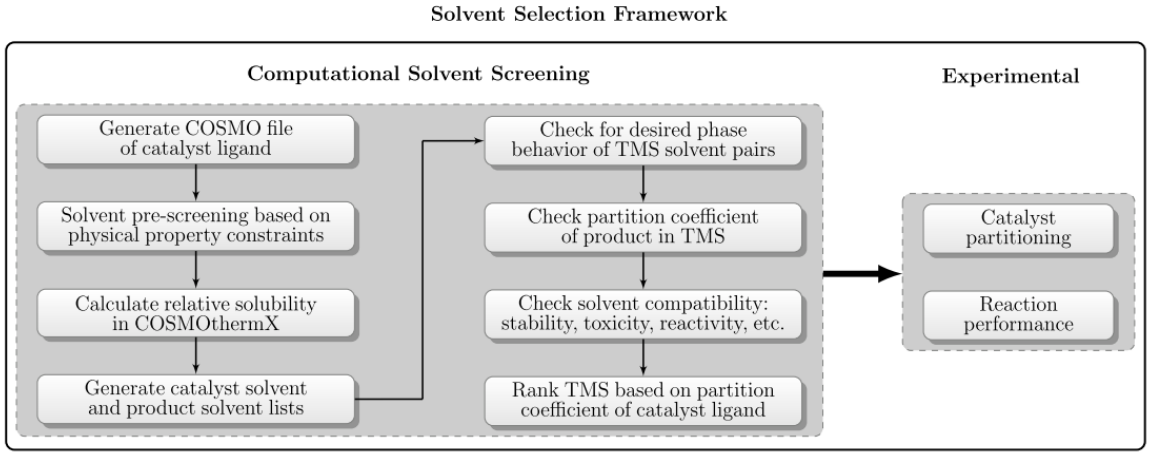

Figure 4.2: Procedure for TMS design.

4.1.4.1. Generate COSMO File of Catalyst Ligand

The first task is to create the COSMO file of the catalyst ligand used in the process. In this case the catalyst is the Biphephos ligand used as part of the catalyst complex for the hydroformylation of 1-dodecene. In this screening work only the catalyst ligand is considered

due to its usually higher concentration in the solution and the fact that catalyst leaching has shown similarities in Rh and phosphorous leaching[172]. The molecular model is developed using TURBOMOLE[183], at the RI-DFT level of theory[184] using the def-TZVP basis set.[185] The resulting Biphephos structure with surface charge is presented in Figure 4.3. This COSMO file contains all required information needed for predicting the thermodynamic properties of Biphephos for solvent screening using COSMOtherm. At a glance, it is possible to obtain much information about a molecule just by observing its σ-profile, seen in Figure 4.4 for Biphephos. Here one can see an expected and large non-polar region locate between−0.01 and 0.01 e/Å, which are usually the accepted boundaries for the hydrogen bonding region[186], outside of which strong hydrogen bonds can be formed. Non-polar molecules usually do not depict such a wide profile as Biphephos. This is due to the negative p-orbitals and positive carbons of the phenyl groups giving two distinct peaks instead of one, typical for aromatic containing compounds. The small shoulder extending from 0.01 to about 0.015 e/ Å corresponds to the negative charge of the oxygen and phosphorous atoms suggesting that the catalyst may prefer to be in solution with solvents showing some type of hydrogen bond donor characteristic. From this it is expected that Biphephos will show a higher affinity for polar solvents and those having broad profiles between the hydrogen bonding borders to non-polar ones.

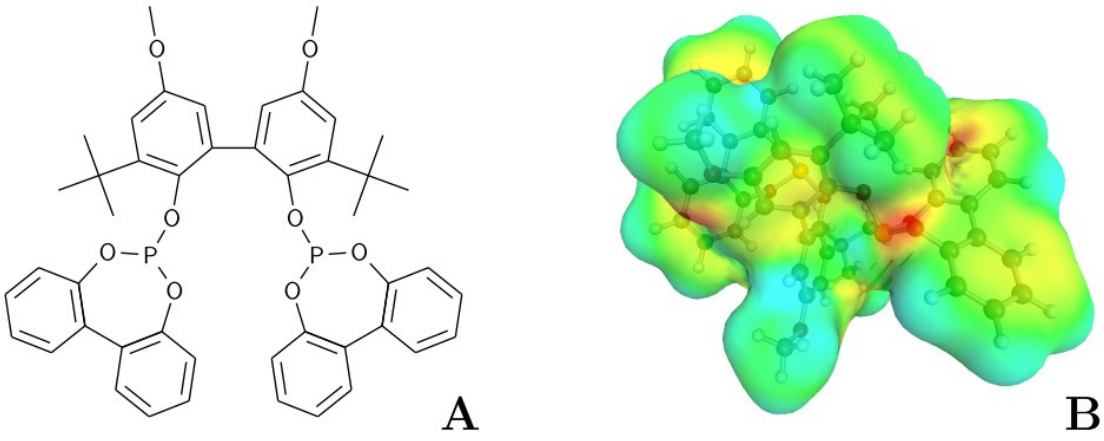

Figure 4.3: Chemical structure formula of Biphephos (A) and its surface charge in a perfect conductor (B) as calculated using TURBOMOLE.

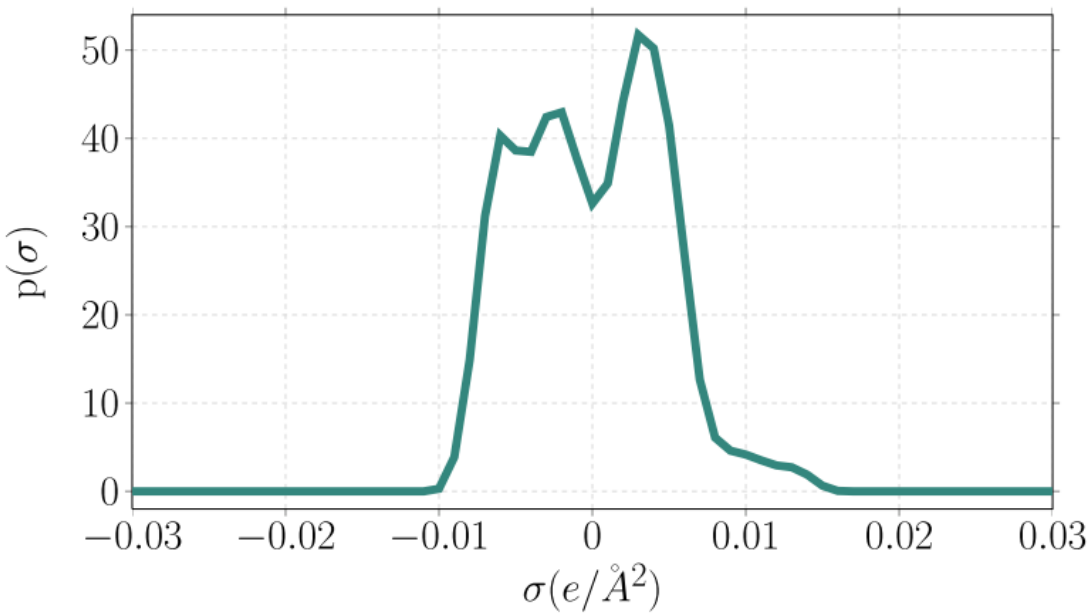

Figure 4.4: Sigma profile of the Biphephos ligand.

4.1.4.2. Pre-Screening of Candidate Solvents

Initially, a list of candidate solvents from the COSMObase (ver.1301, COSMOlogic GmbH) extension has to be generated. To reduce the number of unsuitable molecules from the initial search space, about 7700 in total, certain molecular properties, such as molecular weight, melting temperature, boiling temperature, screening charge, and component atoms, can be used as constraints to prescreen solvent candidates. To intentionally maintain a large search space, only boiling temperature and molecular weight are used as initial constraints. The boiling temperature of each solvent is limited to temperatures between zero and 260 °C. The upper bound is chosen to be 20 °C less than the boiling point of tridecanal in order to avoid possible azeotrope formation in a subsequent distillation unit operation. The molecular weight of each solvent chosen should also not exceed 200 g/mol, as solvents are usually preferably small owing to better solvent functionality. Using these two constraints, the solvent search space is reduced to a list containing 2813 molecules.

4.1.4.3. Solvent Screening: Catalyst Solubility

The next step, and perhaps the most important step, is to predict the relative solubility of Biphephos in each of the candidate solvents. Relative solubility is predicted using only the chemical potential, μ_i^{solvent} of the solute at infinite dilution in the pure solvent. This chemical potential is calculated by COSMO-RS (Eq.(1)) based on statistical thermodynamics using sigma profiles of the involved components (a good reference for how COSMO-RS

calculates potentials is found in [186]). Relative solubilities are calculated in a single batch, which is necessary to allow for direct comparison of different solvents. Once all calculations are complete, the solvents are ranked according to their relative solubilities starting with a maximum value of 0 (referring to maximum solubility) and decreasing therefrom. All relative solubility calculations were made using a temperature of 25 °C.

$$\ln(x_i) = \mu_i^{solvent}/RT \quad (1)$$

4.1.4.4. Solvent Screening: Generation of Two Lists

From this list of ordered solubilities, two new lists are created: one with solvents having high relative solubility of the catalyst ligand (HRSC) and the other with solvents having low relative solubility of the catalyst ligand (LRSC). For each TMS system, two solvents will be used in order to create the desired Type III system. One solvent from the HRSC list will be chosen as the catalyst solvent and one solvent from the LRSC list will be used to recover the product. For example, those solvents predicted as having the highest solubility are presented alongside those having the lowest predicted solubility in Table 4.1. As seen in this list, hydrofluoric acid is predicted as having the highest solubility for Biphephos while water is predicted to have the lowest solubility, being about 18 orders of magnitude less than that of hydrofluoric acid. Interestingly enough, the current HRSC solvent, DMF, used in miniplant experiments, is found to be the solvent with the 24th highest solubility of the catalyst ligand.

Table 4.1: List of top 5 high (HRSC) and low (LRSC) relative solubility catalyst solvents.

HRSC	$\log_{10}(x_i)$	LRSC	$\log_{10}(x_i)$
Hydrofluoric acid	0.0000	H_2O	−18.4128
Selenic acid	−1.0582	Formamide	−12.7388
Chlorosulfonic acid	−1.2406	Hydroxyacetonitrile	−12.2432
ClO_2	−2.6015	Butanedinitrile	−12.1521
1,1,1-Trifluoro-2-bromoethane	−3.0996	Dicyanomethane	−11.6746

It should be quite obvious that not all candidate solvents shown in Table 4.1 are convenient for a multitude of reasons. All of the HRSC solvents listed here are highly reactive acids, strong oxidizers, or CFCs. Those solvents in the LRSC list are also quite unreasonable, with the exception of water, due to their reactivity or toxicity. As it turns out, water is a poor solvent for other reasons, especially due to its also very low solubility of the tridecanal product, something handled later. Obviously it is undesirable to manually screen each one of the almost 3000 solvents based on reactivity, toxicity, or by some other property at this stage. There are various methods of deciding the environmental, health, and

safety aspects of solvents, such as the method developed by Koller et al..[187] However, due to the limited availability of information for many of the solvents in this list and the small size of the EHS tool database[188],it was not suitable for this task. Therefore, selection and exclusion of solvents is based on heuristics, relying more on expertise and process knowledge. This screening step, as seen in Figure 4.2, comes near the end of the process when a much smaller number of candidate solvents remain, greatly reducing the workload of this manual task. It is for this reason that a sizable number of candidate solvents needs to be selected for both the HRSC and LRSC lists. For the HRSC list an arbitrary number of solvents, 100, is chosen. These 100 solvents are those solvents having the highest relative solubility for the catalyst ligand. Due to the availability of some experimental data comparing the chain length of linear alkanes paired with DMF as TMS systems and the amount of catalyst leaching encountered, it was desirable to include several of these alkanes into the screening process.[172] Therefore, octane is chosen as the cut-off point for the LRSC list instead of an arbitrary number as with the HRSC solvents. These solvents, 403 in total, are those solvents having the lowest solubility for the catalyst and are added to the LRSC list.

4.1.4.5. Miscibility Gap Formation

The basis of a functioning TMS is that after the reaction, two phases are formed separating the polar, catalyst containing phase from the less polar, product containing one. This means that for each TMS system, some estimation of miscibility gap formation must be made. Using COSMO-RS once again, liquid–liquid equilibrium calculations are made for each possible pair of solvents from the HRSC and LRSC lists, 40,300 in total. The separation temperature for each calculation was set to −25 °C. This temperature is selected for two reasons: the lower bound for planned experimental validation is about this temperature and that predictive methods for thermodynamic equilibrium are not always accurate. Unreliable phase equilibrium predictions may lead to potentially interesting TMS systems being eliminated during screening due to faulty miscibility predictions made at ambient conditions. Therefore, to avoid these issues and bring predictions more in line with our experimental limits, the lower temperature is used. Solvent mixtures that are found to be feasible at lower temperatures can be investigated at higher separation temperatures at a later time as part of the final process design. In other words, a larger screening net is formed to ensure that TMS systems are not excluded due to poor LLE predictions. The screening criteria are based on simple miscibility gap formation for the same reason. Using this simple constraint, only 5225 potential TMS compositions remain.

4.1.4.6. Product Distribution

The secondary function of TMS usage is the separation of the product from the mixture in the less polar phase. Therefore it is also of interest to check whether or not the TMS systems can remove the tridecanal product from the post-reaction mixture. Remember although water is a great LRSC solvent in that its solubility of the catalyst is low, this is a feature also extended to the slightly polar tridecanal. Using water would lead to practically all of the product being recycled back into the reactor making a functioning process unfeasible. In order to avoid such TMS systems from being included in the list, some measure of product removal ability must be included in the screening process. This is done in a similar way as with Biphephos, but because the screening process now involves binary solvent systems, partition coefficients as predicted by Eq. (2) were used to predict tridecanal distribution. For tridecanal partition coefficients, the volume quotient of the solvents as estimated using the liquid density/volume QSPR method from COSMOtherm is included. The cut-off value is arbitrarily chosen based roughly on doubling the predicted partition coefficient of tridecanal between DMF and decane, which is found to be 0.118. This ensures that the TMS should have similar tridecanal separation as the current TMS while excluding those mixtures with much poorer tridecanal separation. Therefore, the partition coefficient of each TMS is restricted to being less than 0.25 (lower is better), leaving 928 potential solvent pairs.

$$\log_{10}(P_j^{(2,1)}) = \log_{10}(\exp((\mu_j^{(1)} - \mu_j^{(2)})/RT) \cdot V_1/V_2) \quad (2)$$

Here, $\mu_j^{(i)}$ is the chemical potential of species j at infinite dilution in species i, where j stands for the reaction product tridecanal, 1 for the HRSC solvent, 2 for the LRSC solvent, and V for the estimated solvent volume.

4.1.4.7. Suitable Solvent Solutions

The top 30 TMS systems up until now are shown in Table 4.2. TMS systems are ranked according to Biphephos recovery as measured using the partition coefficients as explained in Section 4.1.4.8. The majority of HRSC solvents in this list are small halogen containing alkanes, primarily bromine and iodine. They are usually paired with large alcohols or other multi-functional group containing compounds as the LRSC solvent. Some of these solvents are infeasible based on melting temperature, for example resorcinol melts at 111 °C while others seem quite suitable such as cyclohexanemethanol with a fusion point of −43 °C. The interesting thing about these LRSC solvents is that they have polar characteristics unlike the non-polar solvents expected for product recovery. However, there are several problems with these TMS compositions in addition to phase characteris-

tics. For example, the top two performing HRSC solvents iodomethane and bromomethane are both well known pesticides and, additionally, bromomethane is known to damage the ozone layer and was phased out completely in 2005 according to the Montreal Protocol and the Clean Air Act.[189] Thus it is recommended here to eliminate individual solvents for these and the various reasons mentioned below.

Table 4.2: Unfiltered list of top 30 TMS mixtures.

Rank	HRSC	LRSC	$\log_{10}(P_{tridecanal})$	$\log_{10}(P_{Biphephos})$
1	Iodomethane	Propanal,2-(hydroxyimino)-,oxime	0.1460	3.6040
2	Bromomethane	Propanal,2-(hydroxyimino)-,oxime	−0.0749	3.4292
3	Iodoethane	Propanal,2-(hydroxyimino)-,oxime	0.2419	3.3888
4	Bromoethane	Propanal,2-(hydroxyimino)-,oxime	0.1770	3.3865
5	1-Bromo-1,2-difluoroethylene	Choralhydrate	−0.0339	3.2778
6	Ethylisocyanate	Propanal,2-(hydroxyimino)-,oxime	0.1255	3.2460
7	Iodoethene	Propanal,2-(hydroxyimino)-,oxime	0.0737	3.2343
8	Iodomethane	Resorcinol	0.1454	3.2080
9	Bromomethane	Resorcinol	−0.0754	3.0331
10	Iodoethane	Resorcinol	0.2413	2.9928
11	1-Bromo-1,2-difluoroethylene	4-Methyl-1,3-benzenediol	0.1482	2.9927
12	Bromoethane	Resorcinol	0.1765	2.9905
13	Iodomethane	Methylhydroquinone	0.0589	2.9670
14	1-Bromo-1,2-difluoroethylene	Difluoroacetic acid	−0.2472	2.9523
15	Bromomethane	2,2,2-Trifluoroethanol	−0.0589	2.9509
16	Bromomethane	Pentafluoro-1-propanol	−0.1543	2.9265
17	3-Bromo-3,3-difluoro-1-propene	Pentafluoro-1-propanol	0.2062	2.9130
18	Bromoethane	2,2,2-Trifluoroethanol	0.1930	2.9082
19	Ethyleneoxide	Hexahydroindene	0.2220	2.8928
20	Bromoethane	Pentafluoro-1-propanol	0.0976	2.8838
21	Iodomethane	Orcinol	−0.0620	2.8765
22	Iodoethene	Resorcinol	0.0731	2.8383
23	Acetaldehyde	Tetradecane	0.2308	2.8324
24	Sulfurylchlorideisocyanate	Orcinol	0.2445	2.8260
25	Iodomethane	Cyclohexanemethanol	0.1229	2.8076
26	Acetaldehyde	Tridecane	0.2060	2.8038
27	Acetaldehyde	1-Tridecanol	0.1235	2.7985
28	Bromomethane	Methylhydroquinone	−0.1620	2.7922
29	Acetaldehyde	Dodecanol	0.1046	2.7905
30	2-Butyne	Methylhydroquinone	0.2250	2.7898

Solvents are individually screened here based on several aspects:

1. Species containing halogens

2. Highly reactive species that are considered too unstable

3. Solvents with carbon–carbon double or triple bonds likely to react in the hydroformylation

4. Extremely toxic species not eliminated according to the above criteria

Since there are far fewer unique HRSC solvents left in the binary solvent mixtures, 33 as compared to 158 LRSC solvents, this screening step starts with HRSC solvent elimination. In all, 13 solvents are removed for containing halogens, seven for having a carbon–carbon double or triple bond, and five for either being highly reactive, toxic, or both. This process is then repeated for the LRSC solvents remaining in the reduced number of potential TMS systems with the short list of HRSC solvents. In all, eight solvents remain in this HRSC list: acetaldehyde, DMF, acetone, *N,N*-dimethylacetamide, *N*-methyl-2-pyrrolidone, methylacetate, *N,N*-diethylformamide, and *N*-formylpiperidine (see Table 4.4). Some of these chemicals are still toxic, such as DMF, and require care in handling and exposure, but are commonly used as solvents in industry and can be used in the laborato-

ry without exceptional safety measures. Considering only those systems using one of these eight HRSC solvents, 324 TMS pairs remain. This elimination of various HRSC solvents also reduces the list of LRSC solvents to 65 possibilities in the remaining systems. Of these, 62 are branched, linear, or cyclic alkanes. The three remaining solvents not belonging to this group are dodecanol, tridecanol, and hexahydroindene. Only hexahydroindene is removed here due to its inclusion of a carbon–carbon double bond. With the removal of this solvent, five TMS pairs are eliminated and 319 TMS pairs remain.

For some LRSC solvents, 21 in total, the melting temperature is unknown; however, these solvents are all C 9 or C 10 alkanes which generally have melting temperatures much lower than investigated here and are thus retained. Several remaining LRSC solvents have melting temperatures higher than −25 °C. These include tridecanol, dodecanol, tetradecane, tridecane, dodecane, bicyclohexyl, 2,2,5,5-tetramethylhexane, and cyclodecane. The Liquid–Liquid Equilibrium (LLE) of each TMS system consisting of one of these solvents is calculated again in the same manner as outlined in Section 4.1.4.5, but the minimum temperature used before is substituted with the melting temperature of the LRSC instead. Only 25 TMS pairs consist of one of these solvents. In eight of these systems no miscibility gap is predicted, leaving 311 solvent pairs in our final list of potential TMS systems. It is evident from these results that boiling point limits are not enough in the pre-screening step and it may be desirable to initially add a melting temperature constraint. It is also interesting to check the phase behavior at a reaction temperature of 100 °C, considering this is an often used reaction temperature for the present reaction system.[39] Here, five TMS systems are predicted to form heterogeneous mixtures: DMF with dodecane, tridecane, and tetradecane, and acetaldehyde with tridecane and tetradecane. At a slightly higher maximum of 120 °C, all TMS systems were homogeneous. Due to these systems all having upper critical solution temperatures below 120 °C, they were considered acceptable for further evaluation. These temperatures are still well within the feasible reaction temperature range.

4.1.4.8. Analysis

The final 311 TMS systems are now ranked according to the partition coefficients of Biphephos between the HRSC and LRSC solvents respectively. In this case partition coefficients are calculated using Eq. (3) , with j representing Biphephos. The volume quotient of the solvents is not considered here to ensure consistency with the relative solubility calculations made in the second screening step. When the solvent volume is not considered in Eq. (2), the equation reduces to Eq. (3) which is simply the ratio of the relative solubilities calculated from Eq. (1).

$$\log_{10}(P_j^{(2,1)}) = \log_{10}(\exp((\mu_j^{(1)} - \mu_j^{(2)})/RT)) = \log_{10}(x_j^{(1)}/x_j^{(2)}) \quad (3)$$

Using the partitioning of Biphephos between the two phases should provide a good measure of which systems are best suited for use as a TMS respective to catalyst recovery. Since product partitioning is constrained within a certain performance criteria, each of the remaining solvent systems should feasibly function as a Type III TMS for the hydroformylation of 1-dodecene. The results are presented in the next section.

4.1.5. Screening Results

The top 30 TMS (from the 311 total) systems based on catalyst partition coefficients are presented in Table 4.3. TMS systems composed of catalyst solvents acetaldehyde or DMF paired with product solvents consisting of large alkanes seem to provide good catalyst recovery with functioning product separation. With increasing alkane size, catalyst recovery capacity increases due to the increasing size of the non-polar segments of the product solvents, reducing the amount of catalyst soluble in the non-polar phase. For the same reason, tridecanal partition coefficients also increase, showing reduced solubility of the product in the product phase. This is due to the carbonyl group of the aldehyde providing some polar characteristics and possibilities for hydrogen bonding to the otherwise dominant apolar hydrocarbon backbone. Thus, a trade-off between catalyst recovery and the efficiency of product separation exists when developing a TMS for this reaction.

Table 4.3: List of top 30 TMS mixtures

Rank	HRSC	LRSC	$\log_{10}(P_{tridecanal})$	$\log_{10}(P_{Biphephos})$
1	Acetaldehyde	Tetradecane	0.2308	2.8324
2	Acetaldehyde	Tridecane	0.2060	2.8038
3	Acetaldehyde	Dodecane	0.1750	2.7655
4	Acetaldehyde	Bicyclohexyl	0.0663	2.7507
5	Dimethylformamide	Tetradecane	0.2427	2.7245
6	Acetaldehyde	*n*-Undecane	0.1445	2.7231
7	Acetaldehyde	*n*-Hexylcyclopentane	0.0953	2.7151
8	Acetaldehyde	2-Methyldecane	0.1423	2.7099
9	Acetaldehyde	Pentylcyclohexane	0.0896	2.6978
10	Dimethylformamide	Tridecane	0.2180	2.6959
11	Acetaldehyde	4-Methyldecane	0.1415	2.6850
12	Acetaldehyde	Pentylcyclopentane	0.0522	2.6754
13	Acetaldehyde	*n*-Decane	0.1061	2.6713
14	Acetaldehyde	2-Methyl-nonane	0.1047	2.6643
15	Dimethylformamide	Dodecane	0.1870	2.6577
16	Acetaldehyde	1-Isopropyl-4-methylcyclohexane	0.0360	2.6495
17	Acetaldehyde	*trans*-Decalin	−0.0164	2.6443
18	Dimethylformamide	Bicyclohexyl	0.0783	2.6428
19	Acetone	Bicyclohexyl	0.2485	2.6421
20	Acetaldehyde	2,3-Dimethyloctane	0.0989	2.6407
21	Acetaldehyde	Butylcyclohexane	0.0437	2.6380
22	N,N-Dimethylacetamide	Bicyclohexyl	0.1786	2.6365
23	Acetaldehyde	2,7-Dimethyloctane	0.0997	2.6339
24	Acetaldehyde	2,2-Dimethyloctane	0.0866	2.6334
25	Acetaldehyde	3-Methyl-nonane	0.1041	2.6306
26	Acetaldehyde	4-Methyl-nonane	0.1043	2.6277
27	Acetaldehyde	1-Methyl-3-propylcyclohexane	0.0412	2.6247
28	Acetaldehyde	5-Methyl-nonane	0.1036	2.6218
29	Acetaldehyde	1-Methyl-2-propylcyclohexane	0.0391	2.6218
30	Acetaldehyde	2,2,4,6,6-Pentamethylheptane	0.1305	2.6202

Since all LRSC solvents are large alkanes, a general comparison of HRSC performance can be made when fixing the LRSC to a single solvent. Due to its extensive use in ongoing research with respect to this reaction, the availability of some experimental data, and it

being the benchmark product solvent, *n*-decane is chosen for this task. Results for TMS systems using each one of the remaining HRSC solvents paired with *n*-decane are given in Table 4.4. Acetaldehyde, as expected, is predicted as forming the most promising TMS, due to its increased solubility of the catalyst ligand over DMF and other HRSC solvents. An explanation, based on COSMO-RS analysis, is that a slight increase in excess entropy is observed when using acetaldehyde instead of DMF in a mixture of the solvent and Biphephos. Both solvents are, however, predicted to form approximately ideal solutions with Biphephos. Also noticeable is the difference in tridecanal solubility that arises from solvents having similar catalyst solubilities. DMF and acetone, for example, have similar heats of mixing with tridecanal, but acetone forms a mixture with lower excess entropy than when using DMF leading to a slightly more favourable solution, reducing the ability of the TMS to separate the product. It can also be seen that TMS systems of acetone/decane and *N*-methyl-2-pyrrolidone/decane would have been screened out of the possible TMS systems due to their relatively large tridecanal partition coefficients (>0.25).

Table 4.4: List of high relative solubility solvents and decane TMS candidates

HRSC	LRSC	$\log_{10}(P_{tridecanal})$	$\log_{10}(P_{Biphephos})$
Acetaldehyde	*n*-Decane	0.1061	2.6713
Dimethylformamide	*n*-Decane	0.1180	2.5635
Acetone	*n*-Decane	0.2882	2.5627
N,N-Dimethylacetamide	*n*-Decane	0.2184	2.5572
N-Methyl-2-pyrrolidone	*n*-Decane	0.3017	2.5193
Methyl acetate	*n*-Decane	0.1777	2.2222
N,N-diethylformamide	*n*-Decane	0.1880	2.2166
N-Formylpiperidine	*n*-Decane	0.2487	2.1614

Table 4.5: Comparison of TMS composed of DMF and linear alkanes

HRSC	LRSC	$\log_{10}(P_{tridecanal})$	$\log_{10}(P_{Biphephos})$
Dimethylformamide	*n*-Octane	0.0267	2.4158
Dimethylformamide	*n*-Nonane	0.0759	2.4982
Dimethylformamide	*n*-Decane	0.1180	2.5635
Dimethylformamide	*n*-Undecane	0.1565	2.6152
Dimethylformamide	*n*-Dodecane	0.1870	2.6577
Dimethylformamide	*n*-Tridecane	0.2180	2.6959
Dimethylformamide	*n*-Tetradecane	0.2427	2.7245

As mentioned previously, it is desirable to compare TMS performance with DMF and several linear alkanes. In this case *n*-octane to *n*-tetradecane are used and this is the reason for choosing a larger set of LRSC solvents. Each of these systems is evaluated and listed

in Table 4.5. As expected, the solubility of the catalyst and that of tridecanal in the product phase worsen as the length of the alkane chain increases. This is most likely due to the predicted increase in the heat of mixing caused by the increasing non-polarity of the system. The change in excess entropy is small from mixture to mixture, as the molecular order is not drastically influenced by more of the same non-polar interactions. These results are in qualitative agreement with the experiments conducted by Brunsch[172], where similar trends are observed. This more clearly shows the trade-off between catalyst recovery and product separation performance characteristics of the TMS.

4.1.6. Experimental Validation

The experimental validation of this computationally based solvent selection procedure can be considered a requirement due to the inaccuracies inherent in any predictive model or method. In this section, results from solvent screening are empirically investigated. This is a two-step process that begins with Biphephos ligand being added to binary solvent mixtures where the amount of Biphephos in the product phase is measured. The second step is then to take each of the TMS systems and perform the hydroformylation of 1-dodecene in them. This allows for evaluation of the influence of the reactants and products on the phase behavior as well as the effect of solvent selection on reaction performance. Since the screening results reveal that large alkanes should be used as LRSC solvents, it is preferable to again fix the LRSC solvent to *n*-decane, as is done previously in the screening result comparisons. The reasoning behind this is that the LRSC solvents are all large alkanes and that the trend accompanied by using different sized alkanes is already confirmed experimentally.[172] This makes the selection of the LRSC much less important than the HRSC, where the different structures and functional groups have a stronger effect on physical properties such as boiling temperature and phase characteristics. In this regard, the systems investigated experimentally are chosen from those mixtures listed in Table 4.4. Of these potential TMS mixtures, six are eventually evaluated. Acetaldehyde is not empirically considered due to its low boiling temperature of 20 °C, making experimental validation and analysis difficult. Also, no experimental analysis of *N*-formylpiperidine is conducted as it only appeared in one TMS system. This *N*-formylpiperidine-system suffers from its much higher solubility in alkanes than DMF, for which it is often used as a replacement solvent.

4.1.6.1. Experimental Methods

All phase partitioning and hydroformylation experiments are carried out under an argon atmosphere using standard Schlenk techniques. Chemicals are commercially available

and used without further purification. Each phase partitioning experiment is conducted using a binary mixture of each TMS system with a 1:1 ratio of polar (15 g) and the non-polar (15 g) solvent *n*-decane being added to a double-walled 100 mL separating funnel. An amount of Biphephos proportional to the amount used in the reactions is added (116.9 mg, 0.149 mmol) and thoroughly mixed before being cooled to a temperature of −20 °C. After 20 min, the phases are separated. Samples for Inductively Coupled Plasma Optical Emission Spectrometry (ICP-OES) measurements are prepared using 0.230 g of the non-polar phase weighted into a Teflon cup. To this, 2.5 mL of nitric acid (65%) and 4 mL of sulfuric acid (96%) are added and digestion is conducted in a Micro mPrep A microwave (MWS GmbH, Switzerland). Subsequently 2 mL of distilled water and 1 mL of hydrogen peroxide solution (30–32%, optima grade, Fisher Chemical) are added. Finally, ICP the samples are analyzed with an IRIS Intrepid optical emission spectrometer (Thermo Fisher Scientific GmbH) and the phosphorous content determined.

The hydroformylation experiments follow a similar process with the addition of the reaction step. In a typical reaction setup, the catalyst precursor $Rh(CO)_2acac$ (3.8 mg, 0.0149 mmol) and the ligand Biphephos (58.4 mg, 0.0745 mmol) are weighed in a 40 mL steel autoclave. The autoclave is evaporated and flushed with argon three times. The polar solvent (6.25 g), *n*-decane (6.25 g), and 1-dodecene (2.5 g, 14.9 mmol) are then transferred into the autoclave also under an argon atmosphere. Afterwards, the reactor is pressurized to 20 bar using a mixture of CO/H_2 (1:1) and heated to 100 °C. The stirrer is adjusted to 600 rpm. After 90 min the reaction is stopped by cooling the reactor with ice. After depressurization through removal of the remaining synthesis gas, the reaction mixture is cooled down to −20 °C in a double-walled 100 mL separating funnel. The temperature is controlled by a cooling circulation thermostat (HAAKE K40, Thermo Electron Corporation HAAKE DC50, internal temperature regulation) using ethylene glycol/water (1:1) as cooling medium. The mixture is allowed to settle at this temperature for 20 min before both phases are separated and analyzed using gas chromatography and ICP-OES. For quantitative analysis of the reaction mixture an Agilent Technologies 6890N Network gas chromatograph equipped with an HP-5 column (30 m × 0.320 mm × 0.25 mm film thickness, Agilent J&W GC Columns) and an FI-Detector is used. Leaching values of Rh and phosphorus in the product phase are measured using an IRIS Intrepid ICP-OES spectrometer (Thermo Fisher Scientific GmbH). The identification of the products is carried out by NMR spectroscopy (Bruker model DPX 500) and using a GC–MS (Agilent Technologies 5977A MSD, 70 eV). The same procedure for preparing analysis samples is used here as is used in the phase separation experiments.

4.1.6.2. Phase Partitioning

In each of the six TMS systems examined, two phases are observed at the separation temperature of −20 °C except for the TMS comprised of methyl acetate and *n*-decane. This is unfortunate as methyl acetate is predicted as having a miscibility gap with decane in a binary mixture. This result is similar to the ternary LLE experiments and model comparisons conducted[190], where the ternary LLE of the system methyl acetate, methanol, and *n*-decane is investigated at temperatures from 5 °C to 35 °C. They show that several of the predictive group contribution models used to estimate the phase behaviour predict miscibility gap formation for the binary system methyl acetate and *n*-decane when in fact all experiments show the opposite. This seems to be the case with COSMO-RS as well and may be caused by an over representation of the polar character of the sp^2 oxygen of the otherwise weakly polar methyl acetate. In fact the σ-profile of methyl acetate is quite similar to the more polar acetone, owing to its own similar carbonyl group. Therefore, the careful approach to miscibility gap formation chosen in the solvent screening step is insufficient in only identifying those systems with proper TMS characteristics. Another aspect is that with the increased predicted polarity of methyl acetate, the relative solubility of Biphephos is most likely exaggerated. It may be possible that by using other mixtures of methyl acetate and *n*-decane instead of the 1:1 mass ratio used here would lead to phase separation. This is, however, not investigated in this work and would not eliminate the possible exaggeration in the catalyst solubility prediction.

The amount of Biphephos recovered in each phase is determined from the amount of phosphorous in each phase, seen in Table 4.6 as the distribution of phosphorous, D_P. For example, in the mixture of DMF and *n*-decane, 99% of Biphephos is found in the catalyst phase and 1% is lost in the product phase. All solvents forming two phases had approximately one percent leaching levels outside of acetone which had approximately three percent leaching. Results indicate that COSMO-RS can, in this case, provide good predictions of Biphephos partitioning for those systems actually forming biphasic systems based on the very low leaching of the catalyst in each HRSC solvent. It must be noted, however, that many of the results for catalyst leaching are near the lower limit of detectability of the ICP-OES resolution which make it difficult to exactly define the performance of each solvent system. This makes a qualitative analysis and comparison with the results produced in COSMO-RS somewhat problematic. However, the predicted partition coefficients were very similar and most likely within the expected error.

Table 4.6: Phase Partitioning with Biphephos

HRSC	LRSC	D_{HRSC}	D_{dec}	D_P
Dimethylformamide	*n*-Decane	2/98	94/6	1/99
Acetone	*n*-Decane	10/90	75/25	3/97
N,N-Dimethylacetamide	*n*-Decane	5/95	91/9	1/99
N-Methyl-2-pyrrolidone	*n*-Decane	1/99	93/7	1/99
Methyl acetate	*n*-Decane	/	/	/
N,N-diethylformamide	*n*-Decane	4/96	82/18	1/99

4.1.6.3. Hydroformylation in Each TMS

The final aspect of solvent screening for the hydroformylation of 1-dodecene is to see whether or not the screened TMS systems can facilitate the reaction and provide the desired phase separation with adequate catalyst recovery. For each of the systems that showed some type of phase separation, a reaction based on the procedure outlined in [39] is developed. It is also important to notice that tridecanal is a miscibility enhancer and that the degree of separation between the two phases is expected to worsen with its accumulation in the system. Also, solvent effects on the reaction in regard to conversion and selectivity need to be evaluated, something the screening method does not take into account. This may be related to several aspects such as the solubility of the synthesis gas components carbon monoxide and hydrogen in each TMS, which has strong effects on the active state of the catalyst.[170] This in turn influences the reaction performance and shows that it can be directly influenced by the solvent composition. Also worth mentioning is that the reaction performance also depends on the coordination effects of each solvent with the catalyst complex, something not considered in this screening process.

Results from the reaction experiments are shown in Table 4.7. Most noticeable among the results is that almost all TMS systems lead to similar levels of conversion of 1-dodecene and selectivity for the linear tridecanal. The variation in the n/*iso*-ratio is insignificant and shows that the selectivity of the Biphephos ligand is not significantly affected by the choice of polar solvent. The only exception in reaction performance comes from the yield of tridecanal when using diethylformamide as the HRSC solvent. Here, a substantially lower yield is observed which may be caused by a substantial change in synthesis gas solubility or inhibiting coordination effect when using this solvent.

Table 4.7: Hydroformylation results for each selected TMS system.

	n/iso	Y_{tri}	D_{tri}	D_{dod}	D_{HRSC}	D_{dec}	D_P	D_{Rh}
Dimethylformamide	99/1	80	74/26	94/6	4/96	95/5	1/99	1/99
Acetone	99/1	81	/	/	/	/	/	/
N,N-Dimethylacetamide	98/2	77	68/32	89/11	11/89	90/10	1/99	1/99
N-Methyl-2-pyrrolidone	98/2	79	70/30	91/9	12/88	92/8	1/99	1/99
Methyl acetate	98/2	80	/	/	/	/	/	/
N,N-Diethylformamide	97/3	62	43/57	53/47	28/72	58/42	3/97	5/95

n/iso is the ratio of linear to branched aldehyde product, Y_{tri} is the tridecanal yield, and D_{tri}, D_{dod}, D_{HRSC}, D_{dec}, D_P, and D_{Rh} are the distributions of tridecanal, dodecene, the HRSC solvent, decane, phosphorous, and rhodium between the product and catalyst phases, respectively. All values are given in percents.
Conditions: 0.1 mol% $Rh(CO)_2acac$, 0.5 mol% Biphephos, 14.9 mmol 1-dodecene, 6.25 g polar solvent, 6.25 g decane, T=100 °C, pCO/H_2=20 bar, t=90 min, 600 rpm, yield (Y), ratio of linear and branched hydroformylation products (*n/iso*) and distribution of the solvents, products and substrate are determined by GC-FID, distribution of Biphephos and rhodium is determined by ICP-OES

The miscibility gap formed in each post-reaction mixture is also not as large as in the simple phase separation experiments as seen by the higher distribution of polar solvent between both phases. This is again expected due to the miscibility enhancing effect of the tridecanal product. In the systems using DMF, *N,N*-dimethylacetamide, and *N*-methyl-2-pyrrolidone as the HRSC solvent, the distribution of *n*-decane between the two phases remains almost the same while the distribution of the polar solvent worsens as seen by the increase in polar solvent found in the apolar, product phase. In the case of *N,N*-diethylformamide, the distribution of *n*-decane is much larger than in the phase separation experiment whereas the distribution of *N,N*-diethylformamide, albeit fairly large, changes to a lesser degree. In the case of using acetone as the HRSC, even at a separation temperature of −30 °C, biphasic separation does not occur. The behavior of the unconverted reactant 1-dodecene is unremarkable. The slight polar character of the carbon–carbon double bond in 1-dodecene does not affect its phase behavior strongly as seen in its very similar distribution to *n*-decane. Upon comparison of the predicted tridecanal partition coefficients, no general comparison between the distribution of tridecanal seen here and in the binary mixture predictions can be made. *N,N*-Dimethylacetamide is predicted as having a higher distribution of tridecanal than *N,N*-diethylformamide but performs much better, in fact, almost as well as *N*-methyl-2-pyrrolidone which had the highest tridecanal partition coefficient of all HRSC solvents in Table 4.2. In fact, the TMS with diethylformamide has more tridecanal found in the catalyst phase than in the product phase indicating a much larger partition coefficient than that predicted by COSMO-RS. This could be based on that fact that these partition coefficients do not show much variation and may well be within the average error in predictions for partition coefficients made using COSMO-RS. This suggests that no significant differences in tridecanal affinity can be made therefrom. However, it may be that concentration effects of tridecanal are significant and cannot be effectively predicted using the partition coefficient which assumes a dilute mixture. To compensate, the partition coefficient constraint should be increased to a higher value than

used in this screening example. This would allow more, potentially effective candidate solvents to be considered later in the screening process.

Probably the most interesting aspect of the reaction results are found in the catalyst leaching levels. Very similar levels of catalyst ligand leaching as seen in the phase separation experiments are observed here after the separation of phases in the decanter. This is not only true for the catalyst ligand but for Rh as well. Interestingly enough, even for the poor phase separation of the TMS using *N,N*-diethylformamide and *n*-decane, seemingly low levels of catalyst leaching are observed, being only about five times that of the system DMF and *n*-decane. Catalyst loss is very similar for the systems containing DMF, *N,N*-dimethylacetamide, and *N*-methyl-2-pyrrolidone, each achieving a loss of catalyst of one percent. It can be concluded that the amount of leaching is only roughly comparable to the quality of the distribution of the HRSC solvent between the two phases, showing that LLE behavior does not necessarily correlate to catalyst leaching. Also noticeable is that the leaching levels of Rh and Biphephos are quite similar. Thus the assumption that Rh and Biphephos leaching would be analogous and that predictions of catalyst leaching only require the ligand structure seem to be valid.

In the end, four functioning TMS systems identified using the solvent selection framework presented here are successfully implemented in the hydroformylation of 1-dodecene. It is found the importance of the solvent mixture depends significantly on the polar solvent chosen. Limitations in the screening methods are also evaluated and should be considered when using the method for other homogeneously catalyzed reactions. It is also worth mentioning that the quantum chemical COSMO-RS method employed for thermodynamic predictions is being continuously updated and enhanced. Therefore, screening predictions will continue to improve with time as the theory and methods become more reliable and robust.

4.1.7. Conclusion

A novel method for TMS solvent selection based on quantum chemical COSMO calculations based on reaction specific catalyst recovery is presented. For the hydroformylation of 1-dodecene, it is shown that by selectively screening for solvents based primarily on the Biphephos catalyst ligand solubility and secondarily on product recovery through partition coefficients, functioning TMS systems can be identified. The benefit of using such a model is the absence of experimental data required to make solvent selection decisions at an initial stage of process development.

In addition to the screening framework developed, experimental validation of the catalyst ligand's partitioning between the two solvents is evaluated. This important step in the process allows for the validation of the TMS systems identified in the computational screening framework. Here, it is seen that using thermodynamic models to predict phase equilibrium is still not free of pitfalls. For instance, the inclusion of methyl acetate as a feasible solvent in a TMS with *n*-decane is erroneous; in reality they are completely soluble in one another. Also, predicted partition coefficients between the solvents are found to be inaccurate in predicting which solvent systems would be most affected by tridecanal. These problems illustrate the reason for generating a sizable group of potential TMS systems for experimental validation.

Another aspect that is not covered in the thermodynamically based screening procedure is the reactivity of the solvent species and generally how the reaction proceeds in each sovent mixture. It is shown that for the hydroformylation of 1-dodecene the solvents selected here have a minimal effect on the reaction performance. This would mean that the solvents found here have very similar coordinating effects and/or gas solubilities. Only one exception is found in the case of *N,N*-diethylformamide where a lower yield of tridecanal occurs. In four of the five TMS systems investigated that formed biphasic binary systems, it is very feasible to conduct the hydroformylation of 1-dodecene. In this case, predicted catalyst leaching levels were qualitatively consistent with the predicted catalyst leaching levels found in the partitioning predictions. In the one case using acetone, the reaction proceeded quite well but cannot be used due to the absence of phase separation afterwards.

One bright spot in the use of this method is that DMF was found to be a qualitatively good solvent for catalyst recovery. In this regard, the method is successful in identifying solvents already used in this process. On the downside, expectations were high that a new, feasible solvent would be found with higher catalyst solubility than DMF. Perhaps by using a larger search space, for example a larger batch of HRSC solvents, other interesting candidate solvents can be found that lead to better reaction and recovery performance. Considering the margin of error using this method, future screening examples should also relax some constraints and increase the number of acceptable solvents. However, any increase in the number of solvents chosen during the computational screening section may lead to a larger batch of possible TMS systems, increasing the experimental time and cost. Since thermodynamic models are not yet to the point of accuracy required to really reduce the solvent search space, this may be currently the best course of action for future endeavors in this topic area.

4.1.8. Acknowledgments

This work was conducted in part in cooperation with the Collaborative Research Centre “Integrated Chemical Processes in Liquid Multiphase Systems”. The financial support from the German Research Foundation (DFG) under the grant SFB/TRR 63 is gratefully acknowledged. The authors would also like to thank Umicore AG & Co. KG for donating the Rh precursor, $Rh(CO)_2acac$.

4.2. Isomerization/Hydroformylation Tandem Reaction of a Decene Isomeric Mixture with Subsequent Catalyst Recycling in Thermomorphic Solvent Systems

Tom Gaide, Andreas Jörke, Kim E. Schlipköter, Christof Hamel, Andreas Seidel-Morgenstern, Arno Behr, Andreas J. Vorholt, *Appl. Catal., A.* **2017**, *532*, 50–56.

Graphical Abstract:

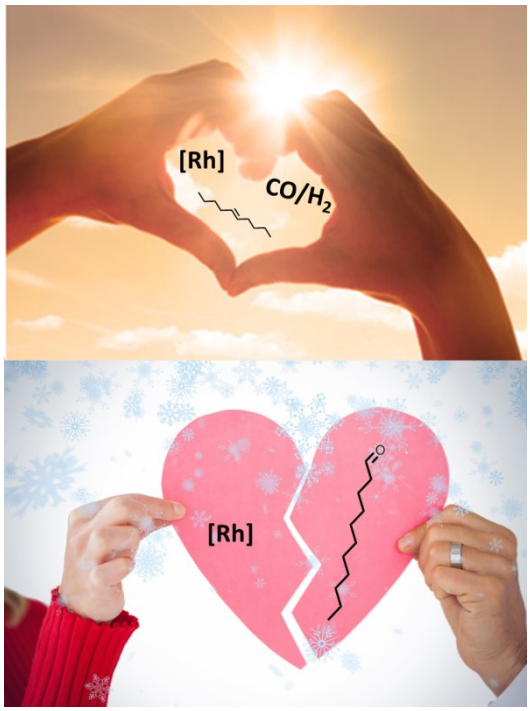

Contributions:

The concept and ideas leading to this publication were contributed by me. Kim E. Schlipköter provided experimental data as part of her master thesis. Art-work, literature search and manuscript preparation were done by me. Andreas Jörke, Andreas Seidel-Morgenstern and Christof Hamel contributed to this work *via* valuable discussions. Andreas J. Vorholt and Arno Behr supervised this project and corrected the manuscript.

4.2.1. Abstract

Herein we report about an efficient isomerization/hydroformylation tandem reaction to convert a technical mixture of decene isomers selectively into the linear undecanal in a thermomorphic solvent system. By applying a rhodium/BIPHEPHOS catalyst a high turnover frequency of 375h^{-1} and high regioselectivity of 92% for the linear product are achieved. Yields up to 70% of the linear aldehyde are obtained. The catalyst can be successfully separated from the product using a thermomorphic solvent system of dimethyl formamide (catalyst phase) and dodecane (product phase). The leaching of the rhodium (0.6% of the initial amount) and phosphorus (1.2% of the initial amount) is very low. The catalyst was successfully recycled five times.

4.2.2. Introduction

The hydroformylation is the most important reaction for the homogeneously catalyzed synthesis of linear aldehydes, which are intermediates of high interest in the chemical industry (e.g. in the synthesis of surfactants, plasticizers or perfumes) (Figure 4.5). Essentially, linear as well as branched aldehydes can be synthesized from a terminal double bond. The hydroformylation of internal double bonds leads to the formation of branched aldehydes. Often the linear aldehydes are of particular interest in technical chemistry. Unfortunately, technical grade olefin feedstocks are often complex mixtures of different olefin isomers, predominately internal olefins. In order to convert these mixtures into linear aldehydes a tandem reaction sequence of double bond isomerization and highly *n*-selective hydroformylation is necessary.

For the realization of this reaction sequence the catalyst plays a crucial role. In consequence, much effort was taken into catalyst development. Several metals like Co, Rh, Ru, Pd, Pt, Ir and iron were tested in combination with different ligands.[126] However, the best results are obtained using rhodium as metal in combination with chelating phosphorous ligands like BISBI and IPHOS[191], XANTPHOS-type ligands[111,192], BIPHEPHOS-type ligands (also in solvent mixtures)[35,110,193–195], H_8-BINOL-derived diphosphite ligands[109], or electronical nonsymmetric acylphosphite ligands[196]. Very good results are also obtained by application of hemilabile ligands[197], anthracenetriol-based triphosphite ligands[198] or tetraphosphorus ligands (for details see[126]). However, all of the above mentioned catalysts have in common, that they use valuable noble metals and tailored ligands, which makes them very expensive. For that reason, catalyst recycling is an essential step in the development of economical processes from an industrial point of view. Compared to the development of suitable catalysts for the isomerization/hydroformylation tandem reaction, their separation and reuse has attracted less attention in academic research.

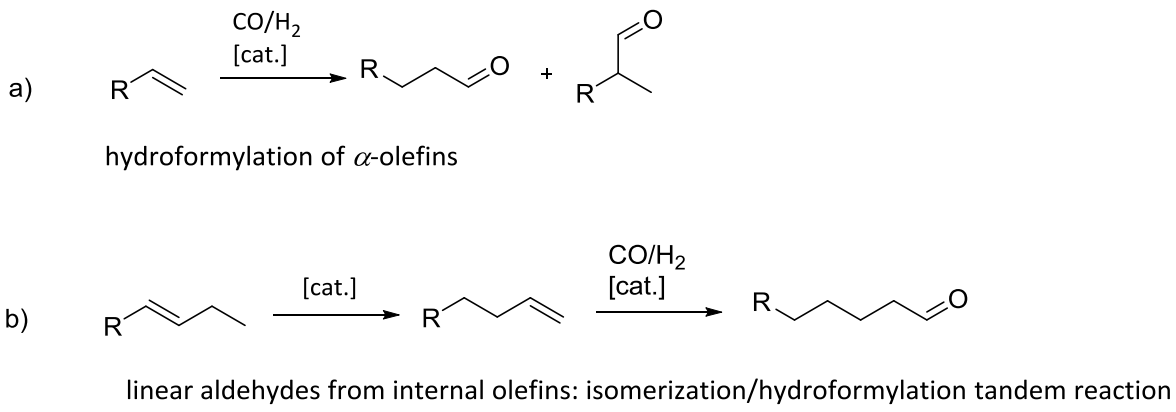

Figure 4.5: Hydroformylation and isomerization/hydroformylation tandem reaction.

To the best of our knowledge there is only one example for an isomerizing hydroformylation of higher olefins with a high regioselectivity and a successful catalyst recycling.[199]

While techniques like product distillation are well suited for separating homogeneous catalysts from low boiling products, the distillation of higher aldehydes requires high temperatures, which often shortens the lifetime of the temperature sensitive catalysts. One other approach for catalyst recycling is the immobilization of the catalyst on a solid carrier or in liquid phase. There are examples for the cobalt/TPPTS catalyzed isomerization/hydroformylation of 2-pentene[200] and technical decene mixtures[201] in aqueous biphasic solvent systems, where the catalyst is immobilized in the aqueous phase. Also a rhodium/TPPTS catalyzed conversion of olefins present in the light-light cracked naphtha in water [202] and a rhodium/XANTphos-type ligand catalyzed hydroformylation of 2-octene in ionic liquids[203] are described. Unfortunately, these catalysts show relatively low *n*-selectivity (between 50% and 75%) in the hydroformylation step.

In order to achieve a highly *n*-selective hydroformylation, Beller et al. used a rhodium/BINAS catalyst for the hydroformylation of isomeric octene mixtures in an aqueous solvent system, which shows a very high regioselectivity (*n/iso* 98:2). The catalyst is immobilized in water[199]. The turnover frequency (TOF) decreases with increasing chain length of the substrate (TOF 113 h^{-1} for 2-butene, TOF 29 h^{-1} for octene mixtures).

Despite the use of water as solvent in industrial plants is very attractive from an economic and ecologic point of view, the conversion of higher olefins in water usually suffers from mass transfer- and solubility limitations, which is displayed by the relatively low TOF values of 29 h^{-1} for higher olefins reported in literature.

One approach to overcome these limitations is the use of thermomorphic solvent systems (TMS systems, Figure 4.6). The idea of these systems is to take advantage of the tem-

perature dependent miscibility gap of a mixture of a polar and a non-polar solvent. While the substrate and the product are better soluble in the non-polar solvent, the catalyst has a high solubility in the polar solvent. Heating the solvent system to reaction temperature leads to the formation of one single homogeneous reaction mixture overcoming mass transfer limitations during the reaction. Cooling after reaction initiates phase separation and the polar, catalyst containing phase can be separated from the non-polar product phase *via* simple decantation.[31,204]

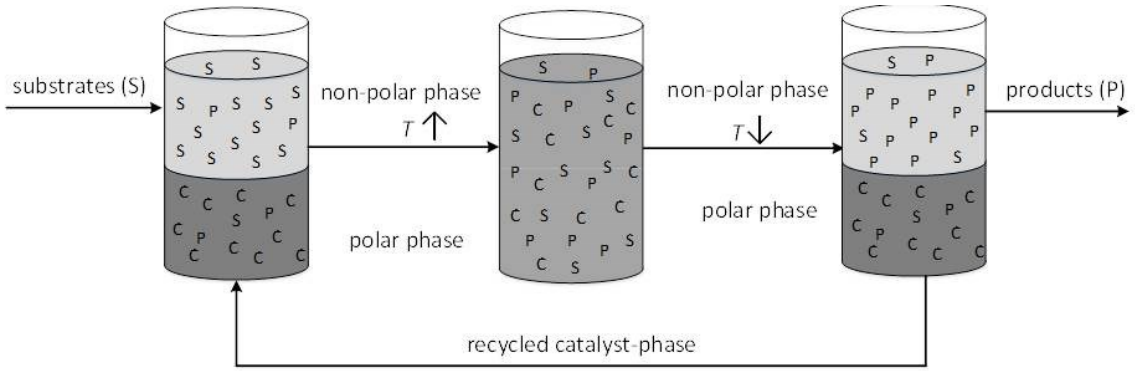

Figure 4.6: Principle of a TMS system.[205]

The TMS system offers several advantages compared to other catalyst immobilization strategies like a homogeneous reaction mixture (no mass transport and solubility limitations during the reaction), straightforward catalyst separation *via* decantation after reaction and the use of cheap commercially available solvents. Usually, there is no need to modify the catalyst, which is of great advantage since catalyst modification means higher prices and, not unusual, lower activities.[15] The concept of TMS systems was already successfully applied in the hydroformylation of long chained olefins.[39,56,58] The hydroformylation of 1-dodecene in a thermomorphic solvent system consisting of *N,N*-dimethylformamide (DMF) and decane using a rhodium/BIPHEPHOS catalyst was already successfully transferred into a continuously operated miniplant.[206]

Figure 4.7 shows the examples from literature for the isomerization/hydroformylation tandem reaction achieving high selectivity towards the linear aldehydes with subsequent catalyst separation, which are already realized. To the best of our knowledge, there is only one example for the isomerization/hydroformylation tandem reaction (synthesis of *n*-hexanal from 2-pentene) demonstrating a recyclability of the catalyst. This work describes the highly selective tandem isomerization – hydroformylation to convert a mixture of decene isomers into undecanal with relatively high turnover frequencies in a TMS system with subsequent catalyst recycling.

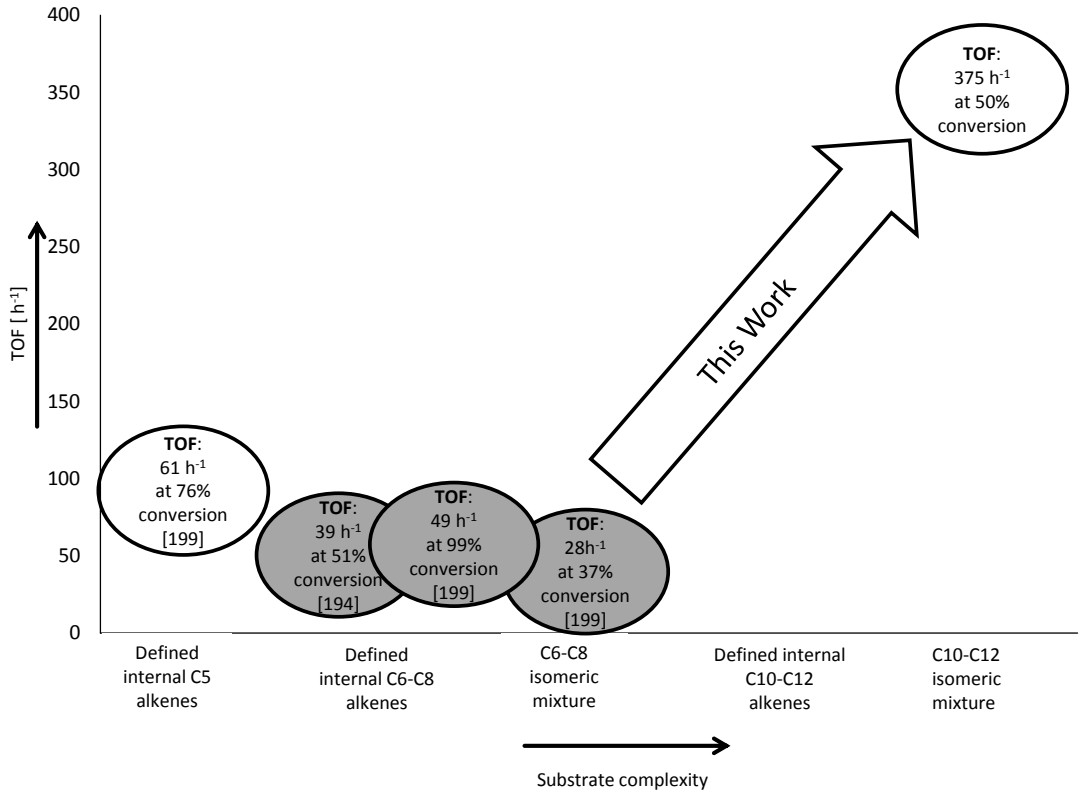

Figure 4.7: Highly selective tandem isomerisation/hydroformylation reactions of internal olefins with subsequent catalyst recycling.
white: catalyst recycling realized; grey: catalyst was not recycled, but separated from the product.

4.2.3. Materials and Methods

4.2.3.1. Chemicals

DMF (>99%), octane (99%), heptane (>99%) and cyclohexane (>99%) were purchased from Acros Organics. Cyclooctane (98%) was purchased from Sigma Aldrich. Dodecane (>99%) and undecanal (97%) were purchased from TCI Chemicals. Nonane (99%) was purchased from Alfa Aesar. BIPHEPHOS (>95%) was purchased from Molisa GmbH. $Rh(CO)_2acac$ was donated by Umicore. The technical decene mixture was donated by Sasol. All chemicals were degassed before use and stored under argon. CO (2.0) and H_2 (5.0) were purchased from Messer Industriegase GmbH.

4.2.3.2. Reaction in a 20 ml Autoclave

The precursor $Rh(CO)_2acac$ and BIPHEPHOS were weighted and added in a homemade 20 ml autoclave. The autoclave was closed, evacuated and flushed with Argon three times. Afterwards degassed DMF, non-polar solvent and decene mixture were transferred into the reactor *via* cannula using standard Schlenk technique. The reactor was pressur-

ized with synthesis gas and heated under stirring to reaction temperature. After reaction time the reactor was cooled in an ice bath and the pressure was released carefully. The reaction mixture was analyzed *via* GC-FID.

4.2.3.3. Reaction in a 300 mL Autoclave

The precursor $Rh(CO)_2acac$ and BIPHEPHOS were weighted and added into a 300 mL autoclave (Parr Instruments). The autoclave was closed, evacuated and flushed with Argon three times. Afterwards the reactor was evacuated again and degassed DMF, non-polar solvent and decene mixture were transferred into the autoclave *via* vacuum using standard Schlenk technique. The reactor was pressurized with synthesis gas and heated to reaction temperature under stirring. For time-resolved experiments samples of the reaction solution were taken *via* a capillary from inside the reactor and analyzed *via* GC-FID. After reaction time the reactor was cooled in an ice bath and the pressure was released carefully. For the determination of the phase behavior the reaction solution was transferred into a temperature controlled separating funnel. After separation, both phases were analyzed *via* GC-FID. The product phase was analyzed *via* ICP-OES.

4.2.3.4. Recycling Experiments

The initial run was set up as described in 4.2.3.3. Before cooling the reactor to end the reaction, a sample was taken from the hot reaction mixture and analyzed *via* GC-FID in order to determine conversion and yield. Afterwards, the reactor was cooled *via* an ice bath. The syngas pressure was then reduced to 10 bar. The autoclave was connected to an inert glass pressure reactor (Büchi AG) *via* flexible tube. The reaction solution was then transferred into the glass pressure autoclave *via* CO/H_2-pressure. The phases were separated in the glass autoclave under syngas atmosphere and 0 °C. Meanwhile the steel autoclave was inerted again *via* the procedure described in 4.2.3.3. and refilled with DMF (small amounts), dodecane and decene mixture. The two reactors were connected again and the catalyst phase was transferred from the glass autoclave into the steel autoclave *via* syngas pressure. Finally, the reaction was started again and the product phase was analyzed *via* GC-FID. In the following reaction runs no samples from the hot reaction mixtures or the catalyst phase were taken.

4.2.3.5. Gas Chromatography – Flame Ionization Detector (GC-FID) Measurements

GC-FID measurements were conducted by HP 6890 Series gas chromatograph (Hewlett Packard). The gas chromatograph was equipped with a capillary column (Agilent J&W GC

Columns-INNOWAX 30 m x 0.25 mm x 0.25 μm) and a flame ionization detector. Helium was used as carrier gas. The method of external standard was used for quantitative analysis of the reaction mixture.

4.2.3.6. Inductive Coupled Plasma Optical Emission Spectrometry (ICP-OES) Measurements

For sample preparation for ICP-OES measurement 0.230 g of the non-polar phase was weighted into a Teflon cup. Then 2.5 mL nitric acid (65%) and 4 mL sulfuric acid (96%) were added and a digestion was conducted in a Micro *m*Prep A microwave apparatus (MWS GmbH). Subsequently 2 mL of distilled water and 1 mL hydrogen peroxide solution (30-32%, optima grade, Fisher Chemical) were added. Finally, ICP-OES measurements were conducted with an IRIS Intrepid optical emission spectrometer (Thermo Elemental).

4.2.4. Results and Discussion

We started our studies on the isomerization/hydroformylation tandem reaction of decene isomeric mixtures by investigating the reaction parameters temperature, synthesis gas pressure, CO/H_2-ratio and decene concentration in pure DMF as solvent. The aim was to determine important influence factors for the tandem reaction and to optimize the yield of the desired linear aldehyde (**2**, Figure 4.8) at low catalyst loadings. Afterwards, suitable TMS systems were developed to realize the catalyst recycling. We decided to use a $Rh(CO)_2$acac/BIPHEPHOS catalyst (Figure 4.8) which was reported to be active in double bond isomerization as well as very *n*-selective in the hydroformylation of olefins.[194]

The substrate mixture (**1**), the desired linear aldehyde (**2**), the branched hydroformylation products (**3**) and the hydrogenated substrates (**4**) are shown in Figure 4.8. Besides these products, small amounts of high boiling byproducts (BP) were detected in some cases.

4.2.4.1. Reaction Optimization

The first paremeter we investigated in order to optimize the yield of **2** was the reaction temperature. The reaction temperature has influence on both the isomerization and the hydroformylation reaction rates. Also the equilibrium concentration of the different decene isomers depends on temperature.[207] Results of the temperature screening are given in Figure 4.9.

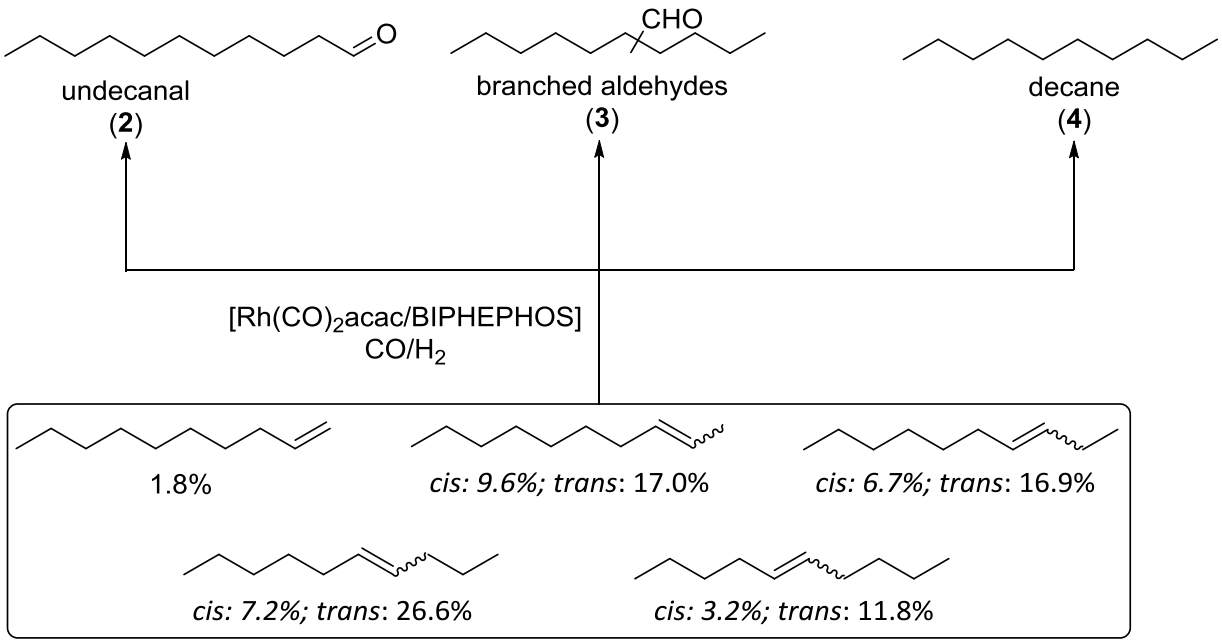

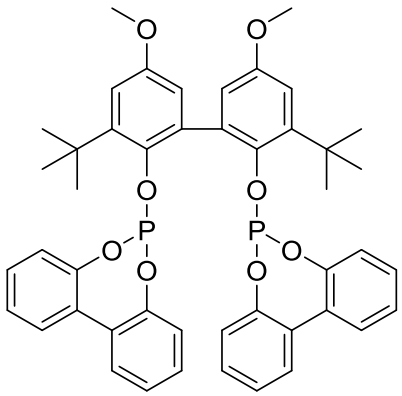

Figure 4.8: Product spectrum/BIPHEPHOS ligand.

The yield of the desired linear hydroformylation product **2** increases from 26% at 95 °C to 75% at 135 °C. Also the overall selectivity towards **2** increases with higher temperatures from 72% (95 °C) to 78% (135 °C). This behaviour can be explained with the reaction network of this tandem reaction (Figure 4.10).

All the isomers of the decene mixture are in equilibrium. While the branched aldehydes and hydrogenated decane can be formed by all isomers, the desired linear product can only be obtained from the terminal 1-decene, which is the thermodynamically less favored alkene. The concentration of 1-decene in the reaction solution increases with higher temperatures[207] and, in consequence, also the reaction rate for the *n*-selective hydroformylation. Also the isomerization rate increases with temperature.[207]

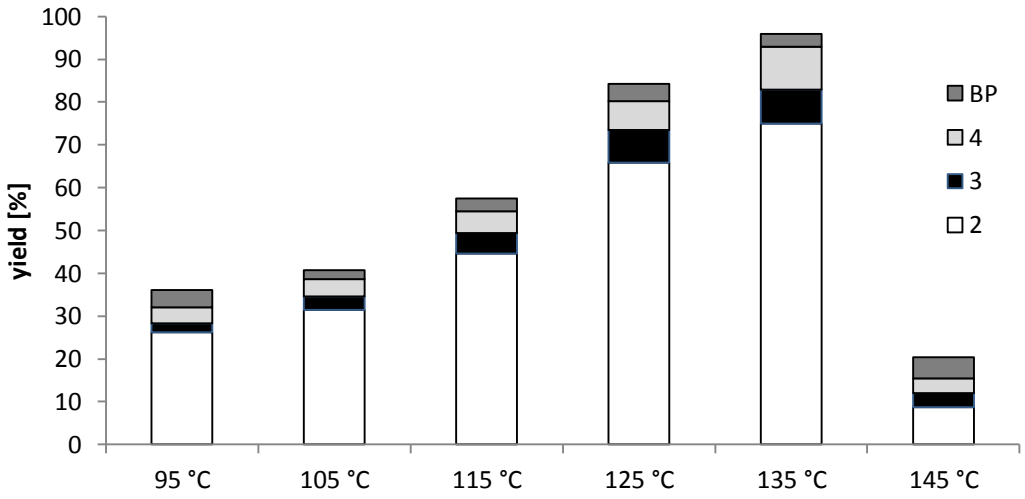

Figure 4.9: Influence of the reaction temperature on the product distribution.
Conditions: 0.5 mol% $Rh(CO)_2acac$ (with regard to 1), 2 mol% BIPHEPHOS (with regard to 1), 5 mL DMF, 2.6 mmol 1, 15 bar syngas (CO/H_2 = 1/1), reaction time=3 h, batch reaction in a 20 mL.

This is beneficial since the converted 1-decene can be reproduced faster from the internal decene isomers. Notably, the regioselectivity in the hydroformylation towards the linear product is between 91% and 92% and not influenced by the temperature in the investigated range. If temperature is raised to 145 °C the yield of all products decreases drastically which can be ascribed to catalyst decomposition at this temperature. However, the best results in terms of reaction rates and selectivity are obtained at 135 °C and further investigations were conducted at this temperature.

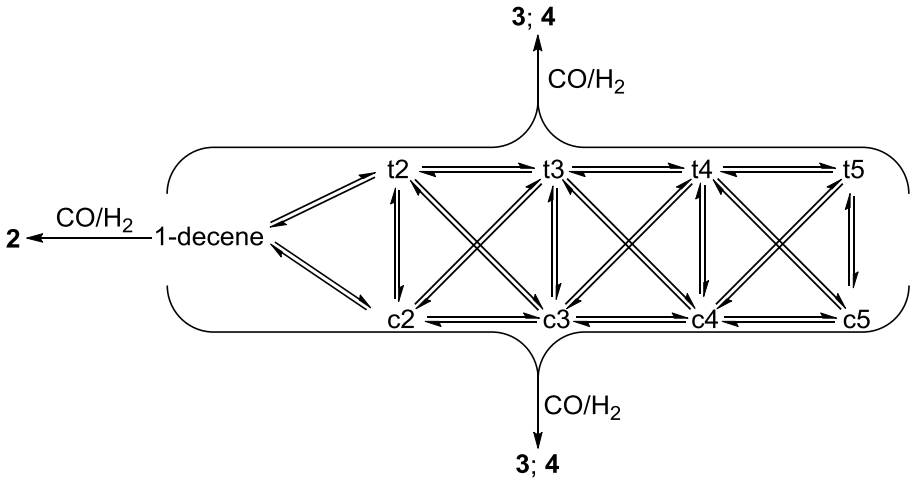

Figure 4.10: Reaction Network of the isomerization/hydroformylation tandem reaction.
t = *trans*-isomers, c = *cis*-isomers, number = double bond position.[207]

After the investigation of the reaction temperature the parameters syngas pressure, CO/H_2-ratio, concentration of **1**, Rh-concentration and rhodium/ligand ratio were optimized for batch operation mode. Table 4.8 shows the optimized conditions for the isomeriza-

tion/hydroformylation tandem reaction of a decene isomeric mixture in batch reaction mode. At a relative high temperature of 135 °C a Rh/ligand ratio of 1/4 is required for a stable and selective catalyst complex. A pressure of 15 bar is required for the reaction in batch operation mode. If the synthesis gas pressure is constant (semi-batch), very good results are obtained at lower pressures of 5 bar. A CO/H_2-ratio of 1:1 turned out to be the best under given conditions. While higher amounts of hydrogen lead to an increasing yield of the hydrogenated substrate **4**, higher amounts of CO lower the reactivity of the catalyst. Kinetic studies for this reaction in semi-batch mode can be found in a related publication.[208]

Table 4.8: Optimized reaction conditions for the isomerization/hydroformylation tandem reaction in batch reaction mode.

Parameter	Optimized Value
Temperature	135 °C
Pressure	15 bar (for batch operation mode); 5 bar (for semi-batch operation mode)
CO/H_2-ratio	1:1
1 concentration	1.5 mmol/mL
Rh concentration	0.2 mol% (with regard to **1**)
BIPHEPHOS concentration	0.8 mol% (with regard to **1**)
DMF volume	5 mL
Reactor volume	20 mL

Under these conditions, a yield of the desired **2** of 34% with a regioselectivity of 92% after one hour can be achieved. With these intermediate results we started to develop a suitable TMS-System for the reaction.

4.2.4.2. Design of the TMS System

After optimizing the reaction conditions the next step was to develop a suitable TMS system to be able to separate the catalyst from the products. The TMS system should meet the following criteria:

- two solvent components (one polar for the catalyst, one non-polar for the product)
- biphasic at room temperature
- homogeneous at reaction temperature

- good reaction performance
- low catalyst leaching into the non-polar phase
- fast an accurate phase separation

Recently we reported about a concept of a COSMO-RS based approach for the solvent selection in TMS systems using Rh/BIPHEPHOS catalyst as model compound. It turned out that DMF is one of the most suitable polar solvents in a TMS system for this catalyst, especially in terms of catalyst leaching.[209] Consequently, we decided to use it as the polar solvent component for the TMS system. Alkanes and cycloalkanes are suitable non-polar components in a TMS system for this type of reaction, since the resulting C11-aldehydes have a higher solubility in them compared to DMF. So we tested the phase behavior of heptane, octane, nonane, dodecane, cyclohexane and cyclooctane (each in 50 v%) in combination with DMF (50 v%). All these mixtures were biphasic at room temperature and homogeneous at reaction temperature, so they meet the first three criteria. Figure 4.11 shows the product distribution in different TMS compositions. All TMS systems show comparable results in the isomerization/hydroformylation tandem reaction. Also there are no significant differences between the use of a TMS system and a reaction in pure DMF. The yield of **2** is at about 40% after one hour. The regioselectivity in the hydroformylation is 92%. As a consequence, all TMS systems are in line for a possible application in view of their reaction performance.

Another important decision criterion is the leaching of the catalyst into the nonpolar product phase. Brunsch et al. already showed that the Rh/BIPHEPHOS-catalyst leaching into the non-polar phase decreases with increasing chain length of the nonpolar solvent.[58] ICP-OES analytic of the DMF/dodecane TMS system showed that the concentrations of rhodium and phosphorus in the dodecane phase after reaction and subsequent phase separation at -9 °C were only 5 ppm for rhodium respectively 25 ppm for phosphorus. If cyclic alkanes like cyclohexane are used as non-polar solvents the concentrations of rhodium (66 ppm) and phosphorus (71 ppm) are much higher compared to simple linear alkanes. While the DMF/cycloalkane TMS-systems were homogeneous at room temperature, the phase separation was accurate for all TMS systems at -9 °C. Taking into account all the criteria made above the DMF/dodecane TMS system seems to be the most promising for further investigations. Table 4.9 shows the distribution of the different components in the two phases after reaction and phase separation.

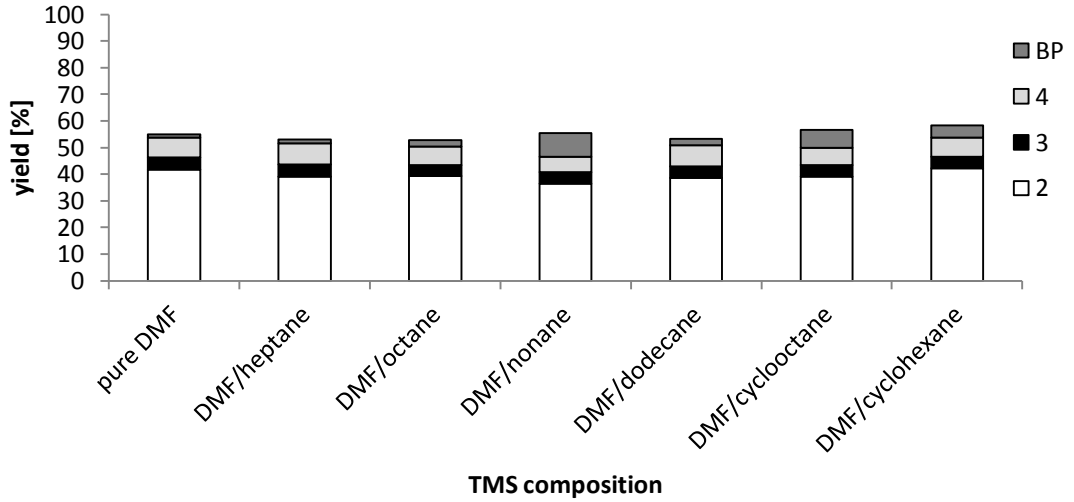

Figure 4.11: Influence of TMS system composition on the reaction behaviour.
Conditions: 0.2 mol% $Rh(CO)_2acac$ (with regard to 1), 0.8 mol% BIPHEPHOS (with regard to 1), 2.5 mL DMF, 2.5 mL nonpolar solvent, 7.5 mmol 1, 15 bar syngas (CO/H_2 = 1/1), reaction temperature = 135 °C, reaction time = 1 h, batch reaction in a 20 mL autoclave, yields were determined by GC-FID, leaching values were determined by ICP-OES.

Table 4.9: Component distribution after phase separation.

Compound	Percentage in DMF phase [%]	Percentage in dodecane phase [%]
1	15	85
4	10	90
2	45	55
3	48	52
rhodium	99.4	0.6
phosphorus (ligand)	98.8	1.2
DMF	94	6
dodecane	6	94

Conditions: 0.2 mol% $Rh(CO)_2acac$ (with respect to 1), 0.8 mol% BIPHEPHOS (with regard to 1), 25 mL DMF, 25 mL dodecane, 75 mmol 1, 15 bar syngas (CO/H_2 = 1/1), reaction temperature = 135 °C, reaction time = 3 h, batch reaction in a 300 mL autoclave, separation temperature = -9 °C, separation time = 0.5 h, distributions of 1, 4, 2, 3, DMF and dodecane were determined by GC-FID, distributions of rhodium and phosphorus were determined by ICP-OES.

The desired **2** as well as the byproducts **4** and **3** have a (slightly) higher solubility in the non-polar dodecane phase; rhodium and the ligand are nearly completely dissolved in the DMF phase. Therefore the phase behaviour of the reaction system is very promising for a catalyst recycling in the ongoing.

Figure 4.12 shows a yield vs. time plot of the reaction in the TMS system under optimized conditions. After 3 h a yield of the desired **2** of 64% is obtained. The regioselectivity in the hydroformylation is 92%. The TOF after 50% conversion (after 40 min) is 375 h^{-1} which is very fast for this tandem reaction in a biphasic solvent system (see Figure 4.7). For example, TOFs obtained in the aqueous reaction system for the conversion of internal octene isomers developed by Beller et al.[200] is only 29 h^{-1} at 36% conversion. With this knowledge we started our investigations on the catalyst recycling in the DMF/dodecane TMS system.

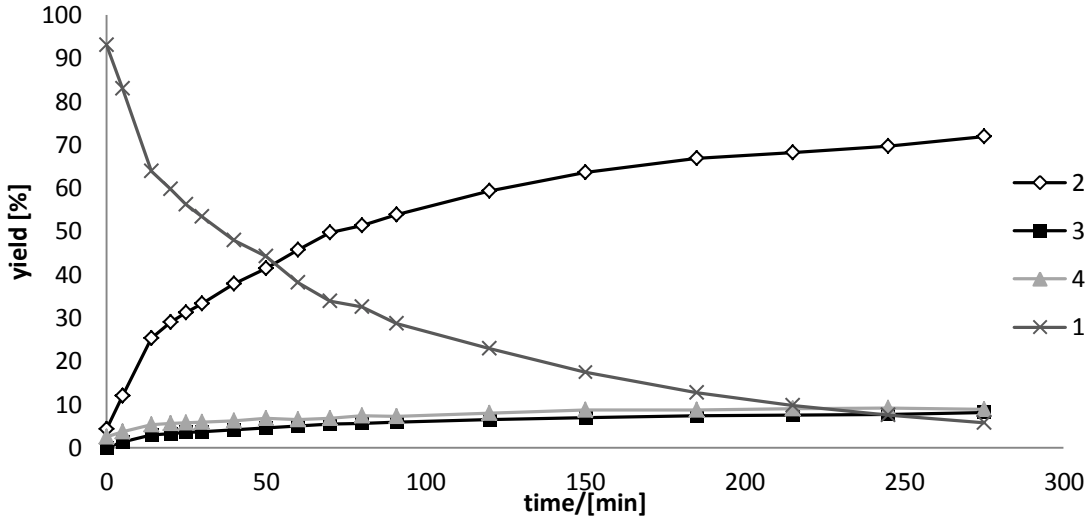

Figure 4.12: Conversion/yield vs. time plot of the isomerization/hydroformylation tandem reaction in a TMS system.
Conditions: 0.2 mol% $Rh(CO)_2acac$ (with regard to 1), 0.8 mol% BIPHEPHOS (with regard to 1), 50 mL DMF, 50 mL dodecane, 150 mmol 1, 15 bar syngas (CO/H_2 = 1/1; reactor was repressurized after taking 4 samples), reaction in a 300 mL autoclave, conversion of 1 and yields of 4, 2 and 3 were determined by GC-FID.

4.2.4.3. Catalyst Recycling

In order to prove the applicability of our TMS system as a recycling concept we conducted a set of recycling experiments (Figure 4.13):

- After the initial run (run 0) the phases were separated.
- Also a sample was taken from the catalyst phase of run 0 to determine the yields of the reaction in the initial run (Figure 4.13a).
- After sampling the catalyst phase was recycled back into the reactor, new dodecane, substrate and synthesis gas were added and the reaction was started again.

The results match the expectations from the results shown in Figure 4.12. The yield of the desired product **2** (95 mmol) is 65% and the regioselectivity in hydroformylation is 91%.

From resulting **2** 58% (55 mmol) were extracted into the product phase which is also in good accordance to the results shown in Table 4.9. In the following recycling runs (run 1-5, Figure 4.13b) no samples of the catalyst phase were taken from the reaction mixture to avoid loss of the catalyst. The yield of the desired **2** is more or less constant over all recycling runs (between 50 and 62 mmol). The same observation was made for the yield of the hydrogenated substrates **4** (6-10 mmol). The regioselectivity in the hydroformylation decreases after run 3 from 90% (run 3) to 64% (run 5). The loss of regioselectivity can be traced back to ligand decomposition, since the ligand is responsible for the high *n*-selectivity in the hydroformylation reaction. It should be noted that a regioselectivity of 64% is still quite high taking into account that less than 1% of all decene isomers is 1-decene in the equilibrium at this temperature.[207] With decreasing regioselectivity in the hydroformylation also the amount of **1** in the product phase decreases from 28 mmol (run 3) to 12 mmol (run 5) since also internal olefins are converted into branched aldehydes. However, with this set of recycling experiments we were able to show that our developed tuneable multiphasic catalyst recycling strategy gives stable yields of **2** over five recycling runs and enhances the reaction kinetic in comparison to the biphasic systems described in literature. Future investigations will be done in a continuously operated miniplant in order to get information about the long time stability and a possible refreshment of the BIPHEPHOS ligand.

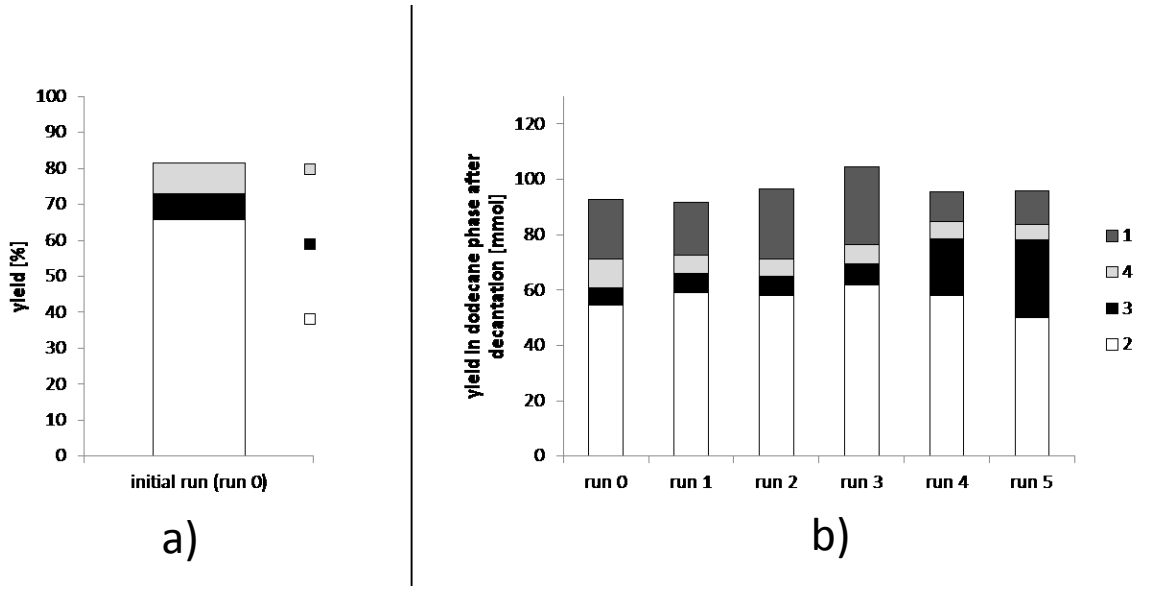

Figure 4.13: Catalyst Recycling.
Figure 4.13a: Product yields after the initial run (run 0) of the recycling experiments. Conditions: 0.2 mol% $Rh(CO)_2acac$ (with regard to 1), 0.8 mol% BIPHEPHOS (with regard to 1), 50 mL DMF, 50 mL dodecane, 150 mmol 1, 15 bar syngas (CO/H2 = 1/1; reactor was repressurized after 1,5 h), reaction temperature = 135 °C, reaction time = 3 h, semi-batch reaction in a 300 mL autoclave, yields were determined by GC-FID.

Figure 4.13b**:** Yield of the different products in the dodecane phase (product phase) after reaction and phase separation. Conditions: run 0: 0.2 mol% $Rh(CO)_2acac$ (with regard to 1), 0.8 mol% BIPHEPHOS (with regard to **1**), 50 mL DMF, 50 mL dodecane, 150 mmol 1, 15 bar syngas (CO/H_2 = 1/1; reactor was repressurized after 1.5 h), reaction temperature = 135 °C, reaction time = 3 h, semi-batch reaction in a 300 mL autoclave, separation temperature = 0 °C, separation time = 0.5 h yields were determined by GC-FID; run 1-5: catalyst phase was recycled into the reactor, addition of: 3 mL DMF, 47 mL dodecane, 94 mmol 1.

4.2.4.4. Conclusion

In this paper we described the first development of an isomerization/hydroformylation tandem reaction of a technical decene isomeric mixture with subsequent recycling of the rhodium/BIPHEPHOS catalyst in a thermomorphic solvent system consisting of DMF/dodecane. With this reaction system highest turnover frequency in a multiphase reaction for this tandem reaction (375 h^{-1} at 50% conversion) in combination with a high regioselectivity of 92% towards the desired linear aldehyde were achieved. The losses of rhodium (5 ppm, <1% of initial amount) and phosphorus (25 ppm, 1.2% of initial amount) into the product phase are very low. A catalyst recycling was successfully realized. The activity of the catalyst was maintained over 6 runs without any refreshment of a catalyst component. This reaction system represents a promising approach for the conversion of internal long chained olefin mixtures into linear aldehydes with an integrated catalyst separation *via* thermomorphic solvent systems. Further investigations should regard the implementation of this reaction in a continuously operated miniplant to get information about the long-term behavior of the TMS system and to get a better understanding of the

BIPHEPHOS decomposition. Also different ligands can be applied to evaluate their reaction performance and the stability in a continuously operated process.

4.2.5. Acknowledgments

The financial support of the German Science Foundation (Project SFB/TRR 63:"InPROMPT – Integrated Chemical Processes in Multi-Phase Fluid Systems") for this joint collaboration (Subprojects A1/A3) is gratefully acknowledged. We are also very grateful to Umicore AG and Co. KG for the supply of the catalyst precursor $Rh(CO)_2acac$.

4.3. Overcoming Phase Transfer Limitations in the Conversion of Lipophilic Oleocompounds in Aqueous Media - A Thermomorphic Approach

Tom Gaide, Jens M. Dreimann, Arno Behr, Andreas J. Vorholt, *Angew. Chem. Int. Ed.*, **2016**, *55*, 2924 –2928; *Angew. Chem.*, **2016**, *128*, 2977-2981.

Graphical Abstract:

Bringing cat and dog together: The intelligent selection of solvents facilitates both the reaction and the recovery of the Rh/SulfoXantphos catalyst. Green solvents (water and 1-butanol) and the use of a renewable feedstock contribute to the development of sustainable processes.

Contributions:

The concept and ideas leading to this publication were contributed by Jens Dreimann and me, while reaction conditions and solvent system are developed by me and catalyst recovery in larger batch scale and continuous operation is developed by Jens Dreimann. Jonas Bianga and Jan Niklas Weimann provided experimental data as part of their bachelor thesis respectively master thesis. Art-work, literature search and manuscript preparation have performed by Jens Dreimann and me in cooperation. Andreas J. Vorholt and Arno Behr supervised this project and corrected the manuscript.

4.3.1. Abstract

This paper describes a new process concept for recycling transition metal catalysts in the synthesis of medium polar products *via* aqueous thermomorphic multicomponent solvent systems. This work focuses on the use of ”green” solvents (1-butanol and water) in the hydroformylation of bio-based substrate methyl 10-undecenoate. Having successfully developed a biphasic reaction system in laboratory scale, the reaction was transferred in a continuously-operated miniplant to demonstrate the robustness of this innovative recycling concept for homogenous catalysts.

4.3.2. Communication

Sustainability and environmental awareness are becoming more and more important in the chemical industry.[210] In terms of green chemistry, which aims, for example, to reduce the use of energy and develop new resource-efficient processes, catalysis is a key technology.[211] Essentially, reactions can be catalysed homogeneously or heterogeneously. Although homogenous catalysis affords many advantages compared to heterogeneous catalysis, such as milder reaction conditions and higher selectivities[9], only 25% of all catalysed processes are conducted homogeneously on an industrial scale due to the complexity of separating the product and the valuable catalyst.[4,212–214] In addition to physical separation methods such as product distillation, homogeneous catalysts can be immobilised on solid carriers or in a liquid phase to allow for easy separation from the product.[215–218] One example for catalyst immobilisation in liquid phases with high industrial relevance is the hydroformylation of propene (Scheme 4.14) in the Ruhrchemie/Rhône-Poulenc-Process (RCh-RP). In this process, the reaction takes place in an aqueous phase on a water soluble rhodium complex containing the ligand triphenylphosphinetrisulfonate (TPPTS, Figure 4.19). The resulting butanals can be separated from the catalyst *via* simple phase separation after the reaction.[18,79] Unfortunately, this process concept is limited to the conversion of short-chained olefins due to the low water solubility of higher alkenes and therefore poor turn over frequencies (TOF) for these substrates.[18,219]

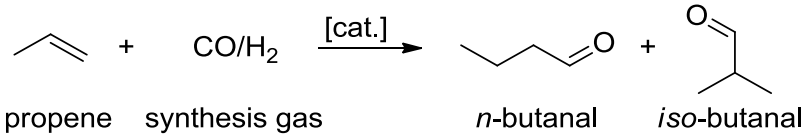

Scheme 4.14: Hydroformylation of propylene.

One strategy for overcoming mass transport limitations is the use of thermoregulated systems such as thermoregulated phase transfer catalysis, microemulsions, fluorinated solvents or polymeric linked catalysts.[204,220–223] One other possibility is the use of thermo-

morphic multicomponent solvent systems (TMS), which have several crucial advantages compared to other process concepts:

- Thermomorphic phase behaviour:
  - Reaction takes place without mass transfer limitations between substrate and catalyst in a single reaction phase
  - Catalyst and product can easily be separated *via* decantation after the reaction within two liquid phases
- Cheap and commercially-available solvents can be used without additional surfactants, etc.
- Typically no modification of the catalyst

TMS systems consist of at least two solvents (S_A, S_B) that have a highly temperature-dependent miscibility gap (Figure 4.15, $T_3>T_2>T_1$). These two solvents form a biphasic mixture at low temperatures. The substrate and the product (lumped to S_C) are better soluble in S_A while the catalyst occurs mainly in S_B. When heated (T_3), this mixture forms a single homogeneous liquid phase, allowing the reaction to take place without any mass transport limitations e.g. at the operation point (OP).[31,204] Cooling the mixture after reaction again (T_1) leads to the formation of two liquid phases, S_A containing the product and S_B containing the catalyst.

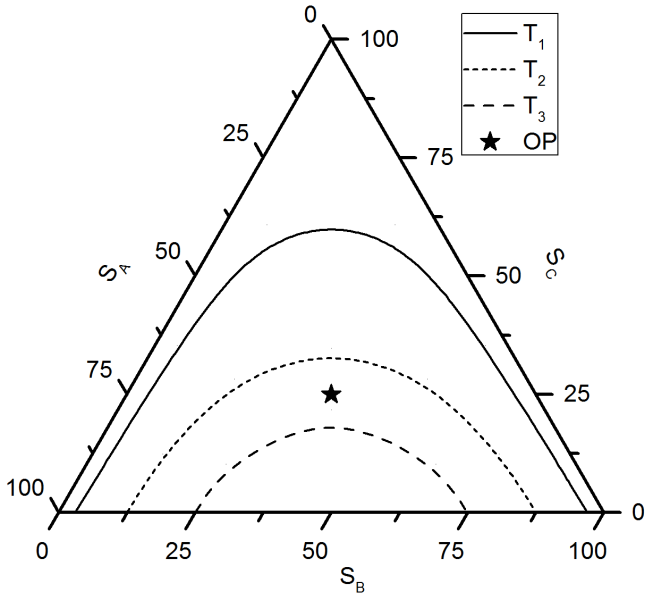

Figure 4.15: Ternary diagram of TMS systems.

The use of TMS systems makes it easy to convert long-chained substrates that are not water soluble in combination with an easy and efficient catalyst recy-

cling.[39,40,42,43,49,56,57,59,224,225] However, known TMS systems based on organic solvents have a limited scope when it comes to synthesizing products with a higher polarity. These products have a better solubility in the polar catalyst phase, which makes an effective separation of product and catalyst impossible.[74,205,226,227] This is why TMS systems have only been used to synthesize non-polar products up to now.[228] The aim of this work is to extend the scope of the TMS concept to the synthesis of middle-polar and polar products. The hydroformylation of methyl 10-undecenoate (**1,** Scheme 4.16) was chosen as model reaction. **1** is easily available through pyrolytic cleavage of ricinoleic acid methyl ester.[229,230] The desired hydroformylation product **2** can be used as a polymer precursor (Scheme 4.17). In addition to **2**, there are some undesired byproducts such as branched aldehydes (**3**), isomers of substrate (**4**) and hydrogenated substrate (**5**). Research by Ternel et al. on the hydroformylation of 10-undecennitril has shown that the known TMS systems are not applicable for functionalising middle-polar substrates that already contain a polar functional group due to the high solubility of the resulting products in the catalyst phase (>90%).[74] As a consequence, new methods have to be developed to allow these substrates to be converted efficiently using a liquid-liquid two-phase technique. With this in mind, laboratory-scale research was conducted with the aim of developing a new concept that allows for both efficient process control with high yields and selectivities as well as easy catalyst recycling. The viability of this concept was then tested in a continuously-operated miniplant.

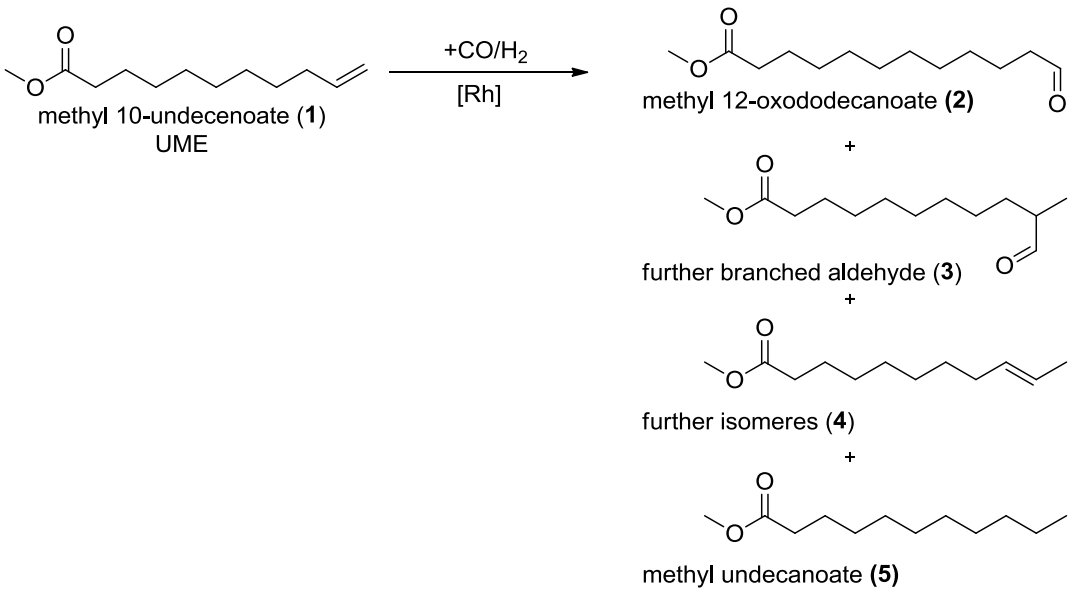

Scheme 4.16: Hydroformylation of 10-undecenoate and observed side reactions.

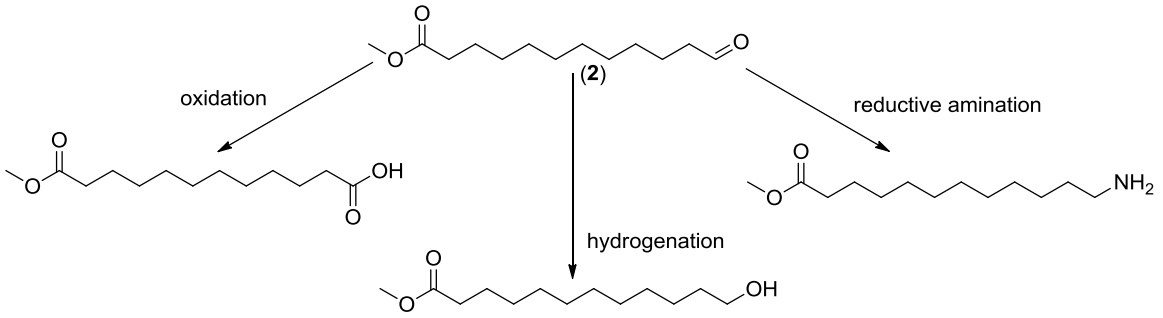

Scheme 4.17: Possible building blocks for the polymer synthesis.

Initially, the catalyst separation in our model reaction was tested using known organic TMS systems. For this purpose, a variety of polar organic solvents were tested as catalyst solvents in combination with *n*-decane as a non-polar product solvent. $Rh(acac)(CO)_2$ was used as a precursor in combination with the Biphephos ligand (Figure 4.19).

This catalyst complex was tested for low catalyst leaching, long term stability and regio selectivity towards the linear aldehyde in the hydroformylation of 1-dodecene in TMS-systems.[70,71,231] High yields of linear product (**2**) of between 40 and 80% were achieved in the hydroformylation of UME (**1**). Furthermore, a high ratio between linear and branched aldehydes (*l*/*b*-ratio) at 99:1 was reached. As the product was highly polar, it was dissolved almost completely in the polar catalyst phase (cp) (Figure 4.18), rendering the efficient separation of catalyst and product impossible.

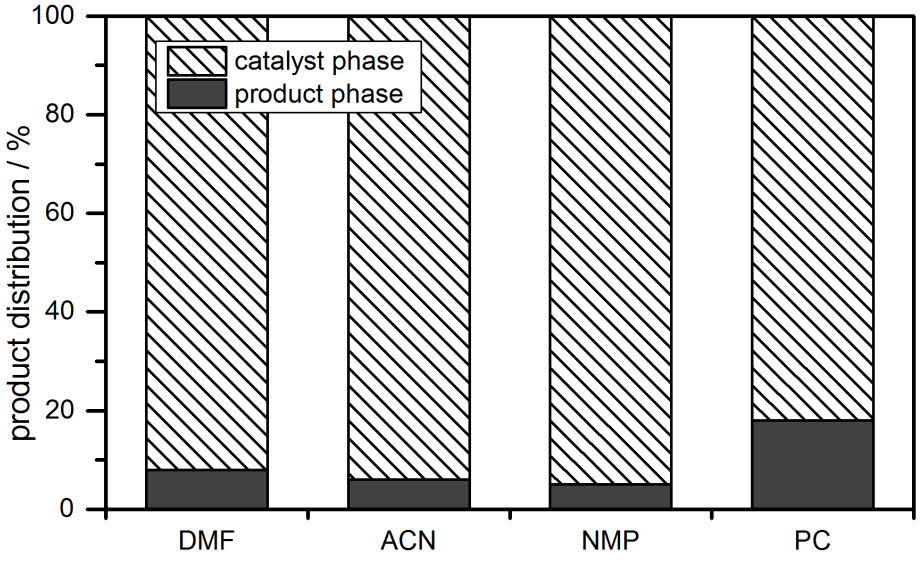

Figure 4.18: Product distribution using polar, organic solvents.
Conditions: n_{UME}= 3.9 mmol, $n_{Rh(acac)(CO)2}$= 0.0039 mmol, $n_{Biphephos}$= 0.0195 mmol, p= 20 bar, $CO:H_2$= 1:1, T= 90 °C, $T_{Separation}$= 25 °C t= 2 h, m_{decane}= 2.1 g, m_{cp}= 2.1 g; catalyst phase (cp)= DMF (dimethylformamide), ACN (acetonitrile), NMP (*N*-methyl-2-pyrrolidone), PC (propylenecarbonate)

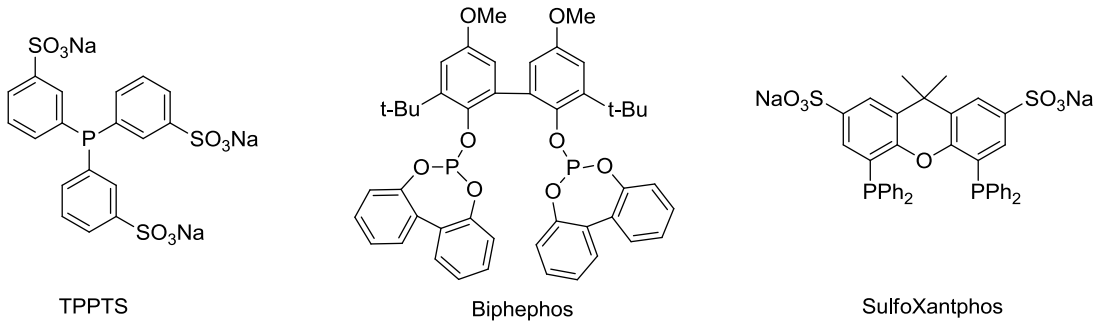

Figure 4.19: Molecular structure of the applied ligands.

However, several requirements needed to be fulfilled to develop a more suitable thermomorphic solvent system:

- Low solubility of product **2** in the polar solvent (catalyst phase)
- High solubility of the catalyst complex in the polar solvent
- High temperature dependency of the miscibility gap

Using water as the polar solvent (catalyst phase) and 1-butanol as the less polar solvent (product phase) fulfilled all postulated requirements. Water and 1-butanol (50:50) have an upper critical solution temperature of 106 °C. Behr et al. have already demonstrated that enzymes can be separated in a solvent system consisting of water, 1-hexanol and methanol.[61] This work is the first to describe the use of aqueous TMS-systems to separate homogeneous transition metal catalysts from medium polar products. Furthermore, solvents such as water and 1-butanol are preferable for continuous processes, as water is non-toxic, non-flammable, odourless, cheap and available in great abundance. 1-butanol is available from renewable feedstocks and is produced *via* biomass fermentation.[232]

A water-soluble rhodium catalyst is required for hydroformylation in aqueous solvent systems. As such, the ligand SulfoXantphos (Figure 4.19) was used for the investigations described in this paper. The combination of this ligand and a rhodium precursor is described as a highly selective hydroformylation catalyst in literature.[233]

The reaction system shows highly temperature-dependent behaviour (Figure 4.20). At a reaction temperature of 140 °C and after a reaction time of 1 h, the highest yield of **2** (76%) is observed. Branched aldehydes (**3**) (5%), isomers of the substrate (**4**) (12%) and the hydrogenation product (**5**) (2%) are observed as byproducts. Compared to these results, lower reaction temperatures lead to a strong decrease in catalyst activity. These results clearly indicate mass transfer limitations during the reaction although the UCST of water/1-butanol is 106 °C. Herein, the presence of the substrate **1** shifts the UCST towards higher temperatures, due to its low polarity compared to the two solvents. Investi-

gations on the phase behaviour of the ternary solvent system (1-butanol/water/**1**) show a biphasic system even at a temperature of 140 °C. However, the yield of 76% corresponds to a TOF of 1500 h^{-1}. To our knowledge, this is the highest TOF in the hydroformylation of long-chained olefins in aqueous solvent systems that has been described in literature thus far. Further increasing of the reaction temperature does not lead to better reaction performance, so that this solvent system provides all advantages of a TMS-system and meanwhile ensures low energy demand by a minimum of temperature change. Additional the stability of the catalyst increases with lower reaction temperatures. Since this mixture does not form one single phase under reaction conditions we call this a “narrow TMS-system”.

Referring to Figure 4.15 the narrow TMS state is outlined at the point T_2. Increasing the reaction temperature leads to a smaller miscibility gap and the components solubility into each other is highly improved, but still the formation of one single phase (T_3) is not achieved. The resulting product is almost completely dissolved in the 1-butanol phase after reaction and the concentration of the rhodium in this phase was at a low level of 5 ppm by weight.

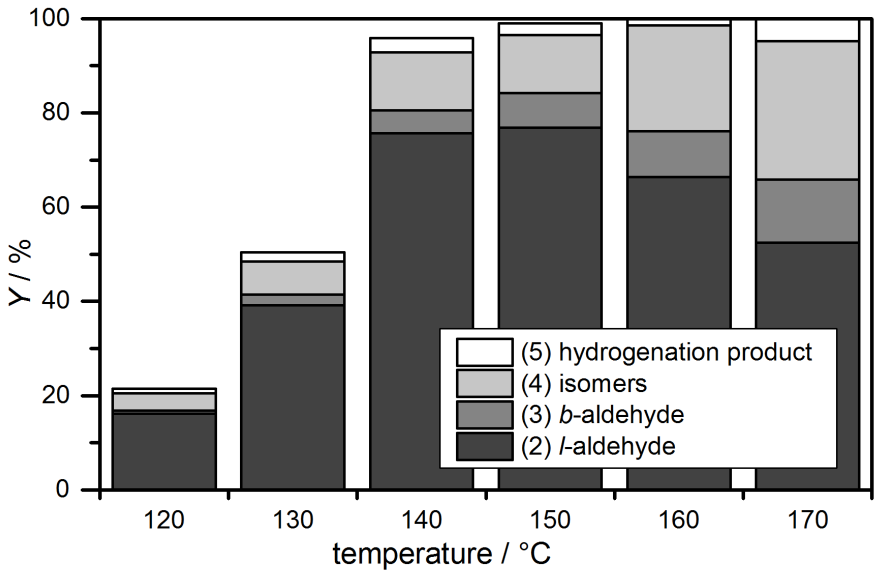

Figure 4.20: Temperature screening.
Conditions: n_{UME}= 4 mmol , $n_{Rh(acac)(CO)2}$= 0.002 mmol, $n_{SulfoXantphos}$ = 0.01 mmol, p= 20 bar, CO:H_2=1:1, t= 1 h, $m_{n\text{-butanol}}$= 2.1 g, m_{H2O}= 2.1 g.

The distribution of the different components among the two phases at 20 °C is presented in Table 4.10.

Table 4.10: Distribution of the components between polar and apolar phase [a]

	H_2O	1-BuOH	**1**	**2**	Rh	P
Product phase	18	92	99	99	5	2
Catalyst phase	82	8	1	1	95	98

[a] distribution in [%] Conditions: $T_{separation}$ = 25 °C

Starting with this suitable reaction system in terms of product yield and catalyst separation, the recycling of the homogeneous transition metal catalyst was then examined. As presented in Figure 4.21, which shows the separation of the catalyst in the aqueous phase and its reuse in a subsequent reaction run, the catalyst was successfully recovered three times.

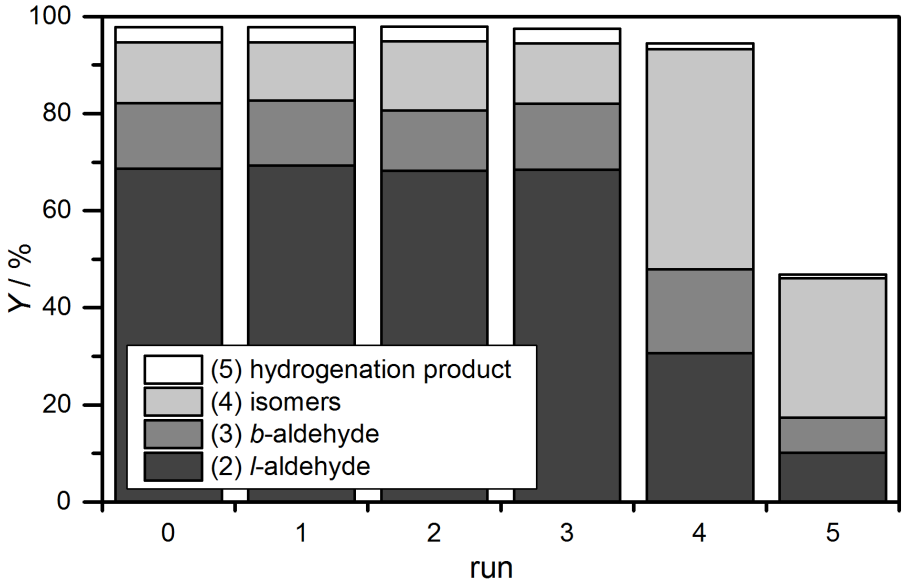

Figure 4.21:Hydroformylation of methyl 10-undecenoate and catalyst recycling using a batch autoclave. catalyst recycling using a batch autoclave, conditions: n_{UME}= 70 mmol, $n_{Rh(acac)(CO)2}$= 0.035 mmol, $n_{SulfoXantphos}$= 0.175 mmol, p= 20 bar, CO:H_2=1:1, $T_{reaction}$= 140 °C, $T_{separation}$=25 °C, t= 1.5 h, $m_{n\text{-}Butanol}$= 37.6 g, m_{H_2O}= 37.6 g.

After each separation of the catalyst and product phases, fresh substrate and 1-butanol was added prior to initiating another hydroformylation run. A significant deactivation was observed in the fourth reaction run. Among the possible explanations for this observation are the exchange of the gaseous atmosphere prior to the phase separation and small amounts of oxygen in the reaction system. In light of this, continuously-operated experiments were conducted in a miniplant consisting of a continuously stirred tank reactor (CSTR) and a phase separator.

At the laboratory scale, both phase separation and catalyst recycling are subject to certain limitations that can be overcome in a continuously-operated miniplant. In contrast to dis-

continuous analyses, it is possible to separate the product from the catalyst at reaction pressure in a synthesis gas atmosphere, ensuring optimal conditions for the catalyst complex at all times. In addition, the operation of a continuous process reveals the following relevant information[174]:

- Long-term stability of the catalyst
- Efficiency of the catalyst recycling under process conditions
- Influence of recycling streams

A process scheme of the miniplant used in these experiments is shown in Figure 4.22. This setup had been used successfully in the hydroformylation of 1-dodecene. A mixture of substrate **1** and non-polar solvent 1-butanol was fed into the reactor using a piston pump. Additionally, the synthesis gas flow was regulated by a mass flow controller. Following phase separation, the catalyst phase was recycled from the decanter to the reactor using a gear pump. In addition, the product phase was removed *via* the phase separator (pulsating).

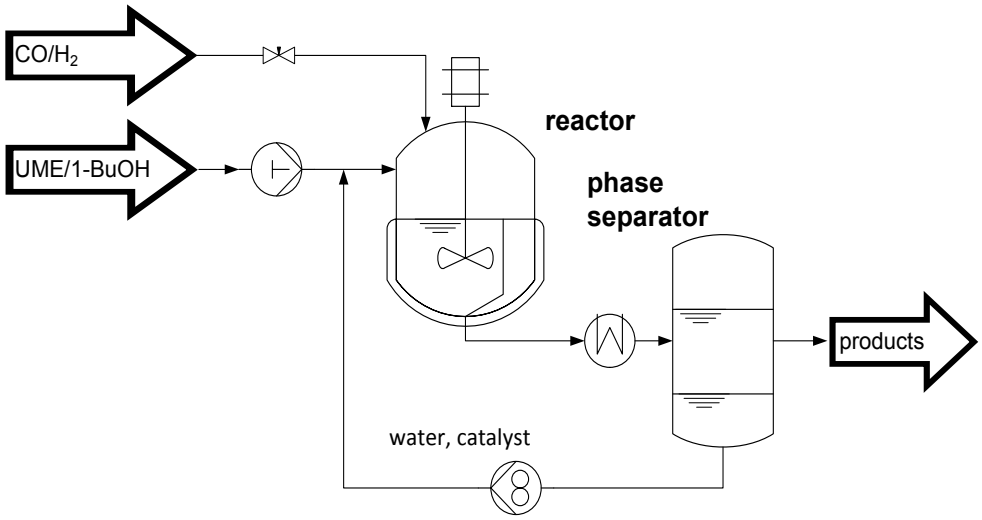

Figure 4.22: Process flow diagram of the miniplant for the hydroformylation of methyl 10-undecenoate.

After the start-up procedure, continuous miniplant operation was achieved (Figure 4.23). A constantly high yield of the linear product **2** at 73% was achieved over the course of miniplant operation over 21 h. In terms of the reaction behavior of the CSTR, virtually the same selectivity was observed compared to prior experiments in the batch autoclave. Only the rhodium loss of 15 ppm by weight into the product stream under continuous operation is higher compared to the batch separation. As the water phase decreased under continuous operation owing to its solubility in 1-butanol, catalyst leaching was likely fa-

vored. Nevertheless, stable process conditions were maintained for 21 h without interference, which demonstrates the stability of the catalyst species under process conditions.

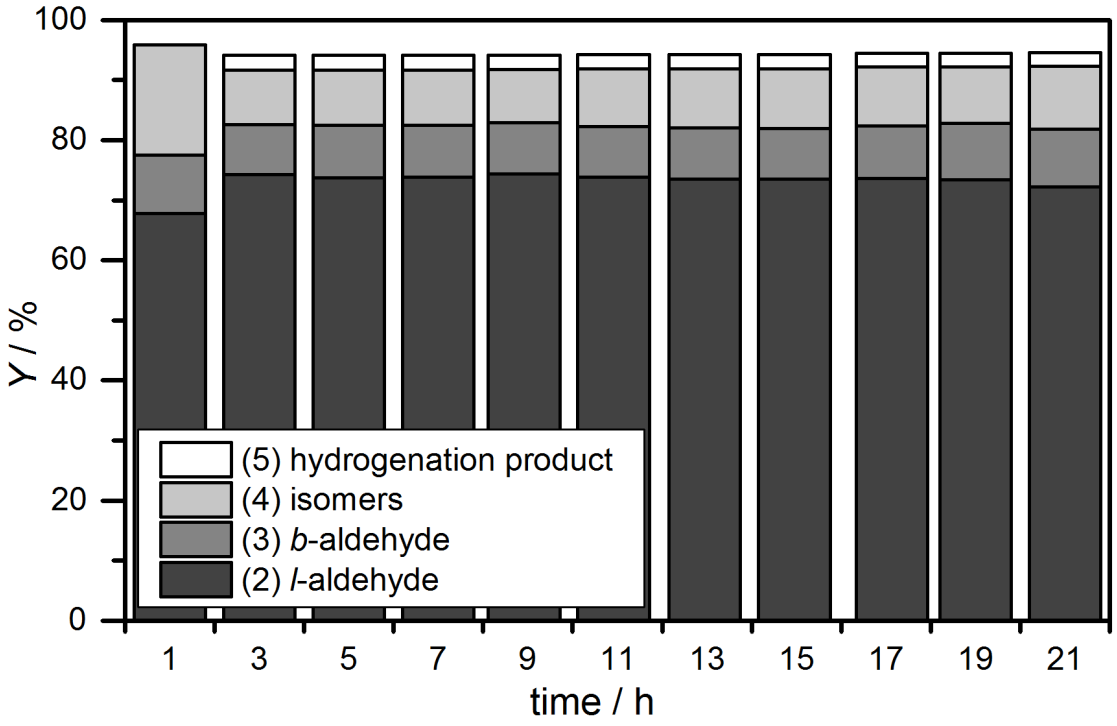

Figure 4.23: Continuous hydroformylation process in a miniplant.
conditions: p= 20 bar, CO:H_2= 1:1, $T_{reaction}$= 140 °C, $T_{separation}$= 5 °C, $w_{n\text{-butanol}}$:w_{H2O}= 1:1, m_{H2O}= 300 g, $m_{Rh(acac)(CO)2}$= 0.275 mmol, $n_{SulfoXantphos}$= 1.375 mmol, $\dot{n}_{UME}$= 100.4 mmol/h, $\dot{V}_{n\text{-butanol}}$= 34.4 g/h

In the scope of this work, an approach for developing of a highly integrated process for the reaction and catalyst separation based on an aqueous TMS-system was explored. This system is especially relevant for separating of medium polar products, as demonstrated by the hydroformylation of 10-undecenoate. The concept, which was initially explored in batch experiments, was then conducted at a continuous miniplant scale. Furthermore, the use of green solvents (water and 1-butanol) suitable for sustainable chemical process development underscores the potential for continued innovation in terms of environmentally-sound chemical processes.

4.3.3. Acknowledgements

This research was conducted in the context of the Sonderforschungsbereich/Transregio 63 “Integrated Chemical Processes in Liquid Multiphase Systems” (TRR63). The authors would like to thank the Deutsche Forschungsgemeinschaft (DFG) for their financial support, Umicore AG & Co.KG for donating the rhodium precursor $Rh(acac)(CO)_2$ and I. Henkel for the ICP-OES analysis. The authors would also like to thank B. Sc. J. Bianga and M.

Sc. J. Weimann for their invaluable support in conducting experiments over the course of this research.

4.4. Hydroesterification of Methyl 10-Undecenoate in Thermomorphic Multicomponent Solvent Systems - Process Development for the Synthesis of Sustainable Polymer Precursors

Tom Gaide, Arno Behr, Alexander Arns, Francesco Benski, Andreas J. Vorholt, *Chem. Eng. Process.* **2016**, *99*, 197–204.

Contributions:

The concept and ideas leading to this publication were developed by me. Alexander Arns and Francesco Benski provided experimental data as part of their bachelor and master thesis respectively. Art-work, literature search and manuscript preparation were done by me. Andreas J. Vorholt and Arno Behr supervised this project and corrected the manuscript.

4.4.1. Abstract

In this paper we present a process concept for the atom economic hydroesterification of renewable methyl 10-undecenoate in thermomorphic multicomponent solvent (TMS) systems. Resulting dimethyl dodecanedioate is a polymer building block used e.g. in Nylon 6,12. As a suitable recycling technique a thermomorphic multicomponent solvent system consisting of methanol and dodecane is employed to recycle the palladium/1,2-bis(di-*tert*-butylphosphinomethyl)benzene/methanesulfonic acid catalyst. Product yields up to 79% and a high regioselectivtiy of 94% to the linear product are obtained. Low leaching of the catalyst into the product phase with 1% in respect of palladium and phosphorous is observed. Robustness and stability of the catalyst is shown in eight recycling runs without any loss of selectivity in the reaction.

4.4.2. Introduction

In times of increasing scarcity of fossil fuels and climatic change the usage of renewable feedstocks in industrial chemistry gets more and more attractive from ecological point of view. For their implementation it would be a great advantage if existing production lines may continue to be used with intermediates gained from renewables.[234] In this paper we describe an alternative process concept for the synthesis of dimethyl dodecanedioate (**2**) based on renewable starting materials.

Main application of dodecanedioic acid is in polyester and polyamide synthesis.[235] Polyamide 6,12 for example, which is synthesised by condensation of dodecanedioic acid with hexamethylenediamine, provides a high melting point (212 °C), high mechanical strength and dimensional stability, high robustness against chemicals and low water absorption.[236]

Industrial synthesis of dodecanedioic acid usually starts from butadiene which is trimerised to 1,5,9-cyclododecatriene (CDT). CDT can be converted into dodecanedioic acid either in a three or a two stage reaction sequence. In case of three reaction steps CDT is initially hydrogenated to cyclododecane. Subsequent oxidation with air or oxygen is carried out yielding in a mixture of cyclododecanol and cyclododecanone. The third reaction step is the oxidation with nitric acid to dodecanedioic acid. The second route consists of a partial hydrogenation of CDT to cyclododecene. Subsequent oxidative ozonolytic cleavage results in desired 1,12-dodecanedioic acid.[235] A possible direct synthesis route based on renewable resources starts from 10-undecenoic acid, which can easily be obtained by pyrolytic cleavage of ricinoleic acid.[230] Andrade and co-workers describe a reaction sequence consisting of hydroformylation of 10-undecenoic acid and subsequent oxidation to the corresponding dicarboxylic acid.[237] Another approach is hydroesterification of methyl

10-undecenoate (**1**) leading to the corresponding linear diester dimethyl dodecanedioate (**2**)[238], which is used instead of the free acid as substrate in condensation reactions to form polyesters or polyamides.

The Hydroesterification is a transition metal catalysed atom-economical direct transformation of unsaturated substrates, carbon monoxide (CO) and an alcohol to form a new ester moiety. In this reaction discovered by Walter Reppe in 1953[76], a wide range of substrates can be applied[239]. In the early 2000s hydroesterification has gained industrial importance since 100.000 tons of methyl propionate per year are synthesised by hydroesterification from ethene.[240–246]

Efficient catalysts for the hydroesterification with high regioselectivity towards the linear product were already described in literature. Cole-Hamilton et al. applied a catalyst consisting of tris(dibenzylideneacetone)dipalladium [$Pd_2(dba)_3$] as precursor, 1,2-bis(di-*tert*-butylphosphinomethyl)benzene (1,2-DTBPMB, Figure 4.26) and methanesulfonic acid (MSA) in hydroesterification of several terminal and internal olefins. This catalyst system is highly selective towards linear products. Even if internal olefins are used as starting materials, linear hydroesterification products are formed *via* isomerisation/hydroesterification tandem reaction (>93% linearity).[143] Since then, this catalyst system was utilised to transform numerous substrates into linear esters. Especially unsaturated esters are interesting starting materials because the corresponding linear diesters are of high interest in polymer synthesis.[152–155] Those linear diesters can be obtained from unsaturated fatty acid methyl esters[144,238], fatty acids[238], triglycerides[145–149] and terpenes[150] with high selectivities. In consequence several studies on catalyst activity[153,157–160] and mechanistic elucidations on isomerising hydroesterification were conducted.[161–163]

A particular challenge in homogeneous palladium-catalysed hydroesterification reactions is the recovery of the valuable noble-metal catalyst. García-Suárez and co-workers reported about palladium/1,2-DTBPMB catalyst immobilisation using ionic liquids in the hydroesterification of ethene.[247] While this system is well suited for simple, short chained olefins, catalyst recycling with more complex substrates is still an issue due to their high boiling points and polar properties.

A promising recycling technique for separating homogeneous catalysts from middle to non-polar products is the application of thermomorphic multicomponent solvent (TMS) systems. These solvent systems take advantage of the temperature dependend miscibility gap of a polar and a non-polar solvent mixture. Heating the solvent system to reaction temperature leads to the formation of one single homogeneous reaction mixture overcom-

ing mass transfer limitations during the reaction. Cooling after reaction initiates phase separation and the polar, catalyst containing phase can be separated from the non-polar product phase *via* simple decantation (Figure 4.24).[31,204]

TMS systems were already successfully applied as catalyst recycling concept in several reactions such as cooligomerisations[42,43], hydrosilylations[40], hydroaminomethylations[49,224,225] and hydroformylations[35,56–59]. The hydroformylation of 1-dodecene was also conducted into miniplant scale enabling a continuous and stable process control.[206]

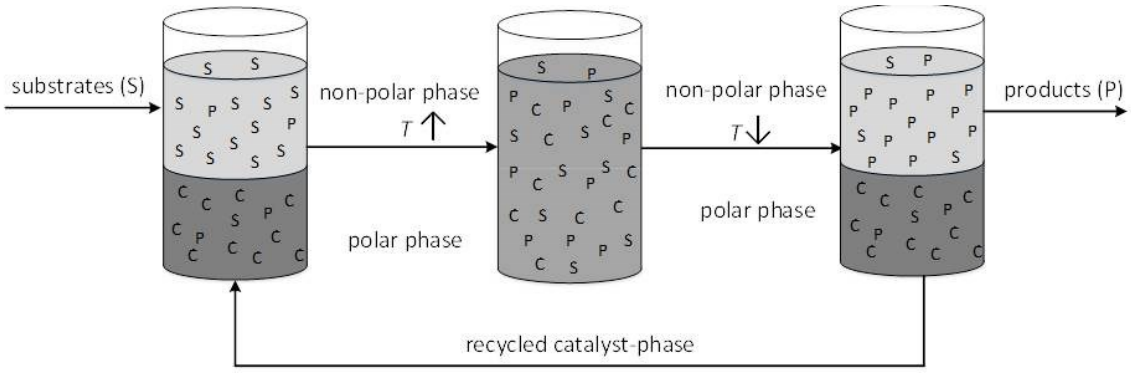

Figure 4.24: Principle of a TMS system.
C=catalyst, P=products, S=substrates, *T*=temperature

The first application of TMS systems in hydroesterification were reported by Behr and Vorholt in the year 2013 in the hydroesterification of methyl oleate[54] and oleyl alcohol[224] using a palladium precursor and XANTphos as ligand (Figure 4.26). Within these reaction systems, the unsaturated C18 compounds were predominately transformed into branched hydroesterification products.

However, application of TMS systems in carbonylation reactions of shorter-chained fatty acid derivates is more challenging due to the higher polarity of substrates and products. Ternel et al. investigated the applicability of TMS systems in hydroformylation of 10-undecenenitrile. The relatively high polarity of the resulting bifunctional product leads to an accumulation (99%) in the polar, catalyst containing phase which made an efficient separation of the catalyst impossible.[74]

Herein, we describe a process concept for the linear hydroesterification of methyl 10-undecenoate (**1**) towards dimethyl dodecanedioate (**2**) using TMS systems as recycling technique.

4.4.3. Materials and Methods

All experiments were conducted under argon atmosphere using Schlenk technique. All chemicals are commercial available. The ligand 1,2-DTBPMB was provided by Digital

Speciality Chemicals Ltd. in a 28 w% solution in methyl propionate. Methyl propionate was removed under reduced pressure before use. Further chemicals were degased and stored under argon. Carbon monoxide was purchased by Messer Industriegase GmbH in 98% purity.

4.4.3.1. Hydroesterification of Methyl 10-Undecenoate

In a typical hydroesterification experiment the palladium precursor and the ligand were weighted into a 20 mL stainless steel autoclave.[248] Afterwards the reactor was evacuated and flushed with argon three times. Then methanol was introduced under inert atmosphere by syringe and the mixture was allowed to stir at 600 rpm for three hours at room temperature under argon atmosphere. Afterwards, dodecane, methyl 10-undecenoate and methanesulfonic acid in methanol were introduced into the reactor inertly. The reactor was pressurised with 30 bar CO and heated to 90 °C. After two hours, the reactor was placed in an ice bath to quench the reaction and was vented. The reaction mixture was introduced into a separating funnel for 20 minutes until phases were separated. Analysis of the composition of phases was conducted by gas chromatography (Hewlett-Packard, HP 6890 Series). The gas chromatograph was equipped with a capillary column (HP-INNOWAX 30 m x 0.25 mm x 0.25 μm) and a flame ionisation detector. 1-Hexanol was used as internal standard. Concentrations of palladium and phosphorous were determined *via* inductive coupled plasma optical emission spectrometry (ICP-OES). For sample preparation for ICP-OES measurement 0.230 g of the non-polar phase was weighted into a Teflon cup. Then 2.5 mL nitric acid (65%) and 4 mL sulfuric acid (96%) were added and a digestion was conducted in a Micro *m*Prep A microwave apparatus (MWS GmbH). Subsequently 2 mL of distilled water and 1 mL hydrogen peroxide solution (30-32%, optima grade, Fisher Chemical) were added. Finally, ICP-OES measurements were conducted with an IRIS Intrepid optical emission spectrometer (Thermo Elemental).

4.4.3.2. Recycling experiments

In a typical hydroesterification recycling experiment, the palladium precursor and the ligand were solved in methanol and stirred at 600 rpm for three hours at room temperature under argon atmosphere. Afterwards, dodecane, methyl 10-undecenoate and methanesulfonic acid in methanol were added to the solution. The reaction solution was transferred into an evacuated 300 mL stainless steel autoclave (Parr Instrument Company), which was purged with argon several times before the transfer. The reactor was pressurised with 30 bar CO and heated to 90 °C. After two hours, the reactor was placed in an ice bath to quench the reaction. Afterwards CO pressure was carefully reduced to 5 bar

and the reaction mixture was transferred into a 40 mL glass pressure tube equipped with a capillary. The mixture was allowed to stand under CO atmosphere at room temperature for 20 minutes to induce phase separation. In this time dodecane, methanol and methyl 10-undecenoate were again introduced inertly into the autoclave using the method described above. Then the catalyst phase was transferred from the pressure tube into the prepared reactor *via* CO excess pressure through a capillary. Finally, the reactor was subjected with 30 bar CO and heated to 90 °C for two hours again.

4.4.4. Results and Discussion

Hydroesterification products of methyl 10-undececenoate (**1**) can be derived into two product groups (Figure 4.25). The desired linear product (**2**) is formed from the terminal double bond. Branched products (**3**) result from hydroesterification of the terminal double bond or internal double bonds generated by isomerisation of the substrate.

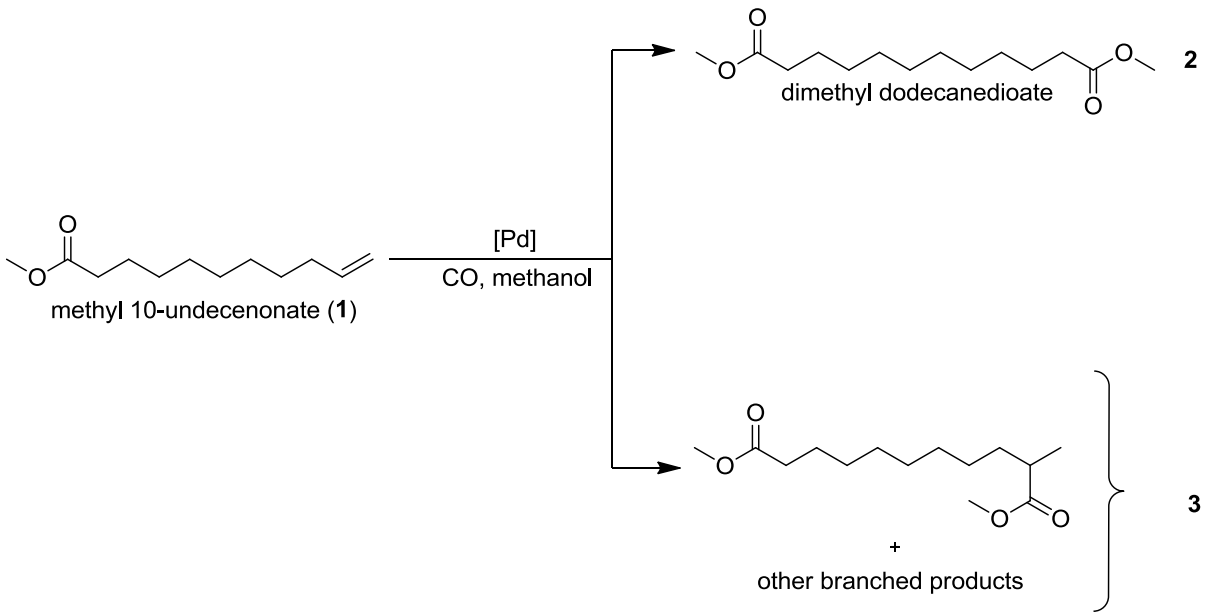

Figure 4.25: Hydroesterification products of methyl 10-undecenoate.

4.4.4.1. Single-phase investigations on the catalyst

For developing a process for the hydroesterification of methyl 10-undecenoate the choice of catalyst is a key parameter. High regioselectivity towards the linear dimethyl dodecanedioate and high catalyst activity are necessary to design an efficient process concept. Investigations on a suitable catalyst were carried out in pure methanol as a polar protic solvent which is also a substrate in the reaction. Previous studies show that steric and electronic properties of the applied ligand have great impact on the reaction rate in hydro-

esterification and isomerisation and the regioselectivity (linear:branched-ratio (*l:b*-ratio)) of the reaction.[157,161]

In this context, we started our studies on catalyst performance by employing several bidentate ligands (Figure 4.26) in order to identify a catalyst, which enables fast reaction rates and a high selectivity towards the desired product (**2**). The employed ligand is also a crucial parameter in terms of catalyst stability.

Different ligands were investigated in combination with the palladium(0)-precursor tris(dibenzylideneacetone)dipalladium ([$Pd_2(dba)_3$]) and methanesulfonic acid (MSA) as co-catalyst. In these first screening experiments the reaction time was set to 16 h.

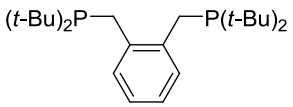

1,2-bis((di-*tert*-butylphosphino)methyl)benzene
1,2-DTBPMB

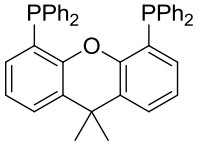

(9,9-dimethyl-9*H*-xanthene-4,5-diyl)bis(diphenylphosphine)
XANTphos

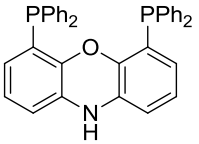

4,6-bis(diphenylphosphino)-10*H*-phenoxazine
NiXANTphos

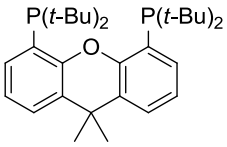

(9,9-dimethyl-9*H*-xanthene-4,5-diyl)bis(di-*tert*-butylphosphine)
t-Bu-XANTphos

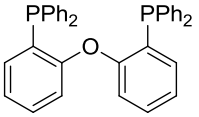

(oxybis(2,1-phenylene))bis(diphenylphosphine)
DPEphos

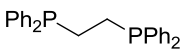

1,2-bis(diphenylphosphino)ethane
DPPE

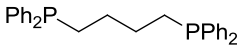

1,4-bis(diphenylphosphino)butane
DPPB

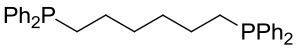

1,6-bis(diphenylphosphino)hexane
DPPH

Figure 4.26: Examined bidentate ligands in hydroesterification of methyl 10-undecenoate.

Usage of 1,2-DTBPMB (Table 4.11, entry 1.1) leads to an outstanding *l:b*-ratio of 96:4 compared with other employed ligands. Previous mechanistical studies show that methanolysis of the linear palladium-acyl species, which is the rate determining step, is faster than methanolysis of branched acyl species due to the steric bulk of the 1,2-DTBPMB ligand.[161] Consequently a high regioselectivtiy towards the linear diester **2** is observed.

In comparison with these results, use of the XANTphos ligand (entry 1.2) leads to a considerably lower *l:b*-ratio of 76:24 under these conditions. Catalyst activity is higher compared with usage of 1,2-DTBPMB and 68% hydroesterification products are obtained instead of 28%. Since the Pd/XANTphos catalyst shows higher reaction rates in hydroesterification under employed conditions and it was shown that a Pd/XANTphos hydroesterification catalyst can be recycled *via* TMS technique already in previous studies [54], we tested different XANTphos derivates with different steric and electronic properties (entries 1.2-1.5) in order to boost the regioselectivity in hydroesterification.

Replacement of XANTphos with *t*-Bu-XANTphos leads to higher basicity of the ligand and a higher steric hindrance around the palladium centre. These changes induce a complete loss of catalytic activity in hydroesterification (entry 1.3).

Already a small enlargement of the bite angle from 111° (XANTphos[249]) to 114° (NiXANTphos[249]) decreases the catalyst activity drastically and only 6% hydroesterification products are formed (entry 1.4). Use of DPEphos (entry 1.5), which has a smaller bite angle (102°) and a less rigid backbone compared with XANTphos, leads to similar results in hydroesterification compared to the Pd/XANTphos catalyst. This results show that basicity and steric properties of the employed ligand are crucial parameters for the performance of the corresponding hydroesterification catalyst. However, in comparison to the use of 1,2-DTBPMB all tested XANTphos-type ligands show lower regioselectivities in hydroesterification.

In respect to the costs of the ligand, simple alkyl-bridged bidentate diphenyl phosphines could be an interesting alternative for a hydroesterification process, if a satisfying reaction performance could be obtained. For this reason we also tested the ligands DPPE, DPPB and DPPH in the hydroesterification of methyl 10-undecenoate (entries 1.6-1.8). The reactivity of the corresponding catalysts increases with growing alkyl bridge chain length and bite angle. Yields of 64% in hydroesterification are reached, but the regioselectivity is significantly lower compared with usage of 1,2-DTBPMB. For this reason further investigations were carried out by use of 1,2-DTBPMB as ligand.

Table 4.11: Investigations on the catalyst [a].

Entry	Ligand [b]	Precursor [c]	X_1 [d]	Y_2	Y_3	*l:b*
1.1	1,2-DTBPMB	$[Pd_2(dba)_3]$	28	27	1	96:4
1.2	XANTphos	$[Pd_2(dba)_3]$	68	52	16	76:24
1.3	*t*-Bu-XANTphos	$[Pd_2(dba)_3]$	-	-	-	-
1.4	NiXANTphos	$[Pd_2(dba)_3]$	6	5	1	83:17
1.5	DPEphos	$[Pd_2(dba)_3]$	63	47	16	75:25
1.6	DPPE	$[Pd_2(dba)_3]$	-	-	-	-
1.7	DPPB	$[Pd_2(dba)_3]$	7	4	3	57:43
1.8	DPPH	$[Pd_2(dba)_3]$	64	48	16	75:25
1.9	1,2-DTBPMB	$Pd(acac)_2$	24	22	2	92:8
1.10	1,2-DTBPMB	$Pd(hfacac)_2$	26	25	1	93:7

[a] 0.1 mol% [Pd], 1 mol% ligand, 20 mol% methanesulfonic acid (MSA), 5 mmol methyl 10-undecenoate, 5 mL methanol, T = 90 °C, p_{CO} = 30 bar, t = 16 h, 600 rpm, yield (*Y*), conversion (*X)* and ratio of linear and branched hydroesterification products (*l:b*) were determined by GC-FID, results in [%].
[b] abbreviations see Figure 4.19
[c] dba=dibenzylideneacetone, acac=acetylacetonate, hfacac=hexafluoroacetylacetonate
[d] double bond isomerisation is not considered in conversion

Since the active catalyst is assumed to be a palladium(II)-hydride species[143], we were interested in the impact of precursors oxidation state and counter ion on the reaction rate (entries 1.1; 1.9-1.10). Use of palladium(II)-precursor palladium(II)acetylacetonate ($Pd(acac)_2$) results in a slightly lower activity and a lower *l:b*-ratio compared to palladium(0)-precursor $[Pd_2(dba)_3]$. The fluorinated equivalent palladium(II)hexafluoroacetylacetonate ($Pd(hfacac)_2$) shows comparable reactivity to the use of $[Pd_2(dba)_3]$. Results show only a small influence of precursors oxidation state and counter ion.

The third component of the catalyst is the acid, which acts as a co-catalyst. The catalytic active cationic palladium(II)-hydride species can be generated and stabilised by strong acids like MSA.[77,250] In order to investigate the influence of the type of the co-catalyst, we tested several different acids as an alternative to MSA, namely trifluoracetic acid, trifluormethanesulfonic acid, sulfuric acid, *para*-toluenesulforic acid, trichloracetic acid and hydrochloric acid (~35 w% in water). Some of them (triflouracetic acid, *para*-toluenesufonic, hydrochloric acid) lead to yields of more than 20% of the desired linear product, some of them (trifluormethanesulfonic acid, sulfuric acid, trichloracetic acid) are less active under the applied conditions. However, highest yields of 27% of **2** are obtained by the use of

MSA, so the catalyst consisting of $[Pd_2(dba)_3]$, 1,2-DTBPMB and methanesulfonic acid MSA, was transferred to TMS systems.

4.4.4.2. Investigation on catalyst activity and stability in TMS systems

In order to design a suitable TMS system we initially imposed several requirements on our solvent system:

- The polar catalyst phase has to be methanol since methanol also acts as substrate in this reaction
- Separating of the product and catalyst phase should be possible at room temperature
- The mixture must be homogenous at the reaction temperature of 90 °C to prevent phase transfer issues

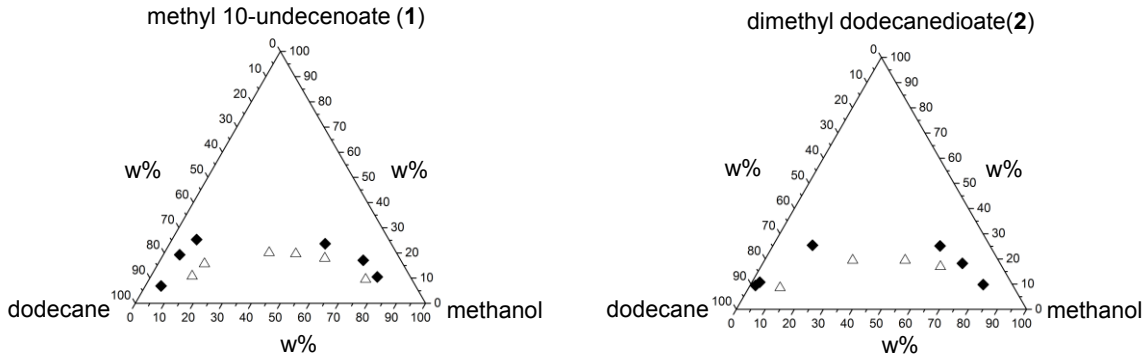

Figure 4.27: Ternary plots of methanol/dodecane/substrate and methanol/dodecane/product at 25 °C (♦) and 60 °C (▲).

Solvent screening experiments showed that a solvent system composed of methanol as polar catalyst phase and dodecane as non-polar product phase meets our requirements made above. Ternary diagrams of methanol/dodecane/**1** and methanol/dodecane/**2** (Figure 4.27) show that this TMS system is suitable if a composition of 40 w% methanol 40 w% dodecane and 20 w% substrate is used even if 100% conversion towards hydroesterification products is achieved. For this reason this composition was chosen as reference system for subsequent investigations on catalyst activity and stability in TMS systems. At first, we tried to transfer the conditions from the investigations with pure methanol (Table 4.11, entry 1.1) into the methanol/dodecane TMS system (Table 4.12, entry 2.1). However, lower activities in hydroesterification reaction are observed and only 9% of the linear product (**2**) is formed, even after 16 h. With dodecane as co-solvent precipitation of palladium black is observed. We concluded that the catalyst is not stable under these

conditions and decided to vary the ratios of palladium to ligand and palladium to MSA in order to determine the influence of these parameters on catalyst activity and stability in the chosen TMS system (Table 4.12 and Table 4.13).

Table 4.12: Investigation on MSA influence in TMS systems [a].

Entry	Pd/MSA	X_1 [b]	Y_2	Y_3	*l:b*
2.1 [c]	1/200	10	9	1	90:10
2.2	1/45	28	27	1	96:4
2.3	1/40	32	31	1	97:3
2.4	1/35	38	36	2	95:5
2.5	1/30	34	33	1	97:3
2.6	1/25	28	27	1	96:4
2.7	1/15	26	25	1	96:4

[a] 0.05 mol% [$Pd_2(dba)_3$], 1 mol% 1,2-DTBPMB, methanesulfonic acid (MSA), 5 mmol methyl 10-undecenoate, 4 g solvent $w_{methanol}/w_{docecane}$ = 50/50, T = 90 °C, p_{CO} = 30 bar, t = 2 h, 600 rpm, yield (*Y*), conversion (*X*) and ratio of linear and branched hydroesterification products (*l:b*) were determined by GC-FID, results in [%].
[b] double bond isomerisation is not considered in conversion
[c] t = 16 h

The active catalyst is assumed to be a palladium(II)-hydride complex, which can be generated and stabilised by strong acids like MSA.[77,250] In consequence, we started our investigations on catalyst activity and stability by varying the amount of MSA (Table 4.12, entries 2.1-2.7). Reduction of MSA amount leads to substantial gain of activity in hydroesterification. Highest yields of **2** (36%) after two hours are reached using a 35 fold excess of MSA to palladium (Entry 2.4). Under these conditions, the catalyst activity is 30 times higher than the activity obtained applying a Pd/MSA-ratio of 1/200. Additionally, no precipitation of palladium black is observed. Higher or lower Pd/MSA ratios lead to catalyst deactivation.

Although presence of MSA is necessary to stabilise the palladium(II)-catalyst, too high acid concentrations may lead to ligand protonation resulting in formation of quaternary phosphonium salts, which are unable to coordinate to the palladium centre. In order to determine the interaction between ligand and MSA, we varied the ratio of these two catalyst components (Table 4.13).

Entries 3.1-3.5 show experiments in which the ratio of palladium and ligand is varied in the range of 1/5 and 1/20 at a 35 fold excess of MSA in respect to palladium. It can be seen that a maximum of catalyst activity exists at a Pd/1,2-DTBPMB-ratio of 1:10 (entry 3.3).

Lowering the amount of ligand leads to formation of palladium black and lower yields of hydroesterification products are obtained. Increasing the amount of ligand also leads to lower activity but no precipitated palladium is observed. It seems that high excess of ligand favours formation of catalytic inactive palladium species while too low amounts result in formation of palladium black. Palladium black is also formed at high concentrations of MSA (Table 4.12, entries 2.1-2.3) indicating, that the ratio of MSA/ligand is a crucial parameter for catalyst stability.

If there is some kind interaction between the ligand and the MSA, comparable catalyst activities should be obtained if the same ligand/MSA ratio is applied in the reaction. Comparison of entry 3.3 with 3.6 shows this coherence. Entry 3.6 shows the results if both the amount of ligand and the amount of MSA are doubled compared to entry 3.3 and nearly the same catalytic activity is obtained. Also no precipitation of palladium black is observed in both cases. In conclusion, if the ratio of MSA/ligand is too high, catalyst deactivates under formation of palladium black. We assume that the amount of protonated ligand is too high, so the ligand is not able to stabilise the palladium catalyst any more. If MSA/ligand ratio is too low, catalytically inactive species are formed without precipitation of palladium black. This is probably due to a blockage of the free coordination sites of the catalyst at high excesses of the free ligand.

Table 4.13: Investigations on catalyst stability and activity in TMS systems [a].

Entry	Pd	1,2-DTBPMB	MSA	X_1 [b]	Y_2	Y_3	*l:b*
3.1	1	5	35	15	14	<1	-
3.2	1	7.5	35	25	24	<1	-
3.3	1	10	35	38	36	2	95:5
3.4	1	15	35	32	30	2	94:6
3.5	1	20	35	13	13	<1	-
3.6	1	20	70	37	35	2	95:5
3.7	1	10	30	34	33	1	97:3
3.8	1	5	15	24	23	1	96:4
3.9 [c]	1	10	35	84	79	5	94:6

[a] 0.05 mol% [$Pd_2(dba)_3$], 1,2-DTBPMB, methanesulfonic acid (MSA), 5 mmol methyl 10-undecenoate, 4 g solvent $w_{methanol}/w_{docecane}$ = 50/50, T=90 °C, p_{CO} = 30 bar, t = 2 h, 600 rpm, yield (Y), conversion (X) and ratio of linear and branched hydroesterification products (*l:b*) were determined by GC-FID, results in [%].
[b] double bond isomerisation is not considered in conversion
[c] t = 23 h

In view of a chemical process, using as low amounts of ligand and co-catalyst as possible is highly desired. Therefore we tried to reduce amounts of MSA and 1,2-DTBPMB (comparing entry 3.7 and entry 3.8). Applying a Pd/1,2-DTBPMB/MSA-ratio of 1/5/15 leads to lower catalyst activity (24% conversion) compared to a ratio of 1/10/30 (34% conversion). So too low concentrations of ligand and MSA lead to lower hydroesterification activity.

In consequence, we decided to use a Pd/1,2-DTBPMB/MSA-ratio of 1/10/35 for our further investigations on phase behaviour and catalyst recycling in TMS systems. With this system, a yield of 79% of **2** after 23 h is obtained (entry 3.9). These results are comparable with the results which were reported before for the hydroesterification of methyl 10-undecenoate in pure methanol.[238]

4.4.4.3. Investigations on TMS composition

For the process, the composition of a TMS system is an important point since key indicators like distribution of product, substrate and catalyst or reactivity depend on it. In case of hydroesterification, impact of reactivity is even higher because methanol has two roles as solvent and substrate.

For this reason, we examined the influence of methanol amounts in the reaction system (Table 4.14**,** entries 4.1-4.3). In respect to hydroesterification performance higher amounts of methanol (comparing entry 4.3 with 4.2 and 4.1) lead to high yields of 50% **2** after 2 h. This observance can mechanistically be attributed to the circumstance that methanolysis of the palladium-acyl complex is the rate determining step using a Pd/1,2-DTBPMB catalyst.[161–163] Values for catalyst leaching into the product phase are less than one percent for palladium and phosphorous if a methanol/dodecane ratio of 70/30 is used. In this case, however, only 9% of the formed product **2** is extracted into the dodecane phase which disqualifies this TMS composition in view of a continuous process. Applying a methanol/dodecane-ratio of 30/70 (entry 4.1) leads to a lower activity in hydroesterification with only 22% yield of **2,** but advantageously 72% of the product is extracted into the product phase. We decided to use a 50/50 ratio of methanol and dodecane (entry 4.2) which seems to be the best compromise between activity in hydroesterification (35% of **2**), catalyst loss (1% Pd and P) and product extraction (40%). Another important aspect in TMS design is the difference of polarity of the used non-polar solvents. In order to determine this influence, we varied the alkane chain length from decane to hexadecane (entries 4.2; 4.4-4.6).

Use of decane, dodecane and tetradecane leads to comparable results in terms of activity and regioselectivity. If hexadecane is applied, slightly lower yields of **2** (29%) are ob-

tained. The catalyst leaching into the product phase is slightly higher by usage of decane (Entry 4.4) as non-polar solvent compared to other applied alkanes.

No significant influence on product extraction is determined by varying alkane chain length. In conclusion, a TMS composition of methanol/dodecane in a ratio 50/50 seems to be the most promising and was used for subsequent recycling experiments.

Table 4.14: Investigations on phase behaviour of the TMS system [a].

Entry	Non-polar solvent	$w_{methanol}/w_{non\text{-}polar\ solvent}$ [b]	X_1 [c]	Y_2	Y_3	*l:b*	w_{Pd} [d]	w_P [d]	w_2 [d]
4.1	dodecane	30/70	25	22	3	88:12	99:1	97:3	28:72
4.2	dodecane	50/50	37	35	2	95:5	99:1	99:1	60:40
4.3	dodecane	70/30	53	50	3	94:6	>99:1	>99:1	91:9
4.4	decane	50/50	38	35	3	92:8	98:2	98:2	66:34
4.5	tetradecane	50/50	41	38	3	93:7	99:1	99:1	66:34
4.6	hexadecane	50/50	31	29	2	94:6	99:1	>99:1	68:32

[a] 0.05 mol% $[Pd_2(dba)_3]$, 1 mol% 1,2-DTBPMB, 3.5 mol% methanesulfonic acid (MSA), 15 mmol methyl 10-undecenoate, 12 g solvent, methanol as polar solvent, T = 90 °C, p_{CO} = 30 bar, t = 2 h, 600 rpm, temperature of phase separation: 25 °C, yield (*Y*), conversion (*X),* ratio of linear and branched hydroesterification products (*l:b*) and distribution of 2 were determined by GC-FID, distribution of Pd and P were determined by ICP-OES, results in %.
[b] ratio before reaction
[c] double bond isomerisation is not considered in conversion
[d] distribution of Pd, P and 2**,** in methanol:non-polar solvent

The component distribution in the methanol/dodecane TMS system after reaction is summarised in Table 4.20.

Table 4.15: Component distribution in methanol/dodecane TMS system.

	Substrate (1) [%]	Product (2) [%]	Methanol [%]	Dodecane [%]	Catalyst [%]
dodecane phase	59	40	11	85	1
methanol phase	41	60	89	15	99

4.4.4.4. Catalyst recycling experiments

In order to prove applicability of the methanol/dodecane TMS system we conducted three sets of recycling experiments. Figure 4.28 shows the yield in grams of **2** in the dodecane phase after reaction and phase separation. In the first set of recycling experiments (set 1) no refreshment of any catalyst component was made. In run 0, which represents an experiment with fresh catalyst, a yield of 1.03 g **2** is obtained which is in good accordance with the results presented above. While in the first recycling run (run 1) the yield of **2** is only slightly lower compared to run 0, catalytic activity drastically decreases in run 2 and 3. In contrast, the *l:b*-ratio of the formed products in run 3 is 99:1 and even higher compared to run 0 (94:6). Precipitation of palladium black is not observed in any recycling run in this set. In accordance to the results discussed in 3.2, we assumed that there is a MSA leaching into the product phase during the phase separation or a deactivation, maybe *via* esterification of MSA with methanol. Also the catalyst phase slightly decreases during these recycling experiments.

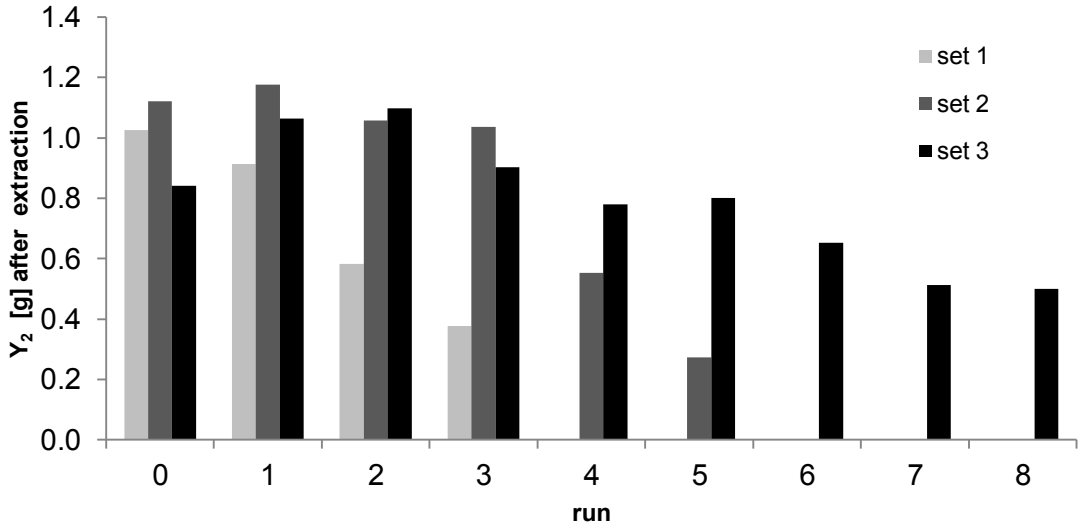

Figure 4.28: Catalyst recycling experiments [a].
[a] run 0: 0.05 mol% [$Pd_2(dba)_3$], 1 mol% 1,2-DTBPMB, 3.5 mol% methanesulfonic acid (MSA), 30 mmol methyl 10-undecenoate, 24 g solvent, methanol/dodecane = 50/50, T = 90 °C, p_{CO} = 30 bar, t = 2 h, 600 rpm, temperature of phase separation: 25 °C, yield (Y) and ratio of linear and branched hydroesterification products (*l:b*) were determined by GC-FID.
set 1: Run 1-3: Addition of 10.2 g dodecane, 1.1 g methanol and 3.6 g 1
set 2: Run 1-5: Addition of 10.2 g dodecane, 1.4 g methanol, 10 mg MSA and 3.6 g 1
set 3: Run 1-8: Addition of 10.2 g dodecane, 2.2 g methanol, 20 mg MSA and 3.6 g 1

For this reason we conducted a second set of recycling experiments (set 2), in which slightly higher amounts of methanol and 10 mg MSA were added after each run. This corresponds to 10% of the starting value of MSA. In these experiments we were able to obtain comparable yields of **2** over three recycling runs. The yield in run 1 is even slightly higher compared to run 0 when fresh catalyst is used. This can be ascribed to an accumu-

lation of the product in the first recycling experiments. Decreasing of catalytic activity is observed from run 4. Ratio of linear and branched hydroesterification products is 99:1 after run 5 in this case. Again, no precipitation of palladium black is observed within all recycling runs, which would indicate to high ratios of MSA/ligand.

In conclusion, we performed a third set of recycling experiments (set 3) doubling the MSA addition after each run (20 mg, 20% of initial value). Reaction behaviour is comparable to the second set of recycling experiments until run 3. Afterwards the catalyst activity decreases distinctly slower compared the second set of recycling experiments. Yield of **2** obtained in run 8 of set 3 is still about two times higher as against the yield of **2** in run 5 in set 2. After run 7 and run 8 precipitating of palladium is observed, which is an indicator for a too high acid concentration.

These experiments show that the developed reaction system is a suitable process concept for the hydroesterification of methyl 10-undecenoate (**1**). The catalyst has a high activity and selectivity in hydroesterification using a TMS system consisting of methanol and dodecane. Figure 4.29 shows a concept for a continuous hydroesterification process. Further purification of the products could be obtained by crystallisation of dimethyl dodecanedioate or distillation of the solvent and the not converted substrate. In respect of a continuous process dodecane and methyl 10-undeceneoate (**1**) could be recycled after these downstream process steps. The concentrations of MSA and 1,2-DTBPMB in the reaction mixture are crucial parameters for the catalyst stability. For further investigations in larger scale an *in operando* pH-control could be implemented in the reactor. The ligand concentration could be monitored by ICP-OES measurements of phosphorus in the product phase. With these analytic improvements well defined make up streams could be applied in order to ensure a stable process control.

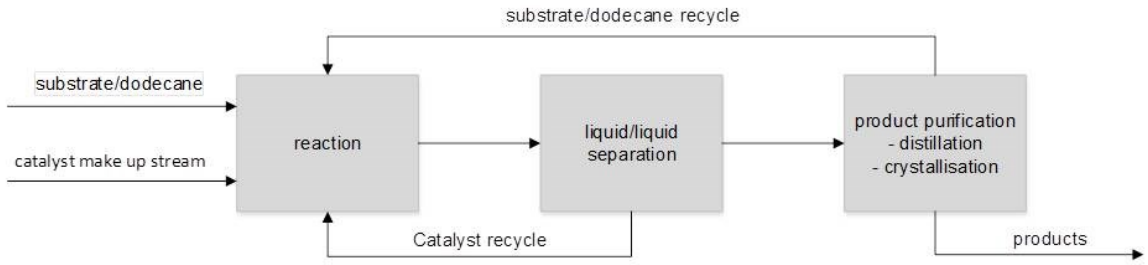

Figure 4.29: Concept for a continuous hydroesterification process.

4.4.5. Conclusion

In this contribution we present the development of a process concept for synthesis of dimethyl dodecanedioate *via* hydroesterification of renewable methyl 10-undecenoate in a

thermomorphic multicomponent solvent (TMS) system consisting of methanol and dodecane. The resulting product is applicable in polyester and polyamide synthesis. The catalytic system consisting of [$Pd_2(dba)_3$)]/1,2-DTBPMB and MSA is highly selective towards the linear dimethyl dodecanedioate (94%) and yields up to 79% are obtained. The ratio of palladium, ligand and MSA is identified as a crucial parameter for catalyst activity and stability. The leaching values of palladium and phosphorous into the product phase are very low (about 1%) and the product can easily be extracted into the non-polar phase. The activity of the catalyst can be maintained over 9 runs without any reduction of the selectivity towards the desired linear diester.

4.4.6. Acknowledgements

This work is part of the Sonderforschungsbereich/Transregio 63 “Integrated Chemical Processes in Liquid Multiphase Systems”. The authors thank the Deutsche Forschungsgemeinschaft (DFG) for financial support, the Umicore AG & Co. KG for the gift of the palladium precursors and the Digital Speciality Chemicals Ltd. for the gift of the ligand 1,2-DTBPMB.

4.5. Catalyst Comparison in the Hydroesterification Methyl 10-undecenoate in Thermomorphic Solvent Systems

Tom Gaide, Arno Behr, Michael Terhorst, Alexander Arns, Francesco Benski, Andreas J. Vorholt, *Chem. Ing. Tech.* **2016**, *88*, 158–167.

Contributions:

The concept and ideas leading to this publication were developed by me. Michael Terhorst, Alexander Arns and Francesco Benski provided experimental data as part of their bachelor and master thesis respectively. Art-work, literature search and manuscript preparation were done by me. Andreas J. Vorholt and Arno Behr supervised this project and corrected the manuscript.

4.5.1. Abstract

This work compares two homogeneous palladium catalysts for the hydroesterification of methyl 10-undecenoate to form dimethyl dodecanedioate. The reaction rates of both catalysts were tested in thermomorphic solvent systems and the reaction conditions were optimized. Afterwards the separation of catalyst and product was investigated and the applicability of thermomorphic solvent systems was validated *via* catalyst recycling experiments.

4.5.2. Einleitung

Aufgrund der zunehmenden Verknappung fossiler Rohstoffe wird die stoffliche Nutzung nachwachsender Ressourcen in der chemischen Industrie aus ökologischen und ökonomischen Gesichtspunkten zunehmend wichtiger. Idealerweise erfolgt die Implementierung von Substraten auf Basis nachwachsender Rohstoffe so, dass bestehende Produktionslinien weiter genutzt werden können.[234] In diesem Zusammenhang wird in dieser Arbeit eine nachhaltige Synthese von Dodecandisäuredimethylester ausgehend vom nachwachsenden Rohstoff 10-Undecensäuremethylester untersucht.

Dodecandisäure findet hauptsächlich Anwendung als Polymerbaustein für die Synthese von Polyestern und Polyamiden.[235] So lässt sich Nylon 6,12 beispielsweise durch die Kondensation von Dodecandisäure mit Hexamethylendiamin herstellen. Nylon 6,12 besitzt einen hohen Schmelzpunkt (212 °C), hohe mechanische und dimensionale Stabilität, sowie eine geringe Wasserabsorption[236].

Industriell wird Dodecandisäure ausgehend von Butadien hergestellt. Zunächst erfolgt die Trimerisierung von Butadien zu 1,5,9-Cylododecatrien (CDT). Ausgehend vom CDT kann die weitere Synthese entweder über einen zwei- oder einen dreistufigen Prozess erfolgen. Im dreistufigen Verfahren erfolgt zunächst eine vollständige Hydrierung von CDT zu Cyclododecan. Anschließend wird Cyclododecan in einer Oxidation zu einem Gemisch aus Cyclododecanol und Cyclododecanon umgesetzt. Dieses Gemisch wird letztlich mit Salpetersäure zur Dodecandisäure oxidiert (Figure 4.30, Route A). Im Zweistufenverfahren wird CDT zunächst partiell zu Cyclododecen hydriert. Die anschließende oxidative, ozonolytische Spaltung des Cyclododecen führt zur Bildung der gewünschten Dodecandisäure (Figure 4.30, Route B).[235]

Eine Synthese unter dem Einsatz nachwachsender Rohstoffe geht von 10-Undecensäure aus, die leicht durch pyrolytische Spaltung aus Rizinolsäure gewonnen werden kann.[230] In einer zweistufigen Variante erfolgt eine Hydroformylierung der Doppelbindung der 10-

Undecensäure gefolgt von der Oxidation der gebildeten Aldehydfunktion zur Dodecandisäure.[237]

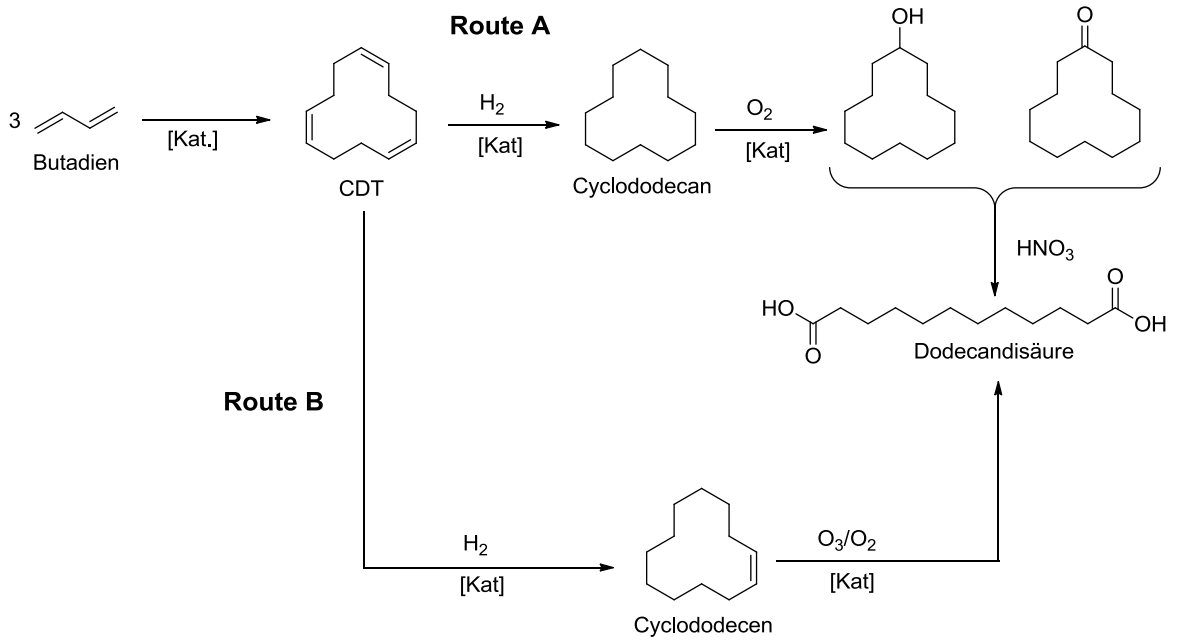

Figure 4.30: Industrielle Synthesen von Dodecandisäure.

Der hier beschriebene alternative Ansatz ist die einstufige Hydroesterifizierung von 10-Undecensäuremethylester mit Kohlenmonoxid und Methanol zum korrespondierenden, linearen 1,12-Dodecandisäuredimethylester (Figure 4.33).[238]

Die Hydroesterifizierung, 1953 entdeckt von Walter Reppe[76], ist eine übergangsmetallkatalysierte, atomökonomische Umsetzung eines ungesättigten Substrates mit Kohlenmonoxid (CO) und einem Alkohol unter Ausbildung einer Esterfunktion (Figure 4.31).

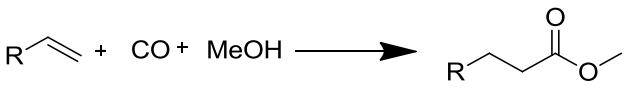

Figure 4.31: Allgemeine Reaktionsgleichung der Hydroesterifizierung.

Seit den frühen 2000er Jahren hat die Hydroesterifizierung durch die Synthese von Propionsäuremethylester ausgehend von Ethen (etwa 100.000 t pro Jahr) auch große industrielle Relevanz erlangt.[240–246] In der Literatur sind bereits effiziente Katalysatoren für die Hydroesterifizierung mit hoher Regioselektivität zur Synthese linearer Ester beschrieben. Cole-Hamilton et al. verwendeten einen Katalysator aus Tris(dibenzylidenaceton)dipalladium ($Pd_2(dba)_3$), dem Liganden 1,2-Bis(di-*tert*-butylphosphinomethyl)benzol (1,2-DTBPMB, Figure 4.34) und Methansulfonsäure (MSA) für die Hydroesterifizierung terminaler und interner Olefine, wobei in allen Fällen eine hohe Regioselektivität (>93%) zum linearen Ester beobachtet wurde.[143] Seit-

dem wurden zahlreiche Substrate mit Hilfe dieses Katalysators hydroesterifiziert, wobei insbesondere der Einsatz ungesättigter Esterverbindungen als Substrat sehr attraktiv ist, da die resultierenden Diester interessant für die Polymersynthese sind.[152–155] Geeignete Substrate auf Basis nachwachsender Rohstoffe sind beispielsweise ungesättigte Fettsäuremethylester[144,238], Fettsäuren[144], Triglyceride[145–149] und Terpene[150]. Aus diesem Grund wurden zahlreiche Studien zur Katalysatoraktivität –und Selektivität[153,157–160] sowie zum Mechanismus der Hydroesterifizierung unter Verwendung des Palladium/1,2-DTBPMB-Katalysators[161–163] durchgeführt.

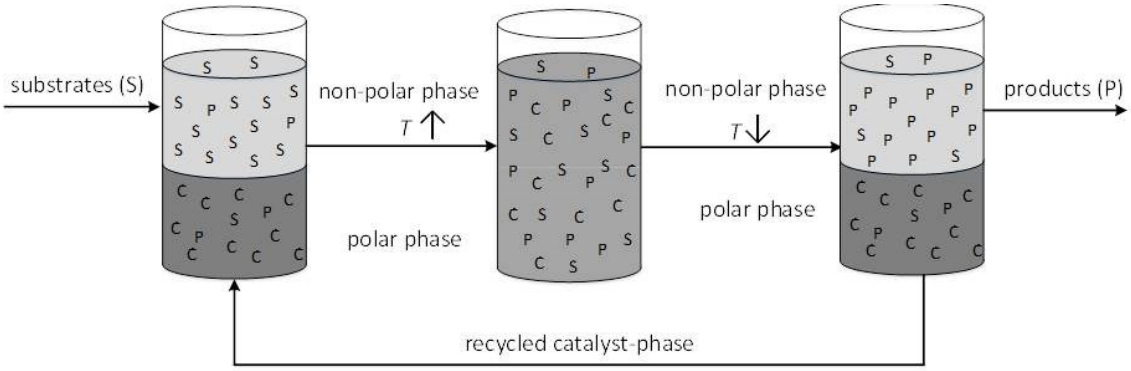

Figure 4.32: Prinzip eines TMS-Systems [a].
[a] C=Katalysator, P=Produkte, S=Substrate, *T*=Temperatur

Die Abtrennung des homogenen Palladiumkatalysators stellt in der Hydroesterifizierung eine besondere Herausforderung dar. García-Suárez et al. berichten über die Hydroesterifizierung von Ethen in ionischen Flüssigkeiten. Der Palladium/1,2-DTBPMB-Katalysator ist dabei in der ionischen Flüssigkeit immobilisiert. Nachdem das Produkt abgetrennt ist, kann der Katalysator erneut verwendet werden.[247] Die Abtrennung von langkettigen Diestern, die durch die Hydroesterifizierung von Ölsäuremethylester an einem Palladium/XANTphos-Katalysator (Figure 4.34) entstehen, wurde von Behr et al. beschrieben[54]. Dabei wird das Prinzip der „Thermomorphen Lösungsmittelsysteme“ (TMS-Systeme) verwendet. TMS-Systeme nutzen die Temperaturabhängigkeit der Mischungslücke eines polaren und eines unpolaren Lösungsmittels aus. Vor Beginn der Reaktion liegt der Katalysator meist in einem polaren Lösungsmittel vor, während das Substrat in einem unpolaren Lösungsmittel gelöst ist. Bei niedrigen Temperaturen bildet ein solches System zwei Phasen aus. Wird die Reaktionsmischung auf Reaktionstemperatur erhitzt, führt dies zur Bildung eines einphasigen, homogenen Reaktionsgemisches und die Reaktion kann ohne Stofftransportlimitierungen stattfinden. Nach Beendigung der Reaktion kann die erneute Phasentrennung durch Abkühlen der Reaktionslösung induziert werden. Die polare Katalysatorphase kann von der unpolaren Produktphase durch einfaches Dekantieren getrennt

werden (Figure 4.32).[31,204] Der Einsatz von TMS-Systemen ermöglicht also eine einfache, effiziente und schonende Trennung von Katalysator und Produkt.

Neben dem Einsatz in der Hydroesterifizierung konnten TMS-Systeme bereits in mehreren Reaktionen, wie Cooligomerisierungen[42,43], Hydrosilylierungen[40], Hydroaminomethylierungen[49,224,225] oder Hydroformylierungen[35,39,56,57,59] erfolgreich als Strategie zum Recycling homogener Katalysatoren eingesetzt werden.

Der Einsatz von TMS-Systemen in Carbonylierungsreaktionen mit kurzkettigen Oleoverbindungen ist aufgrund der höheren Polarität der Produkte verglichen mit langkettigen Fettstoffen eine besondere Herausforderung. Ternel et al. untersuchten die Einsatzmöglichkeiten von TMS-Systemen in der Hydroformylierung von 10-Undecennitril. Die Produkte konnten mit dieser Methode jedoch nicht erfolgreich vom Katalysator getrennt werden.[74]

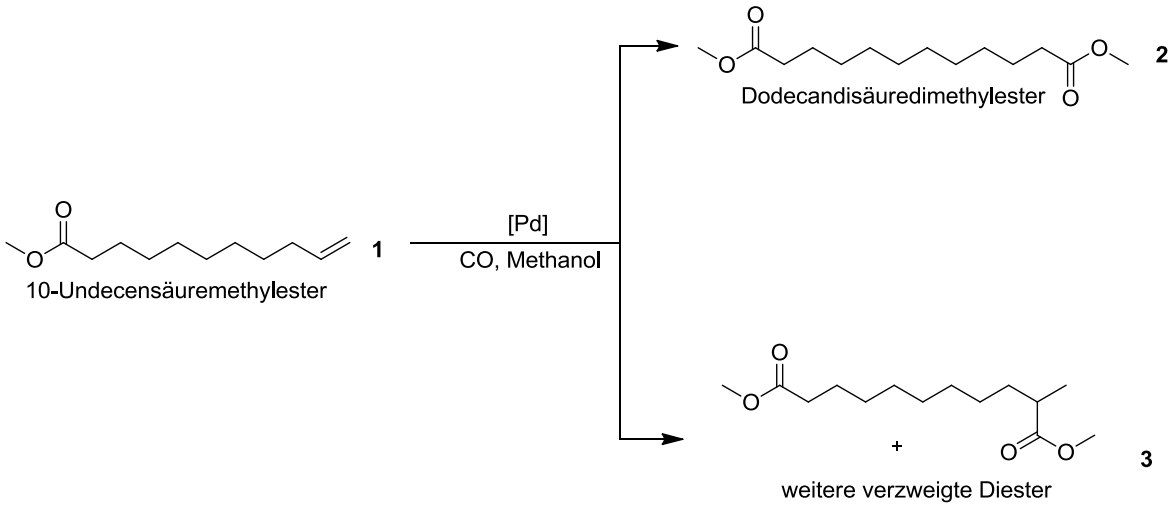

Figure 4.33: Produktspektrum der Hydroesterifizierung von 10-Undecensäuremethylester.

In dieser Arbeit sollen verschiedene Katalysatoren in der Hydroesterifizierung von 10-Undecensäuremethylester in Bezug auf die Reaktionsrate, die Abtrennbarkeit der Produkte in TMS-Systemen und der Robustheit in Bezug auf das Recycling des Katalysators hin untersucht und verglichen werden.

4.5.3. Experimenteller Teil

Alle Experimente wurden unter Argonatmosphäre unter der Verwendung der Schlenk-Technik durchgeführt. Alle Chemikalien sind kommerziell erhältlich. Die Palladiumvorstufe wurde von der Umicore gespendet. Der Ligand 1,2-DTBPMB wurde von Digital Speciality Chemicals Ltd. als 28 w%ige Lösung in Propionsäuremethylester gespendet. Das Lö-

sungsmittel wurde vor Benutzung im Vakuum entfernt. 10-Undecensäuremethylester (96%) wurde von TCI bezogen. Alle Chemikalien wurden entgast und unter Argon gelagert. Kohlenmonoxid wurde von Messer Industriegase GmbH in 98%iger Reinheit bezogen.

In einem typischen Hydroesterifizierungsexperiment werden die Palladiumvorstufe und der Ligand in einem 20 mL-Autoklaven aus Edelstahl vorgelegt. Danach wird der Reaktor evakuiert und mit Argon gespült. Methanol wird hinzugegeben und die Lösung für drei Stunden bei Raumtemperatur gerührt. Anschließend werden Dodecan, 10-Undecensäuremethylester und MSA in den Reaktor gegeben. Der Reaktor wird mit 30 bar CO beaufschlagt und für zwei Stunden bei 90 °C gerührt. Nach der Reaktion wird der Reaktor in einem Eisbad gekühlt und anschließend entspannt. Das Reaktionsgemisch wird entnommen und in einen Scheidetrichter gegeben, um die beiden Flüssigphasen zu trennen. Die Bestimmung der Umsätze und Ausbeuten, sowie der Produktverteilung erfolgt mittels GC-FID (Hewlett-Packard, HP 6890 Series, HP-INNOWAX 30 m x 0.25 mm x 0.25 μm). Die Katalysatorkonzentration in der unpolaren Phase wird mittels ICP-OES (IRIS Intrepid optical emission spectrometer (Thermo Elemental) durchgeführt.

4.5.4. Ergebnisse und Diskussion

Bei der Hydroesterifizierung von 10-Undecensäuremethylester (**1**) entstehen zwei Gruppen von Produkten (Figure 4.33). Der gewünschte, lineare Dodecandisäuredimethylester (**2**) wird durch die Hydroesterifizierung an der terminalen Doppelbindung gebildet. Die verzweigten Hydroesterifizierungsprodukte können entweder durch eine Hydroesterifizierung interner Doppelbindungen, welche wiederum durch Isomerisierung der Doppelbindung gebildet werden, oder, im Falle des Produktes mit der Einführung der Estergruppe an Position 10, auch aus der Hydroesterifizierung der terminalen Doppelbindung entstehen.

4.5.4.1. Auswahl des Katalysatorsystems im Lösungsmittel Methanol

Im Hinblick auf eine effiziente Umsetzung des Substrates zum gewünschten linearen Zielprodukt **2** ist die Entwicklung eines geeigneten Katalysatorsystems, das sowohl eine hohe Regioselektivität als auch eine hohe Aktivität in der Hydroesterifizierung ermöglicht, essenziell. Frühere Studien zeigen, dass der verwendete Ligand einen besonders großen Einfluss auf beide Zielgrößen ausübt.[157,161]

Aus diesem Grund wurden zunächst verschiedene bidentate Liganden in Kombination mit der Katalysatorvorstufe $Pd_2(dba)_3$ und der Säure Methansulfonsäure (MSA) als Cokataly-

sator auf ihre Reaktionsleistung hin untersucht, wobei unter Verwendung der Liganden XANTphos und 1,2-DTBPMB aussichtsreiche Ergebnisse erzielt werden konnten. Anschließend wurden der Einfluss verschiedener Palladiumvorstufen sowie der Einfluss verschiedener Säuren als Co-Katalysator getestet, wobei insbesondere eine Kombination aus $Pd_2(dba)_3$/Ligand/MSA gute Ergebnisse liefert. Die Untersuchungen zum Katalysator wurden zunächst ausschließlich in Methanol durchgeführt, das gleichzeitig als Substrat in der Hydroesterifizierung dient. Auf diese Weise wurden die Katalysatoren $Pd_2(dba)_3$/1,2-DTBPMB/MSA und $Pd_2(dba)_3$/XANTphos/MSA (Figure 4.34) als aussichtsreiche Katalysatoren für die Reaktion zum Zielprodukt **2** identifiziert. Unter Verwendung des Liganden 1,2-DTBPMB wird ein sehr großes Verhältnis von linearen zu verzweigten Diestern (*l/b, 94/6*) und somit eine hohe Regioselektivität bei einer moderaten Aktivität (25% Ausbeute **2**) unter den Testbedingungen beobachtet. Die Verwendung des Liganden XANTphos führt zu einer geringeren Regioselektivität (*l/b*=72/28) aber einer erhöhten Aktivität (52% Ausbeute **2**) in der Hydroesterifizierung. In Hinblick auf die Entwicklung effizienter technischer Prozesse muss der verwendete Katalysator auch auf seine Robustheit hin untersucht werden. Aus diesem Grund wurde die Reaktion in ein TMS-System übertragen und der Einfluss verschiedener Reaktionsparameter auf die beiden Katalysatoren getestet und optimiert, um so ein anschließendes Katalysatorrecycling und einen Vergleich der beiden Katalysatoren zu ermöglichen.

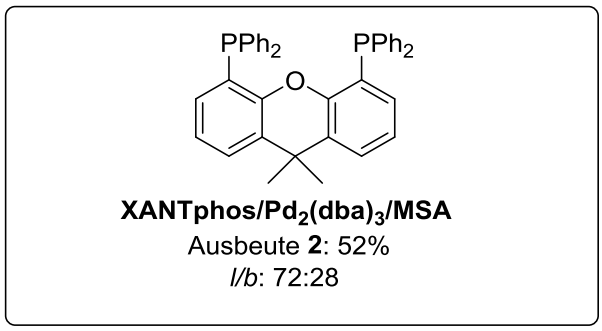

XANTphos/$Pd_2(dba)_3$/MSA
Ausbeute **2**: 52%
l/b: 72:28

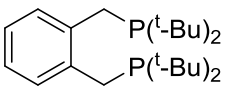

1,2-DTBPMB/$Pd_2(dba)_3$/MSA
Ausbeute **2**: 25%
l/b: 94:6

Figure 4.34: Katalysatorvergleich im Lösungsmittel Methanol.
Bedingungen: T = 90 °C, pCO = 30 bar, t = 16 h, $n_{10\text{-Undecensäuremethylester}}$ = 5 mmol, $m_{Methanol}$ = 4 g, $Pd_2(dba)_3$= 0.05 mol%, n_{Pd}/n_{Ligand} = 1:10, n_{Pd}/n_{MSA}, 600 rpm.
Ergebnisse mittels GC-FID bestimmt.

4.5.4.2. Wahl des TMS-Systems

Um beide Katalysatorsysteme miteinander vergleichen zu können, wurde zunächst ein geeignetes TMS-System aus dem Substrat Methanol als polare Katalysatorphase und Dodecan als unpolare Produktphase im Gewichtsverhältnis Methanol/Dodecan 50/50 ausgewählt. Dieses System ermöglicht eine homogene Reaktionsführung bei 90 °C und eine Abtrennung der Produkte vom Katalysator bei Raumtemperatur.[205]

4.5.4.3. Untersuchungen zur Katalysatorzusammensetzung im TMS-System

Beide untersuchten Katalysatoren setzen sich aus der Palladiumvorstufe $Pd_2(dba)_3$, einem Liganden und dem Cokatalysator MSA zusammen. Im Folgenden soll der Einfluss des Verhältnisses des Säure-Cokatalysators beziehungsweise des Liganden zum Palladium auf die Reaktivität der Katalysatoren untersucht werden.

Zunächst wird der Einfluss des Verhältnisses des Palladiums zur Methansulfonsäure (Pd/MSA) bestimmt und für die Katalysatoren $Pd_2(dba)_3$/1,2-DTBPMB/MSA und $Pd_2(dba)_3$/XANTphos/MSA im TMS-System Methanol/Dodecan optimiert. Die aktive Katalysatorspezies ist eine kationische Palladiumhydrid-Spezies, die in Gegenwart starker Säuren gebildet und stabilisiert werden kann[77,161,250] und so Einfluss auf die Reaktion ausübt. Der Umsatz an 10-Undecensäuremethylester (X_1), die Ausbeute des linearen Diesters (Y_2) und das Verhältnis von linearen zu verzweigten Produkten (*l*/*b*) für das $Pd_2(dba)_3$/1,2-DTBPMB/MSA System sind in Table 4.16 dargestellt.

Table 4.16: Einfluss des Pd/MSA-Verhältnisses auf den $Pd_2(dba)_3$/1,2-DTBPMB/MSA-Katalysator [a, b, c].

Eintrag	Pd/MSA	X_1	Y_2	*l*/*b*
1.1 [d]	1/200	10	9	90/10
1.2	1/45	28	27	96/4
1.3	1/40	32	31	97/3
1.4	1/35	38	36	95/5
1.5	1/30	34	33	97/3
1.6	1/25	28	27	96/4

[a] Bedingungen: T = 90 °C, p_{CO} = 30 bar, t = 2 h, $n_{10\text{-Undecensäuremethylester}}$ = 5 mmol, $m_{Methanol}$ = 2 g, $m_{Dodecan}$ = 2 g, $Pd_2(dba)_3$= 0.05 mol%, $n_{Pd}/n_{1,2\text{-DTBPMB}}$ = 1:10, 600 rpm, Ergebnisse in %. [b] Ergebnisse mittels GC-FID bestimmt.[c] Isomere des Substrats sind im Umsatz nicht berücksichtigt. [d] t=16 h.

Die Aktivität des Katalysators mit dem 1,2-DTBPMB–Liganden ist maßgeblich vom verwendeten Pd/MSA-Verhältnis abhängig. Die höchste Ausbeute des Zielproduktes **2** von 36% wird unter den verwendeten Bedingungen bei einem Pd/MSA-Verhältnis von 1/35 erzielt (Eintrag 1.4, Table 4.16). Wird der Anteil der Methansulfonsäure leicht erhöht oder erniedrigt, verringert sich die Ausbeute von **2**. Ein Einfluss auf das *l*/*b*-Verhältnis ist nur bei sehr hohen MSA-Konzentrationen festzustellen (Eintrag 1.1).

Auch unter Verwendung des XANTphos-Liganden gibt es ein optimales Verhältnis von Pd/MSA. Die höchste Ausbeute an **2** von 21% wird mit einem Pd/MSA-Verhältnis von 1/200 erzielt (Table 4.17, Eintrag 2.3). Des Weiteren hängt auch die Regioselektivität der Reaktion unter Verwendung des XANTphos-Liganden von der MSA-Konzentration ab. Die besten Resultate werden ebenfalls mit einem Pd/MSA-Verhältnis von 1/200 beobachtet. Verglichen mit dem $Pd_2(dba)_3$/1,2-DTBPMB/MSA-Katalysator wird bei Verwendung des XANTphos-Liganden ein deutlich größerer MSA-Überschuss benötigt. Allerdings reagiert das System deutlich weniger sensitiv gegenüber Abweichungen von den optimalen Bedingungen, was eine mögliche Prozessentwicklung erleichtern würde. Für die weiteren Untersuchungen wird ein Pd/MSA-Verhältnis von 1/35 ($Pd_2(dba)_3$/1,2-DTBPMB/MSA) beziehungsweise 1/200 ($Pd_2(dba)_3$/XANTphos/MSA) verwendet.

Table 4.17: Einfluss des Pd/MSA-Verhältnisses auf den $Pd_2(dba)_3$/XANTphos/MSA-Katalysator [a, b, c].

Eintrag	**Pd/MSA**	X_1	Y_2	*l/b*
2.1 [d]	1/800	25	14	56/44
2.2	1/400	30	18	60/40
2.3	1/200	29	21	72/28
2.4	1/100	24	16	67/33
2.5	1/50	22	15	68/32

[a] Bedingungen: T = 90 °C, p_{CO} = 30 bar, t = 5 h, $n_{10\text{-Undecensäuremethylester}}$ = 5 mmol, $m_{Methanol}$ = 2 g, $m_{Dodecan}$ = 2 g, $Pd_2(dba)_3$= 0.05 mol%, $n_{Pd}/n_{XANTphos}$ = 1:10, 600 rpm, Ergebnisse in %.
[b] Ergebnisse mittels GC-FID bestimmt.
[c] Isomere des Substrats sind im Umsatz nicht berücksichtigt.

Die zweite untersuchte Komponente beider Katalysatorsysteme ist der Einfluss der Ligandmenge auf die Reaktivität. Der Ligand eines homogenen Übergangsmetallkatalysators hat im Wesentlichen zwei wichtige Funktionen. Einerseits trägt er entscheidend zur Aktivität und Selektivität des Katalysators bei, andererseits wirkt er stabilisierend auf den Katalysator. Aus diesem Grund werden für den $Pd_2(dba)_3$/1,2-DTBPMB/MSA-Katalysator und den $Pd_2(dba)_3$/XANTphos/MSA-Katalysator der Einfluss des Verhältnisses von Palladium zu Ligand (Pd/L) bestimmt und optimiert. Table 4.18 zeigt die Ergebnisse der Untersuchung des $Pd_2(dba)_3$/1,2-DTBPMB/MSA-Katalysators.

Es wird deutlich, dass die höchsten Ausbeuten von **2** (36%) bei einem Palladium/1,2-DTBPMB-Verhältnis von 1/10 erzielt werden (Eintrag 3.3, Table 4.18). Eine zu niedrige Konzentration des Liganden kann den Katalysatorkomplex nicht ausreichend stabilisieren, während eine zu hohe Ligandenkonzentration zur Blockierung der freien Koordinationsstellen am Pd-zentrum führt.

Ein ähnliches Verhalten ist bei Verwendung des Liganden XANTphos zu beobachten (Tabelle 4). Auch in diesem Fall werden die besten Ausbeuten (21%) und Selektivitäten für das gewünschte Produkt **2** bei einem Palladium/Ligand-Verhältnis von 1/10 erzielt (Eintrag 4.4, Tabelle 4). Aus diesem Grund werden die nachfolgenden Untersuchungen beider Katalysatorsysteme mit einem Pd/Ligand-Verhältnis von 1/10 durchgeführt.

Table 4.18: Einfluss des Pd/Ligand-Verhältnisses auf den $Pd_2(dba)_3$/1,2-DTBPMB/MSA-Katalysator [a, b, c].

Eintrag	Pd/1,2-DTBPMB	X_1	Y_2	*l/b*
3.1 [d]	1/5	15	14	-
3.2	1/7.5	25	24	-
3.3	1/10	38	36	95/5
3.4	1/15	32	30	94/6
3.5	1/20	13	13	-

[a] Bedingungen: T = 90 °C, p_{CO} = 30 bar, t = 2 h, $n_{10\text{-Undecensäuremethylester}}$ = 5 mmol, $m_{Methanol}$ = 2 g, $m_{Dodecan}$ = 2 g, $Pd_2(dba)_3$= 0.05 mol%, n_{Pd}/n_{MSA} = 1:35, 600 rpm, Ergebnisse in %.
[b] Ergebnisse mittels GC-FID bestimmt.
[c] Isomere des Substrats sind im Umsatz nicht berücksichtigt.

Table 4.19: Einfluss des Pd/Ligand-Verhältnisses auf den $Pd_2(dba)_3$/XANTphos/MSA-Katalysator [a, b, c].

Eintrag	Pd/XANTphos	X_1 [b]	Y_2	*l/b*
4.1 [d]	1/1	23	15	60/40
4.2	1/2.5	31	21	67/33
4.3	1/5	29	19	65/35
4.4	1/10	29	21	72/28
4.5	1/50	32	20	64/36

[a] Bedingungen: T = 90 °C, p_{CO} = 30 bar, t = 5 h, $n_{10\text{-Undecensäuremethylester}}$ = 5 mmol, $m_{Methanol}$ = 2 g, $m_{Dodecan}$ = 2 g, $Pd_2(dba)_3$= 0.05 mol%, n_{Pd}/n_{MSA} = 1:200, 600 rpm, Ergebnisse in %.
[b] Ergebnisse mittels GC-FID bestimmt.
[c] Isomere des Substrats sind im Umsatz nicht berücksichtigt.

4.5.4.4. Einfluss der Reaktionsparameter im TMS System

Im Folgenden werden die Einflüsse der Reaktionsparameter Druck und Temperatur auf die Ergebnisse in der Hydroesterifizierung unter Verwendung der beiden Katalysatorsysteme bestimmt und optimiert.

Zunächst wird der Einfluss des CO-Drucks auf die Ausbeuten und Selektivitäten der Reaktion genauer betrachtet. Kohlenmonoxid dient nicht nur als Substrat in der Hydroesterifizierung, sondern kann auch als Ligand an den Katalysatorkomplex koordinieren und so

die Reaktivität beeinflussen. Table 4.20 zeigt den Einfluss des CO-Drucks auf die Reaktion mit dem $Pd_2(dba)_3$/1,2-DTBPMB/MSA-Katalysator. Es zeigt sich, dass die Regioselektivität der Reaktion nicht vom CO-Druck abhängig ist und das *l/b*-Verhältnis zwischen 94/6 und 96/4 liegt. Die Reaktionsgeschwindigkeit steigt mit steigendem CO-Druck in einem engen Bereich zwischen 5 bar und 30 bar (Eintrag 5.1-5.4, Table 4.20). Eine weitere Erhöhung des Drucks hat keinen positiven Effekt auf die Reaktionsgeschwindigkeit.

Table 4.20. Einfluss des CO-Drucks auf den $Pd_2(dba)_3$/1,2-DTBPMB/MSA-Katalysator [a, b, c].

Eintrag	p_{CO}	X_1 [b]	Y_2	*l/b*
5.1 [d]	5	20	19	95/5
5.2	10	25	24	96/4
5.3	20	26	25	96/4
5.4	30	38	36	95/5
5.5	40	35	33	94/6

[a] Bedingungen: T = 90 °C, t = 2 h, $n_{10\text{-Undecensäuremethylester}}$ = 5 mmol, $m_{Methanol}$ = 2 g, $m_{Dodecan}$ = 2 g, $Pd_2(dba)_3$= 0.05 mol%, n_{Pd}/n_{MSA} = 1:35, $n_{Pd}/n_{1,2\text{-DTBPMB}}$ = 1:10, 600 rpm, Ergebnisse in %.
[b] Ergebnisse mittels GC-FID bestimmt.
[c] Isomere des Substrats sind im Umsatz nicht berücksichtigt.

Im Gegensatz dazu steigt die Regioselektivität unter Verwendung des XANTphos-Liganden (Table 4.21) mit sinkendem CO-Druck. Das größte *l/b*-Verhältnis (82/18, Eintrag 6.1) wird bei einem Druck von 5 bar beobachtet. Dieses Ergebnis bestätigt die Beobachtungen von Behr et al..[54] Die Reaktionsgeschwindigkeit hängt ebenfalls vom CO-Druck ab und weist ein Maximum der Ausbeute an **2** bei einem Druck zwischen 30 bar und 40 bar (Eintrag 6.4 und Eintrag 6.5) auf. Die nachfolgenden Untersuchungen der beiden Katalysatorsysteme wurden deshalb bei einem Druck von 30 bar CO durchgeführt.

Auch die Reaktionstemperatur ist ein wichtiger Parameter in chemischen Reaktionen, da Reaktionsgeschwindigkeit und Selektivität, sowie die Gaslöslichkeit von der Temperatur abhängig sind. Außerdem können zu hohe Temperaturen, beispielsweise durch Zersetzung des Liganden, zur Desaktivierung des homogenen Übergangsmetallkatalysators führen.

Table 4.21: Einfluss des CO-Drucks auf den $Pd_2(dba)_3$/XANTphos/MSA-Katalysator [a, b, c].

Eintrag	p_{CO} [bar]	X_1 [b]	Y_2	*l/b*
6.1 [d]	5	11	9	82/18
6.2	10	26	19	73/27
6.3	20	25	18	72/28
6.4	30	29	21	72/28
6.5	50	32	22	69/31

[a] Bedingungen: T = 90 °C, t = 5 h, $n_{10\text{-Undecensäuremethylester}}$ = 5 mmol, $m_{Methanol}$ = 2 g, $m_{Dodecan}$ = 2 g, $Pd_2(dba)_3$= 0.05 mol%, n_{Pd}/n_{MSA} = 1:200, $n_{Pd}/n_{XANTphos}$ = 1:10, 600 rpm, Ergebnisse in %.
[b] Ergebnisse mittels GC-FID bestimmt.
[c] Isomere des Substrats sind im Umsatz nicht berücksichtigt.

Für die Hydroesterifizierung mit dem $Pd_2(dba)_3$/1,2-DTBPMB/MSA-Katalysator ergibt sich ein Maximum in der Ausbeute von **2** (36% nach 2 h) bei einer Reaktionstemperatur von 90 °C. Wird die Temperatur auf 60 °C verringert, sinkt die Ausbeute auf 24%. Eine weitere Erhöhung führt nicht zu einer Erhöhung der Ausbeute von **2**. Da im untersuchten Temperaturbereich kein Einfluss auf das *l/b*-Verhältnis festgestellt werden kann, wurden die weiteren Untersuchungen mit diesem Katalysatorsystem bei einer Temperatur von 90 °C durchgeführt.

Die Verwendung des $Pd_2(dba)_3$/XANTphos/MSA-Katalysators benötigt eine höhere Temperatur von 110 °C, um optimale Ergebnisse in der Hydroesterifizierung zum gewünschten Produkt **2** (49% nach 5 h) zu liefern. Auch unter Verwendung des Liganden XANTphos kann im untersuchten Temperaturbereich kein Einfluss auf die Regioselektivität festgestellt werden.

4.5.4.5. Katalysatorrecycling

In Hinblick auf einen wirtschaftlichen Prozess muss der wertvolle Palladiumkatalysator effizient vom Produkt abgetrennt und wieder eingesetzt werden können. Das in dieser Arbeit verfolgte Konzept zur Rückgewinnung des Katalysators ist die Anwendung von TMS-Systemen. Als polares Lösungsmittel für die Katalysatorphase dient Methanol. Als unpolares Lösungsmittel für die Produktphase wird Dodecan verwendet. Die methanolische Katalysatorphase wird nach der Phasentrennung zurück in den Reaktor überführt, mit neuem Substrat und Dodecan versetzt und zur Reaktion gebracht. Die Produktphase (Dodecanphase) wird auf ihren Produktgehalt untersucht. Table 4.22 zeigt die Verteilung des Produktes **2** und des Substrats **1** auf die Dodecan- und Methanolphase nach der Reaktion. Außerdem ist die Querlöslichkeit der Lösungsmittel Methanol und Dodecan inei-

nander dargestellt. Es zeigt sich, dass nach der Reaktion durch die Phasentrennung etwa 40% des gebildeten Produktes in die unpolare Dodecanphase extrahiert werden. Die Palladiumkonzentration in der Dodecanphase liegt bei beiden verwendeten Katalysatorsystemen bei 2 ppm, was einem Austrag des eingesetzten Palladiums von weniger als einem Prozent entspricht. Die Phosphorkonzentration in der Dodecanphase bei Verwendung des Liganden 1,2-DTBPMB beträgt 14 ppm was etwa einem Prozent der eingesetzten Ligandenmenge entspricht. Unter Verwendung von XANTphos beträgt die Phosphorkonzentration in der Dodecanphase lediglich 2 ppm, sodass weniger als ein Prozent der eingesetzten Ligandenmenge über die Dodecanphase ausgetragen werden. Beide Katalysatorsysteme können also effizient vom Produkt getrennt werden.

Table 4.22: Verteilung der Komponenten auf die beiden Phasen nach der Phasentrennung [a].

	Substrat 1 [%]	Produkt 2 [%]	Methanol [%]	Dodecan [%]
Dodecan-Phase	59	40	11	85
Methanol-Phase	41	60	89	15

[a] Bedingungen: Phasentrenntemperatur = 25 °C

Um Aussagen über die Robustheit beider Katalysatoren treffen zu können, wurden Recyclingexperimente durchgeführt. Abbildung 6 zeigt die absolute Menge des gewünschten Produktes **2** in Gramm, die nach der Trennung der Phasen in der Produktphase (Dodecanphase) detektiert wurde. Nach jedem Reaktionslauf wurde die Katalysatorphase (Methanolphase) zurück in den Reaktor geführt, um die nächste Reaktion durchzuführen. Lauf 0 repräsentiert eine Reaktion mit frischem Katalysator. Die absoluten Ausbeuten von ca. 1 g **2** in den Produktphasen (Dodecanphasen) nach 2 h zeigen eine gute Übereinstimmung mit den zuvor präsentierten Ergebnissen (Erwartet: $Pd_2(dba)_3$/1,2-DTBPMB/MSA: 1,18 g; $Pd_2(dba)_3$/XANTPhos/MSA:0,93 g)

Bei Betrachtung des $Pd_2(dba)_3$/1,2-DTBPMB/MSA-Katalysators (graue Balken) zeigt sich, dass die Ausbeute von **2** nach jedem Recyclinglauf abnimmt. Das *l/b*-Verhältnis der Reaktion beträgt in jedem Reaktionslauf mindestens 95/5. Da die Austragung von Palladium und Ligand in die Produktphase unter einem Prozent liegt, kann dies nicht als Ursache für den Aktivitätsverlust angesehen werden. Die Untersuchungen zum Einfluss der MSA-Konzentration zeigen, dass das Reaktionssystem sehr sensitiv auf Abweichungen vom optimalen Pd/MSA-Verhältnis reagiert. Die verwendete Methansulfonsäure kann unter diesen Bedingungen mit Methanol verestert werden und steht somit nicht mehr zur Stabilisierung des Katalysators zur Verfügung. Auch eine Zersetzung der Säure in Gegenwart

des Palladiumkatalysators ist denkbar. Durch begleitende zeitaufgelöste Analysen der Reaktionsverläufe über 20 h bei verschiedenen MSA-Konzentrationen konnte eine Desaktivierung der MSA nachgewiesen werden. Aus diesem Grund wurde ein zweites Recyclingexperiment (weiße Balken) durchgeführt, bei dem nach jedem Reaktionslauf 10% der anfangs eingesetzten MSA nachdosiert wurden. Mit Hilfe dieser Experimente konnte die Aktivität des Katalysators über vier Reaktionsläufe aufrechterhalten werden, ohne Einbußen in der Selektivität zu beobachten.[205] Da ca. 60% des gebildeten Produktes in der Katalysatorphase verbleiben ist zusätzlich von einer leichten Anreicherung des Produktes **2** durch Extraktion aus der Katalysatorphase in den Läufen 1-3 auszugehen.

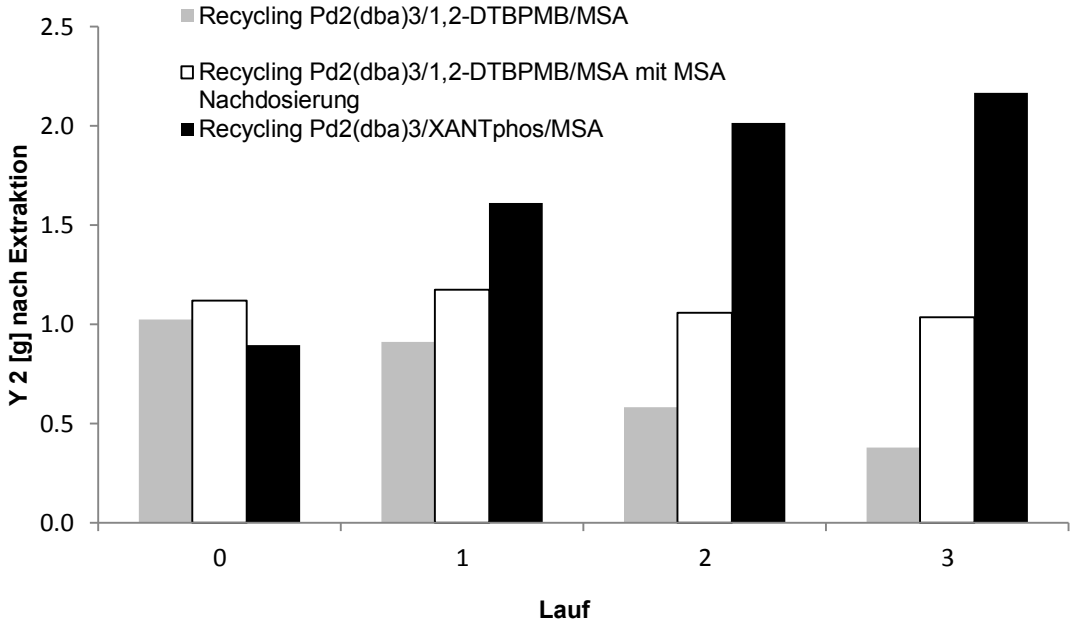

Figure 4.35: Abbildung 6: Recycling-Experimente [a].

[a] Bedingungen:

Recycling $Pd_2(dba)_3$/1,2-DTBPMB/MSA: T = 90 °C, p_{CO} = 30 bar, t = 2 h, $n_{10\text{-Undecensäuremethylester}}$ = 30 mmol, $m_{Methanol}$ = 12 g, $m_{Dodecan}$ = 12 g, $Pd_2(dba)_3$= 0.05 mol%, n_{Pd}/n_{MSA} = 1:35, $n_{Pd}/n_{1,2\text{-DTBPMB}}$ = 1:10, 1000 rpm, Ergebnisse in %, Zugabe nach jedem Reaktionslauf: 10.2 g Dodecan, 1.1 g Methanol, 3.6 g 1
Recycling $Pd_2(dba)_3$/1,2-DTBPMB/MSA mit MSA Nachdosierung: T = 90 °C, p_{CO} = 30 bar, t = 2 h, $n_{10\text{-Undecensäuremethylester}}$ = 30 mmol, $m_{Methanol}$ = 12.5 g, $m_{Dodecan}$ = 12.5 g, $Pd_2(dba)_3$= 0.05 mol%, n_{Pd}/n_{MSA} = 1:35, $n_{Pd}/n_{1,2\text{-DTBPMB}}$ = 1:10, 1000 rpm, Ergebnisse in %, Zugabe nach jedem Reaktionslauf: 10.2 g Dodecan, 1.4 g Methanol, 3.6 g 1, 10 mg MSA
Recycling $Pd_2(dba)_3$/XANTphos/MSA: T = 110 °C, p_{CO} = 30 bar, t = 2 h, $n_{10\text{-Undecensäuremethylester}}$ = 30 mmol, $m_{Methanol}$ = 12.5 g, $m_{Dodecan}$ = 12.5 g, $Pd_2(dba)_3$= 0.05 mol%, n_{Pd}/n_{MSA} = 1:200, $n_{Pd}/n_{1,2\text{-DTBPMB}}$ = 1:10, 1000 rpm, Ergebnisse in %. Zugabe nach jedem Reaktionslauf: 10.2 g Dodecan, 1.4 g Methanol, 3.6 g 1

Im Vergleich zu diesen Ergebnissen zeigt das Recycling des $Pd_2(dba)_3$/XANTphos/MSA-Katalysators (schwarze Balken) ein anderes Verhalten, da die Ausbeute von **2** nach dem Initiallauf deutlich von ca. 0.8 g auf mehr als 2 g (Lauf 3) ansteigt. Begleitende, zeitaufgelöste Untersuchungen zum Reaktionsverlauf zeigen, dass der $Pd_2(dba)_3$/XANTphos/MSA-

Katalysator eine Induktionsdauer von ca. einer Stunde benötigt. Erst nach dieser Zeit werden signifikante Mengen des Produktes **2** gebildet. Aus diesem Grund steigt die Produktausbeute nach dem Initiallauf deutlich an, da der aktive Katalysator nicht erneut gebildet werden muss. Auch in dieser Versuchsreihe ist zusätzlich von einer leichten Anreicherung des Produktes durch Extraktion aus der Katalysatorphase in den Läufen 1-3 auszugehen. Die Desaktivierung der MSA führt bei Verwendung dieses Katalysators nach vier Reaktionsläufen noch nicht zu einer Verminderung der Katalysatoraktivität, was ebenfalls in guter Übereinstimmung zu den Untersuchungen zum Einfluss der MSA-Konzentration (Table 4.16) steht. Die erhöhte Robustheit des Katalysators wird in diesem Experiment bestätigt.

4.5.5. Zusammenfassung und Schlussfolgerungen

In dieser Arbeit wurden die Katalysatoren $Pd_2(dba)_3$/1,2-DTBPMB/MSA und $Pd_2(dba)_3$/XANTphos/MSA in der Hydroesterifizierung von 10-Undecensäuremethylester in einem TMS-System untersucht und hinsichtlich ihrer Reaktionsleistung und Robustheit miteinander verglichen.

Der $Pd_2(dba)_3$/1,2-DTBPMB/MSA-Katalysator zeichnet sich durch eine sehr hohe Regioselektivität in der Hydroesterifizierung zum gewünschten, linearen Diester **2** aus. Es werden sehr gute *l/b*-Verhältnisse von 95/5 erzielt. Dieser Katalysator eignet sich aufgrund seiner Selektivität und der Aktivität in der Isomerisierung auch zur Synthese linearer Ester ausgehend von internen Olefinen.

Die Verwendung des Katalysators $Pd_2(dba)_3$/XANTphos/MSA zeigt im Vergleich eine leicht erhöhte Aktivität, allerdings auch eine deutlich verringerte Regioselektivität (*l/b* = 72/28). Beide Katalysatoren sind grundsätzlich zur Synthese des linearen Diesters **2** geeignet und können nach der Reaktion im TMS-System gut durch Phasentrennung abgetrennt werden. Die Palladiumkonzentration in der Produktphase beträgt lediglich 2 ppm.

Beide Katalysatoren können nach der Reaktion erneut eingesetzt werden, wobei sich insbesondere die Kombination aus $Pd_2(dba)_3$/XANTphos/MSA als robustes Katalysatorsystem zeigt. Unter Verwendung des Liganden 1,2-DTBPMB zeigt sich der Katalysator sehr sensitiv gegen Veränderungen der Konzentration des Cokatalysators MSA. Durch gezielte Nachdosierung von MSA kann die Katalysatoraktivität jedoch ebenfalls aufrecht erhalten werden, so dass beide Katalysatoren prinzipiell wiederverwendet werden können, was für einen kosteneffizienten Prozess von großer Bedeutung ist.

4.5.6. Danksagung

Diese Arbeiten sind Teil des von der Technischen Universität Berlin koordinierten Sonderforschungsbereich/Transregios 63 "Integrierte chemische Prozesse in flüssigen Mehrphasensystemen". Die Autoren bedanken sich bei der Deutschen Forschungsgemeinschaft (DFG) für die finanzielle Unterstützung des Projektes (TRR 63), der Umicore AG & CO für die Spende der Palladiumvorstufe sowie der Digital Speciality Chemicals Ltd. für die Spende des Liganden 1,2-DTBPMB.

4.6. Tandem Reductive Hydroformylation of Castor Oil Derived Substrates and Catalyst Recycling by Selective Product Crystallisation

Marc L. Furst, Vedat Korkmaz, Tom Gaide, Thomas Seidensticker, Arno Behr, Andreas J. Vorholt, ChemCatChem **2017**, 10.1002/cctc.201700965.

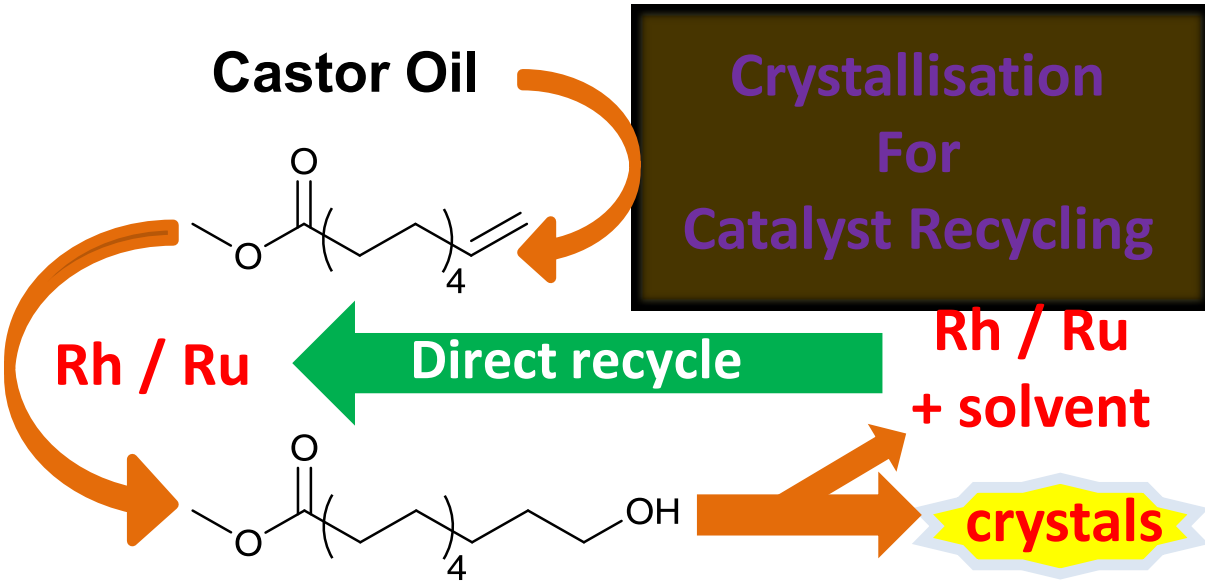

Contributions:

The ideas leading to this publication were contributed by Thomas Seidensticker and me. The concept for this publication was developed by Marc L. Furst, Thomas Seidensticker and me. Experimental data was provided by Vedat Korkmaz as part of his master thesis and Marc L. Furst. Art-work, literature search and manuscript preparation were done by Marc L. Furst, Thomas Seidensticker and me. Andreas J. Vorholt and Arno Behr supervised this project and corrected the manuscript.

4.6.1. Abstract

An orthogonal tandem catalytic system consisting of rhodium and ruthenium complexes yields linear C12 α,ω-bifunctional compounds from commercial, castor oil derived renewable substrates. With alcohol yields up to 88% and selectivities to the linear species of up to 95%, this approach is a direct, atom-economic and easy access to potential polymer precursors for polycondensates. Additionally, a straightforward method for selective product crystallisation has been developed, enabling the recycling of the tandem catalytic system for two runs with excellent activity and simultaneously providing a high purity product.

4.6.2. Communication

The addition of syngas (CO/H_2 mixture) to double bonds under aldehyde formation is generally referred to as hydroformylation. It is one of the most important applications of homogeneous transition metal catalysis in chemical industry, producing more than 12 million metric tons of aldehydes per year.[18] Especially the *n*-selective hydroformylation of terminal alkenes is of high interest since the resulting aldehydes can be converted into the corresponding linear *n*-alcohols, which are of high value. The transformation of alkenes to *n*-alcohols *via* hydroformylation can in principle be done by two different approaches:

- A multistep process consisting of alkene hydroformylation, aldehyde purification, aldehyde reduction, alcohol purification[129]
- A tandem reaction consisting of concurrent alkene hydroformylation and aldehyde reduction in one pot (i.e. reductive hydroformylation) followed by alcohol purification

The tandem reaction approach obviously is a very attractive alternative since energy intensive intermediate aldehyde purification is unnecessary. Consequently, many attempts can be found in the literature to realize this reaction sequence in an auto-tandem catalytic system applying Co[200,251–256], Rh[257–266], Pd[267] or Ru[268–277] as the only catalyst metal in combination with different nitrogen or phosphorus ligands.

Another efficient approach to realize this tandem reaction is the use of two orthogonal catalysts, one for hydroformylation and one for the reduction of aldehydes. Nozaki et al. reported about an orthogonal tandem reaction consisting of Rh/Xantphos hydroformylation catalyst and Shvo's catalyst (Figure 4.36) for aldehyde reduction enabling high yields and selectivity towards the corresponding *n*-alcohols.[275,278] A similar tandem catalytic system consisting of a Rh/Sulfoxantphos catalyst on supported ionic liquid phase in combination

with Shvo's catalyst on SiO_2 for butanol synthesis from propene was reported by Bell *et al.*[279]

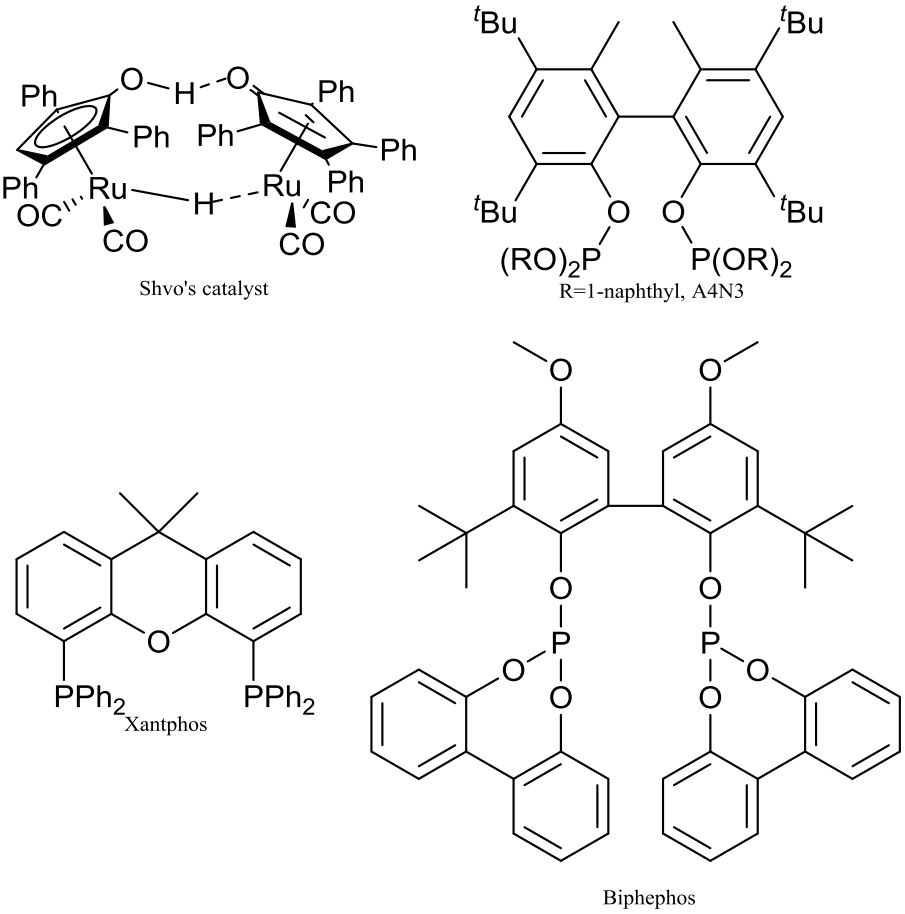

Figure 4.36: Shvo's catalyst and applied ligands in the *n*-selective reductive hydroformylation.

Based on their previously reported system, Nozaki et al. were even able to extend their tandem catalytic system by preceding isomerization yielding linear alcohols from internal olefins by changing the ligand to A4N3 (Figure 4.36) and adding additional $Ru_3(CO)_{12}$.[136] Thus, they yielded 53% linear methyl 19-hydroxynonadecanoate starting from methyl oleate using the catalyst system described above. The application of unsaturated fatty acid methyl esters (FAMEs) is particularly beneficial since the resulting linear bifunctional molecules are interesting AB-type monomers for polycondensates.

In this regard, the readily available and from castor oil renewably derived substrates methyl 10-undecenoate (**1a**), 10-undecenol (**1b**) and 10-undecenoic acid (**1c**) are further very potential starting materials for the production of monomers. For instance, **1a** is already industrially utilized for the production of polyamide-11 (Rilsan®)[280,281], and also other promising approaches have been reported.[74,151,205,238,282–286] However, reductive hydro-

formylation has not been presented so far and would thus considerably broaden the spectrum. Via the corresponding intermediate linear aldehydes **2a-c**, the resulting linear bifunctional alcohols **3a-c** have very high potential as monomers for polycondensates (e.g. polyester 12, Figure 4.37).

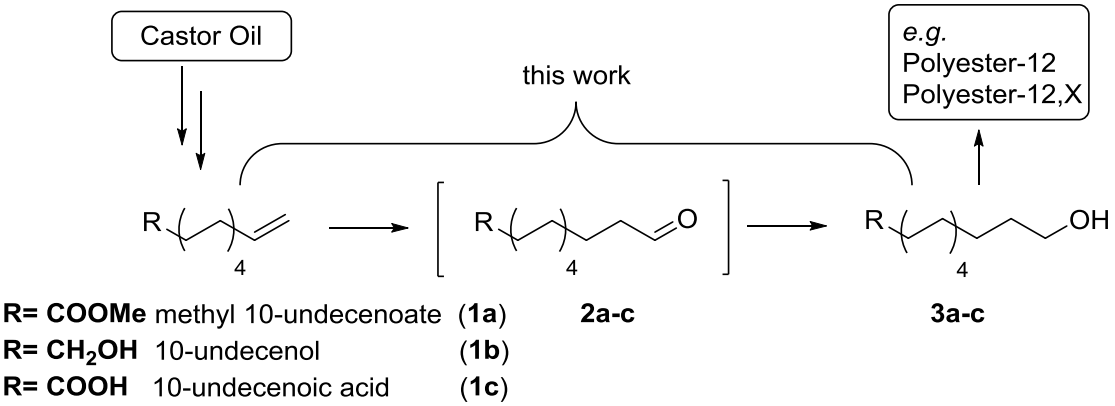

Figure 4.37: Reductive hydroformylation of castor oil derived substrates 1a-c for the synthesis of linear bifunctional alcohols 3a**-c** via the intermediate linear aldehydes 2a-c.

Despite the high potential of transition metal catalyzed tandem reactions for the synthesis of polyester monomers from oleochemicals, their application is still highly limited. This in our opinion is mainly due to two major concerns in the downstream process:

- the required high purity of the monomer
- a considerable lack of efficient catalyst recycling concepts

Ensuring high purity of the product is a prerequisite for the subsequent polycondensation reaction in order to gain substantial molecular weights of the corresponding polymer.[287] Recycling of catalyst is crucial for an economically feasible process since rhodium and ruthenium are very expensive noble metals and also the applied precursors and ligands are tailored and, for that reason, expensive.

We envisaged tackling both of these challenges concurrently, by developing a selective product crystallisation procedure for simultaneous catalyst recycling and product purification. Additionally, the crystallisation approach represents a rather mild method and is therefore less energy-intensive, of high interest and possesses high future potential.[8]

For doing so, we initially combined a Rh/Biphephos system for highly *n*-selective hydroformylation and Shvo's Ru catalyst system for aldehyde reduction. We chose methyl 10-undecenoate (**1a**) as the model substrate for first experiments. Initially, hydroformylation of **1a** for the production of **2a** turned out to be straightforward as expected, with 99% conversion after one hour and a regioselectivity of >98% for the linear aldehyde (see SI for details and conditions).

In ongoing studies on the single step formation of the alcohol **3a** by reduction of **2a**, we discovered, to our surprise, the possibility of generating an active aldehyde reduction system *in situ* by applying Ru_3CO_{12} and tetracyclone (2,3,4,5-Tetraphenyl-2,4-cyclopentadien-1-one). *In situ* generation of the reduction catalyst is of high value from an economic and ecologic perspective, since it saves additional time, effort and auxiliary chemicals in catalyst synthesis and the catalyst precursors are much cheaper compared to Shvo's catalyst.

To compare the activity in aldehyde reduction between the two systems (commercial *ex situ vs. in situ* system), we first performed conversion vs. time plots (Figure 4.38) in the transformation of **2a** into **3a** under hydrogen pressure. We noticed that the reduction of the aldehyde **2a** is straightforward and leads to full conversion to the desired linear alcohol **3a** with either system (Figure 4.38, graphs A and B). However, an induction period does exist using the *in situ* built catalyst (B), which was expected and is not detrimental to the reaction outcome.

Motivated by this fact, the tandem reductive hydroformylation of **1a** to the linear alcohol **3a** *via* the intermediate aldehyde **2a** was tested. Applying the Rh/Biphephos system for hydroformylation leads to a similar conversion path to the desired product **3a**, whatever the reduction system is used (Figure 4.38, *in situ* (graph **C**) or *ex situ* (graph **D**)). Once again, an induction period appears for the *in situ* built Shvo's catalyst. For both systems, full conversion was achieved after 18 h with excellent selectivities. The main undesired reactions were the production of branched aldehydes (**2a**,$_{branched}$), leading to branched alcohols (**3a**,$_{branched}$), and the hydrogenation of methyl 10-undecenoate (**1a**) to methyl undecanoate.

This series of experiments confirms the feasibility, and moreover, the performances of an *in situ* built Shvo's catalyst in reductive hydroformylation for the first time. With these first insights in hand, we modified the reaction conditions for the reductive hydroformylation in order to speed up the reaction sequence and to produce more alcohol product per time. Increasing the amount of catalyst and substrate applied, the reaction time for reaching full conversion could be decreased to one hour, by maintaining high selectivity Moreover, in our effort to provide a greener alternative to toluene, isopropanol worked out very well as a recommended solvent according to CHEM21 solvent guide.[288]

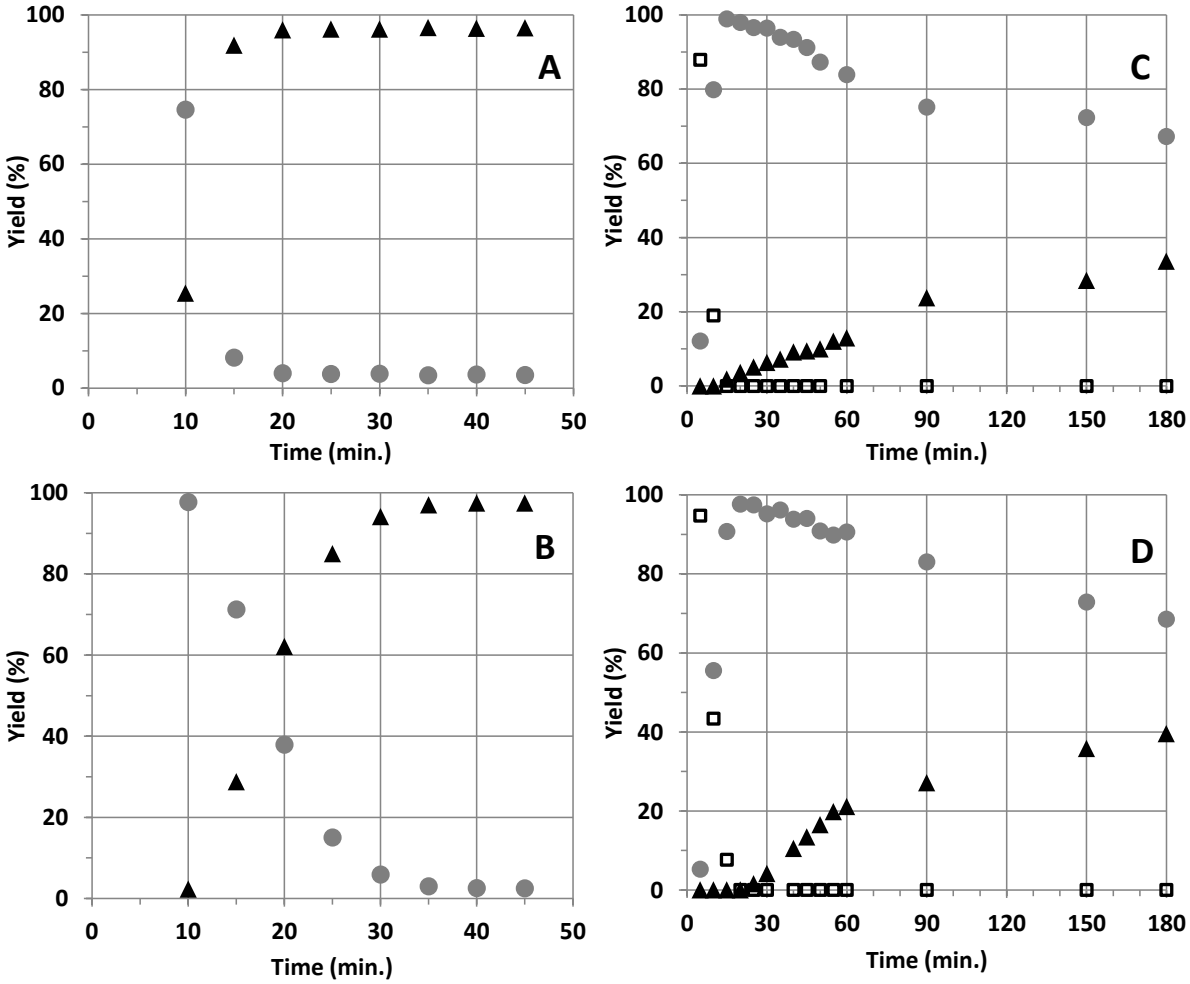

Figure 4.38: Yield vs. time: Reduction of aldehyde 2a to alcohol 3a (with *ex situ* (A) and *in situ* (B) Shvo's catalyst); Reductive hydroformylation of 1a to alcohol 3a (with *ex situ* (C) and *in situ* (D) Shvo's catalyst).

□ methyl 10-undecenoate 1a
• methyl 12-oxododecanoate 2a
▸ methyl 12-hydroxydodecanoate 3a

Conditions: for A and B: n2a = 21.9 mmol, 0.33 mol% Ru_3CO_{12}, 1 mol% tetracyclone, 100 mL toluene, p(H_2) = 10 bar, T = 150 °C; for C and D: n1a = 21.9 mmol, 1 mol% [$Rh(CO)_2$acac], 2 mol% Biphephos, 0.33 mol% Ru_3CO_{12}, 1 mol% tetracyclone, 100 mL toluene, p(CO/H2) = 20 bar, T = 150 °C. Detailed experimentals: see SI

The developed orthogonal tandem catalytic Rh/Ru system proved to tolerate also alcohols and a free carboxylic group by maintaining similar activity and regioselectivity (Table 4.23, Entry 2&3). Under the optimized reaction conditions, substrates **1b** and **1c** were also smoothly transformed into the corresponding alcohol products with 73% and 78% yield and a linear selectivity of 91% and 95%, respectively. However, substrate **1b** gave comparably higher yields for the saturated substrate undecanol of 22%. This is caused by the isomerization of the double bond to the other terminus of the molecule into the vinyl position of the alcohol function. This intermediate tautomerizes to the intermediate undecanal, which is effectively reduced by the present Ru catalyst system. Hence, the higher yield of saturated substrate product for this specific substrate is rather an instance of high

Table 4.23:Reductive hydroformylation of 1a-c under optimized reaction conditions.

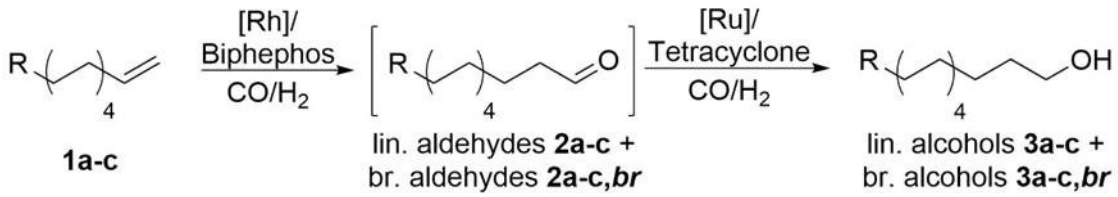

Entry	X_{1a-c} [%]	$Y_{hydr.\ Substrate}$ [%]	$Y_{2a-c,br.}$ [%]	Y_{2a-c} [%]	$Y_{3a-c,br.}$ [%]	Y_{3a-c} [%]	*l/b* in alcohol products
1	98	7	1	2	6	82	93:7
2	99	22	2	2	6	67	91:9
3[a]	95	2	7	8	4	74	95:5

Conditions: Isopropanol 30 mL, 1a-c 41.8 mmol, $Rh(CO)_2acac$ (1 mol%), Biphephos (2 mol%), $Ru_3(CO)_{12}$ (0.33 mol%), tetraphenylcylopentadienone (1 mol%), $p(CO/H_2)$ = 40 bar, T = 150 °C, t = 1 h. Conversion (X) and yields (Y) determined by GC-FID with external standard. [a] Analysed as the corresponding methyl esters after methanolysis of the crude reaction mixture.

aldehyde reduction potential in the tandem system than a lack of chemoselectivity.

Next, the recycling of the Rh/Ru orthogonal catalyst system by developing a temperature induced selective product crystallisation was tackled. For that, we chose ester alcohol product **3a** as the model substrate.

We developed the following working principle: the crude reaction mixture is transferred from the cooled autoclave into a double-jacketed crystalliser equipped with a frit at the bottom. It is cooled down at a certain rate below a temperature at which the product crystallises. Through vacuum filtration, the liquid, catalyst containing reaction mixture is isolated and separated from the solid product, and the latter is analysed by GC-FID for determining its purity and by ICP-OES for residual metals' content.

In an initial experiment, after reductive hydroformylation of **1a** at standard conditions, the reaction mixture was cooled down in the crystalliser at a rate of 2 K per hour (see SI for details). Using this simple method allowed us to obtain large crystals: the filtration was straightforward and quick. The purity of the crystalline linear alcohol **3a** was >97% and ICP analysis provided a leaching of 0.72 mg of Rh and 1.59 mg of Ru (3.3% and 3.0% of initial metal content, respectively).

The catalyst leaching with this non-optimized method is comparable to other recycling strategies for homogeneous transition metal catalysts like thermomorphic multicomponent solvent systems (TMS)[289] or organic solvent nanofiltration[12], making selective product crystallisation a strategy with significant future potential.

The high product purity of **3a** already after the first run in combination with the low leaching values motivated us to tackle the recycling of the orthogonal tandem catalytic system next. After a second experiment, the cooling process in the crystalliser was set to a decrease in temperature from room temperature to -20 °C, letting the product crystallise from the mixture. After vacuum filtration, the liquid filtrate containing the catalysts, the solvent and possible side-products was replenished with the fresh substrate (**1a**). It was introduced via cannula back to the autoclave, which was pressurized once again with syngas and warmed up to 150 °C for one hour. Using this methodology, the orthogonal tandem systems could be successfully reused for three times without a significant loss in activity. While GC-FID conversion of the substrate **1a** was constant, the isolated yield of the desired product after each recycling increased. This phenomenon is due to the fact only that 48% of the desired product **3a** can be recovered after the first crystallisation, and hence the remaining product accumulates in the crude mixture after each recycling. However, this effect shows that recycling of the product does not impede activity, it even enhances crystallisation yield, virtually giving a 74% yield for the first recycling and a 129% yield for the following one.

A third recycling, however, showed the system to substantially lose its ability to convert the starting material into the desired product. The product was then solubilized and crystallised a second time for enhancing its purity. Results of these operations are summarized in Figure 4.39.

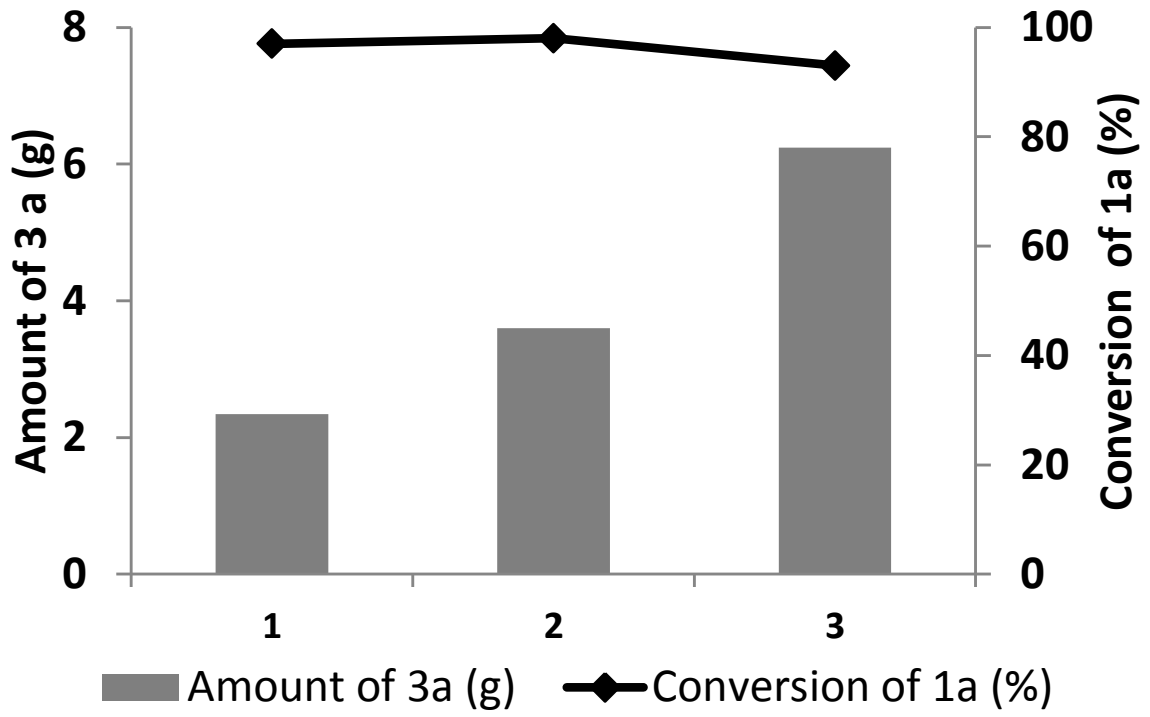

Figure 4.39:1: first reaction; 2: first recycling; 3: second recycling.
Conditions: Isopropanol 30 mL, 1a 5 mL (20.9 mmol), 1 mol% $Rh(CO)_2acac$ (53.9 mg), 0.2 mol% Biphephos (328 mg), 0.33 mol% $Ru_3(CO)_{12}$ (111 mg), 1 mol% tetraphenylcylopentadienone (201 mg), T = 150 °C, t = 1 h.

4.6.3. Conclusions

In conclusion, we proved the high potential of catalyst recycling through the mild method of selective product crystallisation. Moreover, this method allowed us to recycle an orthogonal tandem catalytic system for the first time which consists of two *in situ* built catalytic species, increasing simultaneously the interest of this challenging orthogonal tandem reaction. The tandem-reaction based system simplifies the procedure of converting natural feedstocks into a high-potential polymer precursor. The crystallisation/recycling procedure is currently tested for other substrates and being optimized in order to amplify the number of recycling cycles, lessening the metal leaching and obtaining polymer grade products.

4.6.4. Acknowledgements

We gratefully acknowledge the financial support of the German Science Foundation (Project SFB/TRR 63: ”InPROMPT – Integrated Chemical Processes in Multi-Phase Fluid Systems”) for this work (Subproject A1). We would also like to express our gratitude to Umicore AG & Co. KG for supplying the catalyst precursors.

4.7. Renewable Surfactants *via* Hydroaminomethylation of Terpenes

Thiemo A. Faßbach, Tom Gaide, Michael Terhorst, Arno Behr, Andreas J. Vorholt, *ChemCatChem* **2017**, *9*, 1359-1362.

Graphical Abstract

Contributions:

The ideas leading to this publication were contributed by Thiemo A. Faßbach and me. The concept for this publication was developed Thiemo A. Faßbach and me. Michael Terhorst provided experimental data as part of his master thesis. Art-work, literature search and manuscript preparation were done by Thiemo A. Faßbach. Andreas J. Vorholt and Arno Behr supervised this project and corrected the manuscript.

4.7.1. Abstract

A catalytic system was developed to enable the use of industrially-available terpenes (β-myrcene, β-farnesene) in hydroaminomethylation to obtain renewable building blocks for surfactants in two steps. This homogeneously, tandem-catalyzed reaction includes both a hydroformylation and an enamine condensation, followed by a hydrogenation. Under optimized conditions, the catalytic system ([Rh/dppe]) yields products in high amounts (70%) after short reaction times (3 h), with unprecedentedly high TOFs for the hydroformylation of 1,3-dienes of over 739 [mol·mol^{-1}·h^{-1}]. This is the highest TOF reported to date for a hydroformylation of a 1,3-diene. Furthermore, the highest regioselectivities of 97% and above were observed in the hydroformylation step, which is extraordinarily high for the conversion of 1,3-dienes. The terpene-derived amines obtained were further functionalized to quaternary ammonium compounds, which show surface activity that is quite similar to that of industrially-available quaternary ammonium compounds. The hydroaminomethylation of terpenes achieves higher step-efficiency than industrial means and makes use of an alternative, renewable feedstock to synthesize more environmentally-friendly surfactants.

4.7.2. Communication

Surfactants are among the most important and valuable products in the chemical industry. They are used in a wide range of applications, e.g., as detergents, food additives or in oil field chemistry.[290] Consisting of a polar, and hence hydrophilic, head and a non-polar, lipophilic tail, they show tailor-made properties in surface active behavior, depending on the field of use. They are usually distinguished by their polar group, meaning there are amphoteric, non-ionic, anionic and cationic surfactants. The latter consist of an organic ammonium ion, bearing at least one long chain moiety. They are usually derived from fatty amines, which in turn are synthesized by the hydrogenation of fatty nitriles. Industrial routes to obtain fatty nitriles are usually based on the condensation of fatty acids with ammonia or the hydrocyanation of olefins.[291] Subsequent quaternization of the highly-substituted amine leads to a cationic surfactant. In this work we developed a facile route to access the long chain amine in two steps *via* the hydroaminomethylation of terpenes (Scheme 4.40) and the subsequent hydrogenation of the products. This is favorable for numerous reasons. The turpentine feedstock is renewable – in contrast to petrochemical olefins – and does not interfere with edible resources, such as fatty acids. Furthermore, the hydroaminomethylation route shows higher step-efficiency, as only two steps are needed to obtain saturated amines, whereas industrial routes need at least three steps, starting from bulk chemicals. Hydroaminomethylation is a three step auto-tandem catalytic

conversion, incorporating hydroformylation, a subsequent condensation of the obtained aldehyde with an amine to an enamine, followed by a hydrogenation to obtain saturated amines (Scheme 4.41).[128,292,293]

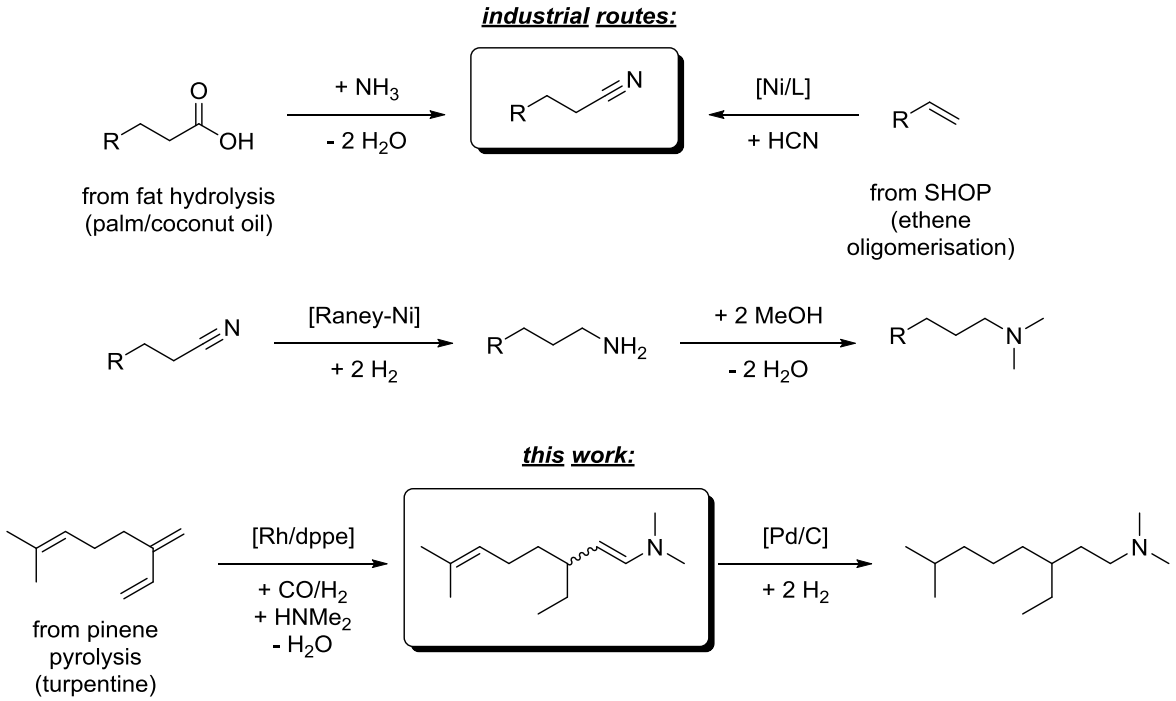

Scheme 4.40: Industrial routes to surfactant-precursors *via* fatty nitriles (top) and *via* hydroaminomethylation of terpenes (bottom).

Although hydroaminomethylation is a well-known conversion that is applied to several unsaturated compounds, there are only few examples for hydroaminomethylations with terpenes, in particular pinene, camphene[294] and limonene[295] or natural occurring allyl benzenes, like eugenol[296] or estragole.[297] None of the hydroaminomethylations mentioned above consist of a conjugated 1,3-diene, but rather an isolated terminal double-bond. The only reported hydroaminomethylations of conjugated 1,3-dienes are isoprene[298] and cyclopentadiene[299]. Both reactions suffer from low regioselectivity of the hydroformylation on the one hand[300,301] and low catalytic activity of rhodium when applied to 1,3-dienes on the other.[302,303] The latter is due to the formation of relatively stable η^3-allyl-Rh complexes.[304,305] Another approach for the hydroaminomethylation of 1,3-dienes is the use of tris(aryl)-hexahydro-1,3,5-triazines as amination substrates and 2-propanol as a transfer hydrogenation reagent using a ruthenium catalyst.[306]

In order to develop a suitable catalytic system for the hydroaminomethylation of terpenes with secondary amines, a model substrate system was required. Myrcene was chosen because of the industrial availability of this compound[307,308] and the chain length of 11 carbon atoms in the final product, thus being structurally similar to the so-called laurics. To

prove the industrial suitability of this concept, myrcene was employed in technical grade (> 90%). Diethylamine was employed as a model substrate for secondary amines.

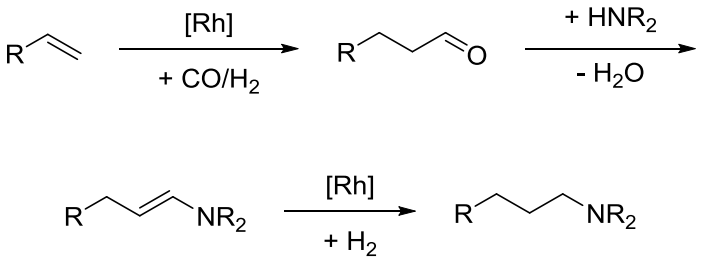

Scheme 4.41: Hydroaminomethylation of an olefin.

Starting from known conditions that work solely for the hydroformylation of 1,3-dienes[300] we tested several catalytic systems based on rhodium with phosphorous ligands. The combination of $[Rh(cod)Cl]_2$ with the dppe (= diphenylphosphinoethane) ligand (Figure 4.42) has shown the best results so far, with a yield of 62% of **3** after 18 hours (for further information about the primary screening for catalysts and solvents see supporting information).

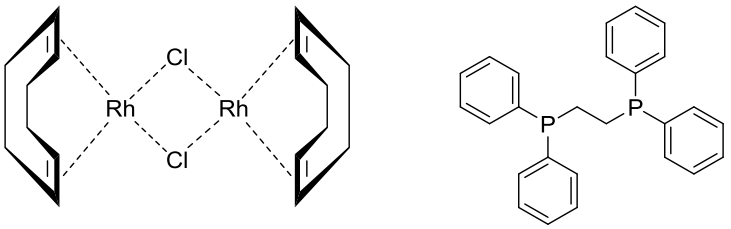

$[Rh(cod)Cl]_2$ DPPE

Figure 4.42: Metal precursor and diphosphine ligand for the catalyst.

NMR studies revealed that the hydroformylation step is highly selective under the applied conditions, yielding the β-ethylidene substituted aldehyde **1**. Furthermore, the reduced form of the condensation product, the diene amine **2**, is not an unsaturated amine, but an enamine **3** (Figure 4.43).

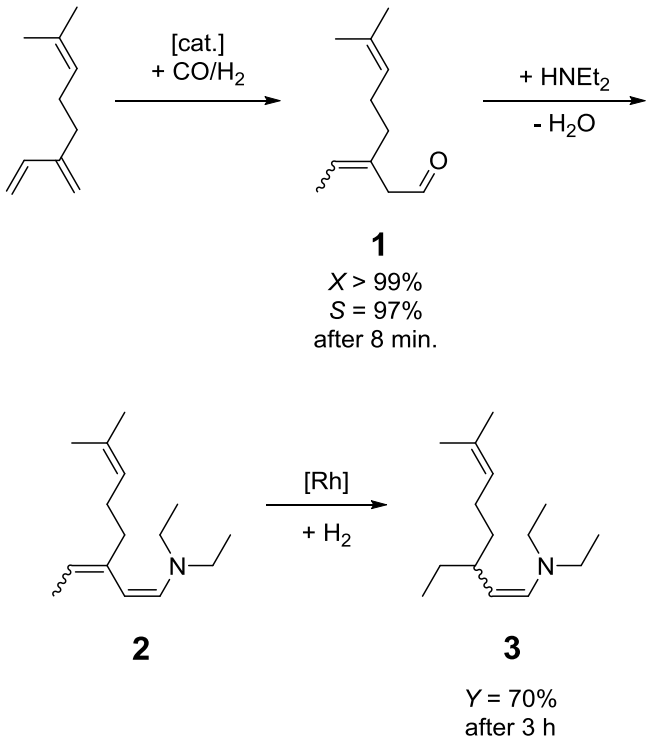

Figure 4.43: Hydroformylation as the regioselectivity determining step in the hydroaminomethylation of myrcene.
Yields (*Y*) and conversions (*X*) are given in % based on myrcene, *S* = Y(**1**)/X(myrcene)), results determined by GC-FID.

Striving for wide applicability to terpenes and amines, the course of the reaction needs to be understood. We decided to aim for enamine **3**, as this is a stable compound that can easily be purified by distillation (bp: 80°C at 1.2 mbar) and further functionalized to obtain surfactants. In order to maximize this yield, the hydroformylation step as well as the hydrogenation step must be accelerated. It is important that the hydrogenation does not reduce the conjugated diene system of myrcene, but only the diene-amine **2**. Several factors make it possible to control the different catalytic steps of the hydroaminomethylation, e.g. temperature, syngas pressure and composition, metal/ligand-ratio or the myrcene/amine-ratio. With a comprehensive study of all these influences (for detailed results, see supporting information) several crucial factors can be identified that accelerate the reaction significantly. The qualitative results are summarized as trends in reactivity in Table 4.24.

Table 4.24: Trends in reactivity of each catalytic step in the hydroaminomethylation of myrcene with diethylamine, depending on reaction conditions.

Parameter	Value	Impact on Hydroformylation step	Impact on Hydrogenation step
Syngas composition (standard: CO/H_2 = 1/1)	2/1	↘	↘
	1/2	→	→
	1/4	→	↗
	1/5	↘	↗
Rh/P-ratio (standard: M/P = 1/3)	1/1	↘	↘
	1/5	↑	→
	1/10	↑	↘
Reaction temperature (standard: 130°C)	80°C	↓	↓
	110°C	↘	↓
	140°C	→	↑
	150°C	→	↑

Reaction conditions: Precursor: $[Rh(cod)Cl]_2$, 1 mol% Rh (hydrogenation step), 0.05 mol% Rh (hydroformylation step) based on myrcene; ligand: DPPE, $n_{myrcene}$=2.5 mmol, $n_{diethylamine}$=3.75 mmol, $m_{toluene+diethylamine}$=3.57 g, p_{syngas}=40 bar, 600 rpm, t=1 h. For detailed results, see supporting information.

To evaluate the reactivity of each catalytic step in this tandem reaction, the investigation of the hydroformylation step was carried out with smaller amounts of catalyst (0.05 mol%) because the hydroformylation step is very fast. To investigate the hydrogenation step, which is the slower step, we employed 1 mol% of Rh. Certain trends emerged. For instance, a slightly higher amount of ligand favors the hydrogenation step without interfering with the hydroformylation step. The same applies with a higher temperature of 140 °C and a modified syngas composition of 1/4 (CO/H_2). A conversion-time plot at the chosen conditions can be seen in Figure 4.44. The hydroformylation reaction, which is fast in any case, is even faster and is completed in as little as 8 minutes. This corresponds to a TOF of over 739 [$mol \cdot mol^{-1} \cdot h^{-1}$], which is the highest rate for a hydroformylation of a 1,3-diene reported to date. Similar hydroformylation reactions of conjugated linear dienes reach a TOF of 90 for myrcene[309], 600 for isoprene[310], 39 for 1,3-piperylene[311] or 500 with 1,3-butadiene[312] (all TOFs were calculated as moles of carbonylation product per mole of Rh and hour at full conversion). Reducing the catalyst concentration leads to even higher TOFs but slows the hydrogenation down significantly. Apparently, the amine has a syner-

gistic effect on the hydroformylation of 1,3-dienes, accelerating the rate-determining step. This was stated before with cyclopentadiene, although the effect was addressed to a suppressed Diels-Alder dimerization.[313]

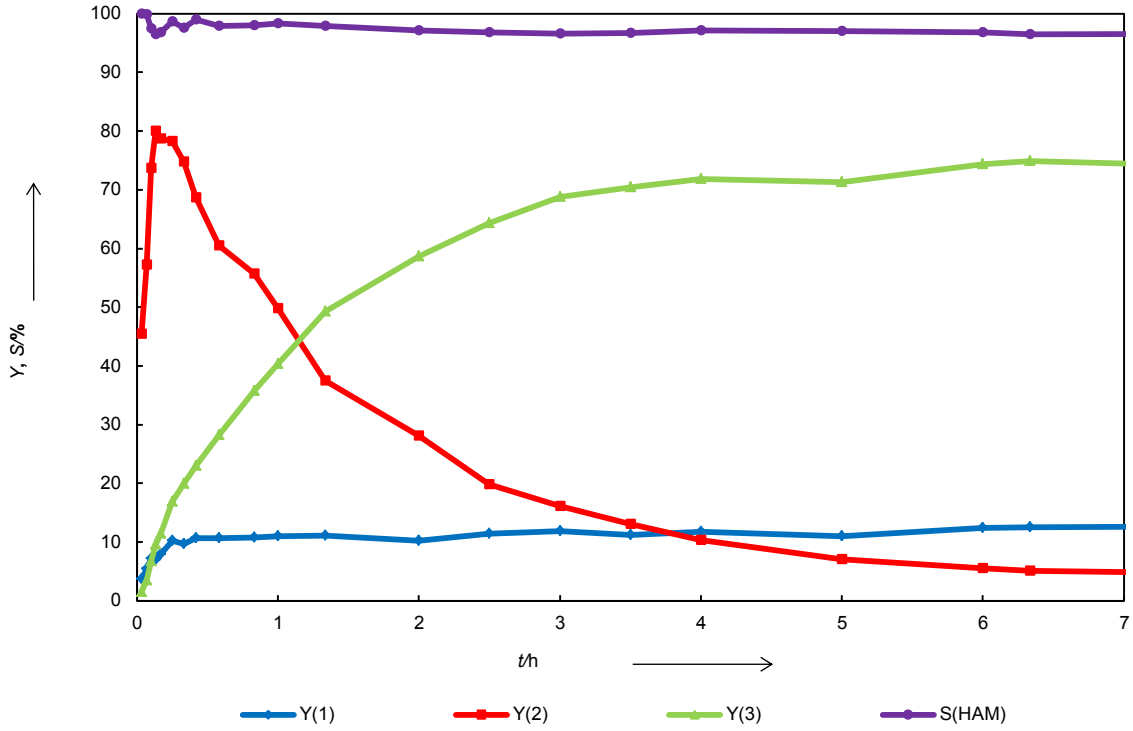

Figure 4.44: Yield-time-plot of the hydroaminomethylation of myrcene with diethylamine.
Reaction conditions: Precursor: $[Rh(cod)Cl]_2$, 1 mol% Rh based on myrcene; ligand: DPPE, M/P = 1/5; $n_{myrcene}$=75 mmol, n_{amine}=300 mmol, $m_{toluene+amine}$=107 g, p_{CO}/p_{H2} = 1/4; p_{syngas}=40 bar, T=140°C, 600 rpm. The reactor was pressurized with H_2 (40 bar) after 40 minutes. Yields (Y) and conversions (X) are given in % based on myrcene, S(HAM) = (Y(1)+Y(2)+Y(3))/X(myrcene)), results determined by GC-FID.

A 70% yield of hydrogenated enamine **3** is obtained in 3 h. Still, 16% of the diene-amine **2** is left, resulting in an overall amines yield of 86% after 3 h. Under these conditions, an aldehyde (1) yield of 10% remains. Hence, the overall selectivity towards the hydroaminomethylation route is 97% because only small amounts of hydrogenated myrcene or diamines are formed.

The enamine condensation can be favored using an excess of the amine. However, this reduces the excellent regioselectivity in the hydroformylation step to about 90% and reduces the hydrogenation activity (see supporting information).

To establish a general procedure for the hydroaminomethylation of terpenes with secondary amines the substrate scope of the reaction must be broadened. To further develop this approach, β-farnesene was employed as a terpene compound and dimethylamine as an amine component. Both are of industrial relevance and availability.[291,314] All of the substrates mentioned were successfully converted to the respective amines in every combi-

nation (see Figure 4.45). Notably, this is the first direct hydroformylation of β-farnesene under the given conditions.

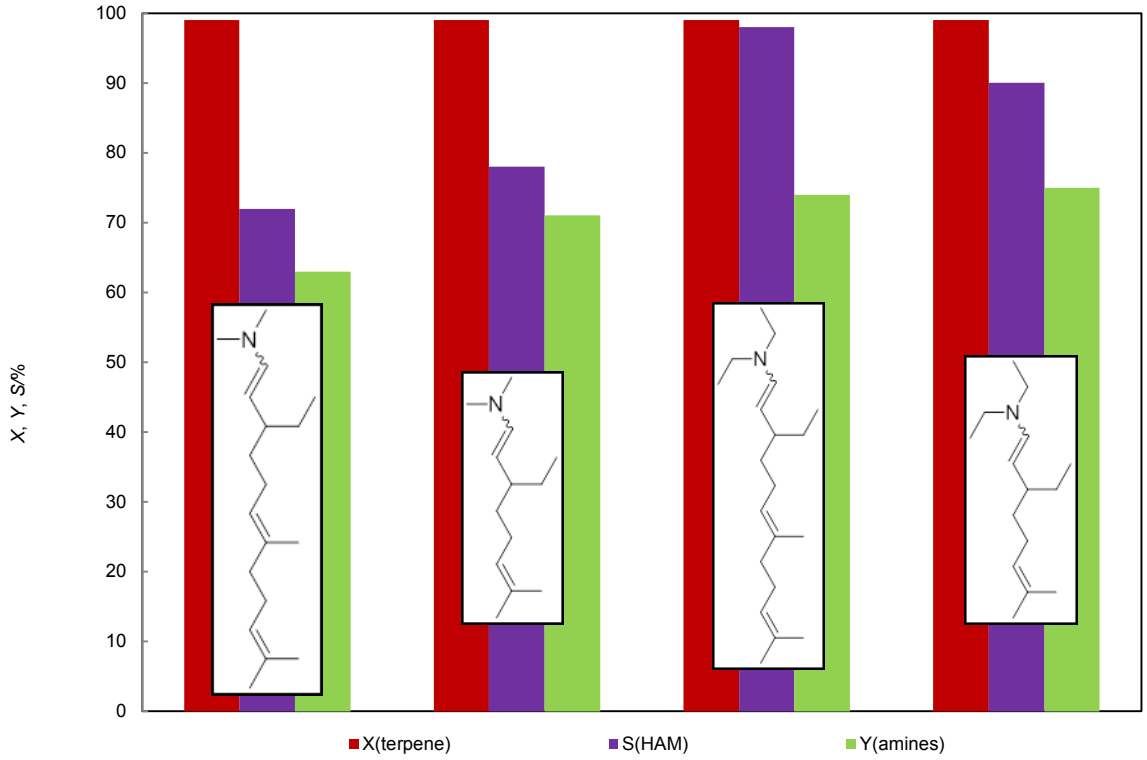

Figure 4.45: Substrate scope for the hydroaminomethylation of terpenes.
Reaction conditions: Precursor: $[Rh(cod)Cl]_2$, 1 mol% Rh based on terpene; ligand: DPPE, M/P = 1/5; $n_{terpene}$=2.5 mmol, n_{amine}=3.75 mmol, $m_{toluene+amine}$=3.57 g, p_{syngas}=40 bar, T=140°C, t=4 h, 600 rpm. Dimethylamine was employed as dimethylammonium dimethylcarbamate. Yields (Y) and conversions (X) are given in % based on myrcene, S(HAM)=(Y(1)+Y(2)+Y(3))/X(terpene)), Y(amines)=Y(2)+Y(3), results determined by GC-FID.

To verify the approach to obtain cationic surfactants, a comparison between the terpene derived amines and industrially available long chain amines is needed. To do so, the corresponding quaternary ammonium compounds were synthesized *via* methylation of the hydrogenated terpenyl amines with methyl iodide. The cmc (= critical micelle concentration) of the prepared surfactants were examined by fluorescence spectroscopy at room temperature, i.e. 20 °C (detailed results can be found in the supporting information). The cmc of the hydrogenated myrcene-derived ammonium compounds align well with the ones of linear quaternary ammonium compounds with similar chain length, e.g. dodecyl trimethyl ammonium bromide. The farnesene derived quaternary ammonium compounds have cmc in the same range as the widely used CTAB (= cetyl trimethyl ammonium bromide). A short overview of the obtained compounds and their respective cmc is given in Figure 4.46, more results with unsaturated compounds as well can be found in the supporting information. These results demonstrate the viability of the presented approach using terpenes as the long-chain component of quaternary ammonium surfactants.[315]

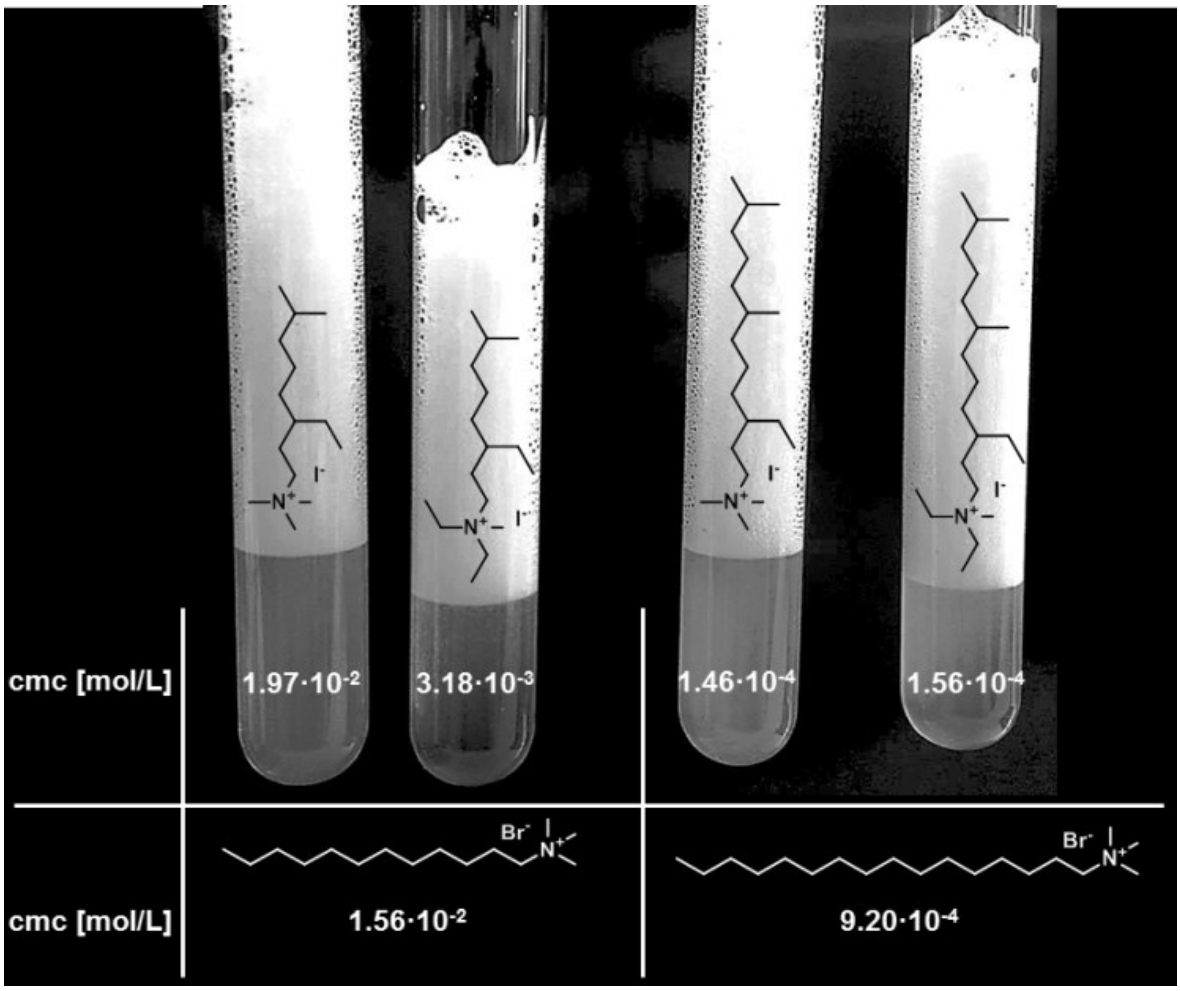

Figure 4.46: Critical micelle concentrations at 20 °C of the synthesized surfactants in comparison to structurally similar, industrially established ones.[315]

In this work, we present the first regioselective (S = 97%) hydroaminomethylation of 1,3-dienes and the first hydroaminomethylation of such terpenes in general. The Rh/dppe catalytic system ensures unprecedentedly high turnover frequencies and is active for other terpenes as well as compatible with other amines. The surface behaviour of the derived quaternary ammonium compounds is similar to long known cationic surfactants, making this approach a valuable contribution to the green synthesis of cationic surfactants.

4.7.3. Acknowledgements

The rhodium precursors were donated by *Umicore*.

We gratefully acknowledge the financial support from *Clariant*.

The financial support of the *German Science Foundation* (Project SFB/TRR 63: ”InPROMPT – Integrated Chemical Processes in Multi-Phase Fluid Systems”) for this work (Subproject A1) is gratefully acknowledged.

4.8. Linear Selective Isomerization/Hydroformylation of Unsaturated Fatty Acid Methyl Esters – A Bimetallic Approach

Tom Gaide, Jonas Bianga, Kim E. Schlipköter, Arno Behr, Andreas J. Vorholt, *ACS Catal*. **2017**, *7*, 4163-4171.

Graphical Abstract

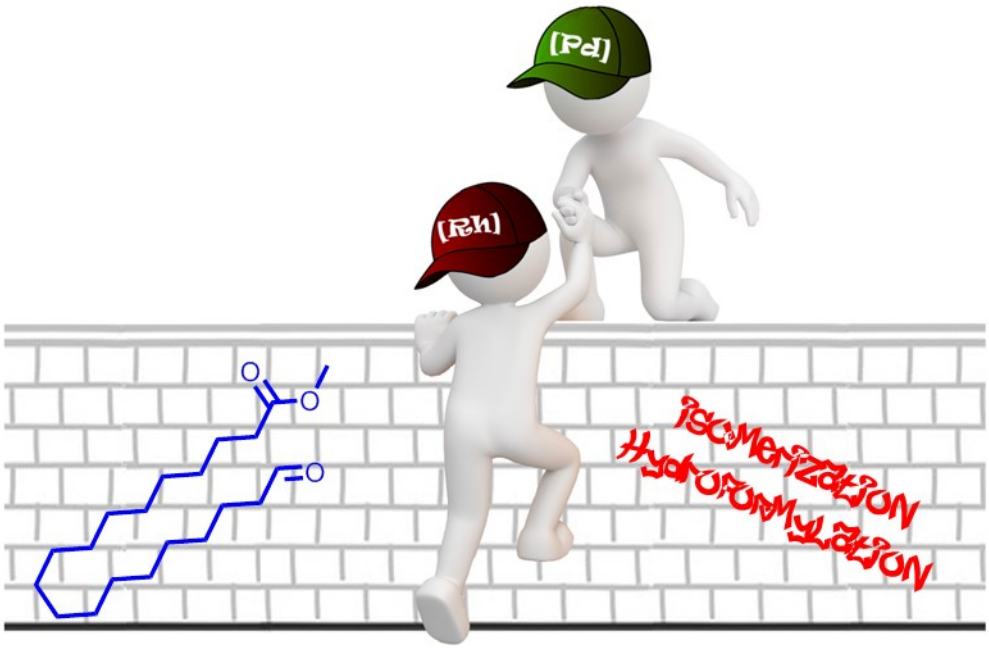

Contributions:

The ideas and the concept leading to this publication were contributed by me. Jonas Bianga and Kim E. Schlipköter provided experimental data as part of their master thesis. Art-work, literature search and manuscript preparation were done by me. Andreas J. Vorholt and Arno Behr supervised this project and corrected the manuscript.

4.8.1. Abstract

Herein we report about the development of an isomerization/hydroformylation tandem reaction to selectively convert fatty acid methyl esters into asymmetric α,ω-functionalized aldehyde esters. An orthogonal tandem catalytic system consisting of a palladium-based isomerization catalyst and a rhodium-based hydroformylation catalyst was developed using methyl 3-hexenoate as a model substrate. Using this catalyst high yields (81% at 99% conversion) and regioselectivities (*l/b*-ratio of 98/2) towards the desired terminal hydroformylation product are obtained in the conversion of methyl 3-hexenoate under mild conditions. Ethyl 4-decenoate was subsequently applied as a second model substrate to identify challenges associated with the longer chain length of the unsaturated ester. Finally, methyl oleate was converted using the developed catalyst system. High aldehyde yields of 74% (at 99% conversion) with an *l/b*-ratio of 91/9 are obtained.

4.8.2. Introduction

Fatty acids and their derivatives are very interesting renewable feedstocks for the chemical industry since they naturally contain both a carboxyl function and a long carbon chain. Consequently, they are widely used as starting material in the chemical industry, e.g., in surfactant synthesis.[290]

Especially the conversion of unsaturated fatty compounds like methyl oleate (**1**) into an α,ω-functionalized long chained molecule (Scheme 4.47) is of great interest in terms of synthesizing new bio based polymer precursors.[152–155] Unfortunately, these are very challenging reaction sequences that place high demands on the applied catalysts. To reach high yields and high selectivities towards the desired products, a catalyst has to be extremely active in double-bond isomerization since the double bond has to be isomerized over many carbon atoms to the end of the chain. High chemoselectivity for the desired functionalization and high regioselectivity towards functionalization in the terminal position are also required. The transformation of unsaturated fatty compounds into α,ω-functionalized long chained molecules is made even more difficult because internal double bonds are thermodynamically favored over terminal ones.[207] In the case of methyl oleate, only 0.2% of all isomers contain a terminal double bond in the equilibrium mixture.[162] Mecking et al. recently published a detailed review of this topic.[135]

Of particular interest in this context are isomerization/carbonylation tandem reactions such as alkoxycarbonylations or hydroformylations. They enable the incorporation of the complete carbon chain of the fatty acid for the synthesis of potential polymer precursors.

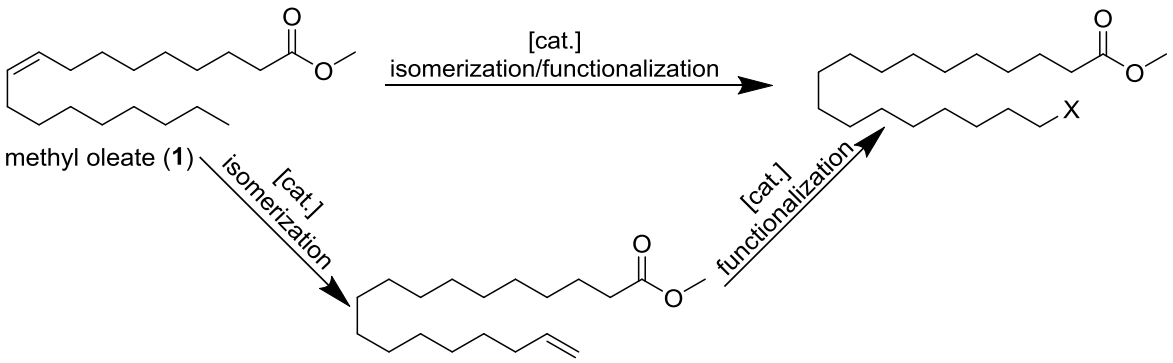

Scheme 4.47: Isomerization/ω-functionalization of methyl oleate (**1**).

The isomerization/methoxycarbonylation (Scheme 4.48) of fatty acid methyl esters (FAMEs) first described by Cole-Hamilton et al. is a very successful example for this kind of transformation.[144] Yields of >85% and selectivities of >95% towards the linear product are achieved using a Pd/dtbx catalyst (Scheme 4.48). Detailed mechanistic studies have been conducted by Mecking et al.[161,162] and Köckritz et al.[163] Recently, successful approaches to recycle the Pd/dtbx catalyst using ionic liquids and thermomorphic solvent systems were also reported by Riisager et al.[247] and our group.[205,316] The conversion of FAMEs *via* alkoxycarbonylation leads directly to symmetric α,ω-functionalized diesters with potential application as AA-type monomers.

For the selective synthesis of valuable asymmetric α,ω-functionalized molecules, which are potential AB-type monomers, *via* isomerizing alkoxycarbonylation at a reasonable reaction time and with high selectivities, FAMEs have to be derivatized prior reaction (e.g. to amides).[151,286]

Isomerizing hydroformylation provides a more straightforward way of synthesizing asymmetric α,ω-functionalized molecules from FAMEs (Scheme 4.48). The isomerizing hydroformylation is well described for simple internal olefins and short chained unsaturated esters such as methyl 3-pentenoate.[126] Unfortunately, all catalysts applied in the isomerizing hydroformylation of FAMEs lead to low yields, chemo- and/or regioselectivities.

Nozaki *et al.* described the synthesis of C19-alcohols from methyl oleate (**1**) *via* an isomerization/hydroformylation/hydrogenation tandem reaction. The resulting aldehydes from the rhodium catalyzed hydroformylation are directly converted into corresponding alcohols by a second ruthenium catalyst. The yield of the linear alcohol is 53% with a *l/b*-ratio of 82/18.[136] Direct synthesis of alcohols may either be desired or not, since they already are an AB-type monomer. On the other hand, the aldehyde, as the more versatile intermedi-

ate, can be easily converted into different products (e.g., alcohols, amines, carboxylic acids).

If the aldehyde itself is targeted, yields of the linear product described in the literature regarding the isomerizing hydroformylation of methyl oleate (**1**) are even lower. A yield of 26% of the linear aldehyde can be achieved by applying a Rh/biphephos (Scheme 4.48) catalyst complex. The yield is slightly higher (34%) using ethyl linoleate as substrate. These are the highest yields yet reported in the literature. The ratio of linear to branched (*l*/*b*) aldehydes is about 75/25 in both reactions, which is unusually low for a Rh/biphephos catalyst.[87] The application of ligand **L1** (Scheme 4.48) leads to similar *l*/*b*-ratios. The yield of the desired linear product cannot be improved with this catalyst either.[125] The main problems this kind of transformation presents are that the hydrogenation of the starting material and the formation of branched aldehydes lead to low chemo- and regioselectivities if the known catalysts are applied.

Consequently, developing a new catalytic system that catalyzes the double bond isomerization from the 9 position to the carbon chains end and the linear selective hydroformylation in an efficient manner is of high interest.

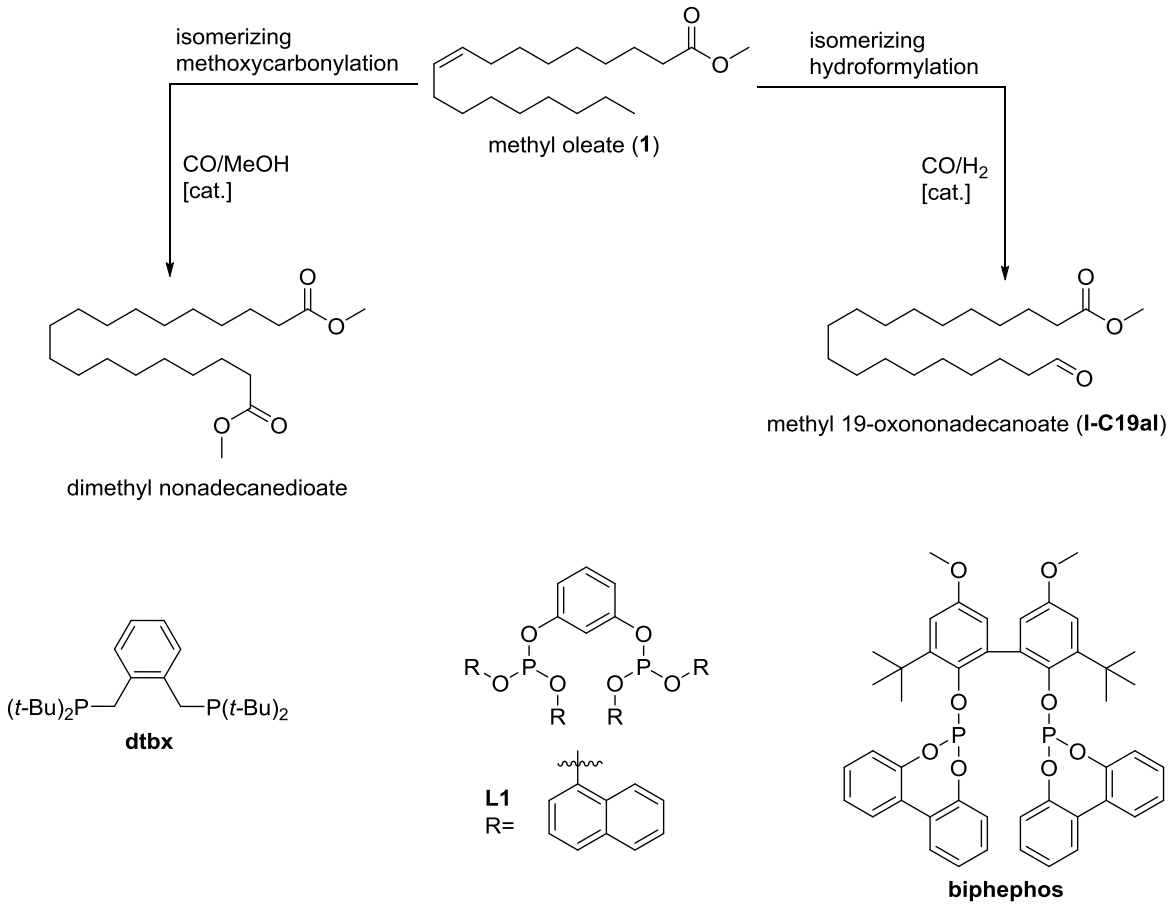

Scheme 4.48: Isomerizing hydroformylation and methoxycarbonylation.

In order to overcome the limitations mentioned above, we decided to develop an orthogonal tandem reaction using two different catalysts: one catalyst for the isomerization and one catalyst for the linear selective hydroformylation of the terminal double bond. This strategy allows the reaction to proceed at mild reaction conditions, enabling the highest yields and the highest regioselectivity towards the linear aldehyde in the hydroformylation of methyl oleate (**1**) described in the literature today (Scheme 4.49).

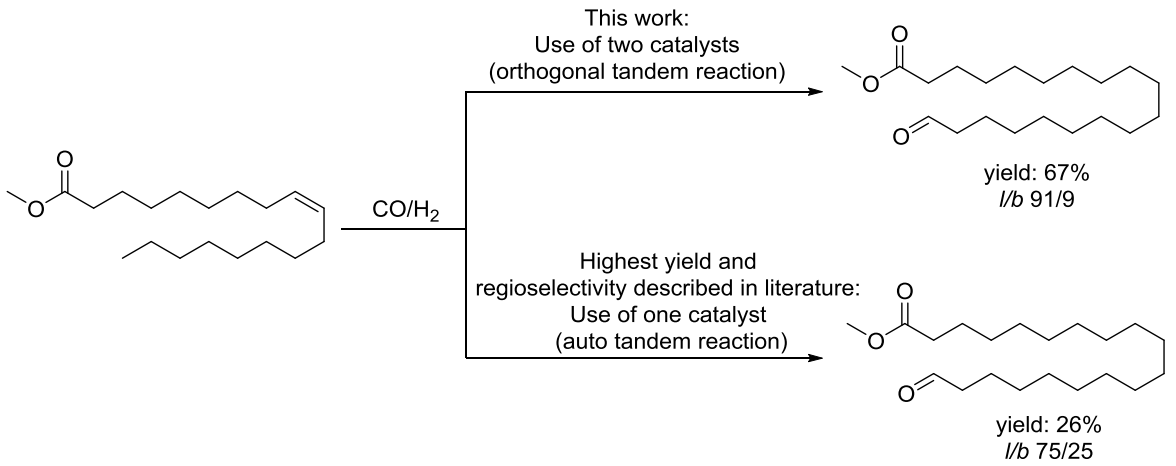

Scheme 4.49: Isomerizing hydroformylation of methyl oleate: This work compared with literature.

4.8.3. Results and Discussion

In order to identify a suitable orthogonal catalyst system as well as suitable reaction conditions, we started our investigation of isomerizing hydroformylation using methyl 3-hexenoate (**2**, Scheme 4.50) as a model substrate. Substrate **2** has an internal double bond and an ester moiety such as the targeted substrate methyl oleate (**1**). In principle, the same qualitative problems as in the conversion of **1** occur. The model substrate 3-methyl hexenoate with its shorter carbon chain provides crucial analytical advantages since isomers can be separated and quantified *via* gas chromatography.

In order to identify problems that occur in connection with the elongation of the substrates carbon chain, we decided to apply the developed catalyst systems and reaction conditions to ethyl 4-decenoate (**3**, Scheme 4.50) as a second model substrate, before optimizing the conditions for the isomerizing hydroformylation of methyl oleate. Scheme 4.50 summarizes the approach for the development of the tandem reaction.

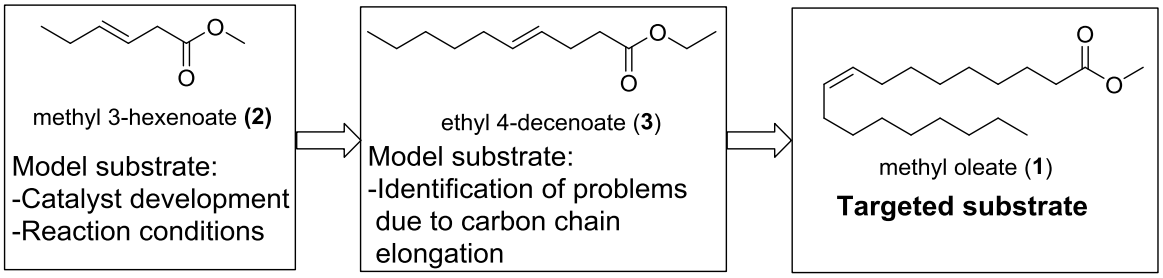

Scheme 4.50: Approach for development of the isomerizing hydroformylation of FAMEs.

4.8.3.1. Catalyst Development

To develop a new orthogonal tandem catalytic system for the isomerization/hydroformylation tandem reaction, we determined several selection criteria for both the hydroformylation and the isomerization catalyst. The hydroformylation catalyst needs to be very selective for functionalization in the terminal position. The activity in double bond hydrogenation needs to be as low as possible. We decided to use a Rh/biphephos catalyst, which is well known for linear selective hydroformylation and also provides the highest yields of the linear aldehyde in the hydroformylation of methyl oleate described in the literature.[87] This catalyst also has some activity in double bond isomerization that is helpful in view of the tandem reaction.

The isomerization catalyst, on the other hand, has to be highly active in double bond isomerization in a synthesis gas atmosphere. Activity in hydrogenation and (non-selective) hydroformylation are highly undesirable. In order to find a suitable isomerization catalyst, we investigated several transition metal catalyst precursors based on Pd, Rh, Ru, Ir, Pt Co and Ni in the isomerization of methyl 3-hexenoate (**2**) under hydroformylation conditions (15 bar CO/H_2, 90 °C, most promising results are shown in Table 4.25, all tested precursors can be found in Table 7.1 and Table 7.2, Chapter 7.4). The most promising candidate was the palladium-dimer **C1** (Table 4.25, Entry 1.2, Scheme 4.52). This catalyst precursor was first synthesized by Vilar et al.[317] and also described by Gooßen et al. as very effective in the double bond isomerization of long chained olefins and oleocompounds in their work regarding the isomerizing metathesis tandem reaction.[318–320]

Table 4.25:Isomerization catalyst screening.

Entry	Catalyst	High isomerization rate	No hydroformylation	No Hydrogenation
1.1	$Pd(t\text{-}Bu_3P)_2$	•	✓	✓
1.2	C1	✓	✓	✓
1.3	$PdCl_2(PPh_3)_2$	•	✓	✓
1.4	$Rh_2(OAc)_2$	✓	•	•
1.5	Shvo's catalyst	✓	✓	•

Conditions: 2.1 g toluene, 3.5 mmol 2, 1 mol% metal, 15 bar synthesis gas (CO/H_2 = 1/1), 16 h, 90 °C, batch reaction in 20 mL autoclave, stirrer speed 500 rpm.
✓= Meets criterion fully, •= Meets criterion in an acceptable manner; ×= does not meet criterion
Isomerization, hydroformylation and hydrogenation are detected by GC-FID.

We began developing an orthogonal tandem catalytic system consisting of Rh/biphephos as the hydroformylation catalyst and **C1** as the isomerization catalyst in the isomerizing hydroformylation of **2**. Scheme 4.51 shows the reaction network of this reaction. The desired linear aldehyde (**l-C7al**) can only be formed from the isomer containing the terminal double bond. Branched aldehydes (**b-C7al**) and the hydrogenated substrate (**C6an**) can be formed from any isomer of **2**. Especially the α,β-unsaturated isomer of **2** is very prone for hydrogenation.[87]

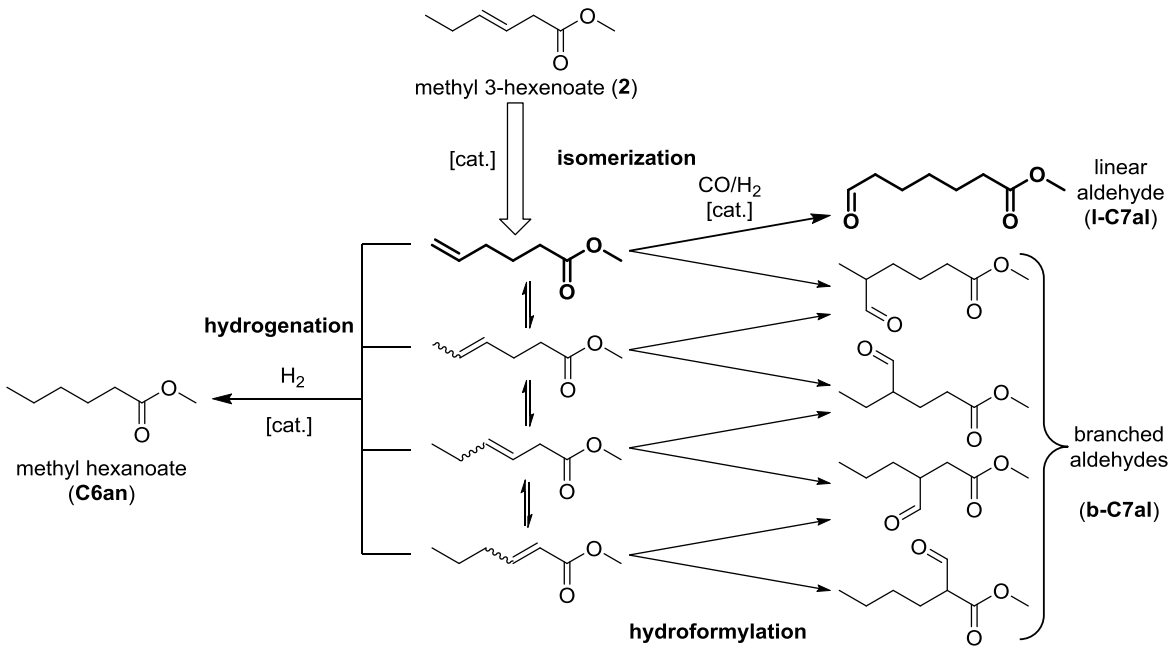

Scheme 4.51: Reaction network of the isomerizing hydroformylation of **2**.

If the Rh/biphephos catalyst was applied without the addition of **C1** (Table 4.26, Entry 2.1), the yield of the linear aldehyde (**l-C7al**) is 59% under the given conditions. The *l/b*-

ratio is 81/19, which is relatively low for this catalyst compared to the results obtained if the internal olefins are converted (>90/10) and the yield of the hydrogenated substrate (**C6an**) is 15%.

When 0.5 mol% of **C1** was added, much better results were obtained. The yield of **l-C7al** increased to 68% with a high *l/b*-ratio of 95/5. Also, substrate hydrogenation was slightly suppressed with 10% of **C6an** obtained.

The **C1** amount added had strong influence on the outcome of the reaction (Entries 2.2 – 2.4). When the amount of **C1** was decreased to 0.25 mol%, yield of **l-C7al** was comparable (65%), but the *l/b*-ratio decreased drastically to 82/18 while the yield of hydrogenated **C6an** was 17%. On the other hand, when 1 mol% **C1** was added, the *l/b*-ratio was even higher (98/2) but the activity of the Rh/biphephos catalyst was inhibited and only 45% of **l-C7al** were formed.

However, in light of these first promising results, we decided to study this orthogonal catalyst system in greater detail. We were first interested in the role of the Pd-dimer **C1**. According to Gooßen et al. this compound can be synthesized *via* comproportionation of $PdBr_2$ and Pd(*t*-$Bu_3P)_2$ (Scheme 4.52).[321]

We wondered if precursor **C1** is necessary to form the catalytically active isomerization species or if it could be formed merely by adding $PdBr_2$ and Pd(*t*-$Bu_3P)_2$ to the reaction mixture under given conditions.

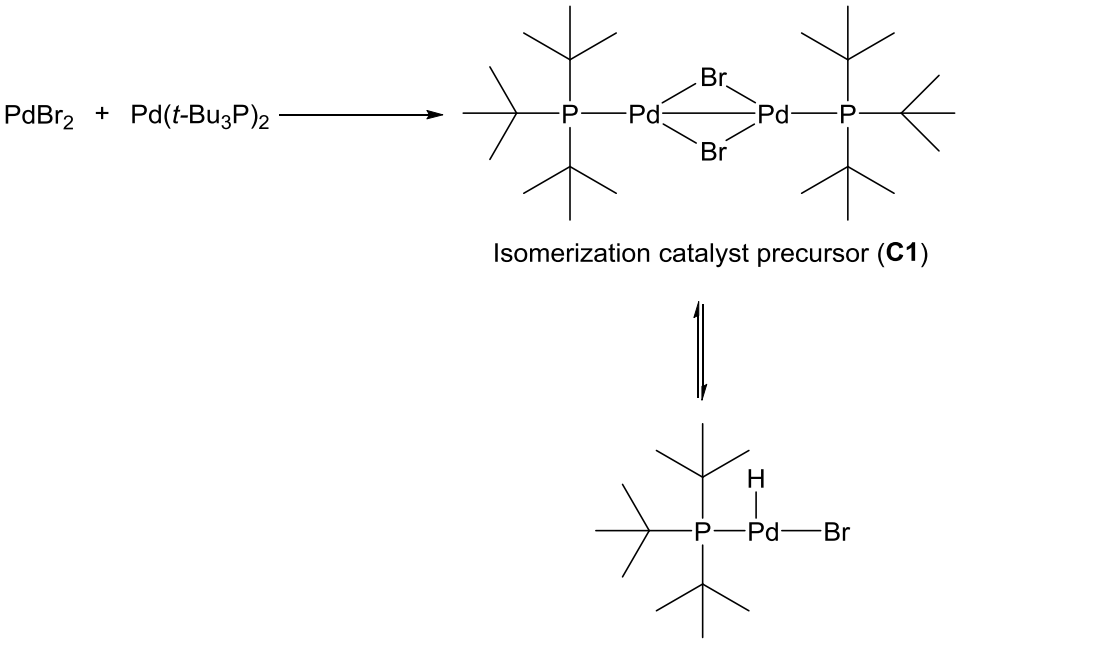

Scheme 4.52: Synthesis of C1 and likely catalytically active species according to Gooßen et al.[321,322]

The latter would be advantageous since additional effort and costs would be avoided if the synthesis of **C1** is not required. A comparison of the results of the reaction using **C1** as isomerization catalyst precursor (Entry 2.2) with the use of $PdBr_2$ and Pd(*t*-$Bu_3P)_2$ (Entry 2.5) showed that the yield of the linear aldehyde **l-C7al** was slightly higher (73% vs 68%) when the active isomerization catalyst was formed directly from $PdBr_2$ and Pd(*t*-$Bu_3P)_2$, but selectivity was slightly lower (*l/b*: 88/12 vs. 95/5; yield **C6an** 15% vs. 10%). In principle, both precursors caused similar results in the tandem reaction, which led us to the assumption that the catalytically active isomerization species is the same in both cases. DFT studies made by Gooßen et al. in their investigations regarding the isomerization of allylic esters suggest that the active isomerization catalyst is species **C1*** (Scheme 4.52).[322] We assume this could also be the active isomerization catalyst in this case.

In order to get more information about the isomerization catalyst we conducted an experiment in which only Pd(*t*-$Bu_3P)_2$ was added as a precursor (Entry 2.6). The results (yield of **l-C7al** 49%, *l/b* = 84/16) obtained were more or less comparable with the reaction without introducing any isomerization catalyst (Entry 2.1), although the activity in hydroformylation and hydrogenation was slightly lower. We also screened the Pd(*t*-$Bu_3P)_2$ precursor in the isomerization of **2** without Rh/biphephos and only small amounts of isomers were formed (Entry S1.3, Table 7.1). Based on these results we concluded that the halide anion is coordinated to the active isomerization catalyst (as in complex **C1***) and that it has a strong influence on the catalyst activity. We further investigated how the nature of the halide influences the tandem reaction (Entries 2.5, 2.7, 2.8). It turned out that the catalytic activity as well as the selectivity towards desired **l-C7al** increases strongly from chloride to iodide. When $PdCl_2$/Pd(*t*-$Bu_3P)_2$ was used as precursor (Entry 2.7), the yield of **l-C7al** was 60% and the *l/b*- ratio was 82/18, which again is quite similar to the results obtained without an additional isomerization catalyst (Entry 2.1). In contrast, by using PdI_2/Pd(*t*-$Bu_3P)_2$, a very high yield of **l-C7al** (81%) and an excellent *l/b*-ratio of 98/2 were obtained. One possible explanation for this effect is that the nature of the halide influences the formation of the catalytically active, three-coordinated Pd-isomerization species from a four-coordinated, halide-bridged dimeric resting state of the catalyst. Also a direct influence of the halide on isomerization activity of the catalytically active species cannot be excluded at this point.

Investigations on the halide source (use of LiI instead of PdI2) show that the cations nature does not influence the outcome of the tandem reaction (comparing Entries 2.8 and 2.11) but, as mentioned above, the amount of Palladium (and therefore the ratio of Pd/I^-) is crucial (comparing Entries 2.8, 2.10 and 2.11) to prevent catalyst deactivation. A Pd/I^--ratio of 1/1 led to excellent yields of **l-C7al** (~80%) and l/b-ratios (98/2) whereas an excess of iodide led to catalyst deactivation. These results also show that the oxidation state of

the Pd precursor is not crucial and both the Pd(0) and the Pd(II) are converted into the active isomerization catalyst under the given conditions.

Table 4.26: Catalyst development for the isomerizing hydroformylation of methyl 3-hexenoate (**2**).

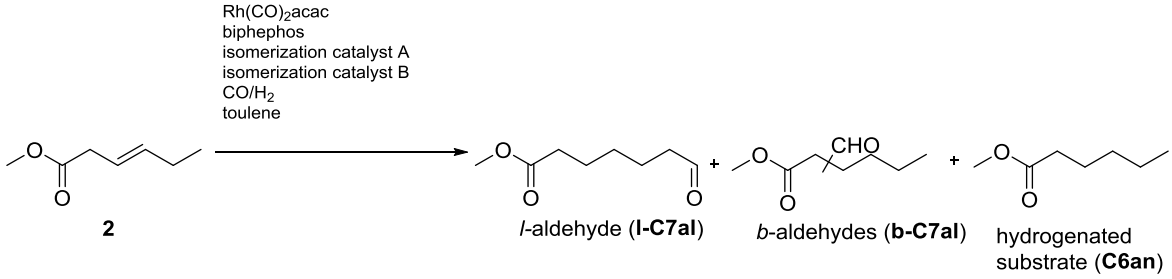

Entry	Isomerization catalyst A	Isomerization catalyst B	Conversion[a] [%]	*l*-aldehyde (l-C7al) [%]	*b*-aldehyde (b-C7al) [%]	Hydrogenated substrate (C6an) [%]	*l*/*b*-ratio
2.1	-	-	87	59	13	15	81/19
2.2	0.5 mol% C1	-	81	68	3	10	95/5
2.3	0.25 mol% C1	-	96	65	14	17	82/18
2.4	1 mol% C1	-	54	45	1	8	98/2
2.5	0.5 mol% $PdBr_2$	0.5 mol% $Pd(t\text{-}Bu_3P)_{2\,2}$	98	73	10	15	88/12
2.6	-	1 mol% $Pd(t\text{-}Bu_3P)_2$	68	49	9	10	84/16
2.7	0.5 mol% $PdCl_2$	0.5 mol% $Pd(t\text{-}Bu_3P)_2$	94	60	13	21	82/18
2.8	0.5 mol% PdI_2	0.5 mol% $Pd(t\text{-}Bu_3P)_2$	>99	81	2	17	98/2
2.9	1 mol% PdI_2	-	<1	-	-	-	-
2.10	1 mol% LiI	0.5 mol% $Pd(t\text{-}Bu_3P)_2$	15	12	<1	2	97/3
2.11	1 mol% LiI	1 mol% $Pd(t\text{-}Bu_3P)_2$	>99	78	2	19	98/2

Conditions: 2.1 g toluene, 3.5 mmol 2, 0.4 mol% $Rh(CO)_2acac$, 1.6 mol% biphephos, 15 bar synthesis gas (CO/H_2 = 1/1), 16 h, 90 °C, batch reaction in 20 mL autoclave, stirrer speed 500 rpm. Conversion yields and *l*/*b*-ratios were determined by GC-FID.
[a] Double bond isomerization not considered in the conversion

We also were interested in the distribution of the isomeric unsaturated C6-esters in the equilibrium and the distribution of the branched C7-aldehydes (b-C7al) (Table 4.27).

Studies of Mecking et al. regarding the isomerization of methyl 5-hexenoate showed that the α,β-unsaturated isomers are the most abundant ones in the thermodynamic equilibrium (54.4% at room temperature). The equilibrium mixture contains only 0.9% of the terminal unsaturated isomers.[162] Consequently, high yield and high selectivity towards the desired linear aldehyde can only be achieved if mainly terminal unsaturated isomers are

hydroformylated and therefore are selectively removed from the equilibrium. These isomers can then be regenerated by isomerization of the internal unsaturated isomers.

The distribution of the branched aldehydes formed if Rh/biphephos is applied as the only catalyst (Table 4.27) shows that in principle also internal double bonds can be hydroformylated under given conditions, if they coordinate to the Rh-center. 67% of all branched aldehydes are formed exclusively by hydroformylation of an internal double bond. Only 33% of the branched aldehydes contain the formyl group in position 5 of the carbon chain. This aldehyde can either be formed by hydroformylation of the terminal unsaturated C6-ester or from the unsaturated C6-ester with the double bond in position 4.

In contrast, application of the orthogonal Rh/Pd-catalyst strongly shifts this distribution towards formation of the branched aldehyde with the formyl group in position 5 (63% of all branched aldehydes; Table 4.27). One possible explanation for this observation is that the coordination of the terminal unsaturated substrate to the Rh/biphephos complex, which is supposed to be the rate determining step in the hydroformylation using this catalyst[323], is strongly favored over coordination of isomers with an internal double bond. If the terminal unsaturated isomers are generated by an additional isomerization catalyst, mainly these isomers will coordinate to the Rh-complex and undergo hydroformylation. This leads to an exceptional high *l/b*-ratio (98/2).

After investigating the reaction parameters temperature, synthesis gas pressure and synthesis gas composition (Figure 7.12 – Figure 7.14) and slightly adjusting (100 °C and 10 bar) the reaction conditions, we studied the kinetics of the reaction to better understand the interplay between both catalysts. Therefore, experiments with the orthogonal tandem catalytic system consisting of Rh/biphephos/PdI_2/Pd(*t*-$Bu_3P)_2$ (Figure 4.53a) were compared with experiments using only the Rh/biphephos catalyst at different temperatures (Figure 4.53b – c).

When the orthogonal catalyst was used (Figure 4.53a), isomerization of methyl 3-hexenoate (**2**) was extremely fast.

After ten minutes the mixture contained only 16% of the starting material and 74% isomers. At this point the isomers seem to be in equilibrium since the concentrations of **2** and its isomers decreased at the same rate. The formation of the linear aldehyde also started instantly (9% after 10 minutes).

During the first four hours, remarkably, no formation of branched aldehydes was observed. Consequently, only isomers containing a terminal double bond were consumed *via* hydroformylation and regenerated from the remaining isomers *via* isomerization. Hydrogenated substrate was also detected from the start of the reaction (1% after 0.5 h).

Based on the results described in previous studies[87], it can be assumed that mainly the α,β–unsaturated isomer is hydrogenated.

Table 4.27:Double bond isomer distribution of **2** in the equilibrium and distribution of branched aldehydes after reaction.

Equilibrium distribution of double bond isomers (at room temperature) [162]	Distribution of branched aldehydes using only Rh/biphephos catalyst	Distribution of branched aldehydes using orthogonal Rh/Pd catalyst [a]
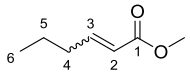 54.4%		
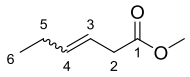 9.1%	**Branched aldehydes exclusively formed from internal double bonds: 67%**	**Branched aldehydes exclusively formed from internal double bonds: 37%**
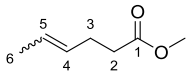 35.6%		
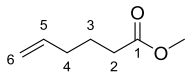 0.9%	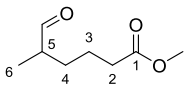 33%	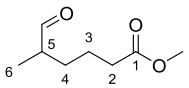 63%

Reaction conditions: Conditions: 2.1 g toluene, 3.5 mmol 2, 0.4 mol% $Rh(CO)_2acac$, 1.6 mol% biphephos, 15 bar synthesis gas (absolute pressure, CO/H2 = 1/1), 16 h, 90 °C, batch reaction in 20 mL autoclave, stirrer speed 500 rpm. Distribution of aldehyde isomers was determined by GC-FID. Identification of the formyl groups position was done by GC-MSD.
[a] Addition of 0.5 mol% PdI_2 and 0.5 mol% $Pd(t\text{-}Bu_3P)_2$

When only Rh/biphephos (Figure 4.53b) was applied as a catalyst at 90 °C, the isomerization rate drastically decreased. The formation of the targeted linear aldehyde **l-C7al** was slower (3% after 0.5 h) and also the formation of undesired branched aldehydes was detected from the start of the reaction (1% after 0.5 h).

Undesired hydrogenation of the substrate was more than two times faster (7% after 2 h instead of 3%) compared to the application of the orthogonal catalyst.

When the temperature was increased to 100 °C (Figure 4.53c), the reaction rates of all partial reactions increased as well. After two hours, aldehyde yield of 52% (*l/b*=90/10) and 14% of the hydrogenated substrate **C6an** were obtained.

The selectivity towards the linear aldehyde in the hydroformylation also increased with temperature. Compared to the orthogonal catalyst system, the isomerization of **2** was still much slower, though the hydroformylation (branched) and hydrogenation reaction rates were higher.

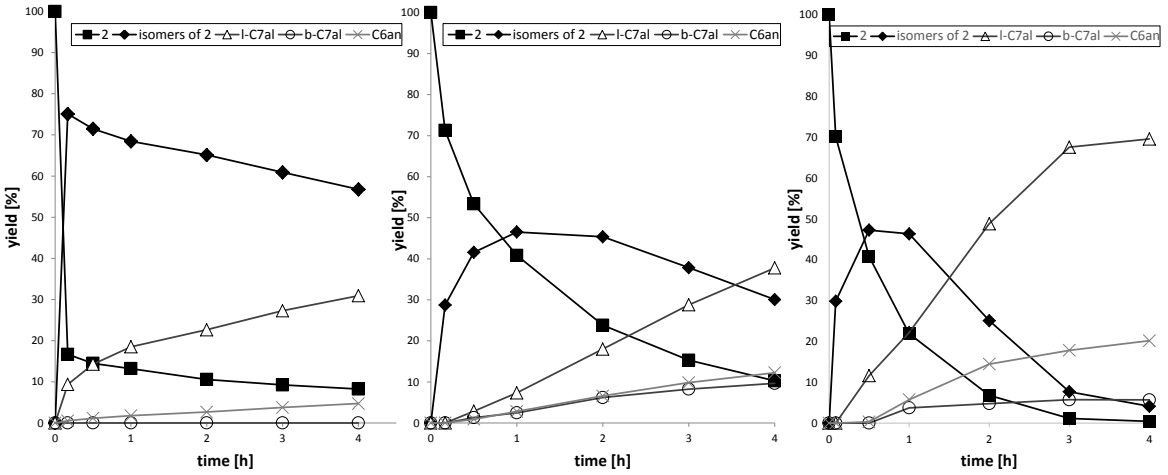

a. Rh/biphephos/PdI_2/Pd(*t*-$Bu_3P)_2$ at 100 °C b. Rh/biphephos at 90 °C c. Rh/biphephos at 100 °C

Figure 4.53: Reaction kinetics of the isomerizing hydroformylation of 2.
a) Conditions: 48 g toluene, 70 mmol 2, 0.4 mol% $Rh(CO)_2$acac, 1.6 mol% biphephos, 0.5 mol% PdI_2, 0.5 mol Pd(*t*-$Bu_3P)_2$ 10 bar synthesis gas (CO/H_2 = 1/1), 100 °C, batch reaction in 300 mL autoclave, stirrer speed 1000 rpm. Yields were determined by GC-FID.
b). Conditions: 48 g toluene, 70 mmol 2, 0.4 mol% $Rh(CO)_2$acac, 1.6 mol% biphephos, 15 bar synthesis gas (CO/H_2 = 1/1), 90 °C, batch reaction in 300 mL autoclave, stirrer speed 1000 rpm. Yields were determined by GC-FID.
c) Conditions: 48 g toluene, 70 mmol 2, 0.4 mol% $Rh(CO)_2$acac, 1.6 mol% biphephos, 10 bar synthesis gas (CO/H_2 = 1/1), 100 °C, batch reaction in 300 mL autoclave, stirrer speed 1000 rpm. Yields were determined by GC-FID.

The use of the orthogonal catalyst inhibits the most important side reactions (hydrogenation and formation of branched aldehydes). The results show that selectivity towards the linear hydroformylation product correlates with the isomerization rate. As outlined above, this could be traced back to a higher coordination affinity of the terminal unsaturated substrates to the Rh/biphephos complex. If an additional isomerization catalyst is present, the "supply" of the terminal unsaturated isomers *via* isomerization of internal unsaturated ones is very fast, resulting in an exceptionally high *l/b*-ratio in the hydroformylation. This could also explain the higher chemoselectivity when the orthogonal tandem catalyst is applied, especially considering that the α,β-unsaturated isomer is very prone to hydrogenation.[87] However, interactions between the transition metals and their ligands cannot be excluded at this point. For example, as shown in Table 4.26 (Entry 2.9 and Entry 2.10), catalytic activity is strongly inhibited if more iodide than palladium is present in the reaction mixture. This demonstrates that components of the isomerization catalyst precursor may potentially interact with the rhodium catalyst.

After successfully developing a promising orthogonal tandem catalytic system, the next step was to apply this system in the isomerizing hydroformylation of ethyl 4-deceneoate (**3**) as a second model substrate bearing a longer carbon chain.

4.8.3.2. Isomerizing Hydroformylation of Ethyl 4-decenoate (**3**)

In order to identify limitations that occur when using a long chained unsaturated ester as a substrate, we tested the catalyst system in the isomerizing hydroformylation of ethyl 4-decenoate (**3**) (Figure 4.54). The results show that reaction rates for hydroformylation and hydrogenation were slower compared to the conversion of **2**. Aldehyde formation (1% **l-C11al**) was observed after two hours. The hydrogenation of the starting material was observed after four hours (1% yield of **C10an**)**.** This was the case because it took more time to reach the equilibrium of the double bond isomers (Figure 7.15). Ratios of the isomers were unchanged after two hours. Afterwards, the reaction proceeded similar to the isomerizing hydroformylation of **2**, albeit more slowly due to the lower equilibrium concentration of the terminal unsaturated ester. After 44 h, the yield of the desired linear product **l-C11al** reached 60%. The *l*/*b*-ratio of the resulting aldehydes was also slightly lower (95/5). As discussed before, this could also be attributed to the lower concentration of the terminal unsaturated isomer of **3**. For the conversion of long chained fatty acid methyl esters such as methyl oleate, the isomerization rate has to be increased in order to reach reasonable yields and *l*/*b*-ratios.

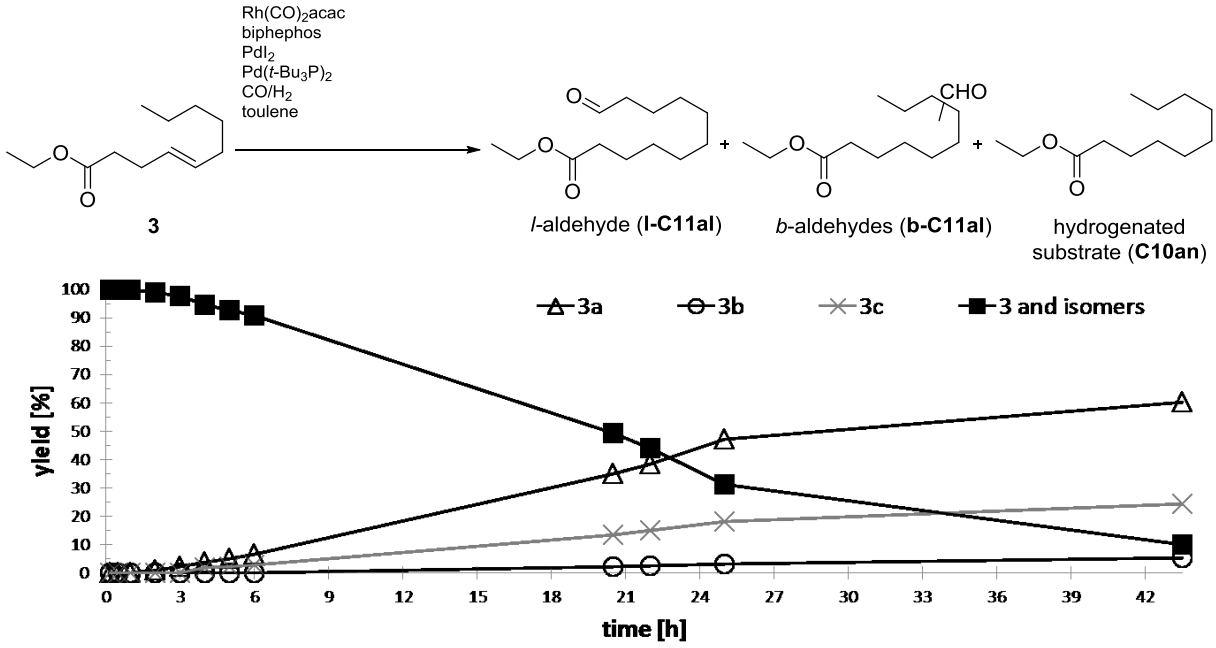

Figure 4.54: Isomerizing hydroformylation of 4-ethyl decenoate.
Conditions: 48 g toluene, 40 mmol **3**, 0.4 mol% $Rh(CO)_2acac$, 1.6 mol% biphephos, 0.5 mol% PdI_2, 0.5 mol $Pd(t\text{-}Bu_3P)_2$ 10 bar synthesis gas (CO/H_2 = 1/1), 100 °C, batch reaction in 300 mL autoclave, stirrer speed 1000 rpm. Yields were determined by GC-FID.

4.8.3.3. Isomerizing hydroformylation of methyl oleate (**1**)

As discussed above, a high isomerization rate is required for an efficient conversion of long chained unsaturated esters such as methyl oleate (**1**). When the developed reaction

conditions are applied directly in the isomerizing hydroformylation of methyl oleate, almost no reaction was observed (Table 4.28, Entry 4.1). A higher isomerization rate can be achieved by increasing the temperature or the isomerization catalyst concentration. Studies on model substrate (**2**) showed that increasing the temperature led to high yields of the undesired hydrogenation product and low *l/b*-ratios (Figure 7.12). The same observation was made in the hydroformylation of methyl oleate (Entry 4.2). The yield of the hydrogenated substrate (c18an) was 15%, whereas the yield of the targeted linear aldehyde (13% **l-C19al**) and also the *l/b*-ratio (55/45) of the resulting aldehydes were low. By contrast, higher palladium concentrations led to more promising results (Entry 4.3). When 2 mol% of both Pd-precursors are used at 100 °C, the yield of **l-C19al** was still low (15%) but the *l/b*-ratio of the aldehydes was 83/17. Investigations on model substrate **2** showed that the ratio of Pd/I^- strongly influences the activity and selectivity of the reaction (Table 4.26, entries 2.10 and 2.11). Therefore we examined the Pd/I^- ratio in greater detail for the isomerizing hydroformylation of methyl oleate (**1**) (Table 4.28, entries 4.3-4.8). The results show that the best yields of **l-C19al** were obtained when the PdI_2 concentration was reduced to 0.33 mol% (Pd/I^- ratio of 3.5, Entry 4.6). The yield of the desired linear aldehyde **l-C19al** was 44% with an *l/b*-ratio of 88/12. Higher iodide concentrations led to lower catalyst activity while lower iodide concentrations also led to a strongly decreased *l/b*-ratio. After this investigation we set the Pd/I^- ratio to 3.5 and varied the total amount of the isomerization catalyst precursor. It seems that a total palladium concentration of 2.33 mol% is sufficient to allow for a high isomerization rate (Entry 4.6).

Higher amounts do not lead to higher yields of desired **l-C19al** (Entry 4.9 and 4.10). Lower concentrations (Entry 4.11) lead to decreased catalytic activity (conversion 40%, yield of **l-C19al** 19% and regioselectivity (*l/b* 70/30), indicating that the “supply” of terminal unsaturated esters for the rhodium catalyst is not fast enough. Longer reaction times lead to a higher conversion and higher yields of the desired product **l-C19al.** After 40h, the yield of **l-C19al** was 62% (Entry 4.12), after 72 h full conversion was reached, yielding in 67% **l-C19al** and a *l/b*-ratio of the aldehydes of 91/9 (Entry 4.13). These are the highest yields and selectivities described in the literature thus far. In the absence of the isomerization catalyst (Entry 4.14), yield of the linear aldehyde (3%) and *l/b*-ratio (20/80) were drastically lower, clearly demonstrating the benefit of the developed orthogonal tandem catalytic system. It allows for the generation of high aldehyde yields (74%) and excellent regioselectivities (*l/b* 91/1) in the hydroformylation.

However, the hydrogenation of the substrate is still an issue using the bimetallic catalyst. In order to arrive at a better understanding of the interplay of the orthogonal catalyst system, *in situ* spectroscopic measurements combined with DFT studies should be conduct-

ed.[324] This could lead to insights that may prove to be very helpful in the design of new, more efficient orthogonal catalysts.

Table 4.28: Catalyst development for the isomerizing hydroformylation of methyl oleate (1).

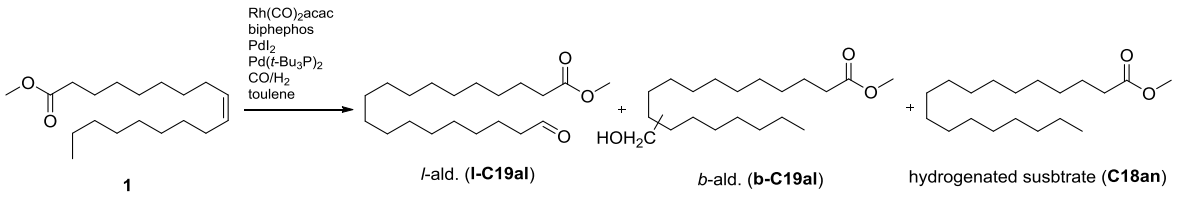

Entry	*T* [°C]	*t* [h]	PdI_2	Pd(*t*-$Bu_3P)_2$	Conv.[a] [%]	*l*-ald. (l-C19al) [%]	*b*-ald. (b-C19al) [%]	Hydrogenated substrate (C18an) [%]	*l*/*b*-ratio
4.1[b]	100	16	0.5 mol%	0.5 mol%	4	-	-	4	-
4.2[b]	140	16	0.5 mol%	0.5 mol%	38	13	10	15	55/45
4.3	100	16	2 mol%	2 mol%	31	15	3	13	83/17
4.4	100	16	1 mol%	2 mol%	45	17	3	25	90/10
4.5	100	16	0.5 mol%	2 mol%	55	33	5	17	87/13
4.6	100	16	0.33 mol%	2 mol%	72	44	6	22	88/12
4.7	100	16	0.2 mol%	2 $mol\%_2$	63	37	7	19	84/16
4.8	100	16	-	2.3 mol%	60	31	14	15	70/30
4.9	100	16	1 mol%	6 mol%	71	45	5	21	91/9
4.10	100	16	0.5 mol%	3 mol%	76	46	6	24	88/12
4.11	100	16	0.17 mol%	1 mol%	40	19	9	12	70/30
4.12	100	40	0.5 mol%	3 mol%	93	62	7	24	89/11
4.13	100	72	0.5 mol%	3 mol%	>99	67	7	25	91/9
4.14	100	16	-	-	21	3	12	6	20/80

Conditions: 2.05 g toluene, 1.3 mmol 1, 0.8 mol% $Rh(CO)_2$acac, 3.2 mol% biphephos, 10 bar synthesis gas (CO/H_2 = 1/1), batch reaction in 20 mL autoclave, stirrer speed 500 rpm. Yields were determined by GC-FID.
[a] Double bond isomerization not considered in the conversion.
[b] 0.4 mol% $Rh(CO)_2$acac, 1.6 mol% biphephos

4.8.4. Conclusions

In this paper we describe the successful development of an orthogonal tandem catalytic system for the linear selective isomerizing hydroformylation of methyl oleate. The isomerization catalyst consists of the palladium precursors Pd(*t*-$Bu_3P)_2$ and PdI_2 at a ratio of 6/1, while a Rh/biphephos complex is used as the hydroformylation catalyst. The use of this catalyst system leads to an aldehyde yield of 74% and an *l*/*b*-ratio of 91/9 for the resulting aldehydes. These are the highest yields and selectivities described for this reaction in the literature thus far.

4.8.5. Experimental

Chemicals

Toluene (Acros Organics, >99%), ethyl acetate (Acros Organics, >99%), cyclohexane (Acros Organics, >99%) methyl 3-hexenoate (Acros Organics, >95%), ethyl 4-decenoate (TCI Chemicals, >98%) were purchased from different commercial suppliers. Methyl oleate (>89%) was donated by Dako Aktiengesellschaft Chemical Products. Biphephos (>95%) was synthesized from Molisa GmbH. $Rh(CO)_2acac$ was donated by Umicore AG & Co. Kg. Palladium precursors, tri-*tert*-butylphosphine and Lithiumiodid were purchased from ABCR. All chemicals were degassed before use and stored under argon. CO (2.0) and H_2 (5.0) were purchased from Messer Industriegase GmbH.

Hydroformylation reactions

$Rh(CO)_2acac$, $Pd(t\text{-}bu_3P)_2$, PdI_2 and biphephos were weighted either in a homemade 20 ml autoclave or in a 300 ml autoclave (Parr Instruments). The autoclave was closed, evacuated and flushed with argon three times. Degassed toluene and the substrate were subsequently transferred into the reactor *via* cannula using the standard Schlenk technique. The reactor was pressurized with synthesis gas and heated while stirring to reaction temperature. In cases of time-resolved experiments, samples were taken from the reactor and analyzed *via* GC-FID. After the reaction time the reactor was put into an ice bath and the pressure was carefully released. The reaction mixture was analyzed *via* GC-FID.

Analytics

Details about the analytics used in this work (GC-FID methods and exemplary chromatograms, NMR spectra) can be found in the supporting information.

4.8.6. Acknowledgments

We gratefully acknowledge the financial support of the German Science Foundation (Project SFB/TRR 63: ”InPROMPT – Integrated Chemical Processes in Multi-Phase Fluid Systems”) for this work (Subproject A1). We would also like to express our gratitude to Umicore AG & Co. KG for supplying the catalyst precursors and to Dako Aktiengesellschaft Chemical Products for supplying the methyl oleate.

5. Summary, Conclusions and Outlook

Two main aspects, which were identified to have high impact on process development, were tackled within this thesis.

The first research focus aimed the recovery of known homogeneous transition metal catalysts. In this context, TMS systems were systematically investigated to extend their application area as catalyst recycling concept. Furthermore, limitations of their applicability were detected. The gained knowledge will be used for the design of a general guide for the application of TMS systems in homogeneous catalysis.

The second research focal point was the design of new catalytic systems for tandem reactions with renewables. Possible catalyst recycling strategies and further developments based on the results in the investigated reactions will be discussed in this chapter.

The results of this work will finally be discussed in light of the guiding principles of *sustainability* and *industrial relevance*.

5.1. Catalyst Recovery *via* Thermomorphic Multicomponent Solvent Systems (TMS Systems)

The evaluation and expansion of the scope of TMS systems as catalyst recycling concept were tackled in four stages:

1. *Development of a new solvent selection strategy for TMS systems*
2. *Application of TMS systems in the conversion of technical grade feedstocks*
3. *Application of TMS systems in the conversion of renewable feedstocks*
4. *Application of TMS systems in reactions with inherently limited degrees of freedom in the solvent choice*

The results are discussed in the following chapters 5.1.1 - 5.1.5.

5.1.1. Development of a New Solvent Selection Strategy for TMS Systems

The design of new TMS systems and therefore the selection of suitable solvents is an important task. In chapter 4.1 a framework based on the “Conductor like Screening Model for Real Solvents” (COSMO-RS) for the systematic selection of solvent combination for TMS was presented. In contrast to the solvent selection strategies described in literature, it allows for considering the thermodynamic properties of the catalyst and the product in an early stage of the process design in the absence of experimental data.

This approach leads to a reduced experimental effort in designing TMS systems for a defined reaction and therefore, is a valuable tool in the process development for homogeneously catalysed reactions in TMS systems.

Further developments should aim for the implementation of green chemistry solvent selection guides into this framework to directly achieve a ranking of potential TMS systems regarding their environmental impact.

5.1.2. Application of TMS Systems in the Conversion of Technical Grade Feedstocks

The next step in extending the scope of TMS systems was to show their applicability in the conversion of technical grade feedstocks. This is described in chapter 4.2 for the tandem isomerisation/hydroformylation for the selective synthesis of undecanal from a technical grade feed of internal C10 olefins (Figure 5.1).

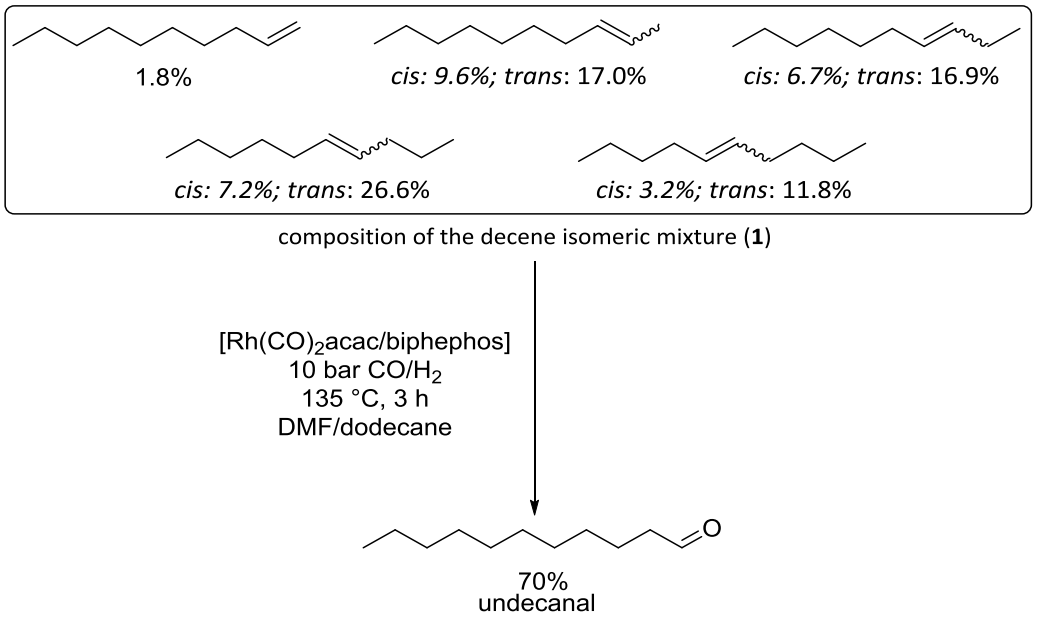

Figure 5.1: Isomerization/hydroformylation of technical grade decene isomers.

The TMS system consisting of DMF and dodecane was selected by application of the COSMO-RS based framework presented in chapter 4.1. It allows for low catalyst leaching into the product phase. Stable phase behaviour of the TMS System and recycling of the catalyst over five runs were obtained.

These results demonstrate the potential applicability of TMS systems in the conversion of technical grade feedstocks. For further validation of these findings, the reaction should be transferred into a continuously operated miniplant to get information about the long-term stability of the developed process concept using this TMS system.

5.1.3. Application of TMS Systemsin the Conversion of Renewable Feedstocks

The next aim was the design of TMS systems for the conversion of renewable feedstocks such as oleocompounds (chapter 4.3). Here, the great challenge is that the substrate already contains a functional group, leading to a higher polarity compared to unfunctionalised olefins. The introduction of an additional aldehyde moiety further increases polarity. This essentially complicates separating the product from a polar catalyst. To find a general approach tackling this challenge, the hydroformylation of methyl 10-undecenotate (Figure 5.2) was chosen as a model reaction, because the substrate has a short carbon chain compared to other oleo chemicals (leading to a higher polarity), expediting the separation problem. Therefore, the developed concept should also be transferable to the hydroformylation of longer chained oleocompounds.

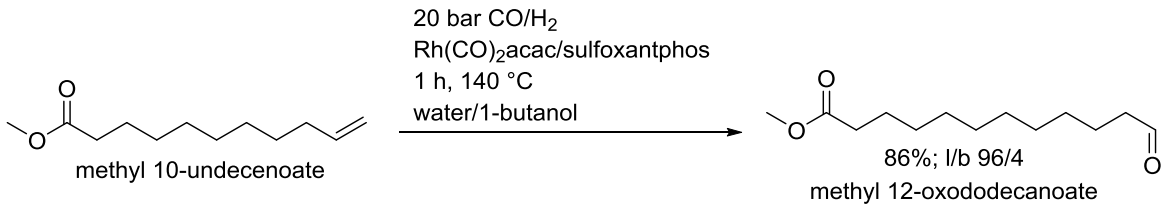

Figure 5.2: Hydroformylation of methyl 10-undecenoate.

Investigations in organic TMS systems showed, that the separation of the catalyst from the product is not sufficient since the product remains in the polar catalyst phase.

To overcome this general limitation in the separation of relatively polar products, new aqueous TMS systems using water as catalyst phase and alcohols as product phase were developed. These TMS systems lead to excellent results in terms of reactivity, product separation and catalyst recycling. The successful application in a continuously operated miniplant demonstrates their applicability for continuously operated processes.

Herein, the phase behaviour of these TMS systems strongly depends on the substrate concentration. Higher concentrations of the substrate shift the upper critical solution temperature towards higher values. Under the chosen process conditions, the reaction mixture contains two liquid phases, but the results obtained are basically the same compared to a homogeneous operation mode (see chapter 7.1.6). The term “narrow” TMS system describes this phenomenon very well.

Although the reaction rates are not influenced by the phase behaviour in this special case, one major drawback of TMS systems is demonstrated. Its application often limits the concentration range of a substrate. If different substrates or catalysts are applied, a biphasic reaction mixture can drastically decrease the reaction rates.

5.1.4. Application of TMS systems in Reactions with Inherently Limited Degrees of Freedom in the Solvent Choice

The applicability of TMS systems in reactions, which inherently limit the degrees of freedom for solvent selection, was investigated in the hydroesterification of methyl 10-uncecenoate with methanol in chapters 4.4 and 4.5 (Figure 5.3).

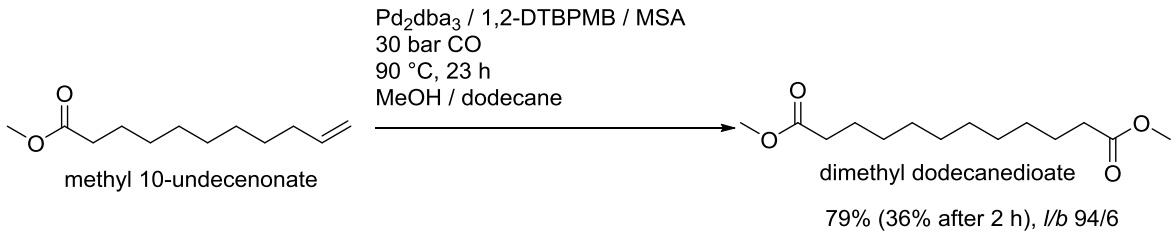

Figure 5.3: Hydroesterification of methyl 10-undecenoate.

A palladium catalyst bearing the 1,2-DTBPMB ligand leads to outstanding results in terms of selectivity towards the desired linear product. If this catalyst is applied, the reaction rates strongly increase with higher methanol concentrations. Therefore, the polar solvent of a TMS system has to be methanol to reach high reaction rates. This has two important consequences for the design of a process:

- Firstly, since the solvent for the catalyst is fixed, the separation of the catalyst and the product can only be influenced by the non-polar solvent. This can cause a poor separation performance.
- Secondly, the reaction rate in a TMS system is inherently lower compared to other catalyst recycling concepts (e.g. consecutive extraction after reaction or product crystallisation). This is due to the fact, that the presence of the additional extracting agent in the reactor leads to a dilution of the reaction mixture and therefore, lowers

the methanol concentration. In case of the hydroesterification catalysed by a Pd/1,2-DTBPMB catalyst, the methanolysis of the Pd-acyl-complex Is rate determining. Therefore, a higher methanol concentration leads to a higher reaction rate.

In this case, a TMS system is not a competitive catalyst recycling concept.

Investigation of the model reaction uncovered a second important limitation of the concept of TMS systems. As outlined in the aims section (chapter 3), TMS systems have not been suitable for the separation of homogeneous transition metal catalysts from relatively polar products. As discussed in chapter 5.1.3, the application of the new developed aqueous, “narrow” TMS systems can be a very effective solution for this challenging separation task. In case of the hydroesterification, these systems are not applicable since water does not act like an inert component in this reaction. In presence of higher amounts of water in addition to an alcohol, mixtures of esters and free carboxylic acids are obtained.

The knowledge gained by the systematic analysis of the scope and limitations of TMS systems as a catalyst recycling concept discussed in the chapters 5.1.1 - 5.1.4 was used for the development of a general application guideline for TMS systems in homogeneously catalysed reactions (chapter 5.1.5).

5.1.5. Guide for the Application of TMS Systems

In this chapter, a general guideline for the application of TMS systems as a catalyst recycling concept in homogeneous catalysis is presented. The aim of this guideline is to help chemists and chemical engineers who work in an early stage of process development to decide, whether a TMS system is a promising catalyst recycling strategy for a certain chemical reaction, or not. If TMS systems are applicable, this guideline will help to identify a suitable type of TMS systems and to design a corresponding process concept for the reaction. Although this guideline was developed based on olefin carbonylation reactions, it is applicable to homogeneously catalysed reactions in general because the underlying principles are the same.

The guideline tries to answer the following three lead-questions:

1. Does the desired process benefit from the inherent advantages of a TMS System?

2. Is there a suitable TMS system for the reaction allowing for an efficient separation without deteriorating the outcome of the reaction?

3. How to design a process for a reaction in a TMS system?

Does the Desired Process Benefit of the Inherent Advantages of a TMS System?

There are several concepts for the recovery of homogeneous transition metal catalysts described in the literature. In general, all of them have different inherent advantageous and disadvantageous. Depending on the process, one has to decide which of these advantages are of high impact and therefore, which recycling technique is principally well suited. Table 5.1 summarises the inherent advantages and disadvantages of a TMS system.

The usage of commercial solvents and catalysts enables for a fast and cost efficient set up of a potential process for a given reaction. The integrated reactor-mixer design and the separation *via* decantation allow for a simple apparatus setup, since in principle only a reactor and a decanter are necessary for evaluating a potential process. Additionally, the reaction takes place under "real homogeneous" conditions and therefore, is not limited by mass transport between two liquids or a liquid and a solid phase. This leads to three major advantages of the TMS technique:

- Fast and cost efficient development of a new process concept.
- Potentially low investment costs and fast setup of an industrial process.
- No additional mass transport limitations during the reaction.

Table 5.1: Inherent advantages and disadvantages of TMS systems.

Advantages	Disadvantages
Use of commercial catalysts	Limitations in substrate concentration
Use of commercial solvents	Limitations in the amount of the extraction agent
No liquid-liquid phase transfer or solubility limitations	Limited range of reaction and separation temperature
Integration of reaction and extraction	Energy intensive cooling and heating procedures to induce phase separation / homogenisation
Catalyst separation *via* simple decantation	Dilution of the reaction mixture due to the second solvent (lower space/time yields)
	Long residence time in the decanter, if the phase separation is slow

Disadvantages of the TMS technique are limitations regarding the substrate concentration, the amount of the extraction agent and the limited ranges of the reaction and separation temperatures. Additionally, the reaction mixture is comparably diluted due to the presence of a second solvent, leading to lower space/time yields. In some cases also the phase separation in the decanter is slow, requiring long residence times in the decanter. Also the heating/cooling procedure of the reaction mixture is relatively energy intensive.

If the advantages of a TMS system outweigh its limitations, the next question regards the applicability of the TMS concept for the desired reaction.

Is There a Suitable TMS System for the Reaction Allowing for an Efficient Separation Without Deteriorating the Outcome of the Reaction?

In order to answer this question, a decision tree (Figure 5.4) was developed based on simple yes-or-no questions. This decision tree also shows which kind of the TMS system will probably do the best job for a given task.

If more than one liquid substrate is converted and a high concentration of one these substrates strongly accelerates the reaction, a TMS system will be inherently inferior compared to other recycling strategies. Ideally, this substrate serves as the only solvent in these reactions. One example for such a reaction is the Pd/1,2-DTBPMB-catalysed methoxycarbonylation of methyl 10-undecenoate presented in chapters 4.4 and 4.5 and discussed in chapter 5.1.4. In this case, a different catalyst recycling strategies such as product crystallisation or consecutive extraction after reaction are more promising approaches.

If there is only one liquid substrate or a high concentration of one of the substrates is not required to reach high reaction rates, TMS systems are in principle a promising catalyst recycling strategy. If the resulting products are of low polarity, organic TMS systems are well suited for the separation of the catalyst and the product. One example, the isomerization/hydroformylation tandem reaction of internal decene isomers, was presented in chapter 4.2 and discussed in chapter 5.1.2. Catalyst was separated from the substrate using a DMF/dodecane TMS system. An example for the conversion of two liquid substrates is the hydroamination of myrcene with diethylamine in an acetonitrile/heptane TMS system.[44]

For the separation of polar products from the catalyst, application of water can lead to a good performance. Requirement for this is that water acts like an inert component in the reaction. If water is not applicable in the reaction, a TMS system will probably not lead to a satisfying separation of the catalyst and a polar product.

If water acts like an inert component and the product is soluble in water, a “reversed” aqueous TMS system can be applied, where the catalyst is immobilised in the less polar,

non-aqueous phase. One example for such a strategy (although not homogenous at reaction temperature) was developed by Kuhlmann et al. They used a liquid-liquid biphasic solvent system consisting of water and 2-ethylhexanol for the synthesis of DMF from CO_2.The DMF is soluble in the aqueous phase, while the ruthenium catalyst remains in the organic 2-ethylhexanol.[325]

If the product is not soluble in water and there is a competitive water soluble catalyst complex, aqueous TMS system will be a promising solution for the separation task, as demonstrated in the hydroformylation of methyl 10-undecenoate, presented in chapter 4.3 and discussed in chapter 5.1.3. If such a catalyst does not exist, a recycling approach which is not based on the principle of extraction should be chosen.

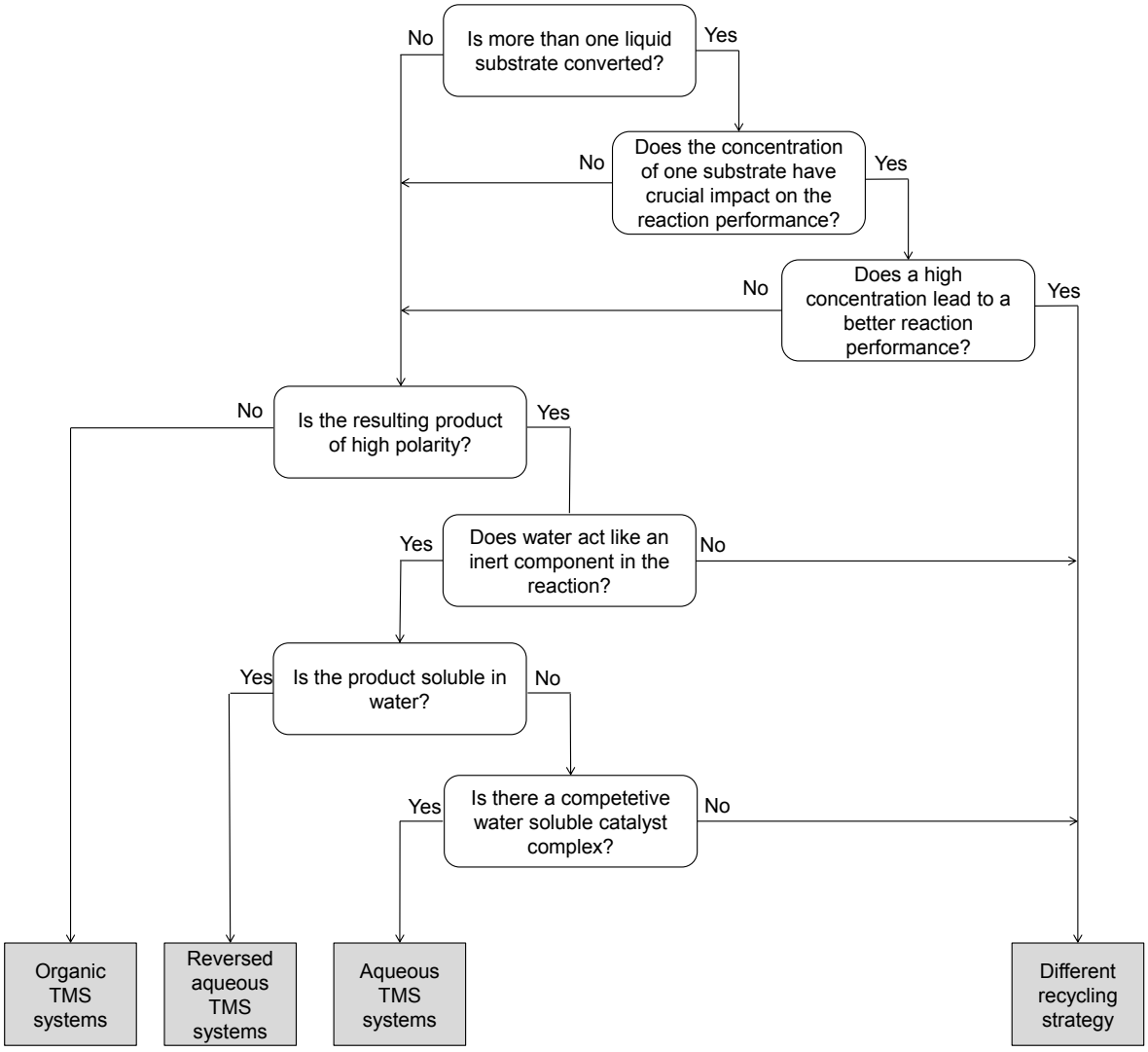

Figure 5.4: Decision tree for TMS systems.

After determining the most promising type of TMS system, the next question regards the development of the potential process.

How to Design a Process for a Reaction in a TMS System?

The first important task in designing processes using TMS systems is the development of the solvent system itself. A systematic workflow for the TMS system development based on the experience made in within this thesis is shown in Figure 5.5.

As discussed in chapter 2.2.1, type III TMS systems are favourable for process development since they are less complex compared to type I and II TMS systems. Consequently, type III TMS systems should initially be evaluated for catalyst separation in a given reaction.

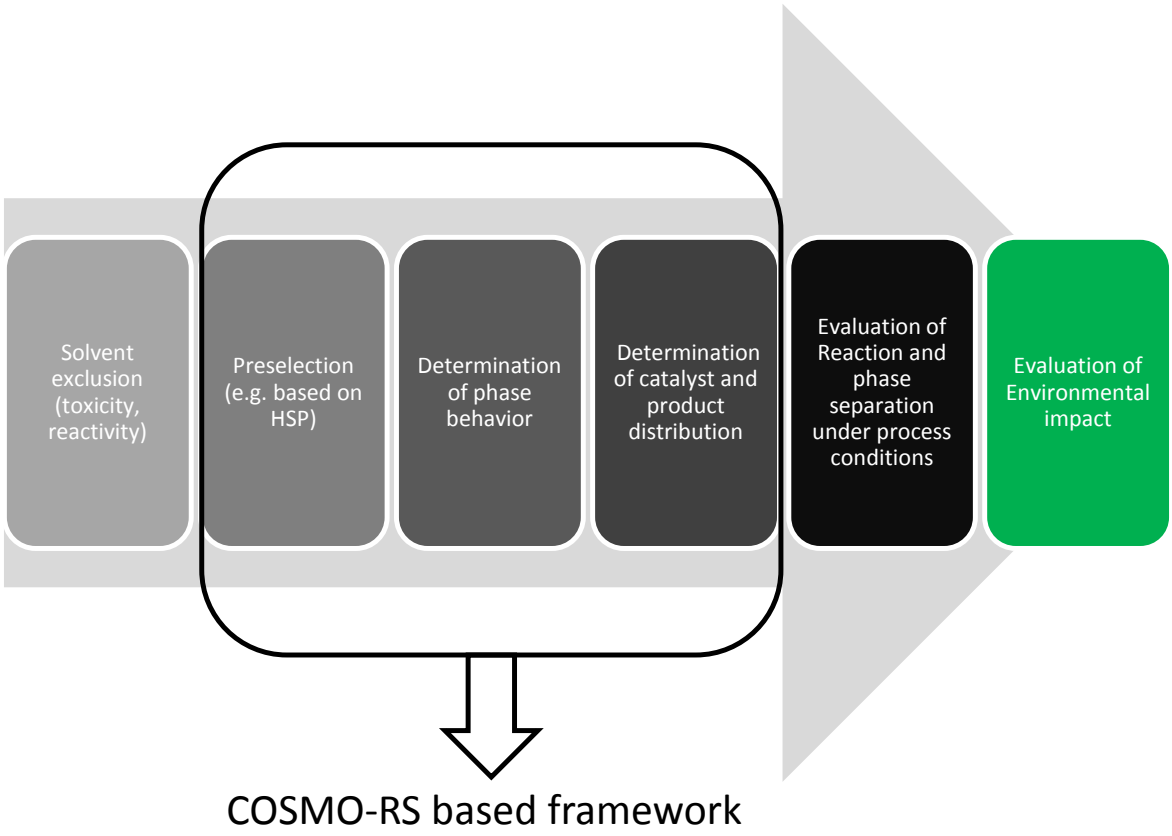

Figure 5.5: Workflow for the systematic development of TMS systems.

In a first step, solvents which are not suitable for the reaction (e.g. because they are not inert or toxic) should be excluded.

Afterwards a preselection (e.g. based on the HSP values) should be done, followed by determination of the UCST of potential pairs of polar and non-polar solvents.

Substrates and products should also be considered in the experimental identification of suitable TMS systems. For example, this can be achieved by measuring the ternary diagram of the two solvents and the substrate at reaction temperature. If more than one liquid

substrate is present during the reaction, they can be lumped together in a certain ratio (that leads to a good reaction performance) to one pseudo component.

After reaction, most of the substrate(s) should be converted into the desired product. Consequently, measuring the ternary diagram of the two solvents and the product(s) at the aimed separation temperature gives a good idea about the phase behaviour after the reaction.

After identifying suitable TMS systems and promising operating areas, preliminary investigations on the catalyst and product separation can be carried out. This can be done by the following procedure:

- Adding the catalyst to a mixture of the TMS system and the product
- Heating up this mixture to reaction temperature
- Cooling down the mixture to separation temperature
- Measuring the catalyst and the product distribution

This procedure allows for a fast evaluation of different TMS system candidates in terms of catalyst and product distribution. The phase behaviour of the catalyst is often determined by its ligand and therefore, the ligand can be investigated instead of the whole catalyst.

The new developed COSMO-RS framework (presented in chapter 4.1 and discussed in chapter 5.1.1) can strongly simplify the solvent selection process.

Promising TMS systems can then be tested regarding the reaction step and the separation step under real conditions. Final candidates can be further be rated regarding their environmental impact by applying green chemistry solvent selection guides.[188,288,326–328]

If a type III TMS system does not lead to satisfying results, a third solvent (type I or type II TMS system) can be added. In principle, the same experimental procedure for the TMS system development described above can be used. For determining the influence of a substrate, the measurement of the ternary diagrams of the three solvent components as well as the separation behaviour can be carried out at a certain substrate or product concentration, which leads to good results in the reaction.

Afterwards, the reaction conditions have to be optimised and the principal recyclability of the catalyst *via* the developed TMS system has to be evaluated. Both can be done in laboratory scale batch experiments. Finally, the reaction should be transferred into a continuously operated miniplant. In long term experiments, information about the stability of the phase behaviour and the catalyst complex can be obtained. Also accumulation of by-products and their influence on the reaction system can be evaluated. Figure 5.6 summa-

rises the holistic workflow for designing new processes for homogenously catalysed reactions in TMS systems.

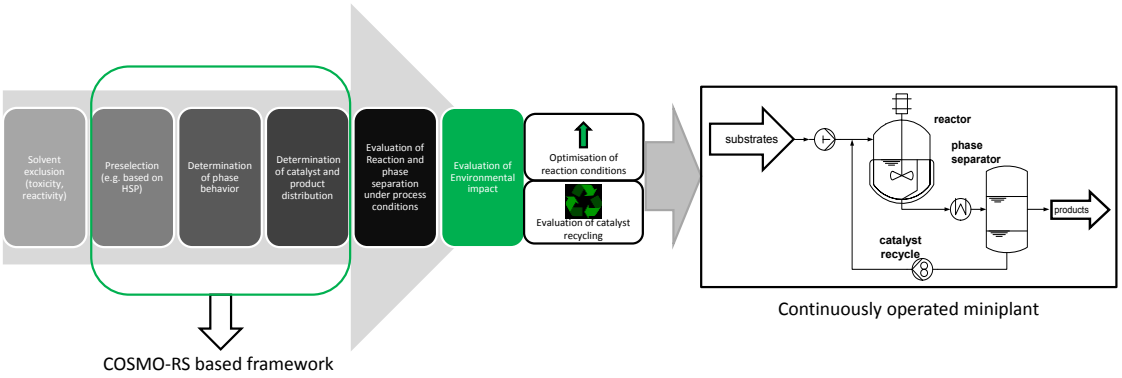

Figure 5.6: Workflow for process design for TMS systems.

5.2. Design of New Catalytic Systems for Tandem Reactions with Renewables

Three new catalytic systems for tandem hydroformylation reactions with renewable feedstocks were developed within this thesis. Two systems (one for the hydroformylation/hydrogenation or reductive hydrofromylation; one for the hydroaminomethylation) were designed for utilising the hydroformylation as the first step in a tandem reaction sequence. One catalyst allows to slot an isomerisation in ahead of the hydroformylation.

5.2.1. Catalyst Development for the Reductive Hydroformylation of Castor Oil Derived Substrates

The investigations for developing a new catalyst for the tandem hydroformylation/hydrogenation (or reductive hydroformylation) reaction for the conversion of functionalised, terminal unsaturated substrates derived from castor oil into the corresponding α,ω-functionalised products are presented in chapter 4.6. These investigations aimed for simplifying the well-known bimetallic orthogonal Rh/Ru (Shvo's catalyst) catalyst by *in situ* synthesis of Shvo's catalyst from Ru_3CO_{12} and tetracyclone. Comparison of the *ex situ* with the *in situ* generated catalysts showed, that the same catalytic performance can be achieved. With this new catalyst, effort in synthesising Shvo's catalyst can be avoided which is beneficial from an economic and an ecologic point of view.

A catalyst recycling *via* TMS systems is not promising in this case since the resulting products show high polarity and the applied catalyst is not soluble in water. For these reasons, catalyst recycling *via* product crystallisation was successfully investigated. This

strategy enables the recycling of a complex homogeneous orthogonal catalyst system consisting two different metals with two different ligands for the first time.

In general, this *in situ* generated catalyst is of high value for the synthesis of *n*-alcohols from olefins. Since crystallisation of the product is not always an option, sulfonating the tetracyclone ligand leading to a water soluble derivate of Shvo's catalyst is interesting. This would also allow for the application of hybrid separation techniques leading to very powerful process concepts (Figure 5.7). For instance, the tandem hydroformylation/hydrogenation of methyl 10-undecenoate could be carried out in an aqueous TMS system (e.g. water/1-butanol) using a [Rh/TPPTS]/[sulfonated Shvo's catalyst] system resulting in the formation of both, the linear and the *iso*-alcohol. Cooling this mixture would lead to the formation of two liquid phases (water phase containing the catalyst, 1-butanol phase containing the branched alcohol) and to the crystallisation of the linear alcohol at the same time. Such a process would enable the *selective* synthesis of linear *and* branched alcohols *at the same time* in a very efficient manner.

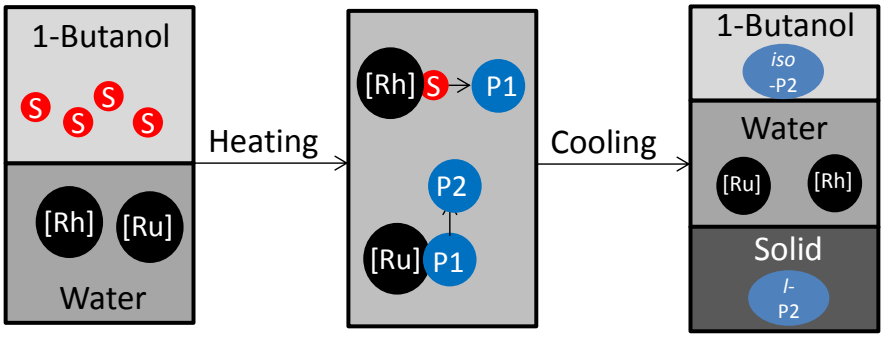

Figure 5.7: Future concept of a hybrid separation process for the tandem hydroformylation/hydrogenation of methyl 10-undecenoate. [Rh] = Rh/TPPTS; [Ru] = sulfonated Shvo's catalyst, P1 = ester-aldehyde, P2= ester-alcohol

5.2.2. Catalyst Development for the Hydroaminomethylation of 1,3-Dienic Substrates

A Rh/dppe catalyst was developed for the hydroaminomethylation of 1,3-dienic substrates (chapter 4.7). This catalyst allows for an exceptional high regioselectivity in the hydroformylation of myrcene (97%, no higher values are reported in literature).

Even more interesting, a TOF of 739 h^{-1} for the hydroformylation was achieved which is the highest TOF for the hydroformylation of 1,3-dienes reported in literature. Investigations on the origin of this unprecedented high reaction rate showed, that the hydroformylation is strongly accelerated in the presence of amines. Future investigations should lead to a deeper understanding of the accelerating effect of the amine in the hydroformylation of 1,3-dienes. If this phenomena can be observed independently of the applied substrate

and catalyst complex, this would be a major breakthrough in the hydroformylation of 1,3-dienes.

It was also shown, that the hydroaminomethylation is a powerful tool for the synthesis of new bio-based surfactants. Application of different amines could lead to additional interesting surfactants. *N*-methyl glucamine for example, which is an amine synthesised from glucose, could directly lead to non-ionic surfactants. Subsequent synthesis of the quats after hydroaminomethylation is not necessary in this case (Figure 5.8).

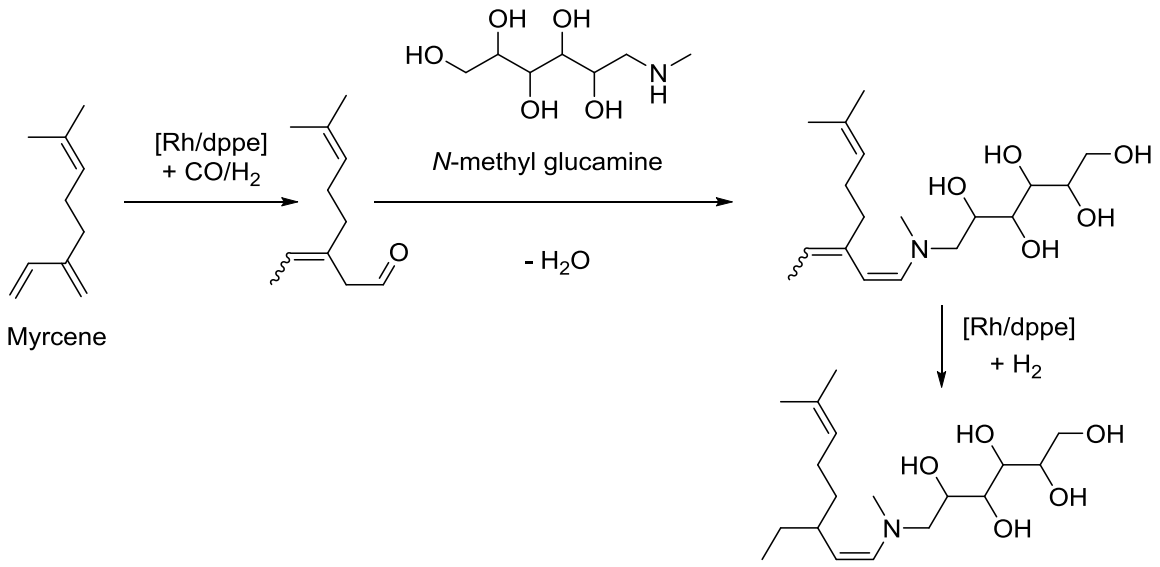

Figure 5.8: Direct surfactant synthesis *via* hydroaminomethylation of myrcene with N-methyl glucamine.

In terms of catalyst recycling, TMS systems are a promising alternative. Two liquid substrates are used in this transformation, but the reactivity does not strongly depend on their concentration, if the ratio of both substrates is in a certain range. The polarity of the resulting products is moderate. Preliminary studies or COSMO-RS modelling could show, if a sufficient separation of the catalyst and the product can be achieved using organic TMS systems. Alternatively, there is sulfonated derivative of the applied dppe ligand available and water does not disturb the reaction. Consequently, also the application of aqueous TMS systems is conceivable.

5.2.3. Catalyst Development for the Tandem Isomerisation/Hydroformylation of Fatty Acid Methyl Esters (FAMEs)

The developed orthogonal tandem catalytic system consisting of a Rh/biphephos catalyst for the hydroformylation and a PdI_2/$Pd(^tbu_3P)_2$ for the isomerisation enables the highest yield for the tandem isomerisation/hydroformylation of methyl oleate (67%) as well as the highest regioselectivity (91% towards the linear ester-aldehyde) reported in literature.

Although this catalytic system is a major improvement compared to all catalysts described in literature, it is still far away from a technical application due to the high catalysts loadings and the low reaction rates. Also, double bond hydrogenation as a side reaction is still an issue, which could be tackled by the usage of different hydroformylation catalysts. Finding isomerisation catalysts with a higher activity would also strongly contribute to a more effective system.

Further improvement of this orthogonal catalyst would be of high value. The systematic investigation showed that it can be used for the conversion of unsaturated esters of different chain lengths. Broadening the scope towards the conversion of multiple unsaturated FAMEs such as linoleic acid or even longer FAMEs like erucic acid should be aimed in further investigations. Also usage of crude mixtures of FAMEs, triglycerides and free fatty acids or other derivatives as starting materials may be of interest.

Resulting α,ω-ester-aldehydes (or derivatives) enable a versatile and straightforward follow-up chemistry aiming for the synthesis of different polymer precursors (

Figure 5.9).

The orthogonal tandem catalyst could also be an alternative approach to tackle other isomerisation/hydroformylation problems, e.g. in the synthesis of adipaldehyde from butadiene.

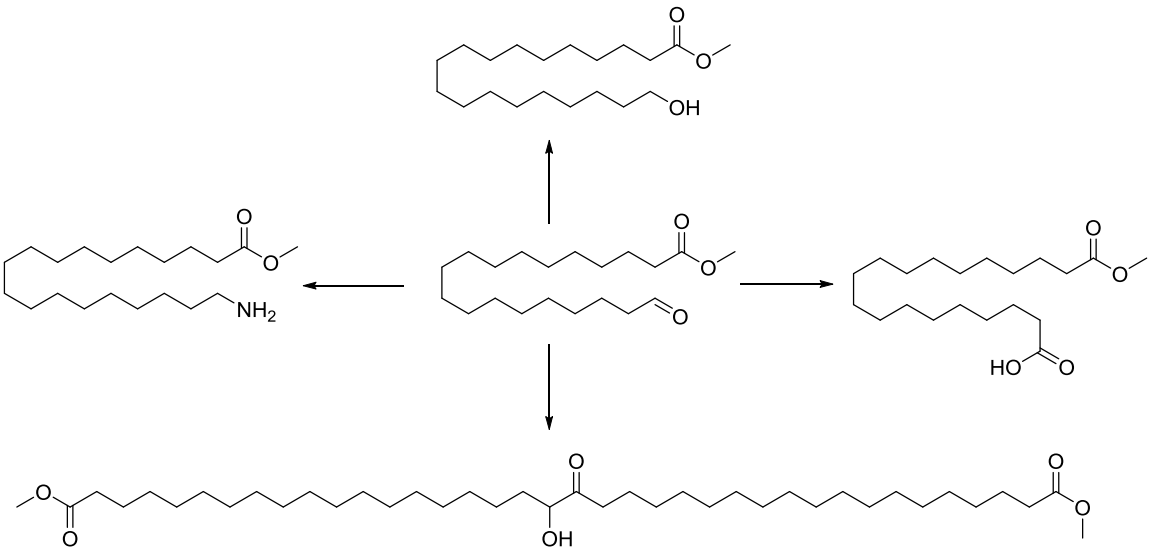

Figure 5.9: Follow-up chemistry of α,ω- ester-aldehydes.

5.3. This Work in the Context of Sustainable Chemistry and Industrial Relevance

The overarching objective of this work was to enhance the knowledge in the field of sustainable process development for olefin carbonylation reactions. The impact of developments in this field on the environment is strongly linked to their industrial relevance. Therefore, both sustainability and industrial relevance build the framework for this thesis. While sustainability was achieved *via* consideration of the green chemistry principles, industrial relevance was given by converting readily available substrates into high-value products.

The production of undecanal from a technical mixture of internal decene isomers represents an interesting conversion since the product can be used for fragrance or surfactant synthesis. Amine synthesis from renewable terpenes myrcene and farnesene also offers access to valuable surfactants. ω–Functionalisation of the FAMEs methyl 10-undeceneoate (and derivatives) and methyl oleate under formation of diesters, ester-aldehydes, diols and ester-alcohols lead to renewable polymer building blocks. In the synthesis of these compounds, the green chemistry principles waste prevention (principle 1), atom economy (principle 2), usage of safe solvents (principle 4), designing energy efficient processes (principle 6), use of renewables (principle 7), reduce derivatives (principle 8) and catalysis (principle 9) were considered wherever possible.

The two research focal points *catalyst recycling* and *catalyst design* were extensively studied.

The concept of TMS systems for *catalyst recycling* was systematically investigated leading to a general guide for their application in homogeneous catalysis. Additionally, two new tools in this area were created turning process development more “green”:

Aqueous “narrow” TMS systems allow for the application of the “green solvents” water and benign alcohols in continuously operated carbonylation processes in a very efficient manner.

The application of the **COSMO-RS framework for designing TMS systems** helps to reduce the experimental effort in the early stage of process development, and therefore reduces waste production.

Catalyst Design for tandem reactions with renewables was tackled using the hydroformylation as the core element. In principle, the hydroformylation can be the initial or the terminal part of a tandem reaction sequence. Both cases are investigated within this thesis. Two catalysts (one for the hydroformylation/hydrogenation; one for the hydroam-

inomethylation) were designed for utilising the hydroformylation as the first step in a tandem reaction sequence. These catalysts allow for more straightforward process design since no intermediate purification of the aldehydes is necessary, which meets several of the green chemistry principles (1, 4, 6, 8, 9).

One catalyst paves the way for slot an isomerisation in ahead of the hydroformylation of FAMEs. This catalyst was designed to enable a new pathway for the implementation of renewable feedstocks into the value-creation chain.

All developments in this work, which are published in eight research articles, help to design processes for homogeneously catalysed reactions in a sustainable manner and show new ways for the implementation of alternative feedstocks into future chemical processes.

6. References

[1] PricewaterhousCoopers, "Megatrends", http://www.pwc.co.uk/issues/megatrends.html, **2017**.

[2] "Living planet report 2016. Risk and resilience in a new era", WWF International, Gland, Switzerland, **2016**.

[3] J. von Hoyningen-Huene, T. Rings, F. Forrest, O. Schulz, "Chemical Industry Vision 2030: A European Perspective", https://www.atkearney.de/chemicals/ideas-insights/article/-/asset_publisher/LCcgOeS4t85g/content/chemical-industry-vision-2030-a-european-perspective/10192, **2012**.

[4] B. Cornils, W. Hermann, "Concepts in homogeneous catalysis. The industrial view", *J. Catal.* **2003**, *216*, 23–31.

[5] A. Behr, A. J. Vorholt, "Homogeneous Catalysis With Renewables", Springer, Heidelberg, **2017**.

[6] P. T. Anastas, J. C. Warner, "Green chemistry. Theory and practice", Oxford University Press, New York, **2000**.

[7] W. Gösele, W. Egel-Hess, K. Wintermantel, F. R. Faulhaber, A. Mersmann, "Feststoffbildung durch Kristallisation und Fällung", *Chem. Ing. Tech.* **1990**, *62*, 544–552.

[8] T. Seidensticker, H. Busch, C. Diederichs, J. J. von Dincklage, A. J. Vorholt, "From Oleo Chemicals to Polymer. Bis -hydroaminomethylation as a Tool for the Preparation of a Synthetic Polymer from Renewables", *ChemCatChem* **2016**, *8*, 2890–2893.

[9] A. Behr, P. Neubert, "Applied homogeneous catalysis", Wiley-VCH, Weinheim, **2012**.

[10] H. Bahrmann, H. Bach, G. D. Frey, "Oxo Synthesis" in *Ullmann's Encyclopedia of Industrial Chemistry*, Wiley-VCH, Weinheim, Germany, **2000**.

[11] J. H. Jones, "The Cativa™ Process for the Manufacture of Acetic Acid", *Platinum Metals Rev.* **2000**, *44*, 94–105.

[12] J. M. Dreimann, M. Skiborowski, A. Behr, A. J. Vorholt, "Recycling Homogeneous Catalysts Simply by Organic Solvent Nanofiltration. New Ways to Efficient Catalysis", *ChemCatChem* **2016**, *8*, 3330–3333.

[13] J. M. Dreimann, A. J. Vorholt, M. Skiborowski, A. Behr, "Removal of Homogeneous Precious Metal Catalysts via Organic Solvent Nanofiltration", *Chem. Eng. Trans.* **2016**, *47*, 343–348.

[14] M. Janssen, J. Wilting, C. Muller, D. Vogt, "Continuous rhodium-catalyzed hydroformylation of 1-octene with polyhedral oligomeric silsesquioxanes (POSS) enlarged triphenylphosphine", *Angew. Chem., Int. Ed.* **2010**, *49*, 7738–7741.

[15] S. Hübner, J. G. de Vries, V. Farina, "Why Does Industry Not Use Immobilized Transition Metal Complexes as Catalysts?", *Adv. Synth. Catal.* **2016**, *358*, 3–25.

[16] K. M. Dyballa, H. Hahn, R. Franke, D. Fridag, "Immobilized Catalytically Active Composition Having Tridentate Phosphorus Ligands In An Ionic Liquid for the Hydroformylaiton of Olefin-Containing Mixtures", WO/2015/071266, **2015**.

[17] R. Franke, D. Selent, A. Börner, "Applied Hydroformylation", *Chem. Rev.* **2012**, *112*, 5675–5732.

[18] G. Frey, G. Dämbkes, "75 Jahre Oxo-Synthese. = 75 years of oxo synthesis", Klartext, Essen, **2013**.

[19] R. S. Bauer, H. Chung, P. W. Glockner, W. Keim, H. van Zwet, "Ethylene polymerization", US3635937 A, **1972**.

[20] E. F. Lutz, "Ethylene oligomerization process carried out in a monohydric/dihydric alcohol solvent mixture", US4528416 A, **1985**.

[21] Z. J. Ji, J. Y. Jiang, Y. H. Wang, "A novel thermoregulated phosphine ligand used for the Rh-catalyzed hydroformylation of mixed C11–12 olefins in aqueous/organic biphasic system", *Chin. Chem. Lett.* **2010**, *21*, 515–518.

[22] Y. Wang, J. Jiang, Q. Miao, X. Wu, Z. Jin, "Thermoregulated phase transfer ligands and catalysis: Part XIII. Use of nonionic water-soluble phosphine ligands to effect homogeneous catalyst separation and recycling", *Catal. Today* **2002**, *74*, 85–90.

[23] T. Pogrzeba, D. Müller, T. Hamerla, E. Esche, N. Paul, G. Wozny, R. Schomäcker, "Rhodium-Catalyzed Hydroformylation of Long-Chain Olefins in Aqueous Multiphase Systems in a Continuously Operated Miniplant", *Ind. Eng. Chem. Res.* **2015**, *54*, 11953–11960.

[24] M. Schwarze, T. Pogrzeba, I. Volovych, R. Schomäcker, "Microemulsion systems for catalytic reactions and processes", *Catal. Sci. Technol.* **2015**, *5*, 24–33.

[25] M. Kahlweit, R. Strey, G. Busse, "Microemulsions. A qualitative thermodynamic approach", *J. Phys. Chem.* **1990**, *94*, 3881–3894.

[26] T. Hamerla, M. Schwarze, R. Schomäcker, "Katalyse in modifizierten Flüssig/flüssig-Mehrphasensystemen", *Chem. Ing. Tech.* **2012**, *84*, 1861–1872.

[27] I. T. Horváth, J. Rábai, "Facile Catalyst Separation Without Water: Fluorous Biphase Hydroformylation of Olefins", *Science* **1994**, *266*, 72–75.

[28] M. Wende, J. A. Gladysz, "Fluorous Catalysis under Homogeneous Conditions without Fluorous Solvents: A “Greener” Catalyst Recycling Protocol Based upon Temperature-Dependent Solubilities and Liquid/Solid Phase Separation", *J. Am. Chem. Soc.* **2003**, *125*, 5861–5872.

[29] D. E. Bergbreiter, Y.-S. Liu, P. L. Osburn, "Thermomorphic Rhodium(I) and Palladium(0) Catalysts", *J. Am. Chem. Soc.* **1998**, *120*, 4250–4251.

[30] K. Stephan, F. Mayinger, "Thermodynamik. Band 2: Mehrstoffsysteme und chemische Reaktionen. Grundlagen und technische Anwendungen", Springer, Heidelberg, **1999**.

[31] A. Behr, G. Henze, L. Johnen, C. Awungacha, "Advances in thermomorphic liquid/liquid recycling of homogeneous transition metal catalysts", *J. Mol. Catal. A: Chem.* **2008**, *285*, 20–28.

[32] C. M. Hansen, "The three-dimensional solubility parameter - key to paint component affinities: solvents, plasticizers, polymers, and resins. II. Dyes, emulsifiers, mutual solubility and compatibility, and pigments. III. Independent calculation of the parameter components", *J. Paint Technol.* **1967**, *39*, 505–510.

[33] C. M. Hansen, "The Three Dimensional Solubility Parameter - Key to Paint Component Affinities I. - Solvents, Plasticizers, Polymers, and Resins", *J. Paint Technol.* **1967**, *39*, 104–117.

[34] A. Behr, A. Kleyensteiber, M. Becker, "A novel approach to selecting thermomorphic multicomponent solvent systems (TMS) for hydroaminomethylation reactions", *Chem. Eng. Process.* **2013**, *69*, 15–23.

[35] A. Behr, G. Henze, D. Obst, B. Turkowski, "Selection process of new solvents in temperature-dependent multi-component solvent systems and its application in isomerising hydroformylation", *Green Chem.* **2005**, *7*, 645.

[36] C. M. Hansen, "Hansen solubility parameters. A user's handbook", Taylor & Francis, Boca Raton, **2007**.

[37] A. F. M. Barton, "CRC handbook of solubility parameters and other cohesion parameters", CRC Press, Boca Raton, **1991**.

[38] "Test Method for Kauri-Butanol Value of Hydrocarbon Solvents", ASTM International, West Conshohocken, **1998**.

[39] E. Schäfer, Y. Brunsch, G. Sadowski, A. Behr, "Hydroformylation of 1-Dodecene in the Thermomorphic Solvent System Dimethylformamide/Decane. Phase Behavior–Reaction Performance–Catalyst Recycling", *Ind. Eng. Chem. Res.* **2012**, *51*, 10296–10306.

[40] A. Behr, N. Toslu, "Einphasige und zweiphasige Reaktionsführung der Hydrosilylierungsreaktion", *Chem. Ing. Tech.* **1999**, *71*, 490–493.

[41] A. Behr, N. Toslu, "Hydrosilylation Reactions in Single and Two Phases", *Chem. Eng. Technol.* **2000**, *23*, 122–125.

[42] A. Behr, C. Fängewisch, "Rhodium-catalysed synthesis of branched fatty compounds in temperature-dependent solvent systems", *J. Mol. Catal. A: Chem.* **2003**, *197*, 115–126.

[43] A. Behr, Q. Miao, "A new temperature-dependent solvent system based on polyethylene glycol 1000 and its use in rhodium catalyzed cooligomerization", *J. Mol. Catal. A: Chem.* **2004**, *222*, 127–132.

[44] A. Behr, L. Johnen, N. Rentmeister, "Novel Palladium-Catalysed Hydroamination of Myrcene and Catalyst Separation by Thermomorphic Solvent Systems", *Adv. Synth. Catal.* **2010**, *352*, 2062–2072.

[45] T. Färber, R. Schulz, O. Riechert, T. Zeiner, A. Górak, G. Sadowski, A. Behr, "Different Recycling Concepts in the Homogeneously Catalysed Synthesis of Terpenyl Amines", *Chem. Eng. Process.* **2015**, *98*, 22–31.

[46] T. Färber, O. Riechert, T. Zeiner, G. Sadowski, A. Behr, A. J. Vorholt, "Homogeneously Catalyzed Hydroamination in a Taylor–Couette Reactor Using a Thermormorphic Multicomponent Solvent System", *Chem. Eng. Res. Des.* **2016**, *112*, 263–273.

[47] A. Behr, L. Johnen, A. J. Vorholt, "Telomerization of Myrcene and Catalyst Separation by Thermomorphic Solvent Systems", *ChemCatChem* **2010**, *2*, 1271–1277.

[48] A. Behr, A. Kleyensteiber, L. Domke, "Herstellung von Glycerin-tert-butylethern – Entwicklung vom Labor bis zur Miniplant", *Chem. Ing. Tech.* **2016**, *88*, 1082–1094.

[49] A. Behr, R. Roll, "Hydroaminomethylation in thermomorphic solvent systems", *J. Mol. Catal. A: Chem.* **2005**, *239*, 180–184.

[50] A. Behr, Q. Miao, "Selective rhodium catalysed synthesis of trans-1,4-hexadiene in polyethylene glycol 1000-water solvent systems", *Green Chem.* **2005**, *7*, 617–620.

[51] D.-H. Chang, D.-Y. Lee, B.-S. Hong, J.-H. Choi, C.-H. Jun, "A New Solvent System for Recycling Catalysts for Chelation-Assisted Hydroacylation of Olefins with Primary Alcohols", *J. Am. Chem. Soc.* **2004**, *126*, 424–425.

[52] S. Huang, H. Bilel, F. Zagrouba, N. Hamdi, C. Bruneau, C. Fischmeister, "Olefin metathesis transformations in thermomorphic multicomponent solvent systems", *Catal. Commun.* **2015**, *63*, 31–34.

[53] A. Keraani, T. Renouard, C. Fischmeister, C. Bruneau, M. Rabiller-Baudry, "Recovery of Enlarged Olefin Metathesis Catalysts by Nanofiltration in an Eco-Friendly Solvent", *ChemSusChem* **2008**, *1*, 927–933.

[54] A. Behr, A. J. Vorholt, N. Rentmeister, "Recyclable homogeneous catalyst for the hydroesterification of methyl oleate in thermomorphic solvent systems", *Chem. Eng. Sci.* **2013**, *99*, 38–43.

[55] S. Kim, K. Yamamoto, K. Hayashi, K. Chiba, "A cycloalkane-based thermomorphic system for palladium-catalyzed cross-coupling reactions", *Tetrahedron* **2008**, *64*, 2855–2863.

[56] Y. Yang, J. Jiang, Y. Wang, C. Liu, Z. Jin, "A new thermoregulated PEG biphasic system and its application for hydroformylation of 1-dodecene", *J. Mol. Catal. A: Chem.* **2007**, *261*, 288–292.

[57] M. S. Shaharun, B. K. Dutta, H. Mukhtar, S. Maitra, "Hydroformylation of 1-octene using rhodium–phosphite catalyst in a thermomorphic solvent system", *Chem. Eng. Sci.* **2010**, *65*, 273–281.

[58] Y. Brunsch, A. Behr, "Temperature-Controlled Catalyst Recycling in Homogeneous Transition-Metal Catalysis. Minimization of Catalyst Leaching", *Angew. Chem., Int. Ed.* **2013**, *52*, 1586–1589.

[59] J. Tijani, B. El Ali, "Selective thermomorphic biphasic hydroformylation of higher olefins catalyzed by $HRhCO(PPh_3)_3/P(OPh)_3$", *Appl. Catal., A* **2006**, *303*, 158–165.

[60] S. Kim, N. Ikuhisa, K. Chiba, "A Cycloalkane-based Thermomorphic System for Organocatalytic Cyclopropanation Using Ammonium Ylides", *Chem. Lett.* **2011**, *40*, 1077–1078.

[61] A. Behr, L. Johnen, B. Daniel, "A liquid immobilisation concept for enzymes by thermomorphic solvent systems", *Green Chem.* **2011**, *13*, 3168–3172.

[62] S. Kim, A. Tsuruyama, A. Ohmori, K. Chiba, "Solution-phase oligosaccharide synthesis in a cycloalkane-based thermomorphic system", *Chem. Commun.* **2008**, 1816–1818.

[63] K. Chiba, Y. Kono, S. Kim, K. Nishimoto, Y. Kitano, M. Tada, "A liquid-phase peptide synthesis in cyclohexane-based biphasic thermomorphic systems", *Chem. Commun.* **2002**, 1766–1767.

[64] A. Behr, H. Witte, A. Kämper, J. Haßelberg, M. Nickel, "Entwicklung und Untersuchung eines Verfahrens zur Herstellung verzweigter Fettstoffe im Miniplant-Maßstab", *Chem. Ing. Tech.* **2014**, *86*, 458–466.

[65] J. Haßelberg, A. Behr, C. Weiser, J. B. Bially, I. Sinev, "Process development for the synthesis of saturated branched fatty derivatives", *Chem. Eng. Sci.* **2016**, *143*, 256–269.

[66] C. Vogelpohl, C. Brandenbusch, G. Sadowski, "High-pressure gas solubility in multicomponent solvent systems for hydroformylation. Part II. Syngas solubility", *J. Supercrit. Fluids* **2014**, *88*, 74–84.

[67] C. Vogelpohl, C. Brandenbusch, G. Sadowski, "High-pressure gas solubility in multicomponent solvent systems for hydroformylation. Part I. Carbon monoxide solubility", *J. Supercrit. Fluids* **2013**, *81*, 23–32.

[68] J. Markert, Y. Brunsch, T. Munkelt, G. Kiedorf, A. Behr, C. Hamel, A. Seidel-Morgenstern, "Analysis of the reaction network for the Rh-catalyzed hydroformylation of 1-dodecene in a thermomorphic multicomponent solvent system", *Appl. Catal., A* **2013**, *462–463*, 287–295.

[69] G. Kiedorf, D. M. Hoang, A. Müller, A. Jörke, J. Markert, H. Arellano-Garcia, A. Seidel-Morgenstern, C. Hamel, "Kinetics of 1-dodecene hydroformylation in a thermomorphic solvent system using a rhodium-biphephos catalyst", *Chem. Eng. Sci.* **2014**, *115*, 31–48.

[70] M. Zagajewski, J. Dreimann, A. Behr, "Verfahrensentwicklung vom Labor zur Miniplant. Hydroformylierung von 1-Dodecen in thermomorphen Lösungsmittelsystemen", *Chem. Ing. Tech.* **2014**, *86*, 449–457.

[71] M. Zagajewski, A. Behr, P. Sasse, J. Wittmann, "Continuously Operated Miniplant for the Rhodium Catalyzed Hydroformylation of 1-Dodecene in a Thermomorphic Multicomponent Solvent System (TMS)", *Chem. Eng. Sci.* **2014**, *115*, 88–94.

[72] J. Dreimann, P. Lutze, M. Zagajewski, A. Behr, A. Górak, A. J. Vorholt, "Highly integrated reactor–separator systems for the recycling of homogeneous catalysts", *Chem. Eng. Process.* **2016**, *99*, 124–131.

[73] J. M. Dreimann, H. Warmeling, J. N. Weimann, K. Künnemann, A. Behr, A. J. Vorholt, "Increasing selectivity of the hydroformylation in a miniplant. Catalyst, solvent, and olefin recycle in two loops", *AIChE J.* **2016**, *62*, 4377–4383.

[74] J. Ternel, J.-L. Couturier, J.-L. Dubois, J.-F. Carpentier, "Rhodium-Catalyzed Tandem Isomerization/Hydroformylation of the Bio-Sourced 10-Undecenenitrile. Selective and Productive Catalysts for Production of Polyamide-12 Precursor", *Adv. Synth. Catal.* **2013**, *355*, 3191–3204.

[75] D. E. Fogg, E. N. dos Santos, "Tandem catalysis. A taxonomy and illustrative review", *Coord. Chem. Rev.* **2004**, *248*, 2365–2379.

[76] W. Reppe, H. Kröper, "Carbonylierung II. Carbonsäuren und ihre Derivate aus olefinischen Verbindungen und Kohlenoxyd", *Justus Liebigs Ann. Chem.* **1953**, *582*, 38–71.

[77] G. Kiss, "Palladium-Catalyzed Reppe Carbonylation", *Chem. Rev.* **2001**, *101*, 3435–3456.

[78] M. Baerns, A. Behr, A. Brehm, J. Gmehling, H. Hofmann, U. Onken, A. Renken, K.-O. Hinrichsen, R. Palkovits, "Technische Chemie", Wiley-VCH, Weinheim, **2013**.

[79] B. Cornils, W. A. Herrmann, M. Rasch, "Otto Roelen, Pioneer in Industrial Homogeneous Catalysis", *Angew. Chem., Int. Ed.* **1994**, *33*, 2144–2163.

[80] G. D. Frey, "75 Years of oxo synthesis – The success story of a discovery at the OXEA Site Ruhrchemie", *J. Organomet. Chem.* **2014**, *754*, 5–7.

[81] A. I. M. Keulemans, A. Kwantes, T. van Bavel, "The structure of the formylation (OXO) products obtained from olefines and watergas", *Recl. Trav. Chim. Pays-Bas* **1948**, *67*, 298–308.

[82] A. Börner, R. Franke, "Hydroformylation. Fundamentals, processes, and applications in organic systhesis", Wiley-VCH, Weinheim, **2016**.

[83] R. F. Heck, D. S. Breslow, "The Reaction of Cobalt Hydrotetracarbonyl with Olefins", *J. Am. Chem. Soc.* **1961**, *83*, 4023–4027.

[84] D. Evans, J. A. Osborn, G. Wilkinson, "Hydroformylation of alkenes by use of rhodium complex catalysts", *J. Chem. Soc., A* **1968**, 3133–3142.

[85] J. F. Hartwig, "Organotransition metal chemistry. From bonding to catalysis", University Science Books, Sausalito, **2010**.

[86] C. Li, E. Widjaja, W. Chew, M. Garland, "Rhodium Tetracarbonyl Hydride. The Elusive Metal Carbonyl Hydride", *Angew. Chem.* **2002**, *114*, 3939–3943.

[87] A. Behr, D. Obst, A. Westfechtel, "Isomerizing hydroformylation of fatty acid esters: Formation of ω-aldehydes", *Eur. J. Lipid Sci. Technol.* **2005**, *107*, 213–219.

[88] Z. S. Petrović, I. Cvetković, D. Hong, X. Wan, W. Zhang, T. W. Abraham, J. Malsam, "Vegetable oil-based triols from hydroformylated fatty acids and polyurethane elastomers", *Eur. J. Lipid Sci. Technol.* **2010**, *112*, 97–102.

[89] P. Eilbracht, L. Bärfacker, C. Buss, C. Hollmann, B. E. Kitsos-Rzychon, C. L. Kranemann, T. Rische, R. Roggenbuck, A. Schmidt, "Tandem Reaction Sequences under Hydroformylation Conditions: New Synthetic Applications of Transition Metal Catalysis", *Chem. Rev.* **1999**, *99*, 3329–3366.

[90] H. Bahrmann, H.-D. Hahn, D. Mayer, G. D. Frey, "2-Ethylhexanol" in *Ullmann's Encyclopedia of Industrial Chemistry*, Wiley-VCH, Weinheim, Germany, **2000**.

[91] J. Pospech, I. Fleischer, R. Franke, S. Buchholz, M. Beller, "Alternative Metals for Homogeneous Catalyzed Hydroformylation Reactions", *Angew. Chem., Int. Ed.* **2013**, *52*, 2852–2872.

[92] "Rhodium - From 1992 to present", http://www.kitco.com/charts/historicalrhodium.html, **2017**.

[93] Johnson Matthey (Ed.), "PGM Market Report November 2016. Forecast of Platinum - Supply and Demand in 2016", **2016**.

[94] I. Piras, R. Jennerjahn, R. Jackstell, A. Spannenberg, R. Franke, M. Beller, "A general and efficient iridium-catalyzed hydroformylation of olefins", *Angew. Chem., Int. Ed.* **2011**, *50*, 280–284.

[95] H. Zhang, Y.-Q. Li, P. Wang, Y. Lu, X.-L. Zhao, Y. Liu, "Effect of positive-charges in diphosphino-imidazolium salts on the structures of Ir-complexes and catalysis for hydroformylation", *J. Mol. Catal. A: Chem.* **2016**, *411*, 337–343.

[96] A. Behr, A. Kämper, M. Nickel, R. Franke, "Crucial role of additives in iridium-catalyzed hydroformylation", *Appl. Catal., A* **2015**, *505*, 243–248.

[97] A. Behr, A. Kämper, R. Kuhlmann, A. J. Vorholt, R. Franke, "First efficient catalyst recycling for the iridium-catalysed hydroformylation of 1-octene", *Catal. Sci. Technol.* **2016**, *6*, 208–214.

[98] R. Jennerjahn, I. Piras, R. Jackstell, R. Franke, K.-D. Wiese, M. Beller, "Palladium-catalyzed isomerization and hydroformylation of olefins", *Chem. - Eur. J.* **2009**, *15*, 6383–6388.

[99] J. Ternel, J.-L. Couturier, J.-L. Dubois, J.-F. Carpentier, "Rhodium versus Iridium Catalysts in the Controlled Tandem Hydroformylation-Isomerization of Functionalized Unsaturated Fatty Substrates", *ChemCatChem* **2015**, *7*, 513–520.

[100] W. Ren, W. Chang, J. Dai, Y. Shi, J. Li, Y. Shi, "An Effective Pd-Catalyzed Regioselective Hydroformylation of Olefins with Formic Acid", *J. Am. Chem. Soc.* **2016**, *138*, 14864–14867.

[101] L. Le Goanvic, J.-L. Couturier, J.-L. Dubois, J.-F. Carpentier, "Ruthenium-catalyzed hydroformylation of the functional unsaturated fatty nitrile 10-undecenitrile", *J. Mol. Catal. A: Chem.* **2016**, *417*, 116–121.

[102] C. Kubis, I. Profir, I. Fleischer, W. Baumann, D. Selent, C. Fischer, A. Spannenberg, R. Ludwig, D. Hess, R. Franke, A. Borner, "In Situ FTIR and NMR Spectroscopic Investigations on Ruthenium-Based Catalysts for Alkene Hydroformylation", *Chem. - Eur. J.* **2016**, *22*, 2746–2757.

[103] I. Fleischer, L. Wu, I. Profir, R. Jackstell, R. Franke, M. Beller, "Towards the development of a selective ruthenium-catalyzed hydroformylation of olefins", *Chem. - Eur. J.* **2013**, *19*, 10589–10594.

[104] K. Takahashi, M. Yamashita, Y. Tanaka, K. Nozaki, "Ruthenium/C5 Me5/bisphosphine- or bisphosphite-based catalysts for normal-selective hydroformylation", *Angew. Chem., Int. Ed.* **2012**, *51*, 4383–4387.

[105] A. Lofù, P. Mastrorilli, C. F. Nobile, G. P. Suranna, P. Frediani, J. Iggo, "(Diphosphane monosulfide)platinum(II) Complexes for Hydroformylation Reactions. Their Catalytic Activity and a High-Pressure NMR Mechanistic Study", *Eur. J. Inorg. Chem.* **2006**, *2006*, 2268–2276.

[106] M. Gottardo, A. Scarso, S. Paganelli, G. Strukul, "Efficient Platinum(II) Catalyzed Hydroformylation Reaction in Water. Unusual Product Distribution in Micellar Media", *Adv. Synth. Catal.* **2010**, *352*, 2251–2262.

[107] P. Pongrácz, L. Kollár, A. Kerényi, V. Kovács, V. Ujj, G. Keglevich, "Hydroformylation of styrene in the presence of platinum(II) complex catalysts incorporating cyclic phosphines and phosphonous diesters as P-ligands", *J. Organomet. Chem.* **2011**, *696*, 2234–2237.

[108] A. Kämper, P. Kucmierczyk, T. Seidensticker, A. J. Vorholt, R. Franke, A. Behr, "Ruthenium-catalyzed hydroformylation. From laboratory to continuous miniplant scale", *Catal. Sci. Technol.* **2016**, *6*, 8072–8079.

[109] I. Piras, R. Jennerjahn, R. Jackstell, W. Baumann, A. Spannenberg, R. Franke, K.-D. Wiese, M. Beller, "Synthesis of novel rhodium phosphite catalysts for efficient and selective isomerization–hydroformylation reactions", *J. Organomet. Chem.* **2010**, *695*, 479–486.

[110] C. Vogl, E. Paetzold, C. Fischer, U. Kragl, "Highly selective hydroformylation of internal and terminal olefins to terminal aldehydes using a rhodium-BIPHEPHOS-catalyst system", *J. Mol. Catal. A: Chem.* **2005**, *232*, 41–44.

[111] E. Zuidema, P. E. Goudriaan, B. H. G. Swennenhuis, P. C. J. Kamer, P. W. N. M. van Leeuwen, M. Lutz, A. L. Spek, "Phenoxaphosphine-Based Diphosphine Ligands. Synthesis and Application in the Hydroformylation Reaction", *Organometallics* **2010**, *29*, 1210–1221.

[112] S. H. Chikkali, J. I. van der Vlugt, J. N. Reek, "Hybrid diphosphorus ligands in rhodium catalysed asymmetric hydroformylation", *Coord. Chem. Rev.* **2014**, *262*, 1–15.

[113] A. Pizzano, "Features and Application in Asymmetric Catalysis of Chiral Phosphine-Phosphite Ligands", *Chem. Rec.* **2016**, *16*, 2595–2618.

[114] Y. Deng, H. Wang, Y. Sun, X. Wang, "Principles and Applications of Enantioselective Hydroformylation of Terminal Disubstituted Alkenes", *ACS Catal.* **2015**, *5*, 6828–6837.

[115] J.-Z. Wei, J.-W. Lang, H.-Y. Fu, R.-X. Li, X.-L. Zheng, M.-L. Yuan, H. Chen, "Aqueous biphasic hydroformylation of higher alkenes and highly efficient catalyst recycling in the presence of a polar low boiling solvent", *Transit. Met. Chem.* **2016**, *41*, 599–603.

[116] A. Scrivanti, V. Beghetto, M. M. Alam, S. Paganelli, P. Canton, M. Bertoldini, E. Amadio, "Biphase hydroformylation catalyzed by rhodium in combination with a water-soluble pyridyl-triazole ligand", *Inorg. Chim. Acta* **2017**, *455*, 613–617.

[117] L. Obrecht, P. C. J. Kamer, W. Laan, "Alternative approaches for the aqueous–organic biphasic hydroformylation of higher alkenes", *Catal. Sci. Technol.* **2013**, *3*, 541–551.

[118] C. A. Henriques, F. M. S. Rodrigues, R. M. B. Carrilho, M. Silva, A. Fernandes, M. Filipa Ribeiro, M. M. Pereira, "Reusable MCM-41 Immobilized Rh(I) Hydroformylation Catalysts Built on Binaphthyl-based Phosphoramidite and Phosphite Ligands", *Curr. Org. Chem.* **2016**, *20*, 1445–1453.

[119] P. Purwanto, H. Delmas, "Gas-liquid-liquid reaction engineering. Hydroformylation of 1-octene using a water soluble rhodium complex catalyst", *Catal. Today* **1995**, *24*, 135–140.

[120] M. Illner, D. Müller, E. Esche, T. Pogrzeba, M. Schmidt, R. Schomäcker, G. Wozny, J.-U. Repke, "Hydroformylation in Microemulsions. Proof of Concept in a Miniplant", *Ind. Eng. Chem. Res.* **2016**, *55*, 8616–8626.

[121] Y. Zhao, X. Zhang, J. Sanjeevi, Q. Yang, "Hydroformylation of 1-octene in Pickering emulsion constructed by amphiphilic mesoporous silica nanoparticles", *J. Catal.* **2016**, *334*, 52–59.

[122] T. Vanbésien, A. Sayede, E. Monflier, F. Hapiot, "A self-emulsifying catalytic system for the aqueous biphasic hydroformylation of triglycerides", *Catal. Sci. Technol.* **2016**, *6*, 3064–3073.

[123] H. Warmeling, R. Koske, A. J. Vorholt, "Procedural Rate Enhancement of Lean Aqueous Hydroformylation of 1-Octene without Additives", *Chem. Eng. Technol.* **2017**, *40*, 186–195.

[124] S. L. Desset, D. J. Cole-Hamilton, "Carbon dioxide induced phase switching for homogeneous-catalyst recycling", *Angew. Chem., Int. Ed.* **2009**, *48*, 1472–1474.

[125] S. Pandey, S. H. Chikkali, "Highly Regioselective Isomerizing Hydroformylation of Long-Chain Internal Olefins Catalyzed by a Rhodium Bis(Phosphite) Complex", *ChemCatChem* **2015**, *7*, 3468–3471.

[126] M. Vilches-Herrera, L. Domke, A. Börner, "Isomerization–Hydroformylation Tandem Reactions", *ACS Catal.* **2014**, *4*, 1706–1724.

[127] T. Seidensticker, J. M. Vosberg, K. A. Ostrowski, A. J. Vorholt, "Rhodium-Catalyzed Bis-Hydroaminomethylation of Linear Aliphatic Alkenes with Piperazine", *Adv. Synth. Catal.* **2016**, *358*, 610–621.

[128] C. Chen, X.-Q. Dong, X. Zhang, "Recent progress in rhodium-catalyzed hydroaminomethylation", *Org. Chem. Front.* **2016**, *3*, 1359–1370.

[129] G. M. Torres, R. Frauenlob, R. Franke, A. Börner, "Production of alcohols via hydroformylation", *Catal. Sci. Technol.* **2015**, *5*, 34–54.

[130] K. A. Ostrowski, T. A. Faßbach, D. Vogelsang, A. J. Vorholt, "Decreasing Side Products and Increasing Selectivity in the Tandem Hydroformylation/Acyloin Reaction", *ChemCatChem* **2015**, *7*, 2607–2613.

[131] K. A. Ostrowski, T. A. Faßbach, A. J. Vorholt, "Tandem Hydroformylation/Acyloin Reaction - The Synergy of Metal Catalysis and Organocatalysis Yielding Acyloins Directly from Olefins", *Adv. Synth. Catal.* **2015**, *357*, 1374–1380.

[132] T. Vanbesien, F. Hapiot, E. Monflier, "Hydroformylation of vegetable oils and the potential use of hydroformylated fatty acids", *Lipid Technol.* **2013**, *25*, 175–178.

[133] T. Vanbésien, E. Monflier, F. Hapiot, "Supramolecular Emulsifiers in Biphasic Catalysis. The Substrate Drives Its Own Transformation", *ACS Catal.* **2015**, *5*, 4288–4292.

[134] H. F. Ramalho, K. M. di Ferreira, P. M. Machado, R. S. Oliveira, L. P. Silva, M. J. Prauchner, P. A. Suarez, "Biphasic hydroformylation of soybean biodiesel using a rhodium complex dissolved in ionic liquid", *Ind. Crops Prod.* **2014**, *52*, 211–218.

[135] V. Goldbach, P. Roesle, S. Mecking, "Catalytic Isomerizing ω-Functionalization of Fatty Acids", *ACS Catal.* **2015**, *5*, 5951–5972.

[136] Y. Yuki, K. Takahashi, Y. Tanaka, K. Nozaki, "Tandem isomerization/hydroformylation/hydrogenation of internal alkenes to n-alcohols using Rh/Ru dual- or ternary-catalyst systems", *J. Am. Chem. Soc.* **2013**, *135*, 17393–17400.

[137] A. J. Vorholt, S. Immohr, K. A. Ostrowski, S. Fuchs, A. Behr, "Catalyst recycling in the hydroaminomethylation of methyl oleate. A route to novel polyamide monomers", *Eur. J. Lipid Sci. Technol.* **2016**, *119*, 1–10.

[138] P. J. Baricelli, M. Rodriguez, L. G. Melean, M. M. Alonso, M. Borusiak, M. Rosales, B. Gonzalez, K. C. d. Oliveira, E. V. Gusevskaya, E. N. dos Santos, "Rhodium catalyzed aqueous biphasic hydroformylation of naturally occurring allylbenzenes in the presence of water-soluble phosphorus ligands", *Appl. Catal., A* **2015**, *490*, 163–169.

[139] C. G. Vieira, M. d. Freitas, K. C. d. Oliveira, A. d. Camargo Faria, E. N. dos Santos, E. V. Gusevskaya, "Synthesis of fragrance compounds from renewable resources. The aqueous biphasic hydroformylation of acyclic terpenes", *Catal. Sci. Technol.* **2015**, *5*, 960–966.

[140] Q. Liu, L. Wu, I. Fleischer, D. Selent, R. Franke, R. Jackstell, M. Beller, "Development of a ruthenium/phosphite catalyst system for domino hydroformylation-reduction of olefins with carbon dioxide", *Chem. - Eur. J.* **2014**, *20*, 6888–6894.

[141] Lucite International, "Alpha Technology", http://www.luciteinternational.com/monomers-emea-manufacturing-alpha-technology-15/, **2011**.

[142] Harris. B, "Acryls for the future", *Ingenia* **2010**, *45*, 18–23.

[143] C. Jimenez Rodriguez, D. F. Foster, G. R. Eastham, D. J. Cole-Hamilton, "Highly selective formation of linear esters from terminal and internal alkenes catalysed by palladium complexes of bis-(di-tert-butylphosphinomethyl)benzene", *Chem. Commun.* **2004**, 1720–1721.

[144] C. Jiménez-Rodriguez, G. R. Eastham, D. J. Cole-Hamilton, "Dicarboxylic acid esters from the carbonylation of unsaturated esters under mild conditions", *Inorg. Chem. Commun.* **2005**, *8*, 878–881.

[145] M. R. L. Furst, R. Le Goff, D. Quinzler, S. Mecking, C. H. Botting, D. J. Cole-Hamilton, "Polymer precursors from catalytic reactions of natural oils", *Green Chem.* **2012**, *14*, 472–477.

[146] F. M. Petrat, F. E. Baumann, H. Häger, G. Walther, A. Martin, A. Köckritz, "Verfahren zur herstellung von linearen alpha,omega-dicarbonsäurediestern", WO2011110249 A1, **2011**.

[147] P. Roesle, F. Stempfle, S. K. Hess, J. Zimmerer, C. Río Bártulos, B. Lepetit, A. Eckert, P. G. Kroth, S. Mecking, "Synthetic polyester from algae oil", *Angew. Chem., Int. Ed.* **2014**, *53*, 6800–6804.

[148] G. Walther, J. Deutsch, A. Martin, F.-E. Baumann, D. Fridag, R. Franke, A. Köckritz, "α,ω-Functionalized C19 Monomers", *ChemSusChem* **2011**, *4*, 1052–1054.

[149] G. Walther, A. Martin, A. Köckritz, "Direct Transesterification/Isomerization/Methoxycarbonylation of Various Plant Oils", *J. Am. Oil Chem. Soc.* **2013**, *90*, 141–145.

[150] H. Busch, F. Stempfle, S. Heß, E. Grau, S. Mecking, "Selective isomerization–carbonylation of a terpene trisubstituted double bond", *Green Chem.* **2014**, *16*, 4541–4545.

[151] T. Witt, F. Stempfle, P. Roesle, M. Häußler, S. Mecking, "Unsymmetrical α,ω-Difunctionalized Long-Chain Compounds via Full Molecular Incorporation of Fatty Acids", *ACS Catal.* **2015**, *5*, 4519–4529.

[152] D. J. Cole-Hamilton, "Nature's polyethylene", *Angew. Chem., Int. Ed.* **2010**, *49*, 8564–8566.

[153] F. Stempfle, D. Quinzler, I. Heckler, S. Mecking, "Long-Chain Linear C 19 and C 23 Monomers and Polycondensates from Unsaturated Fatty Acid Esters", *Macromolecules* **2011**, *44*, 4159–4166.

[154] C. Vilela, A. F. Sousa, A. C. Fonseca, A. C. Serra, J. F. J. Coelho, C. S. R. Freire, A. J. D. Silvestre, "The quest for sustainable polyesters – insights into the future", *Polym. Chem.* **2014**, *5*, 3119–3141.

[155] G. Walther, "High-Performance Polymers from Nature: Catalytic Routes and Processes for Industry", *ChemSusChem* **2014**, *7*, 2081–2088.

[156] V. Goldbach, L. Falivene, L. Caporaso, L. Cavallo, S. Mecking, "Single-Step Access to Long-Chain α,ω-Dicarboxylic Acids by Isomerizing Hydroxycarbonylation of Unsaturated Fatty Acids", *ACS Catal.* **2016**, *6*, 8229–8238.

[157] J. T. Christl, P. Roesle, F. Stempfle, P. Wucher, I. Göttker-Schnetmann, G. Müller, S. Mecking, "Catalyst activity and selectivity in the isomerising alkoxycarbonylation of methyl oleate", *Chem. - Eur. J.* **2013**, *19*, 17131–17140.

[158] J. J. Frew, K. Damian, H. van Rensburg, A. M. Slawin, R. P. Tooze, M. L. Clarke, "Palladium(II) Complexes of New Bulky Bidentate Phosphanes: Active and Highly Regioselective Catalysts for the Hydroxycarbonylation of Styrene", *Chem. - Eur. J.* **2009**, *15*, 10504–10513.

[159] A. Grabulosa, J. J. Frew, J. A. Fuentes, A. M. Slawin, M. L. Clarke, "Palladium complexes of bulky ortho-trifluoromethylphenyl-substituted phosphines: Unusually regioselective catalysts for the hydroxycarbonylation and alkoxycarbonylation of alkenes", *J. Mol. Catal. A: Chem.* **2010**, *330*, 18–25.

[160] A. Pews-Davtyan, X. Fang, R. Jackstell, A. Spannenberg, W. Baumann, R. Franke, M. Beller, "Synthesis of new diphosphine ligands and their application in Pd-catalyzed alkoxycarbonylation reactions", *Chem. - Asian J.* **2014**, *9*, 1168–1174.

[161] P. Roesle, L. Caporaso, M. Schnitte, V. Goldbach, L. Cavallo, S. Mecking, "A comprehensive mechanistic picture of the isomerizing alkoxycarbonylation of plant oils", *J. Am. Chem. Soc.* **2014**, *136*, 16871–16881.

[162] P. Roesle, C. J. Dürr, H. M. Möller, L. Cavallo, L. Caporaso, S. Mecking, "Mechanistic features of isomerizing alkoxycarbonylation of methyl oleate", *J. Am. Chem. Soc.* **2012**, *134*, 17696–17703.

[163] G. Walther, L. R. Knöpke, J. Rabeah, M. P. Chęciński, H. Jiao, U. Bentrup, A. Brückner, A. Martin, A. Köckritz, "From sunflower oil toward 1,19-diester: Mechanistic elucidation", *J. Catal.* **2013**, *297*, 44–55.

[164] H. Li, K. Dong, H. Jiao, H. Neumann, R. Jackstell, M. Beller, "The scope and mechanism of palladium-catalysed Markovnikov alkoxycarbonylation of alkenes", *Nat. Chem.* **2016**, *8*, 1159–1166.

[165] K. Dong, X. Fang, S. Gulak, R. Franke, A. Spannenberg, H. Neumann, R. Jackstell, M. Beller, "Highly active and efficient catalysts for alkoxycarbonylation of alkenes", *Nat. Commun.* **2017**, *8*, 14117.

[166] A. Behr, C. Fängewisch, "Temperature-Dependent Multicomponent Solvent Systems – An Alternative Concept for Recycling Homogeneous Catalysts", *Chem. Eng. Technol.* **2002**, *25*, 143–147.

[167] D. E. Bergbreiter, S. D. Sung, J. Li, D. Ortiz, P. N. Hamilton, "Designing Polymers for Biphasic Liquid/Liquid Separations after Homogeneous Reactions", *Org. Process Res. Dev.* **2004**, *8*, 461–468.

[168] B. Hentschel, A. Peschel, H. Freund, K. Sundmacher, "Simultaneous design of the optimal reaction and process concept for multiphase systems", *Chem. Eng. Sci.* **2014**, *115*, 69–87.

[169] B. Hentschel, H. Freund, K. Sundmacher, "Modellbasierte Ermittlung der optimalen Reaktionsführung für integrierte Mehrphasenprozesse", *Chem. Ing. Tech.* **2014**, *86*, 1080–1087.

[170] B. Hentschel, G. Kiedorf, M. Gerlach, C. Hamel, A. Seidel-Morgenstern, H. Freund, K. Sundmacher, "Model-Based Identification and Experimental Validation of the Optimal Reaction Route for the Hydroformylation of 1-Dodecene", *Ind. Eng. Chem. Res.* **2015**, *54*, 1755–1765.

[171] A. Klamt, "Conductor-like Screening Model for Real Solvents. A New Approach to the Quantitative Calculation of Solvation Phenomena", *J. Phys. Chem.* **1995**, *99*, 2224–2235.

[172] Y. Brunsch, "Temperaturgesteuertes Katalysatorrecycling für die homogen katalysierte Hydroformylierung langkettiger Alkene", Technische Universität Dortmund, **2013**.

[173] K. McBride, K. Sundmacher, "Data Driven Conceptual Process Design for the Hydroformylation of 1-Dodecene in a Thermomorphic Solvent System", *Ind. Eng. Chem. Res.* **2015**, *54*, 6761–6771.

[174] H. Witte, M. Zagajewski, A. Behr, "Scale-up durch Miniplant-Technik: Anwendungsbeispiele aus der homogenen Katalyse", *Chem. Ing. Tech.* **2012**, *84*, 694–703.

[175] A. Fredenslund, R. L. Jones, J. M. Prausnitz, "Group-contribution estimation of activity coefficients in nonideal liquid mixtures", *AIChE J.* **1975**, *21*, 1086–1099.

[176] F. Eckert, A. Klamt, "COSMOtherm, version C13", COSMOlogic GmbH & Co. KG, Leverkusen, **2014**.

[177] A. Klamt, G. Schüürmann, "COSMO. A new approach to dielectric screening in solvents with explicit expressions for the screening energy and its gradient", *J. Chem. Soc., Perkin Trans. 2* **1993**, 799–805.

[178] H.-H. Tung, J. Tabora, N. Variankaval, D. Bakken, C.-C. Chen, "Prediction of pharmaceutical solubility Via NRTL-SAC and COSMO-SAC", *J. Pharm. Sci.* **2008**, *97*, 1813–1820.

[179] I. Hahnenkamp, G. Graubner, J. Gmehling, "Measurement and prediction of solubilities of active pharmaceutical ingredients", *Int. J. Pharm.* **2010**, *388*, 73–81.

[180] A. Pozarska, C. da Costa Mathews, M. Wong, K. Pencheva, "Application of COSMO-RS as an excipient ranking tool in early formulation development", *Eur. J. Pharm. Sci.* **2013**, *49*, 505–511.

[181] B. Bouillot, S. Teychené, B. Biscans, "An evaluation of thermodynamic models for the prediction of drug and drug-like molecule solubility in organic solvents", *Fluid Phase Equilib.* **2011**, *309*, 36–52.

[182] K. Wichmann, A. Klamt, "Drug Solubility and Reaction Thermodynamics" in *Chemical Engineering in the Pharmaceutical Industry: R&D to Manufacturing (ed. D. J. am Ende)*, John Wiley & Sons, Ltd, Hoboken (USA), **2010**.

[183] "TURBOMOLE, V6.5, Program packager for ab initio electronic structure calculations", COSMOlogic GmbH & Co. KG, Leverkusen, **2013**.

[184] K. Eichkorn, F. Weigend, O. Treutler, R. Ahlrichs, "Auxiliary basis sets for main row atoms and transition metals and their use to approximate Coulomb potentials", *Theor. Chem. Acc.* **1997**, *97*, 119–124.

[185] A. Schäfer, C. Huber, R. Ahlrichs, "Fully optimized contracted Gaussian basis sets of triple zeta valence quality for atoms Li to Kr", *J. Chem. Phys.* **1994**, *100*, 5829–5835.

[186] A. Klamt, "COSMO-RS. From Quantum Chemistry to Fluid Phase Thermodynamics and Drug Design", Elsevier Science Limited, Amsterdam, Boston, **2005**.

[187] G. Koller, U. Fischer, K. Hungerbühler, "Assessing Safety, Health, and Environmental Impact Early during Process Development", *Ind. Eng. Chem. Res.* **2000**, *39*, 960–972.

[188] C. Capello, U. Fischer, K. Hungerbühler, "What is a green solvent? A comprehensive framework for the environmental assessment of solvents", *Green Chem.* **2007**, *9*, 927.

[189] United States Environmental Protection Agency, "Ozone Layer Protection", http://www.epa.gov/ozone/mbr/index.html, **2014**.

[190] L. M. Casás, B. Orge, C. Díaz, J. Tojo, "Liquid–liquid equilibria for mixtures of {methyl acetate+methanol+n-alkane (C10–C12)} at several temperatures and 1 atm", *J. Chem. Thermodyn.* **2004**, *36*, 237–243.

[191] H. Klein, R. Jackstell, K.-D. Wiese, C. Borgmann, M. Beller, "Highly Selective Catalyst Systems for the Hydroformylation of Internal Olefins to Linear Aldehydes", *Angew. Chem., Int. Ed.* **2001**, *40*, 3408–3411.

[192] L. A. van der Veen, P. C. J. Kamer, P. W. N. M. van Leeuwen, "Hydroformylation of Internal Olefins to Linear Aldehydes with Novel Rhodium Catalysts", *Angew. Chem., Int. Ed.* **1999**, *38*, 336–338.

[193] E. Billig, A. G. Abatjoglou, Bryant, D. R. Union Carbide Corporation, "Bis-phosphite compounds", EP 213639, **1987**.

[194] A. Behr, D. Obst, B. Turkowski, "Isomerizing hydroformylation of trans-4-octene to n-nonanal in multiphase systems. Acceleration effect of propylene carbonate", *J. Mol. Catal. A: Chem.* **2005**, *226*, 215–219.

[195] A. Behr, D. Obst, C. Schulte, "Kinetik der isomerisierenden Hydroformylierung von trans-4-Octen", *Chem. Ing. Tech.* **2004**, *76*, 904–910.

[196] D. Selent, D. Hess, K.-D. Wiese, D. Röttger, C. Kunze, A. Börner, "New Phosphorus Ligands for the Rhodium-Catalyzed Isomerization/Hydroformylation of Internal Octenes", *Angew. Chem., Int. Ed.* **2001**, *40*, 1696–1698.

[197] D. Selent, K.-D. Wiese, D. Röttger, A. Börner, "Novel Oxyfunctionalized Phosphonite Ligands for the Hydroformylation of Isomeric n-Olefins", *Angew. Chem., Int. Ed.* **2000**, *39*, 1639–1641.

[198] A. Christiansen, R. Franke, D. Fridag, D. Hess, B. Kreidler, D. Selent, A. Börner, Evonik Oxeno GmbH, "Novel organophosphorus compounds based on anthracenetriol", WO2013068232, **2016**.

[199] H. Klein, R. Jackstell, M. Beller, "Synthesis of linear aldehydes from internal olefins in water", *Chem. Commun.* **2005**, 2283–2285.

[200] M. Beller, J. G. Krauter, "Cobalt-catalyzed biphasic hydroformylation of internal short chain olefins", *J. Mol. Catal. A: Chem.* **1999**, *143*, 31–39.

[201] M. Kant, A. Martin, G. Giuffrida, S. Rosano, "Hydroformylierung langkettiger interner Olefine mit wasserlöslichen Cobalt/Phosphin-Komplexen", *Chem. Ing. Tech.* **2006**, *78*, 913–921.

[202] N. C. Kokkinos, E. Kazou, A. Lazaridou, C. E. Papadopoulos, N. Psaroudakis, K. Mertis, N. Nikolaou, "A potential refinery process of light–light naphtha olefins conversion to valuable oxygenated products in aqueous media – Part 1. Biphasic hydroformylation", *Fuel* **2013**, *104*, 275–283.

[203] R. P. J. Bronger, S. M. Silva, P. C. J. Kamer, P. W. N. M. van Leeuwen, "A novel dicationic phenoxaphosphino-modified Xantphos-type ligand. A ligand for highly active and selective, biphasic, rhodium catalysed hydroformylation in ionic liquids", *Dalton Trans.* **2004**, 1590–1596.

[204] A. Behr, G. Henze, R. Schomäcker, "Thermoregulated Liquid/Liquid Catalyst Separation and Recycling", *Adv. Synth. Catal.* **2006**, *348*, 1485–1495.

[205] T. Gaide, A. Behr, A. Arns, F. Benski, A. J. Vorholt, "Hydroesterification of methyl 10-undecenoate in thermomorphic multicomponent solvent systems - Process development for the synthesis of sustainable polymer precursors", *Chem. Eng. Process.* **2016**, *99*, 197–204.

[206] A. Behr, J. Dreimann, M. Zagajewski, A. J. Vorholt, "Hydroformylierung von 1-Dodecen im Miniplantmaßstab unter Verwendung von thermomorphen Mehrkomponenten-Lösungsmittelsystemen", *Chem. Ing. Tech.* **2014**, *86*, 1535–1536.

[207] A. Jörke, A. Seidel-Morgenstern, C. Hamel, "Isomerization of 1-decene. Estimation of thermodynamic properties, equilibrium composition calculation and experimental validation using a Rh-BIPHEPHOS catalyst", *Chem. Eng. J.* **2015**, *260*, 513–523.

[208] A. Jörke, T. Gaide, A. Behr, A. J. Vorholt, A. Seidel-Morgenstern, C. Hamel, "Hydroformylation and tandem isomerization–hydroformylation of n-decenes using a rhodium-BiPhePhos catalyst. Kinetic modeling, reaction network analysis and optimal reaction control", *Chem. Eng. J.* **2017**, *313*, 382–397.

[209] K. McBride, T. Gaide, A. J. Vorholt, A. Behr, K. Sundmacher, "Thermomorphic solvent selection for homogeneous catalyst recovery based on COSMO-RS", *Chem. Eng. Process.* **2016**, *99*, 97–106.

[210] American Chemical Society, "Sustainability and the Chemical Enterprise", Washington, DC, **2014**.

[211] P. T. Anastas, T. C. Williamson, "Green chemistry. Designing chemistry for the environment", American Chemical Society, Washington, DC, **1996**.

[212] D. J. Cole-Hamilton, R. P. Tooze, "Catalyst separation, recovery and recycling. Chemistry and process design", Springer, Dordrecht, **2006**.

[213] M. Röper, "Homogene Katalyse in der Chemischen Industrie. Selektivität, Aktivität und Standzeit", *Chem. unserer Zeit* **2006**, *40*, 126–135.

[214] A. Behr, "Catalysis, Homogeneous" in *Ullmann's Encyclopedia of Industrial Chemistry*, Wiley-VCH, Weinheim, Germany, **2000**.

[215] M. Benaglia, "Recoverable and Recyclable Catalysts", John Wiley & Sons, Ltd, Chichester, **2009**.

[216] P. Barbaro, F. Liguori, "Heterogenized homogeneous catalysts for fine chemicals production. Materials and processes", Springer, Dordrecht, **2010**.

[217] D. E. Bergbreiter, P. L. Osburn, A. Wilson, E. M. Sink, "Palladium-Catalyzed C−C Coupling under Thermomorphic Conditions", *J. Am. Chem. Soc.* **2000**, *122*, 9058–9064.

[218] A. Riisager, R. Fehrmann, M. Haumann, P. Wasserscheid, "Supported Ionic Liquid Phase (SILP) Catalysis: An Innovative Concept for Homogeneous Catalysis in Continuous Fixed-Bed Reactors", *Eur. J. Inorg. Chem.* **2006**, *2006*, 695–706.

[219] K. Kunna, C. Müller, J. Loos, D. Vogt, "Aqueous-Phase Hydroformylation of 1-Octene: Styrene Latices as Phase-Transfer Agents", *Angew. Chem., Int. Ed.* **2006**, *45*, 7289–7292.

[220] D. E. Bergbreiter, S. D. Sung, "Liquid/Liquid Biphasic Recovery/Reuse of Soluble Polymer-Supported Catalysts", *Adv. Synth. Catal.* **2006**, *348*, 1352–1366.

[221] C. Liu, X. Li, Z. Jin, "Progress in thermoregulated liquid/liquid biphasic catalysis", *Catal. Today* **2015**, *247*, 82–89.

[222] M. Lombardo, A. Quintavalla, M. Chiarucci, C. Trombini, "Multiphase Homogeneous Catalysis: Common Procedures and Recent Applications", *Synlett* **2010**, 1746–1765.

[223] B. J. Cohen, M. A. Kraus, A. Patchornik, ""Wolf and Lamb" reactions equilibrium and kinetic effects in multipolymer systems", *J. Am. Chem. Soc.* **1981**, *103*, 7620–7629.

[224] A. J. Vorholt, P. Neubert, A. Behr, "Katalytische Funktionalisierungen von Oleylalkohol in thermomorphen Lösungsmittelsystemen zur Synthese potenzieller Biotenside und -Monomere", *Chem. Ing. Tech.* **2013**, 1540–1547.

[225] A. Behr, T. Seidensticker, A. J. Vorholt, "Diester monomers from methyl oleate and proline via tandem hydroaminomethylation-esterification sequence with homogeneous catalyst recycling using TMS-technique", *Eur. J. Lipid Sci. Technol.* **2014**, *116*, 477–485.

[226] D. E. Bergbreiter, "Thermomorphic Catalysts" in *Recoverable and Recyclable Catalysts (ed. M. Benaglia)*, John Wiley & Sons, Ltd, **2009**.

[227] D. E. Bergbreiter, P. L. Osburn, J. D. Frels, "Nonpolar Polymers for Metal Sequestration and Ligand and Catalyst Recovery in Thermomorphic Systems", *J. Am. Chem. Soc.* **2001**, *123*, 11105–11106.

[228] A. Behr, A. Wintzer, "Baukastensystem zur Auswahl von Lösungsmitteln in homogenkatalytischen Reaktionen", *Chem. Ing. Tech.* **2011**, *83*, 1356–1370.

[229] U. Biermann, U. Bornscheuer, M. A. R. Meier, J. O. Metzger, H. J. Schäfer, "Oils and Fats as Renewable Raw Materials in Chemistry", *Angew. Chem., Int. Ed.* **2011**, *50*, 3854–3871.

[230] A. Thomas, "Fats and Fatty Oils" in *Ullmann's Encyclopedia of Industrial Chemistry*, Wiley-VCH, Weinheim, Germany, **2000**.

[231] Y. Brunsch, A. Behr, "Temperaturgesteuertes Katalysatorrecycling in der homogenen Übergangsmetallkatalyse: Minimierung des Katalysatorleachings", *Angew. Chem.* **2013**, *125*, 1627–1631.

[232] H.-D. Hahn, G. Dämbkes, N. Rupprich, H. Bahl, G. D. Frey, "Butanols" in *Ullmann's Encyclopedia of Industrial Chemistry*, Wiley-VCH, Weinheim, Germany, **2000**.

[233] T. Hamerla, A. Rost, Y. Kasaka, R. Schomäcker, "Hydroformylation of 1-Dodecene with Water-Soluble Rhodium Catalysts with Bidentate Ligands in Multiphase Systems", *ChemCatChem* **2013**, *5*, 1854–1862.

[234] P. T. Anastas, J. B. Zimmerman, "Through the 12 Principles of Green Engineering", *Environ. Sci. Technol.* **2003**, *37*, 94A–101A.

[235] B. Cornils, P. Lappe, U. by Staff, "Dicarboxylic Acids, Aliphatic" in *Ullmann's Encyclopedia of Industrial Chemistry*, Wiley-VCH, Weinheim, Germany, **2000**.

[236] B. Herzog, M. I. Kohan, S. A. Mestemacher, R. U. Pagilagan, K. Redmond, "Polyamides" in *Ullmann's Encyclopedia of Industrial Chemistry*, Wiley-VCH, Weinheim, Germany, **2000**.

[237] J. D. Andrade, K. Köhler, G. D. Prescher, "Verfahren zur Herstellung von 1,12-Dodecandisäure II", EP0258535 A2, **1988**.

[238] M. R. L. Furst, T. Seidensticker, D. J. Cole-Hamilton, "Polymerisable di- and triesters from Tall Oil Fatty Acids and related compounds", *Green Chem.* **2013**, *15*, 1218–1225.

[239] A. Brennführer, H. Neumann, M. Beller, "Palladium-Catalyzed Carbonylation Reactions of Alkenes and Alkynes", *ChemCatChem* **2009**, *1*, 28–41.

[240] G. R. Eastham, R. P. Tooze, X. L. Wang, K. Whiston, "Process for the carbonylation of ethylene and catalyst system for use therein", WO 96/19434, **1996**.

[241] W. Clegg, M. R. J. R. J. Elsegood, G. R. Eastham, R. P. Tooze, X. L. Wang, K. Whiston, "Highly active and selective catalysts for the production of methyl propanoate via the methoxycarbonylation of ethene", *Chem. Commun.* **1999**, 1877–1878.

[242] W. Clegg, G. R. Eastham, M. R. J. R. J. Elsegood, B. T. Heaton, J. A. Iggo, R. P. Tooze, R. Whyman, S. Zacchini, "Synthesis and reactivity of palladium hydrido-solvento complexes, including a key intermediate in the catalytic methoxycarbonylation of ethene to methyl propanoate", *J. Chem. Soc., Dalton Trans.* **2002**, 3300–3308.

[243] W. Clegg, G. R. Eastham, M. R. J. R. J. Elsegood, B. T. Heaton, J. A. Iggo, R. P. Tooze, R. Whyman, S. Zacchini, "Characterization and Dynamics of $[Pd(L{-}L)H(solv)]^+$, $[Pd(L{-}L)(CH_2CH_3)]^+$, and $[Pd(L{-}L)(C(O)Et)(THF)]^+$ (L−L = 1,2-$(CH_2PBu^t_2)_2C_6H_4$): Key Intermediates in the Catalytic Methoxycarbonylation of Ethene to Methylpropanoate", *Organometallics* **2002**, *21*, 1832–1840.

[244] V. de la Fuente, M. Waugh, G. R. Eastham, J. A. Iggo, S. Castillón, C. Claver, "Phosphine Ligands in the Palladium-Catalysed Methoxycarbonylation of Ethene: Insights into The Catalytic Cycle through an HP NMR Spectroscopic Study", *Chem. - Eur. J.* **2010**, *16*, 6919–6932.

[245] T. Fanjul, G. Eastham, N. Fey, A. Hamilton, A. G. Orpen, P. G. Pringle, M. Waugh, "Palladium Complexes of the Heterodiphosphine o-$C_6H_4(CH_2P^tBu_2)(CH_2PPh_2)$ Are Highly Selective and Robust Catalysts for the Hydromethoxycarbonylation of Ethene", *Organometallics* **2010**, *29*, 2292–2305.

[246] D. Cole-Hamilton, G. R. Eastham, C. Jimenez, "Process for the carbonylation of ethylenically unsaturated compouds", WO2004/0148434 A1, **2004**.

[247] E. J. García-Suárez, S. G. Khokarale, O. N. van Buu, R. Fehrmann, A. Riisager, "Pd-catalyzed ethylene methoxycarbonylation with Brønsted acid ionic liquids as promoter and phase-separable reaction media", *Green Chem.* **2013**, *16*, 161–166.

[248] A. Behr, G. Henze, L. Johnen, S. Reyer, "Selective catalytic formation of unsaturated amino acids from petrochemicals and carbon dioxide—Application of high-throughput catalyst screening", *J. Mol. Catal. A: Chem.* **2008**, *287*, 95–101.

[249] P. W. N. M. van Leeuwen, P. C. J. Kamer, J. N. Reek, "The bite angle makes the catalyst", *Pure Appl. Chem.* **1999**, *71*, 1443–1452.

[250] V. V. Grushin, "Hydrido Complexes of Palladium", *Chem. Rev.* **1996**, *96*, 2011–2034.

[251] L. H. Slaugh, R. D. Mullineaux, "Novel Hydroformylation catalysts", *J. Organomet. Chem.* **1968**, *13*, 469–477.

[252] R. F. Mason, R. C. Morris, J. L. van Winkle, "Single stage hydroformylation of olefins to alcohols", US3420898 A, **1969**.

[253] P. K. Wong, A. A. Moxey, "Hydroformylation of alpha-alcohol-diolefins to dialcohols", US6114588 A, **2000**.

[254] C. Crause, L. Bennie, L. Damoense, C. L. Dwyer, C. Grove, N. Grimmer, W. J. van Rensburg, M. M. Kirk, K. M. Mokheseng, S. Otto, P. J. Steynberg, "Bicyclic phosphines as ligands for cobalt-catalysed hydroformylation", *Dalton Trans.* **2003**, 2036–2042.

[255] P. N. Bungu, S. Otto, "Bicyclic phosphines as ligands for cobalt catalysed hydroformylation. Crystal structures of $[Co(Phoban[3.3.1]\text{-}Q)(CO)_3]_2$ (Q = C_2H_5, C_5H_{11}, $C_3H_6NMe_2$, C_6H_{11})", *Dalton Trans.* **2007**, 2876–2884.

[256] D. Wu, Y. Wang, G. Li, J. Jiang, Z. Jin, "Thermoregulated phase-transfer cobalt catalyst for production of linear higher alcohols from C11–12 internal olefins in aqueous/organic biphasic system", *Catal. Commun.* **2014**, *44*, 54–56.

[257] J. K. MacDougall, D. J. Cole-Hamilton, "Direct formation of alcohols in homogeneous hydroformylation catalysed by rhodium complexes", *J. Chem. Soc., Chem. Commun.* **1990**, 165–167.

[258] J.-A. M. Andersen, A. W. S. Currie, "Improved regioselectivity in the hydroformylation reaction catalysed by zeolite-encapsulated rhodium(I) species", *Chem. Commun.* **1996**, 1543–1544.

[259] M. C. Simpson, A. W. S. Currie, J.-A. M. Andersen, D. J. Cole-Hamilton, M. J. Green, "Hydrocarbonylation of prop-2-en-1-ol to butane-1,4-diol and 2-methylpropan-1-ol catalysed by rhodium triethylphosphine complexes", *J. Chem. Soc., Dalton Trans.* **1996**, 1793–1800.

[260] J. R. Briggs, D. L. Packett, D. R. Bryant, A. G. Phillips, D. J. Schreck, A. S. Guram, K. D. Olson, T. C. Eisenschmid, E. B. Tjaden, "Processes for producing 1,6-hexanediols", US6187970 B1, **2001**.

[261] L. Ropartz, R. E. Morris, D. F. Foster, D. J. Cole-Hamilton, "Phosphine-containing carbosilane dendrimers based on polyhedral silsesquioxane cores as ligands for hydroformylation reaction of oct-1-ene", *J. Mol. Catal. A: Chem.* **2002**, *182-183*, 99–105.

[262] T. Ichihara, K. Nakano, M. Katayama, K. Nozaki, "Tandem hydroformylation-hydrogenation of 1-decene catalyzed by Rh-bidentate bis(trialkylphosphine)s", *Chem. - Asian J.* **2008**, *3*, 1722–1728.

[263] I. I. F. Boogaerts, D. F. S. White, D. J. Cole-Hamilton, "High chemo and regioselective formation of alcohols from the hydrocarbonylation of alkenes using cooperative ligand effects", *Catal. Commun.* **2010**, *46*, 2194–2196.

[264] L. L. W. Cheung, G. Vasapollo, H. Alper, "Synthesis of Alcohols via a Rhodium-Catalyzed Hydroformylation- Reduction Sequence using Tertiary Bidentate Amine Ligands", *Adv. Synth. Catal.* **2012**, *354*, 2019–2022.

[265] B. A. Rodriguez, W. J. Tenn, "Direct formation of propanol from a dilute ethylene feed via reductive-hydroformylation using homogeneous rhodium catalysts at low feed pressures", *Appl. Catal., A* **2012**, *421-422*, 161–163.

[266] O. Diebolt, C. Müller, D. Vogt, "On-water rhodium-catalysed hydroformylation for the production of linear alcohols", *Catal. Sci. Technol.* **2012**, *2*, 773–777.

[267] D. Konya, K. Q. Almeida Leñero, E. Drent, "Highly Selective Halide Anion-Promoted Palladium-Catalyzed Hydroformylation of Internal Alkenes to Linear Alcohols", *Organometallics* **2006**, *25*, 3166–3174.

[268] E. M. Gordon, R. Eisenberg, "Photochemical hydroformylation catalysis using ruthenium complexes", *J. Organomet. Chem.* **1986**, *306*, C53-C57.

[269] J. F. Knifton, "Syngas reactions", *J. Mol. Catal. A: Chem.* **1987**, *43*, 65–77.

[270] L. Alvila, T. A. Pakkanen, O. Krause, "Hydroformylation of olefins catalysed by supported Ru3(CO)12 with 2,2′-bipyridine or with other heterocyclic nitrogen base", *J. Mol. Catal. A: Chem.* **1993**, *84*, 145–156.

[271] L. Alvila, J. Pursiainen, J. Kiviaho, T. A. Pakkanen, O. Krause, "$Ru_3(CO)_{12}$/2,2′-bipyridine supported on inorganic carriers as 1-hexene hydroformylation catalysts", *J. Mol. Catal. A: Chem.* **1994**, *91*, 335–342.

[272] T.-a. Mitsudo, N. Suzuki, T.-a. Kobayashi, T. Kondo, "$Ru_3(CO)_{12}$/1,10-phenanthroline-catalyzed hydroformylation of styrene and acrylic esters", *J. Mol. Catal. A: Chem.* **1999**, *137*, 253–262.

[273] M. A. Moreno, M. Haukka, S. Jääskeläinen, S. Vuoti, J. Pursiainen, T. A. Pakkanen, "Synthesis, characterization, reactivity and theoretical studies of ruthenium carbonyl complexes containing ortho-substituted triphenyl phosphanes", *J. Organomet. Chem.* **2005**, *690*, 3803–3814.

[274] M. Moreno, M. Haukka, A. Turunen, T. Pakkanen, "Monomeric ruthenium carbonyls containing 2-substituted pyrazinesFrom synthesis to catalytic activity in 1-hexene hydroformylation", *J. Mol. Catal. A: Chem.* **2005**, *240*, 7–15.

[275] K. Takahashi, M. Yamashita, K. Nozaki, "Tandem hydroformylation/hydrogenation of alkenes to normal alcohols using Rh/Ru dual catalyst or Ru single component catalyst", *J. Am. Chem. Soc.* **2012**, *134*, 18746–18757.

[276] L. Wu, I. Fleischer, R. Jackstell, I. Profir, R. Franke, M. Beller, "Ruthenium-catalyzed hydroformylation/reduction of olefins to alcohols: extending the scope to internal alkenes", *J. Am. Chem. Soc.* **2013**, *135*, 14306–14312.

[277] I. Fleischer, K. M. Dyballa, R. Jennerjahn, R. Jackstell, R. Franke, A. Spannenberg, M. Beller, "From olefins to alcohols: efficient and regioselective ruthenium-catalyzed domino hydroformylation/reduction sequence", *Angew. Chem., Int. Ed.* **2013**, *52*, 2949–2953.

[278] K. Takahashi, M. Yamashita, T. Ichihara, K. Nakano, K. Nozaki, "High-yielding tandem hydroformylation/hydrogenation of a terminal olefin to produce a linear alcohol using a Rh/Ru dual catalyst system", *Angew. Chem., Int. Ed.* **2010**, *49*, 4488–4490.

[279] D. G. Hanna, S. Shylesh, P. A. Parada, A. T. Bell, "Hydrogenation of butanal over silica-supported Shvo's catalyst and its use for the gas-phase conversion of propene to butanol via tandem hydroformylation and hydrogenation", *J. Catal.* **2014**, *311*, 52–58.

[280] H. Mutlu, M. A. R. Meier, "Castor oil as a renewable resource for the chemical industry", *Eur. J. Lipid Sci. Technol.* **2010**, *112*, 10–30.

[281] M. van der Steen, C. V. Stevens, "Undecylenic acid: a valuable and physiologically active renewable building block from castor oil", *ChemSusChem* **2009**, *2*, 692–713.

[282] O. Türünç, M. A. R. Meier, "The thiol-ene (click) reaction for the synthesis of plant oil derived polymers", *Eur. J. Lipid Sci. Technol.* **2013**, *115*, 41–54.

[283] X. Miao, C. Fischmeister, C. Bruneau, P. H. Dixneuf, J.-L. Dubois, J.-L. Couturier, "Tandem catalytic acrylonitrile cross-metathesis and hydrogenation of nitriles with ruthenium catalysts: direct access to linear alpha,omega-aminoesters from renewables", *ChemSusChem* **2012**, *5*, 1410–1414.

[284] M. Winkler, M. A. R. Meier, "Olefin cross-metathesis as a valuable tool for the preparation of renewable polyesters and polyamides from unsaturated fatty acid esters and carbamates", *Green Chem.* **2014**, *16*, 3335–3340.

[285] A. Behr, S. Toepell, S. Harmuth, "Cross-metathesis of methyl 10-undecenoate with dimethyl maleate. An efficient protocol with nearly quantitative yields", *RSC Adv.* **2014**, *4*, 16320–16326.

[286] C. Jimenez-Rodriguez, A. A. Nunez-Magro, T. Seidensticker, G. R. Eastham, M. R. L. Furst, D. J. Cole-Hamilton, "Selective formation of alpha, omega-ester amides from the aminocarbonylation of castor oil derived methyl 10-undecenoate and other unsaturated substrates", *Catal. Sci. Technol.* **2014**, *4*, 2332–2339.

[287] D. Quinzler, S. Mecking, "Linear semicrystalline polyesters from fatty acids by complete feedstock molecule utilization", *Angew. Chem., Int. Ed.* **2010**, *49*, 4306–4308.

[288] D. Prat, A. Wells, J. Hayler, H. Sneddon, C. R. McElroy, S. Abou-Shehada, P. J. Dunn, "CHEM21 selection guide of classical- and less classical-solvents", *Green Chem.* **2016**, *18*, 288–296.

[289] T. Gaide, J. M. Dreimann, A. Behr, A. J. Vorholt, "Overcoming Phase-Transfer Limitations in the Conversion of Lipophilic Oleo Compounds in Aqueous Media-A Thermomorphic Approach", *Angew. Chem., Int. Ed.* **2016**, *55*, 2924–2928.

[290] K. Kosswig, "Surfactants" in *Ullmann's Encyclopedia of Industrial Chemistry*, Wiley-VCH, Weinheim, Germany, **2000**.

[291] P. Roose, K. Eller, E. Henkes, R. Rossbacher, H. Höke, "Amines, Aliphatic" in *Ullmann's Encyclopedia of Industrial Chemistry*, Wiley-VCH, Weinheim, Germany, **2000**.

[292] D. Crozet, M. Urrutigoïty, P. Kalck, "Recent Advances in Amine Synthesis by Catalytic Hydroaminomethylation of Alkenes", *ChemCatChem* **2011**, *3*, 1102–1118.

[293] T. Rische, P. Eilbracht, "One-Pot Synthesis of Secondary and Tertiary Amines by Carbonylative Hydroaminomethylation of Alkenes Catalyzed by Di(μ-chloro)bis(η4-1,5-cyclooctadiene)dirhodium", *Synthesis* **1997**, *1997*, 1331–1337.

[294] D. S. Melo, S. S. Pereira-Júnior, E. N. dos Santos, "An efficient method for the transformation of naturally occurring monoterpenes into amines through rhodium-catalyzed hydroaminomethylation", *Appl. Catal., A* **2012**, *411-412*, 70–76.

[295] A. Behr, A. Wintzer, "Hydroaminomethylation of the Renewable Limonene with Ammonia in an Aqueous Biphasic Solvent System", *Chem. Eng. Technol.* **2015**, *38*, 2299–2304.

[296] K. C. d. Oliveira, A. G. Santos, E. N. dos Santos, "Hydroaminomethylation of eugenol with di-n-butylamine catalyzed by rhodium complexes. Bringing light on the promoting effect of Brönsted acids", *Appl. Catal., A* **2012**, *445-446*, 204–208.

[297] K. C. d. Oliveira, S. N. Carvalho, M. F. Duarte, E. V. Gusevskaya, E. N. dos Santos, J. E. Karroumi, M. Gouygou, M. Urrutigoïty, "Phospholes as efficient ancillaries for the rhodium-catalyzed hydroformylation and hydroaminomethylation of estragole", *Appl. Catal., A* **2015**, *497*, 10–16.

[298] A. Behr, S. Reyer, V. Manz, "Hydroaminomethylierung des Isoprens. Rückführung des homogenen Rhodiumkatalysators in wässrigen Zweiphasensystemen", *Chem. Ing. Tech.* **2012**, *84*, 108–113.

[299] A. Behr, D. Levikov, E. Nürenberg, "Rhodium-catalyzed hydroaminomethylation of cyclopentadiene", *RSC Adv.* **2015**, *5*, 60667–60673.

[300] C. M. Foca, H. V. Barros, E. N. dos Santos, E. V. Gusevskaya, J. Carles Bayón, "Hydroformylation of myrcene. Metal and ligand effects in the hydroformylation of conjugated dienes", *New J. Chem.* **2003**, *27*, 533–539.

[301] H. Barros, C. C. Guimarães, E. N. dos Santos, E. V. Gusevskaya, "Rhodium-Catalyzed Hydroformylation of Isoprene. Unusual Accelerating Effects of Phosphorus Ligands and Gas Pressure", *Organometallics* **2007**, *26*, 2211–2218.

[302] W. H. Clement, M. Orchin, "Hydroformylation of Terpenes", *Ind. Eng. Chem. Prod. Res. Dev.* **1965**, *4*, 283–286.

[303] S. Bertozzi, N. Campigli, G. Vitulli, R. Lazzaroni, P. Salvadori, "Selective hydroformylation of open-chain conjugated dienes promoted by mesitylene-solvated rhodium atoms to give β,γ unsaturated monoaldehydes", *J. Organomet. Chem.* **1995**, *487*, 41–45.

[304] S. Schmidt, E. Baráth, T. Prommnitz, T. Rosendahl, F. Rominger, P. Hofmann, "Synthesis and Characterization of Crotyl Intermediates in Rh-Catalyzed Hydroformylation of 1,3-Butadiene", *Organometallics* **2014**, *33*, 6018–6022.

[305] S. Schmidt, E. Baráth, C. Larcher, T. Rosendahl, P. Hofmann, "Rhodium-Catalyzed Hydroformylation of 1,3-Butadiene to Adipic Aldehyde. Revealing Selectivity and Rate-Determining Steps", *Organometallics* **2015**, *34*, 841–847.

[306] S. Oda, J. Franke, M. J. Krische, "Diene hydroaminomethylation via ruthenium-catalyzed C–C bond forming transfer hydrogenation. Beyond carbonylation", *Chem. Sci.* **2016**, *7*, 136–141.

[307] T. R. Savich, L. A. Goldblatt, "Process for Producing Myrcene from beta-Pinene", US 2507546, **1950**.

[308] A. Behr, L. Johnen, "Myrcene as a natural base chemical in sustainable chemistry: a critical review", *ChemSusChem* **2009**, *2*, 1072–1095.

[309] H. Barros, J. G. da Silva, C. C. Guimarães, E. N. dos Santos, E. V. Gusevskaya, "Hydroformylation of Monoterpenic Polyenes. Effect of the Conjugation of Double Bonds on Reactivity", *Organometallics* **2008**, *27*, 4523–4531.

[310] H. Barros, C. C. Guimarães, E. N. dos Santos, E. V. Gusevskaya, "Rhodium catalyzed hydroformylation of conjugated dienes. Remarkable accelerative effect of triphenylphosphine", *Catal. Commun.* **2007**, *8*, 747–750.

[311] P. Neubert, S. Fuchs, A. Behr, "Hydroformylation of piperylene and efficient catalyst recycling in propylene carbonate", *Green Chem.* **2015**, *17*, 4045–4052.

[312] P. W. N. M. van Leeuwen, C. F. Roobeek, "The hydroformylation of butadiene catalysed by rhodium-diphosphine complexes", *J. Mol. Catal. A: Chem.* **1985**, *31*, 345–353.

[313] A. Behr, D. Levikov, D. Vogelsang, "First rhodium-catalyzed hydroformylation of cyclopentadiene", *J. Mol. Catal. A: Chem.* **2015**, *406*, 114–117.

[314] S. N. Renninger, Mephee J D, "Fuel Compositions Comprising Farnesane and Farnesene Derivates and Method of Making and Using Same", US 7399323 B2, **2008**.

[315] T. F. Tadros, "An introduction to surfactants", De Gruyter, Boston, **2014**.

[316] T. Gaide, A. Behr, M. Terhorst, A. Arns, F. Benski, A. J. Vorholt, "Katalysatorvergleich bei der Hydroesterifizierung von 10-Undecensäuremethylester in thermomorphen Lösungsmittelsystemen", *Chem. Ing. Tech.* **2016**, *88*, 158–167.

[317] R. Vilar, D. M. P. Mingos, C. J. Cardin, "Synthesis and structural characterisation of [$Pd_2(\mu\text{-}Br)_2(PBu^t_3)_2$], an example of a palladium(I)–palladium(I) dimer", *J. Chem. Soc., Dalton Trans.* **1996**, *25*, 4313–4314.

[318] D. M. Ohlmann, N. Tschauder, J.-P. Stockis, K. Gooßen, M. Dierker, L. J. Gooßen, "Isomerizing Olefin Metathesis as a Strategy To Access Defined Distributions of Unsaturated Compounds from Fatty Acids", *J. Am. Chem. Soc.* **2012**, *134*, 13716–13729.

[319] S. Baader, P. E. Podsiadly, D. J. Cole-Hamilton, L. J. Goossen, "Synthesis of tsetse fly attractants from a cashew nut shell extract by isomerising metathesis", *Green Chem.* **2014**, *16*, 4885–4890.

[320] S. Baader, D. M. Ohlmann, L. J. Goossen, "Isomerizing ethenolysis as an efficient strategy for styrene synthesis", *Chem. - Eur. J.* **2013**, *19*, 9807–9810.

[321] L. Gooßen, M. Arndt, P. Mamone, Gruenberg, "Method for the preparation of palladium(i) tri-tert-butylphosphine bromide dimer and process for its use in isomerization reactions", WO 2013000874 A1, **2013**.

[322] P. Mamone, M. F. Gruenberg, A. Fromm, B. A. Khan, L. J. Goossen, "Pd(μ-Br)(P(t)Bu_3)$_2$ as a highly active isomerization catalyst: synthesis of enol esters from allylic esters", *Org Lett.* **2012**, *14*, 3716–3719.

[323] A. Jörke, A. Seidel-Morgenstern, C. Hamel, "Rhodium-BiPhePhos catalyzed hydroformylation studied by operando FTIR spectroscopy. Catalyst activation and rate determining step", *J. Mol. Catal. A: Chem.* **2017**, *426*, 10–14.

[324] C. Li, L. Chen, M. Garland, "Synchronicity of Mononuclear and Dinuclear Events in Homogeneous Catalysis. Hydroformylation of Cyclopentene Using $Rh_4(CO)_{12}$ and $HRe(CO)_5$ as Precursors", *J. Am. Chem. Soc.* **2007**, *129*, 13327–13334.

[325] R. Kuhlmann, S. Schmitz, K. Haßmann, A. Prüllage, A. Behr, "Synthesis of N,N- dimethylformamide from carbon dioxide in aqueous biphasic solvent systems", *Appl. Catal., A* **2017**, *539*, 90–96.

[326] D. Prat, O. Pardigon, H.-W. Flemming, S. Letestu, V. Ducandas, P. Isnard, E. Guntrum, T. Senac, S. Ruisseau, P. Cruciani, P. Hosek, "Sanofi's Solvent Selection Guide. A Step Toward More Sustainable Processes", *Org. Process Res. Dev.* **2013**, *17*, 1517–1525.

[327] K. Alfonsi, J. Colberg, P. J. Dunn, T. Fevig, S. Jennings, T. A. Johnson, H. P. Kleine, C. Knight, M. A. Nagy, D. A. Perry, M. Stefaniak, "Green chemistry tools to influence a medicinal chemistry and research chemistry based organisation", *Green Chem.* **2008**, *10*, 31–36.

[328] R. K. Henderson, C. Jiménez-González, D. J. C. Constable, S. R. Alston, G. G. A. Inglis, G. Fisher, J. Sherwood, S. P. Binks, A. D. Curzons, "Expanding GSK's solvent selection guide – embedding sustainability into solvent selection starting at medicinal chemistry", *Green Chem.* **2011**, *13*, 854.

7. Appendix

7.1 Supporting Information to Chapter 4.3

7.1.1. Experimental Procedure for the Continuously-Operated Mini-plant

The Ligand (SulfoXantphos) and the catalyst precursor ($Rh(acac)(CO)_2$) were dissolved in degassed water at a molar ratio of 1:5 ($m_{Rh(acac)(CO)_2}$=71 mg, $m_{SulfoXantphos}$=1071 mg) and transferred to the miniplant reactor using the standard Schlenk technique. The reactor was then heated to the reaction temperature (T_R=140 °C) and the decanter was cooled to the separation temperature (T_S=5 °C). The miniplant was simultaneously pressurized with 20 bar synthesis gas (CO/H_2=1:1). As soon as the desired reaction conditions were achieved, the reactor was continuously fed with the substrate solution ($\dot{V}$=60 mL/h, $m_{UME}/m_{n\text{-Butanol}}$=31.5/68.5). The startup is finished after the hold-up (V_{ges}=790 mL) of the miniplant was completely filled and the product solution was continuously discharged from the process, which denotes the starting point (t=0) in Figure 4.23.

7.1.2. Gas Chromatography

To examine samples *via* gas chromatography, a Hewlett Packard 6890 Series GC System gas chromatograph was used, which is equipped with a thermal conductivity detector, a flame ionization detector and a Hewlett Packard Innowax column (30 m x 0.25 mm x 0.25 µm). The injection volume was 1 µL, the split ratio is 1:200. Helium was used as carrier gas with a flow of 1.3 mL/min. The starting temperature of the oven was 40 °C. After one minute the temperature was increased to 155 °C with a rate of 7 °C/min. The temperature was then increased to 250 °C at a rate of 20 °C/min. This temperature was maintained for five minutes. The external standard quantification method was used.

7.1.3. ICP-OES

An Iris Intrepid ICP (Thermo Elemental) was used to determine of the rhodium and phosphorous content in both phases. For this, 0.23 g of a sample were measured out in a Teflon cup and 2.5 mL nitric acid (65%) and 4 mL sulfuric acid (96%) were added. The digestion process was conducted in a MWS µPrep start-system microwave (MLS). Upon

completion of the digestion process, the samples were treated with 2 ml double-distilled water and 1 mL of H_2O_2 (Fisher Scientific, Optima grade, phosphorous free). The prepared samples were allowed to rest for twelve hours before measurement.

7.1.4. Process Chart

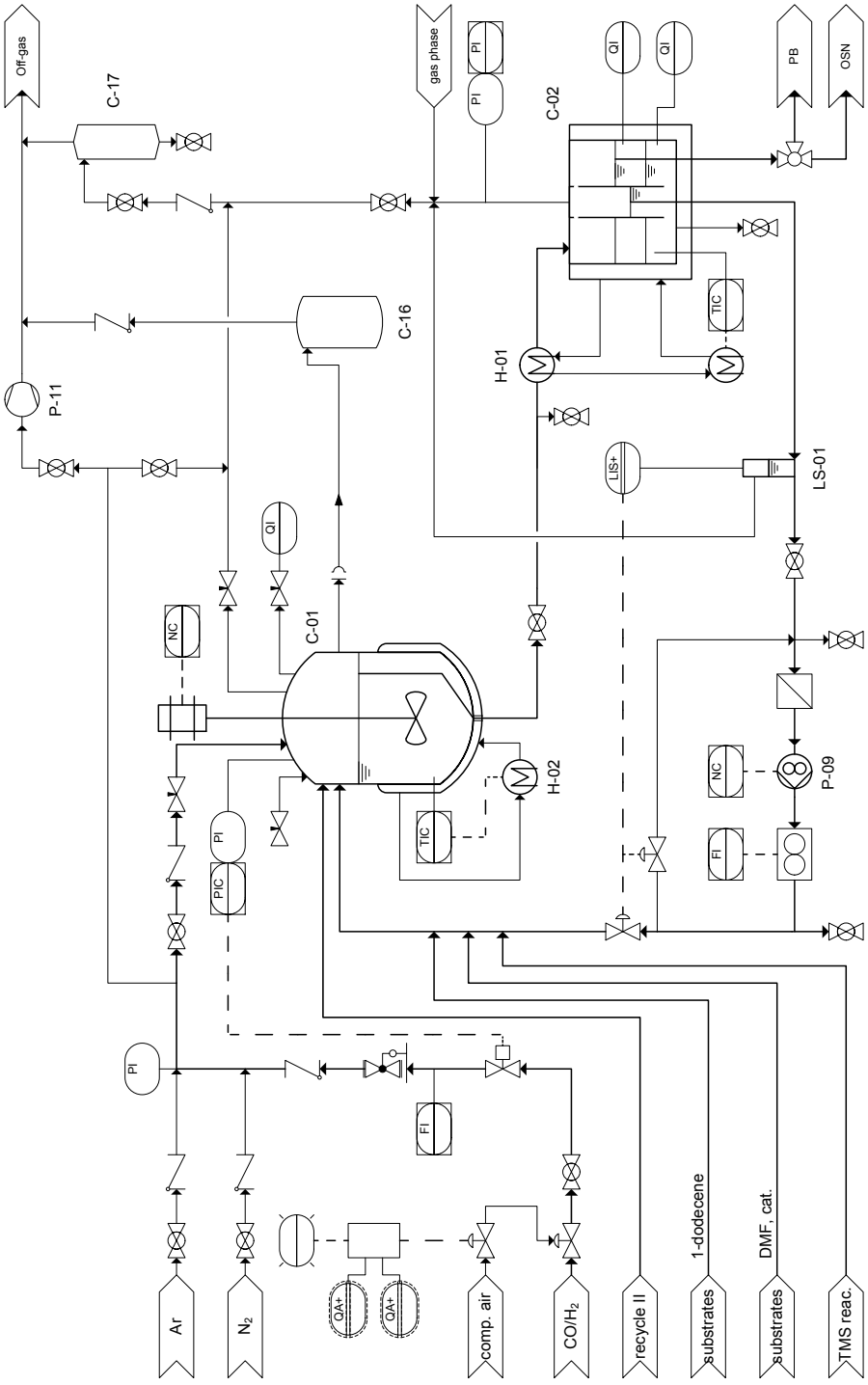

Figure 7.1: Process chart for the continuously operated hydroformylation miniplant.

.

7.1.5. Product Isolation

A discontinuous hydroformylation was transduced to isolate the linear hydroformylation product. Afterwards, the phases were separated and the product was separated from the 1-butanol phase by removing the solvent under reduced pressure *via* a rotary evaporator. The crude product was purified with a Kugelrohr at a reduced pressure of 0.8 mbar and a temperature of 140 °C.

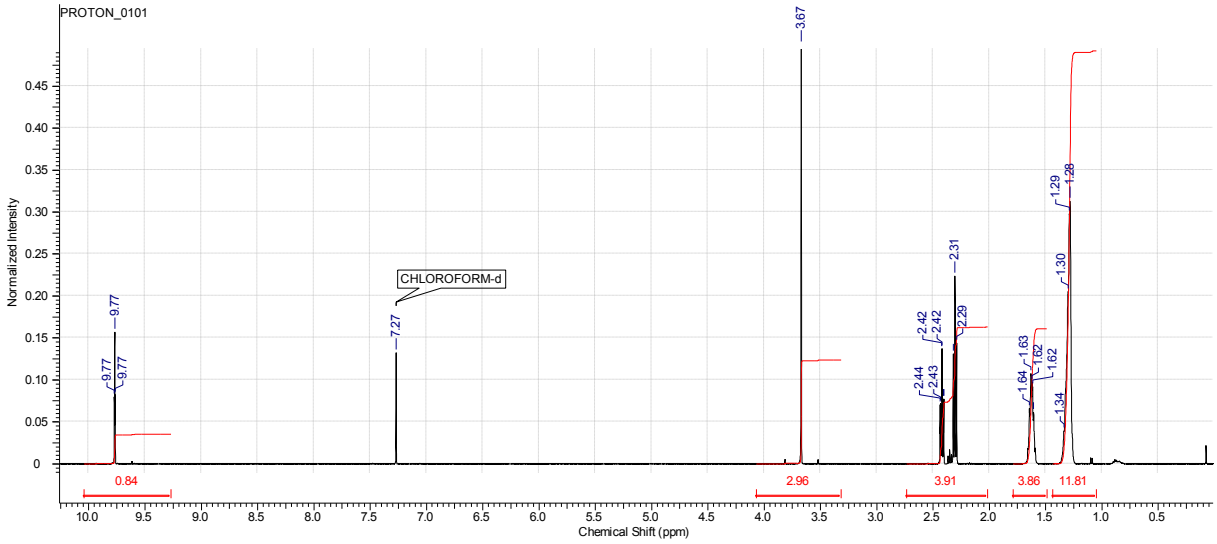

Figure 7.2: 1-H NMR of the linear hydroformylation product (**2**).

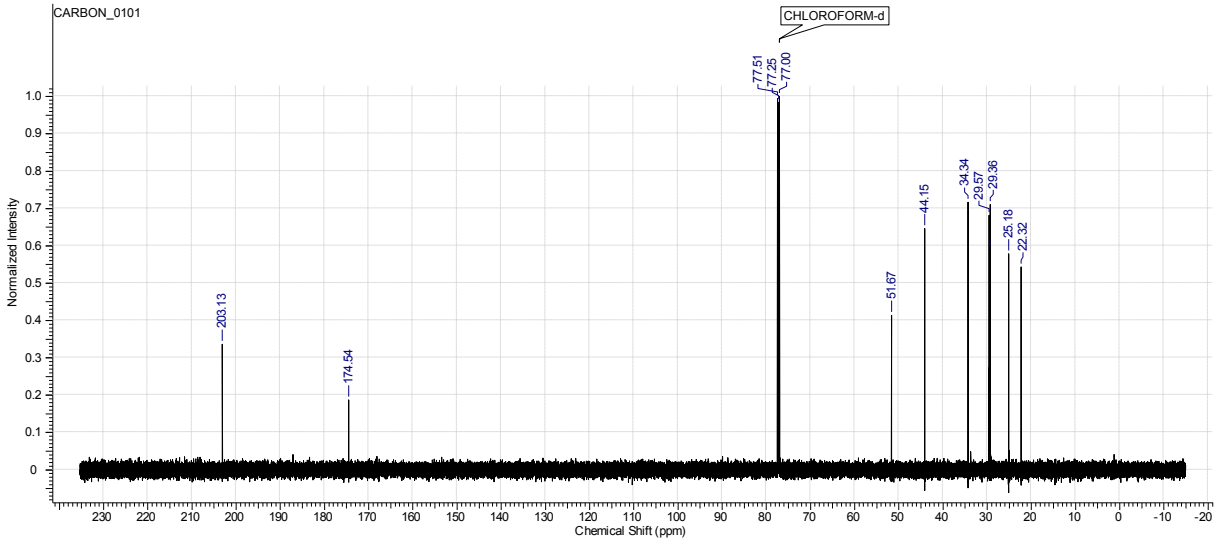

Figure 7.3: 13-C NMR of the linear hydroformylation product (**2**).

7.1.6. Additional Investigations on the Influence of the Substrate Concentration on the Reaction Rates and Catalyst Preforming (not published)

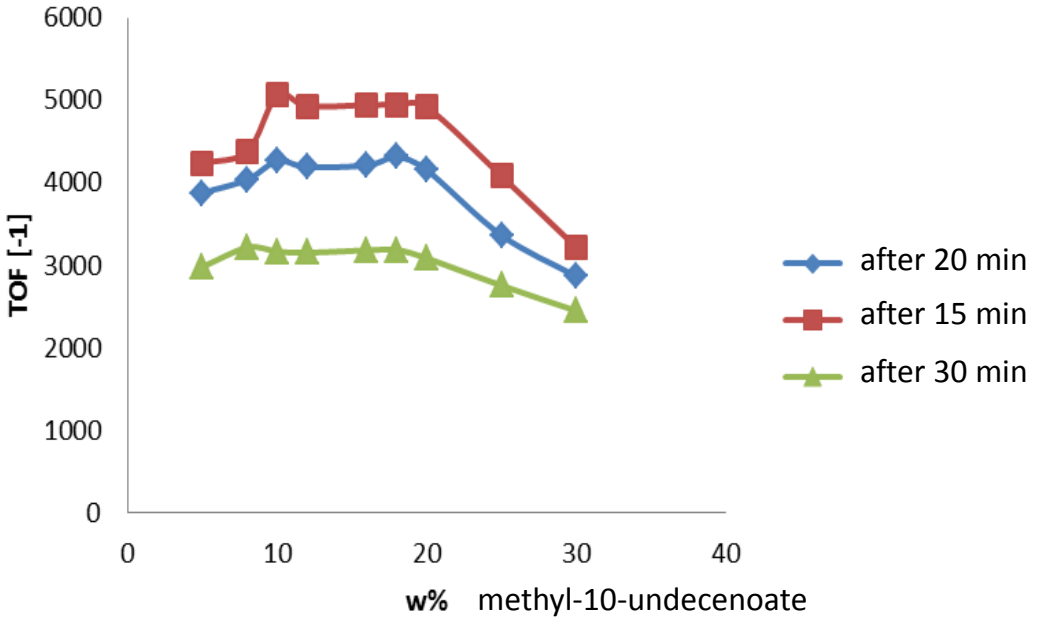

Figure 7.4: Turnover frequencies at different substrate concentrations.
Conditions: n(Rh)/n(methyl 10-undecenoate) = 1:2000, n(Rh)/n(P) = 1:10, p = 20 bar, T = 140 °C, CO/H2 = 1, w(water)/w(1-butanol) = 1:1, $Rh(acac)(CO)_2$, Sulfoxantphos. The catalyst was preformed *via* heating precursor and ligand in water to 140 °C prior addition of 1-butanol and substrate.

The reaction mixture was biphasic at a concentration of methyl 10-undecenoate >5%.

Catalyst preforming under 140 °C and 5 bar synthesis gas for 10 minutes lead to an improved catalytic performance yielding in 86% of the linear aldehyde and a *l/b* ratio of 96/4 after one hour.

7.2. Supporting Information to Chapter 4.6

7.2.1. Preparation of Methyl 12-hydroxydodecanoate

Under air with a flow of argon, a 300 mL stainless steel autoclave was filled with $Rh(CO)_2acac$ (53.9 mg, 0.209mmol), Biphephos (328 mg, 0.418 mmol), $Ru_3(CO)_{12}$ (222 mg, 0.523 mmol Ru) and tetraphenylcyclopentadienone (402 mg, 0.523 mmol). The autoclave was sealed, and then flushed four times with 5 bar of argon. Isopronanol (30 mL) and methyl 10-undecenoate (5 mL, 20.9 mmol) were introduced using a syringe. The autoclave pressurized with syngas (40 bar) and heated up to 150 °C for 60 minutes (stirring bar: 500 rpm). After 60 minutes the autoclave was cooled down to room temperature.

7.2.2. Methodology for the Recycling Experiment

The remaining syngas was removed and the autoclave purged three times with 5 bar of argon. Using the argon pressure, the crude reaction mixture was extracted from the autoclave *via* canola and introduced into a crystalliser. The mixture was continuously mechanically stirred under an inert atmosphere of argon. The temperature of the mixture was decreased using a cryostat until crystals stopped to form. The temperature decrease profiles for the initial reaction and the two following recycling experiments are depicted in Figure 7.5 to Figure 7.7. The crystallisation starts when the temperature slightly increases after 3900 s.

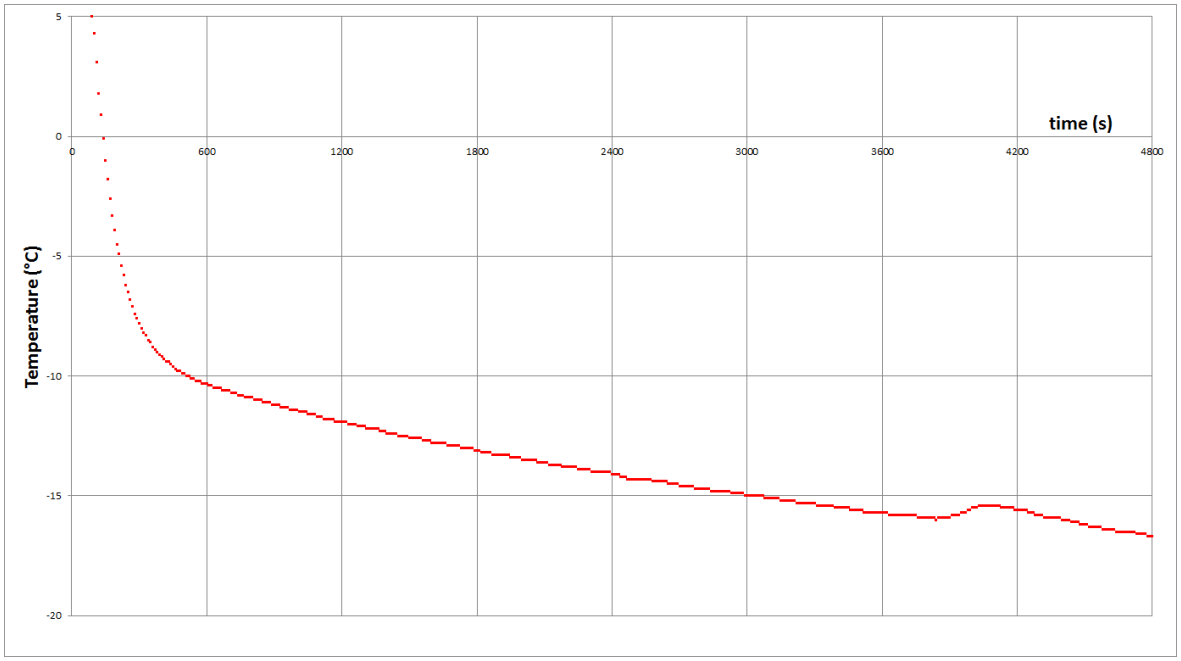

Figure 7.5: Decrease in temperature of the first crude mixture.

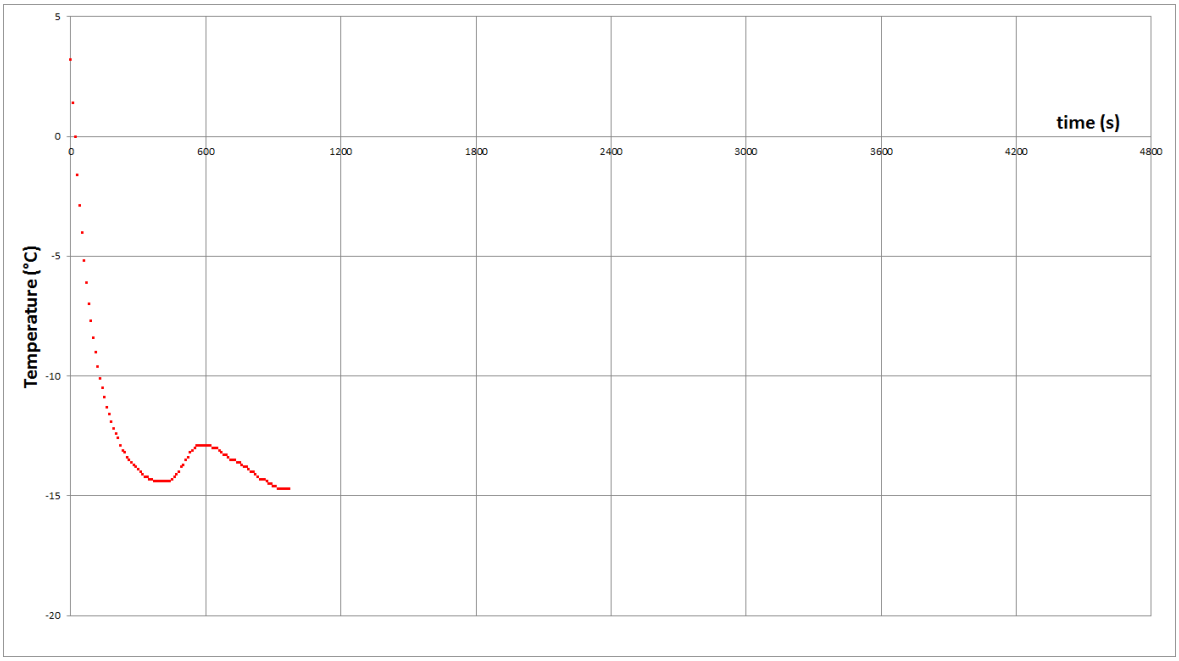

Figure 7.6: Decrease in temperature of the first recycled mixture.

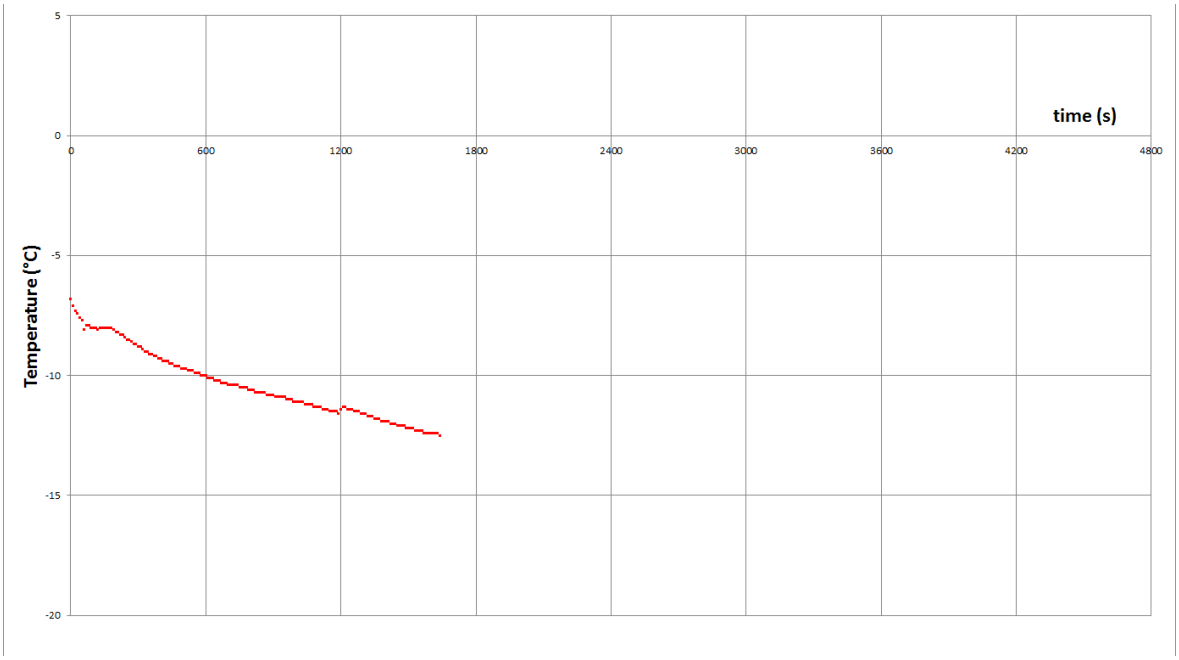

Figure 7.7: Decrease in temperature of the second recycled mixture.

After crystallisation occurred, the mixture was filtered through a frit glass. The liquid phase was recovered under argon. 5 mL of methyl 10-undecenoate were added to the mixture, and the overall liquid phase was reintroduced in the autoclave (previously set under vacuum) *via* canola. The autoclave was heated up to 150 °C for 60 minutes, and then cooled down to room temperature. The recycling process was then repeated once again.

7.2.3. Methodology for an Optimised Crystallisation:

Under air with a flow of argon, a 300 mL stainless steel autoclave was filled with $Rh(CO)_2acac$ (53.9 mg, 0.209 mmol), Biphephos (328 mg, 0.418 mmol), $Ru_3(CO)_{12}$ (222 mg, 0.523 mmol Ru) and tetraphenylcyclopentadienone (402 mg, 0.523 mmol). The autoclave was sealed, and then flushed four times with 5 bar of argon. Isopronanol (30 mL) and methyl 10-undecenoate (5 mL, 20.9 mmol) were introduced using a syringe. The autoclave was pressurised with syngas (40 bar) and heated up to 150°C for 60 minutes (stirring bar: 500 rpm). After 60 minutes the autoclave was cooled down to room temperature. The autoclave is opened and the crude mixture is introduced into a crystalliser under air. The mixture is let to stabilise at -5°C and then cooled down. The temperature decreases according to the following ramps:

- -5 °C to -11 °C in 60' (6 °C/h)
- -11 °C to -15 °C in 120' (2 °C/h)
- -15 °C to -20 °C in 30' (10 °C/h)

The desired temperature and the real measured temperatures are depicted in Figure 7.8.

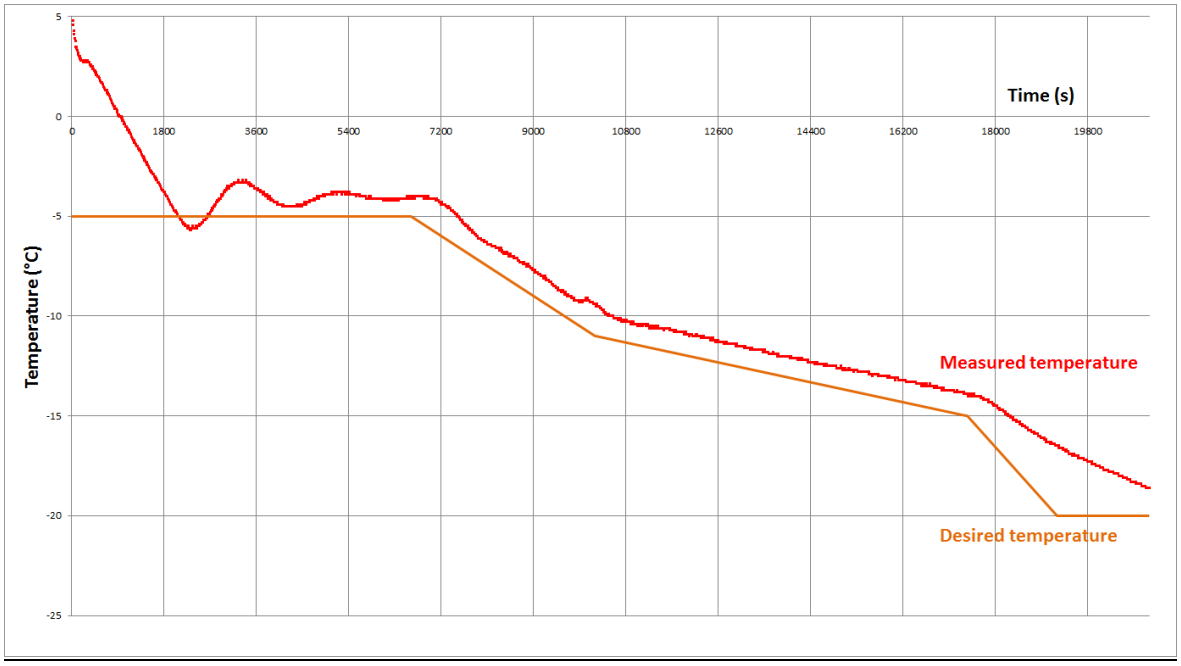

Figure 7.8: Desired and measured temperatures.

7.2.4. Conversion *vs* Time Experiments: Methodology

7.2.4.1. Hydrogenation of Methyl 12-oxododecanoate to Methyl 12-hydroxydodecanoate with *in situ* Shvo's Catalyst

Under air with a flow of argon, a 300 mL stainless steel autoclave was filled with $Ru_3(CO)_{12}$ (46.5 mg, 0.22 mmol Ru) and tetraphenylcyclopentadienone (88.5 mg, 0.22 mmol). The autoclave was sealed, and then flushed two times with 5 bar of argon, and then put under vacuum. Toluene (100 mL) and methyl 12-oxododecanoate (5 g = 5.25 mL, 21.9 mmol) were introduced *via* canola. The autoclave was pressurised with hydrogen (10 bar). The hydrogen pressure was maintained at 10 bar for the whole experiment. The mixture was mechanically stirred at 500 rpm. The heather was switched on and the autoclave was heated up to 150 °C. The sampling was achieved using a canola. The first sample was taken after 10 minutes (T = 135 °C). The following samples were taken every five minutes for 35 minutes. The desired 150 °C were achieved at the 20th minute.

7.2.4.2. Hydrogenation of Methyl 12-oxododecanoate to Methyl 12-hydroxydodecanoate with *ex situ* Shvo's Catalyst

Under air with a flow of argon, a 300 mL stainless steel autoclave was filled with Shvo's catalyst (118.8 mg, 0.22 mmol Ru). The autoclave was sealed, and then flushed two times with 5 bar of argon, and then put under vacuum. Toluene (100 mL) and methyl 12-oxododecanoate (5 g = 5.25 mL, 21.9 mmol) were introduced *via* canola. The autoclave was pressurised with hydrogen (10 bar). The hydrogen pressure was maintained at 10 bar for the whole experiment. The mixture was mechanically stirred at 500 rpm. The heather was switched on and the autoclave was heated up to 150 °C. The sampling was achieved using a canola. The first sample was taken after 10 minutes (T = 150 °C). The following samples were taken every five minutes for 35 minutes.

7.2.4.3. Hydroformylation Followed by Hydrogenation of Methyl 10-undecenoate to Methyl 12-hydroxydodecanoate with *in situ* Shvo's Catalyst

Under air with a flow of argon, a 300 mL stainless steel autoclave was filled with $Ru_3(CO)_{12}$ (46.5 mg, 0.22 mmol Ru), tetraphenylcyclopentadienone (88.5 mg, 0.22 mmol), $Rh(CO)_2$acac (56.5 mg, 0.22 mmol), biphephos (344.6 mg, 0.44 mmol). The autoclave was sealed, and then flushed two times with 5 bar of argon, and then put under vacuum. Toluene (100 mL) and methyl 10-undecenoate (5 g = 5.30 mL, 21.9 mmol) were introduced *via* canola. The autoclave was pressurised with syngas (20 bar). The syngas pressure was maintained at 20 bar for the whole experiment. The mixture was mechanically stirred at 500 rpm. The heather was switched on and the autoclave was heated up to 150 °C. The sampling was achieved using a canola. The first sample was taken after 5 minutes (T = 68 °C). The following samples were taken every five minutes until the 60th

minutes, then at 90, 150 and 180minutes. The desired 150 °C were achieved at the 15th minute.

7.2.4.4. Hydroformylation Followed by Hydrogenation of Methyl 10-undecenoate to Methyl 12-hydroxydodecanoate with *ex situ* Shvo's catalyst

Under air with a flow of argon, a 300 mL stainless steel autoclave was filled with Shvo's catalyst (118.8 mg, 0.22 mmol Ru), $Rh(CO)_2acac$ (56.5 mg, 0.22 mmol), biphephos (344.6 mg, 0.44 mmol). The autoclave was sealed, and then flushed two times with 5 bar of argon, and then put under vacuum. Toluene (100 mL) and methyl 10-undecenoate (5 g = 5.30 mL, 21.9 mmol) were introduced *via* canola. The autoclave was pressurised with syngas (20 bar). The syngas pressure was maintained at 20 bar for the whole experiment. The mixture was mechanically stirred at 500 rpm. The heather was switched on and the autoclave was heated up to 150°C. The sampling was achieved using a canola. The first sample was taken after 5 minutes (T = 58 °C). The following samples were taken every five minutes until the 60th minutes, then at 90, 150 and 180minutes. The desired 150 °C were achieved at the 20th minute.

7.2.4.5. Conversion *vs* Time experiments: plots

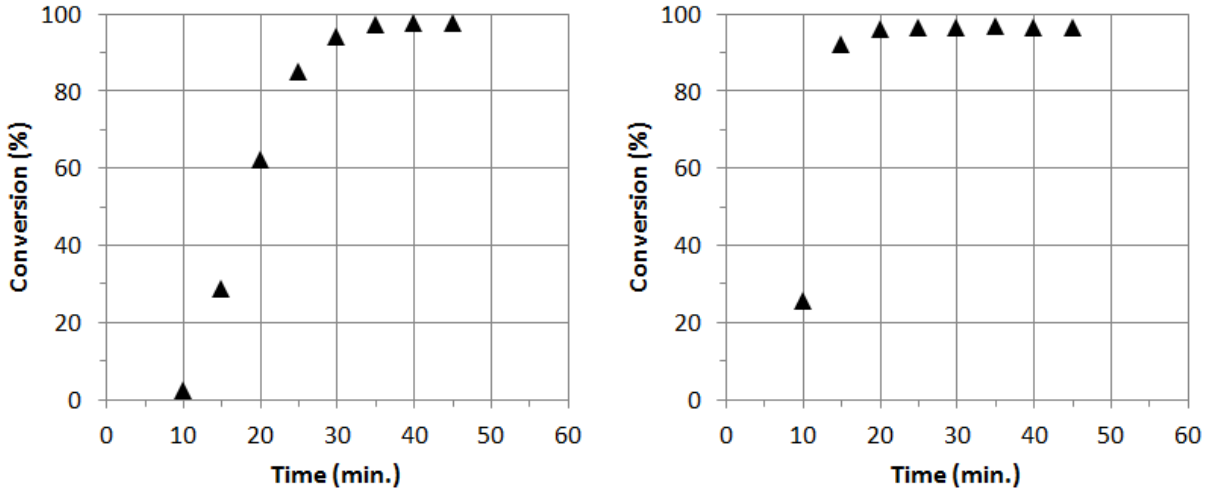

Figure 7.9 (left) Hydrogenation of methyl 12-oxododecanoate to methyl 12-hydroxydodecanoate using *in situ* Shvo's catalyst.
Figure 7.9 (right) Hydrogenation of methyl 12-oxododecanoate to methyl 12-hydroxydodecanoate using *ex situ* Shvo's catalyst.

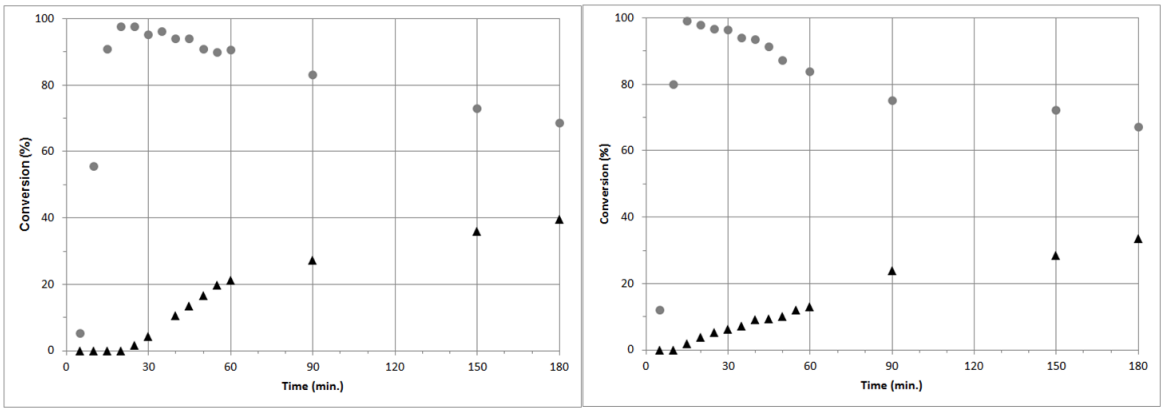

Figure 7.10: (left) Hydroformylation and hydrogenation of methyl 10-undecenoate to methyl 12-hydroxydodecanoate using *in situ* Shvo's catalyst.
Figure 7.11: (right) Hydroformylation and hydrogenation of methyl 10-undecenoate to methyl 12-hydroxydodecanoate using *ex situ* Shvo's catalyst.

7.2.4.6. Preparation of 12-hydroxydodecanoic Acid and its Derivatization:

Preparation: under air with a flow of argon, a 300 mL stainless steel autoclave was filled with $Rh(CO)_2acac$ (53.9 mg, 0.209mmol), Biphephos, 328 mg, 0.418 mmol, $Ru_3(CO)_{12}$ (111 mg, 0.262 mmol Ru), tetraphenylcyclopentadienone (201 mg, 0.262 mmol) and 10-undecenoic acid (3851 mg, 20.9 mmol). The autoclave was sealed, and then flushed four times with 5 bar of argon. Isopronanol (30 mL) was introduced using a syringe. The autoclave was pressurized with syngas (40 bar) and heated up to 150 °C for 120 minutes (stirring bar: 500 rpm).

Derivatization: The procedure was followed from the one from Sigma Aldrich designed for the analysis of carboxylic acids using GC. The overall mixture was introduced into a round-bottom flask. 250 mg of the solid mixture was sampled into a Schlenk flask. 20 mL of a mixture BCl3/MeOH was added and put to the boil for 10 minutes. Water (10 mL) and dichloromethane (10 mL) were added and the mixture stirred. The mixture was left to settle for a few minutes and the organic phase was extracted and dried with sodium sulfate. A sample was taken for GC-FID.

7.2.4.7. Preparation of 1,12-dodecanediol:

Under air with a flow of argon, a 300 mL stainless steel autoclave was filled with Rh(CO)2acac (53.9 mg, 0.209mmol), Biphephos, 328 mg, 0.418 mmol, Ru3(CO)12 (111 mg, 0.262 mmol Ru), tetraphenylcyclopentadienone (201 mg, 0.262 mmol) and 10-undecen-1-ol (3559 mg, 20.9 mmol). The autoclave was sealed, and then flushed four times with 5 bar of argon. Isopronanol (30 mL) was introduced using a syringe. The auto-

clave was pressurized with syngas (40 bar) and heated up to 150 °C for 90 minutes (stirring bar: 500 rpm)

7.2.5. NMRs of Methyl 12-hydroxydodecanoate and Methyl 12-oxododecanoate

^{1}H NMR of methyl 12-hydroxydodecanoate:

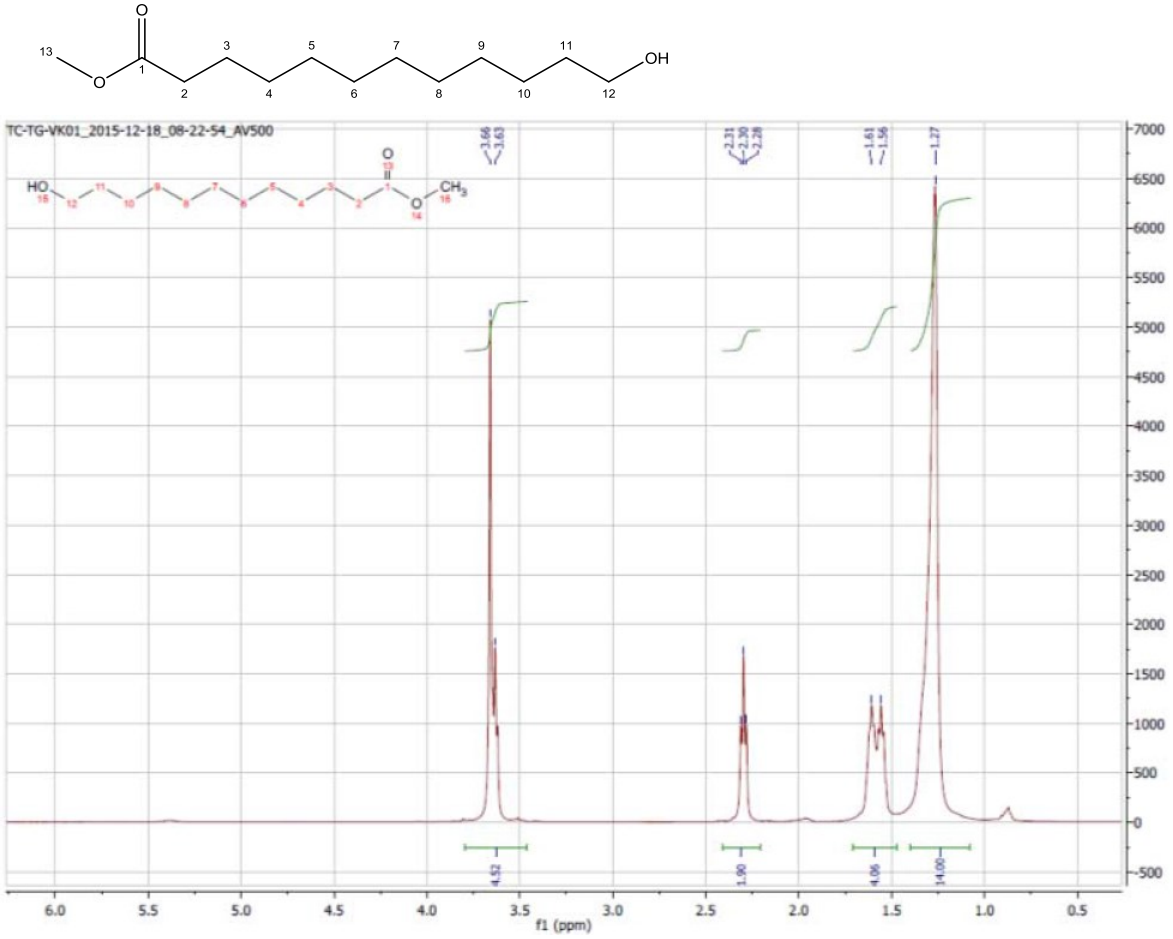

^{1}H NMR (500 MHz, CDCl3): δ(ppm) = 1.27 (m, 14H, C(4)H_2 - C(10)H_2), 1.56-1.61 (m, 4H, C(3)H_2, C(11)H_2), 2.28-2.31 (t,3JHH = 7.6 Hz, 2H, C(2)H_2), 3.63 (t, 3JHH = 6.6 Hz, 2H, C(12)H_3), 3.66 (m, 3H, C(13)H_2).

- ^{13}C NMR of methyl 12-hydroxydodecanoate:

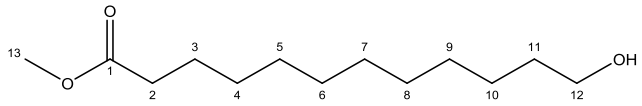

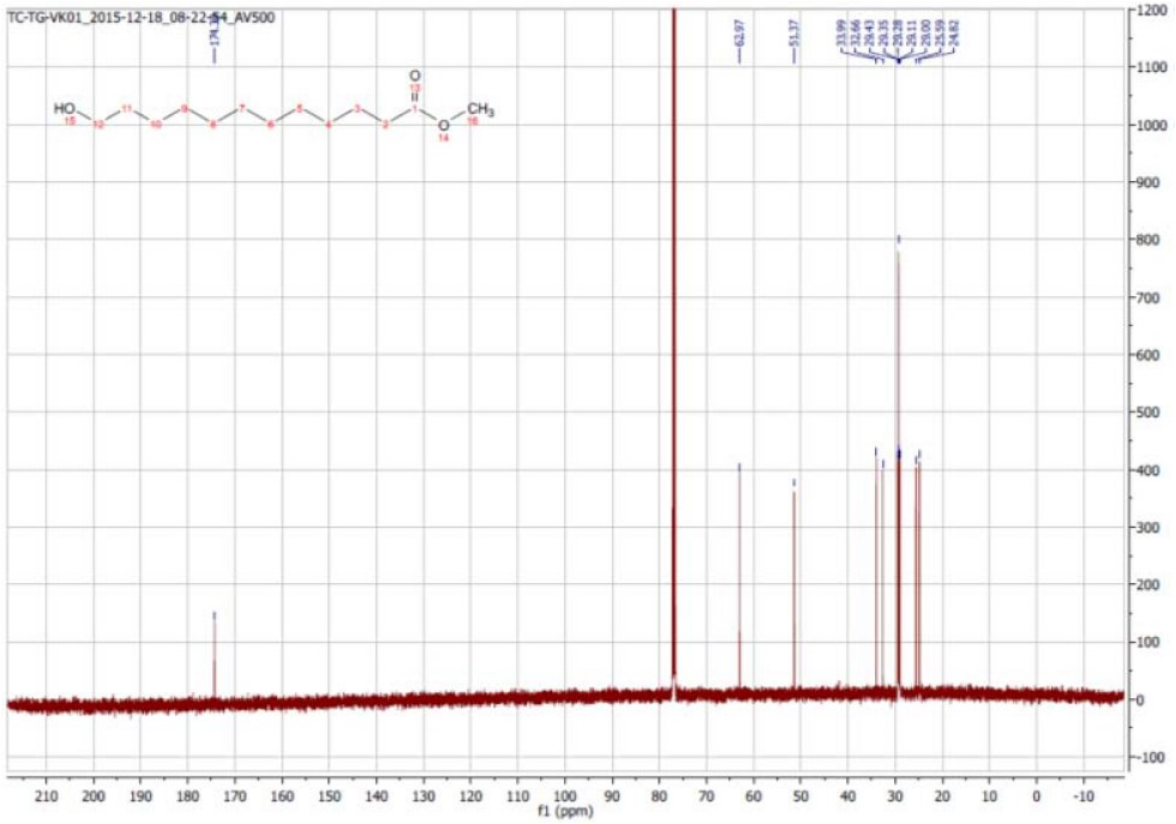

^{13}C NMR (100 MHz, CDCl3) δ(ppm) = 22.32 (s, C(3)H_2), 25.18 (s, C(10)H_2), 28.78 - 30.03 (m, C(4)H_2 - C(13)H_2), 34.34 (s, C(2)H_2), 44.15 (s, C(11)H_2), 51.67 (s, C(13)H_3), 174.54 (s, C(1)), 203.13 (s, C(12)).

7.2.6. Recycling Experiments: FIDs and ICPs Analyses

Main compounds: **1** methyl 10-undecanoate; **2** methyl undecenoate isomers; **3** methyl 12-oxododecanoate; **4** methyl 11-hydroxydodecanoate; **5** methyl 12-hydroxydodecanoate

First reaction crude mixture:

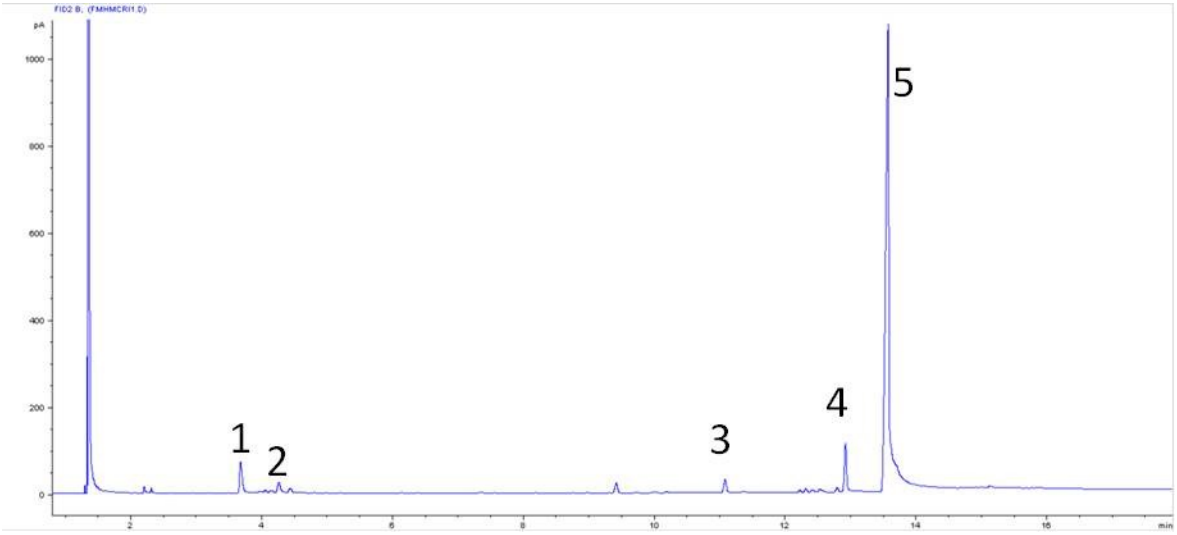

First reaction crude mixture:

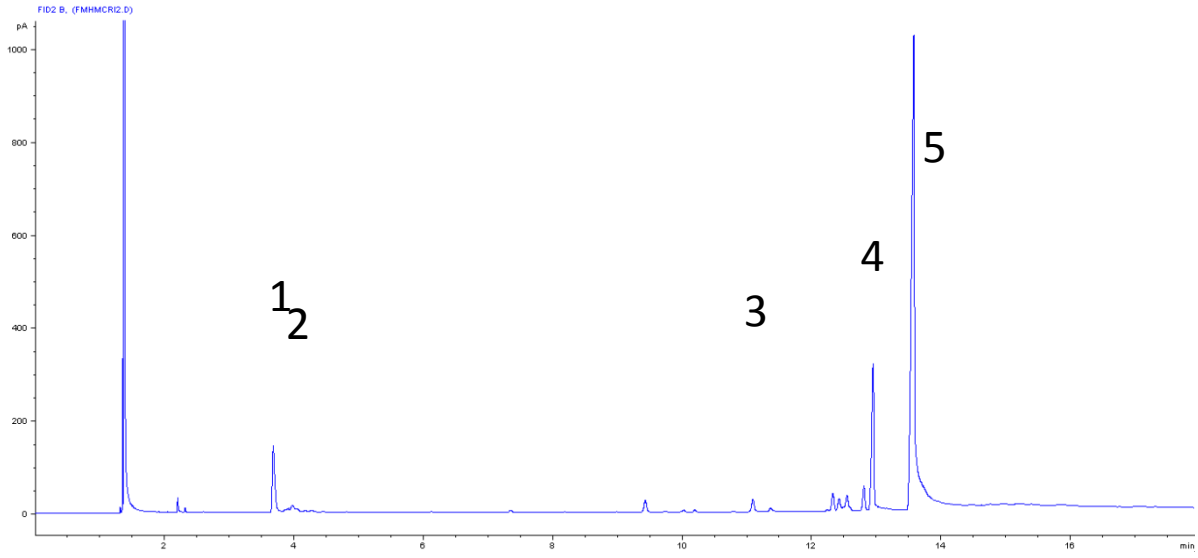

Second recycling crude mixture:

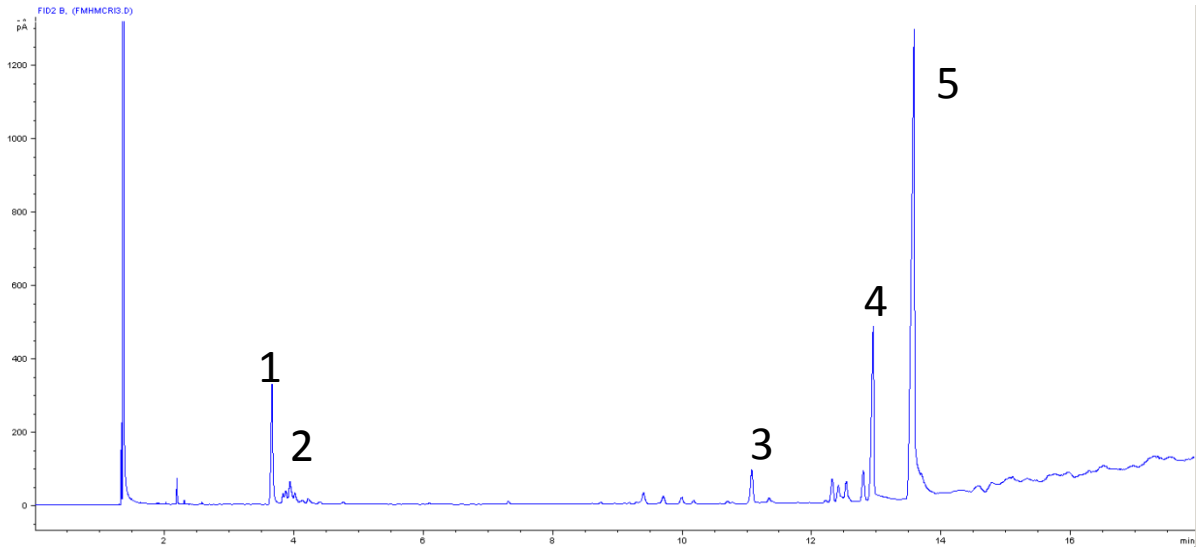

Third recycling crude mixture:

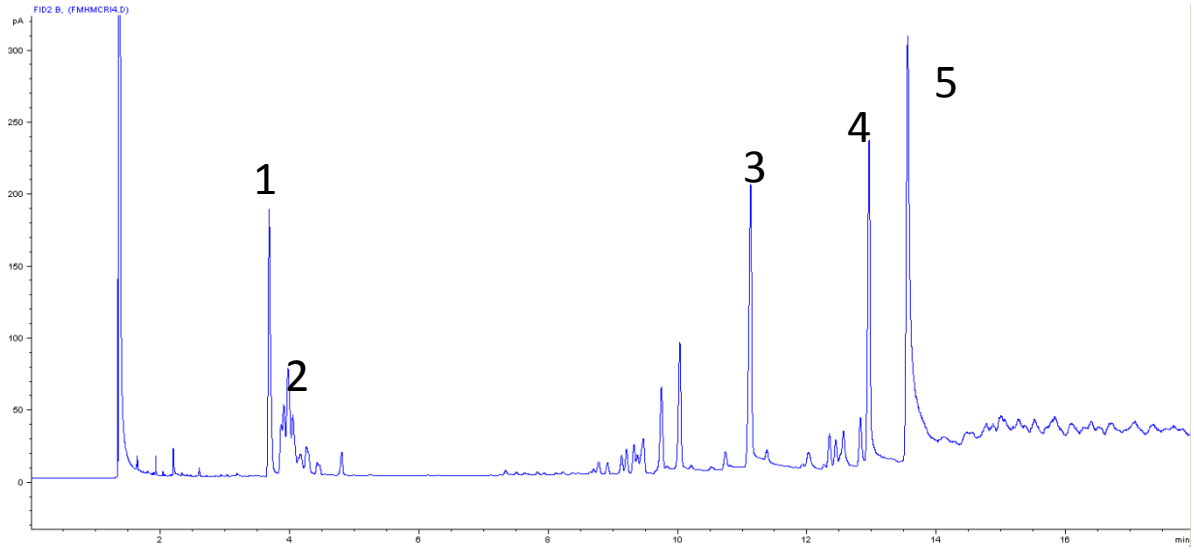

ICP analysis (Rh content):

Datenblatt Rhodium ICP - Proben

Name:	Marc Furst
Probenbezeichnung:	s. u.
Ausgeführt von:	Iris Henkel
Ausgeführt am:	30.01.2017

Probenbez.	FMCC002/1	FMCC002/2	FMCRI1_2/1	FMCRI1_2/2	FMCRI2_2/1	FMCRI2_2/2	FMCRI2_3/1	FMCRI2_3/2
Rh_3396	**0,1880**	**0,1908**	**0,5278**	**0,5635**	**0,2257**	**0,2055**	**0,0142**	**0,0119**
Rh_3434	**0,1917**	**0,1944**	**0,5411**	**0,5648**	**0,2257**	**0,2133**	**0,0094**	**0,0053**
Rh_3657	**0,2070**	**0,2293**	**0,5523**	**0,5800**	**0,2483**	**0,2323**	**0,0308**	**0,0240**
MW (ppm)	0,196	0,205	0,540	0,569	0,233	0,217	0,018	0,014
Verd. Faktor	68,985	71,924	70,975	65,213	62,779	73,468	69,211	65,423
Konz. (ppm)	**13**	**15**	**38**	**37**	**15**	**16**	**1**	**1**
MW (ppm)		**14**		**38**		**15**		**1**

Sample FMCC002 57.6 mg solubilised in isopropanol, weight of sample 1077.2 mg: 261 ppm (0.7 mg Rh in 2762.3 mg of product).

ICP analysis (Ru content):

Datenblatt Ruthenium ICP - Proben

Name:	Marc Furst
Probenbezeichnung:	s. u.
Ausgeführt von:	Iris Henkel
Ausgeführt am:	30.01.2017

Probenbez.	FMCC002/1	FMCC002/2	FMCRI1_2/1	FMCRI1_2/2	FMCRI2_2/1	FMCRI2_2/2	FMCRI2_3/1	FMCRI2_3/2
Ru2402	**0,437**	**0,4436**	**0,5231**	**0,5495**	**0,1707**	**0,1624**	**0,0253**	**0,0331**
Ru2678	**0,4318**	**0,4407**	**0,5278**	**0,5614**	**0,1655**	**0,1499**	**0,0186**	**0,0276**
MW (ppm)	0,434	0,442	0,525	0,555	0,168	0,156	0,022	0,030
Verd. Faktor	68,985	71,924	70,975	65,213	62,779	73,468	69,211	65,423
Konz. (ppm)	**30**	**32**	**37**	**36**	**11**	**11**	**2**	**2**
MW (ppm)		**31**		**37**		**11**		**2**

Sample FMCC002 57.6 mg solubilised in isopropanol, weight of sample 1077.2 mg: 579 ppm (1.6 mg Ru in 2762.3 mg of product).

7.3. Supporting Information to Chapter 4.7

The supporting information of this chapter contains 93 pages and is available online under the following DOI: 10.1002/cctc.201700097

7.4. Supporting Information to Chapter 4.8

CHEMICALS

Toluene (Acros Organics, >99%), ethyl acetate (Acros Organics, >99%), cyclohexane (Acros Organics, >99%), methyl 3-hexenoate (TCI Chemicals, >98%), ethyl 4-decenoate (TCI Chemicals, >98%) were purchased from different commercial suppliers. Methyl oleate (dakolub 9001, 90% GC) was donated from Dako. Biphephos (>95%) was synthesized from Molisa GmbH. Precursors bis[1,2-bis(diphenylphosphino)ethane]palladium(0) (Pd(DPPE), Sigma Aldrich), bis(dibenzylideneacetone)palladium(0) ($Pd(dba)_2$, TCI), di-μ-bromobis(tri-tert-butylphosphine)dipalladium(I) (C1, ABCR), palladium(II)acetate ($Pd(OAc)_2$, ABCR), bis(triphenylphosphine)palladium(II)dichloride ($PdCl_2(PPh_3)_2$, Sigma Aldrich), allylpalladium(II)-chloride dimer ($Pd(allyl)_2Cl_2$), rhodium on aluminia (Alfa Aesar), rhodium on activated carbon (Degussa AG), rhodiumacetate dimer ($Rh_2(acac)_2$, ABCR), allylrhodium(II)-chloride dimer, carbonylhydrido-tris(triphenylphosphine)rhodium(I) ($HRh(PPh_3)(CO)$, Strem Chemicals), acetylacetonatoplatin(II) ($Pt(acac)_2$, Degussa AG), di-μ-chloroobis(ethylene)diplatin(II) ($[PtCl(C_2H_4)]$, Alfa Aesar), trirutheniumdodecacarbonyl ($Ru_3(CO)_{12}$, ABCR), Shvo's catalyst (ABCR), dicobaltoctacarbonyl (Acros organics), trichlorobis(tributylphosphine)nickel(II) ($NiCl_2(PBu_3)_2$, Sigma Aldrich), palladium(II)-iodide (PdI_2, ABCR), palladium(II)-chloride ($PdCl_2$, ABCR), palladium(II)-bromide ($PdBr_2$, ABCR), bis(tri-tert-butylphosphine)palladium(0) ($Pd(t\text{-}Bu_3P)_2$, ABCR) were purchased from different commercial suppliers.

Acetylacetonatodicarbonylrhodium ($Rh(CO)_2acac$), bis(1,4-naphtoquinone(bis[1,3-bis(2,6-diisopropylphenyl)imidazol-2-ylidene]dipalladium(0) (Umicore CX-11, $[(iPr)Pd(NQ)]_2$)), allylpalladium(II)-chloride dimer ($Pd(allyl)_2Cl_2$), bis(1,5-cyclooctadien)diiridium(I)dichloride ([Ir(cod)Cl]), dichloro(1,5-cyclooctadien)platin(II) ($Pt(cod)_2Cl_2$), dichlrorobis(p-cymene)ruthenium(II)dimer ($Ru_2(p\text{-}cymene)Cl_2$) were donated from Umicore AG & Co. Kg. Lithiumiodid was purchased from ABCR. All chemicals were degassed before use and stored under argon. CO (2.0) and H_2 (5.0) were purchased from Messer Industriegase GmbH.

Table 7.1: PALLADIUM-PRECURSORS IN THE ISOMERIZATION OF METHYL 3-HEXENOATE UNDER HYDROFORMYLATION CONDITIONS.

Entry	Metall	Catalyst	High isomerization rate	No hydroformylation	No Hydrogenation
S1.1	**Pd(0)**	Pd(DPPE)	×	✓	✓
S1.2		$Pd(dba)_2$	×	✓	✓
S1.3		$Pd(t\text{-}Bu_3P)_2$	•	✓	✓
S1.4		$[(iPr)Pd(NQ)]_2$	×	✓	✓
S1.5	**Pd(I)**	C1	✓	✓	✓
S1.6	**Pd(II)**	$PdCl_2$	×	✓	✓
S1.7		$Pd(OAc)_2$	×	✓	✓
S1.8		$PdCl_2(PPh_3)_2$	•	✓	✓
S1.9		$Pd(allyl)_2Cl_2$	×	✓	✓

Conditions: 2.1 g toluene, 3.5 mmol **2**, 1 mol% metal, 15 bar synthesis gas (CO/H_2 = 1/1), 16 h, 90 °C, batch reaction in 20 mL autoclave, stirrer speed 500 rpm.
✓= Meets criterion, •= Meets criterion partially; ×= does not meet criterion
Isomerization, hydroformylation and hydrogenation are detected by GC-FID.

Table 7.2: DIFFERENT METAL PRECURSORS IN THE ISOMERIZATION OF METHYL 3-HEXENOATE UNDER HYDROFORMYLATION CONDITIONS.

Entry	Metall	Catalyst	High isomerization rate	No hydroformylation	No Hydrogenation
S2.1	**Rh**	Rh on alumnia	•	✓	✓
S2.2		Rh on activated carbon	•	✓	✓
S2.3		$Rh_2(acac)_2$	✓	•	•
S2.4		$[Rh(Cl)(C_2H_4)]_2$	×	✓	✓
S2.5		$HRh(PPh_3)(CO)$	✓	×	•
S2.6	**Ir**	$[Ir(cod)Cl]_2$	×	✓	✓
S2.7	**Pt**	$Pt(cod)_2Cl_2$	✓	•	×
S2.8		$Pt(acac)_2$	×	✓	✓
S2.9		$[PtCl_2(C_2H_4)]_2$	×	✓	✓
S2.10	**Ru**	$Ru_2(p\text{-}cymene)Cl_2$	•	✓	×
S2.11		$Ru_3(CO)_{12}$	✓	×	•
S2.12		Shvo-Katalysator	✓	✓	•
S2.13	**Co**	$Co_2(CO)_8$	•	•	✓
S2.14	**Ni**	$NiCl_2(PBu_3)_2$	×	✓	✓

Conditions: 2.1 g toluene, 3.5 mmol **2**, 1 mol% metal, 15 bar synthesis gas (CO/H_2 = 1/1), 16 h, 90 °C, batch reaction in 20 mL autoclave, stirrer speed 500 rpm.
✓= Meets criterion, •= Meets criterion partially; ×= does not meet criterion
Isomerization, hydroformylation and hydrogenation are detected by GC-FID.

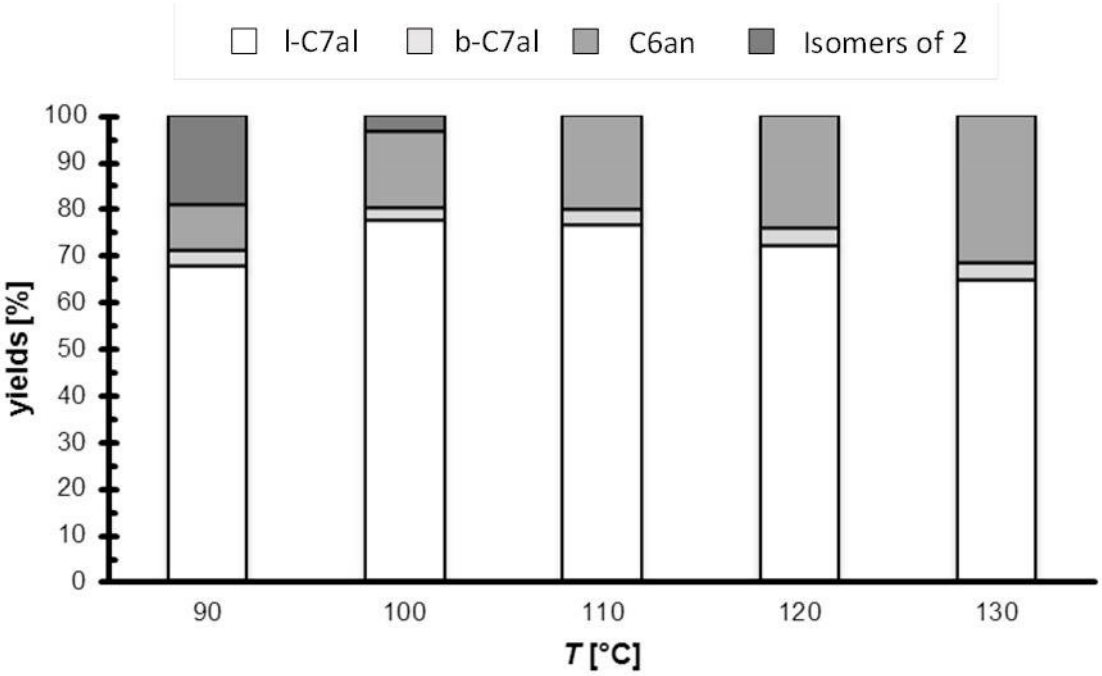

Figure 7.12: TEMPERATURE SCREENING.
Conditions: 2.1 g toluene, 3.5 mmol 2, 0.4 mol% $Rh(CO)_2acac$, 1.6 mol% biphephos, 0.5 mol% C1, 15 bar synthesis gas (CO/H_2 = 1/1), 100 °C, batch reaction in 20 mL autoclave, stirrer speed 500 rpm. Yields were determined by GC-FID.

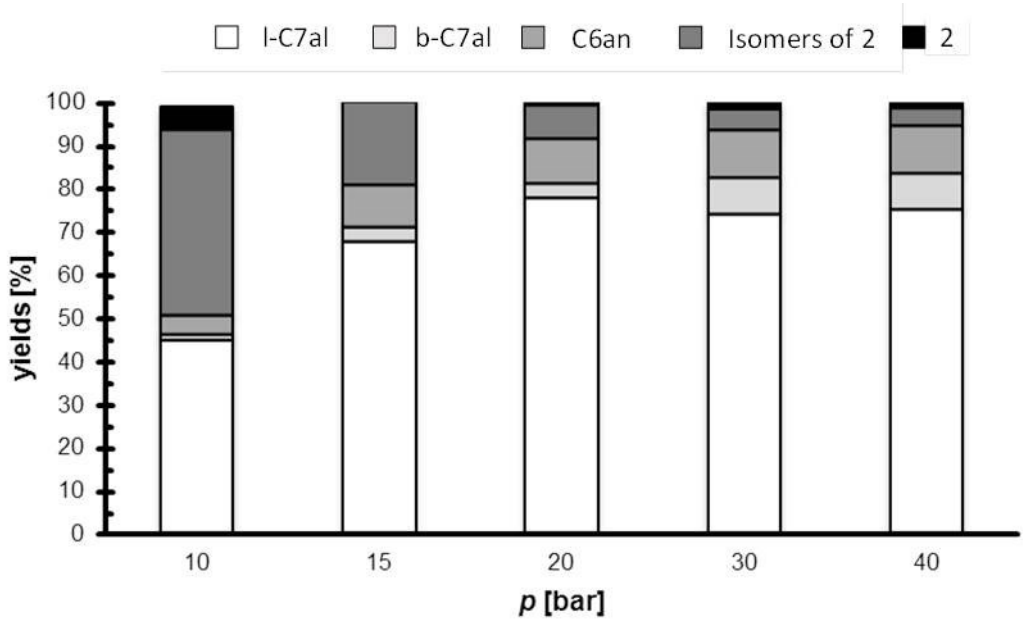

Figure 7.13: PRESSURE SCREENING.
Conditions: 2.1 g toluene, 3.5 mmol 2, 0.4 mol% $Rh(CO)_2acac$, 1.6 mol% biphephos, 0.5 mol% C1, 90 °C, (CO/H_2 = 1/1), batch reaction in 20 mL autoclave, stirrer speed 500 rpm. Yields were determined by GC-FID.

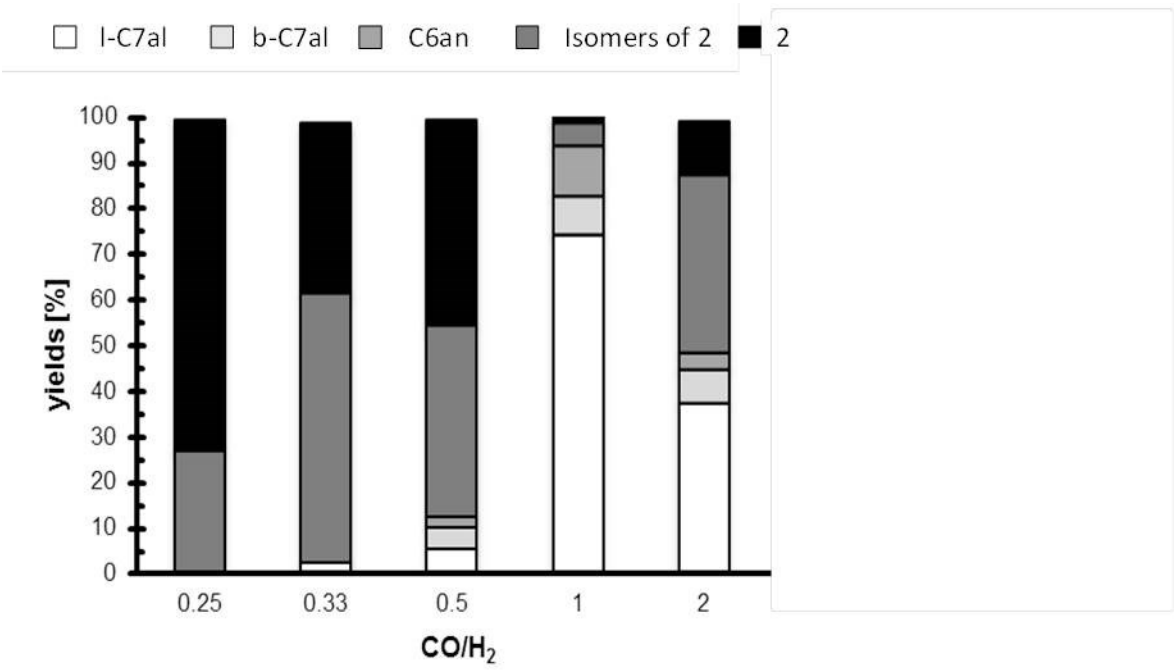

Figure 7.14: SYNGAS COMPOSITION SCREENING.
Conditions: 2.1 g toluene, 3.5 mmol **2**, 0.4 mol% $Rh(CO)_2acac$, 1.6 mol% biphephos, 0.5 mol% C1, 90 °C, 30 bar synthesis gas, batch reaction in 20 mL autoclave, stirrer speed 500 rpm. Yields were determined by GC-FID.

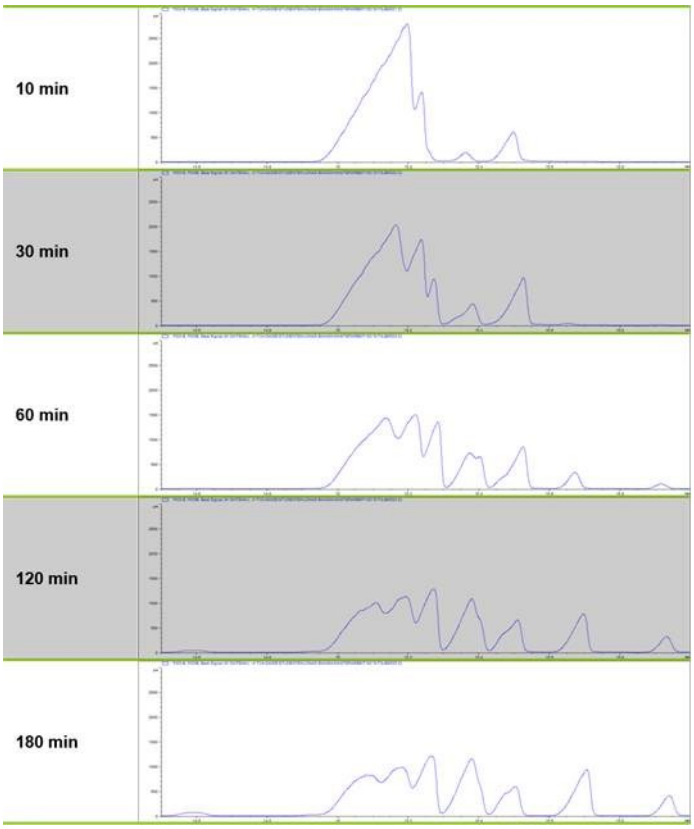

Figure 7.15: GC-CHROMATOGRAMS SHOWING THE PROGRESS OF ISOMERIZATION IN THE ISOMERIZING HYDROFORMYLATION OF **3**.
Conditions: 48 g toluene, 40 mmol 3, 0.4 mol% Rh(CO)2acac, 1.6 mol% biphephos, 0.5 mol% PdI2, 0.5 mol Pd(*t*-Bu3P)2 10 bar synthesis gas (CO/H_2 = 1/1), 100 °C, batch reaction in 300 mL autoclave, stirrer speed 1000 rpm. Yields were determined by GC-FID.

ANALYTIC ISOMERZING HYDROFORMYLATION OF METHYL 3-HEXENOATE (**2**)

Product isolation and characterization

Linear aldehyde (**l-C7al**) was isolated from reaction mixture *via* column chromatography using a mixture of cylcohexane/ethyl acettate (5/1). Product **l-C7al** was obtained as slightly yellow colored liquid and analyzed by ^{1}H-NMR (Figure 7.16) and ^{13}C-NMR spectroscopy (Figure 7.17) using a Bruker DRX-400 spectrometer. Branched aldehydes (**b-C7al**), isomers of the substrate (2) and the hydrogenated substrate (2c) were identified *via* gas chromatography coupled with mass spectrometry (GC/MS) using an Agilent Technologies 7890B GC System and a 5977A MSD detector from crude reaction mixture.

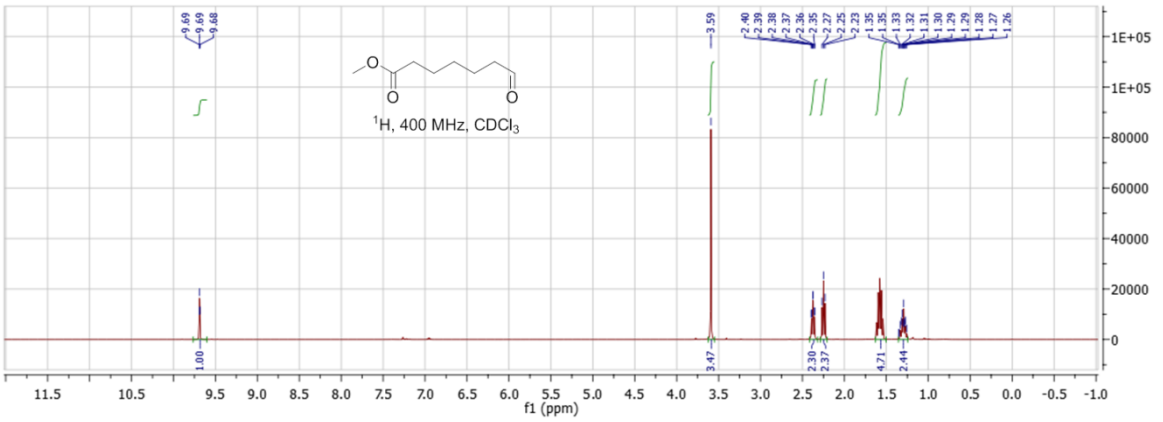

Figure 7.16: ^{1}H-NMR of **I-C7al**.

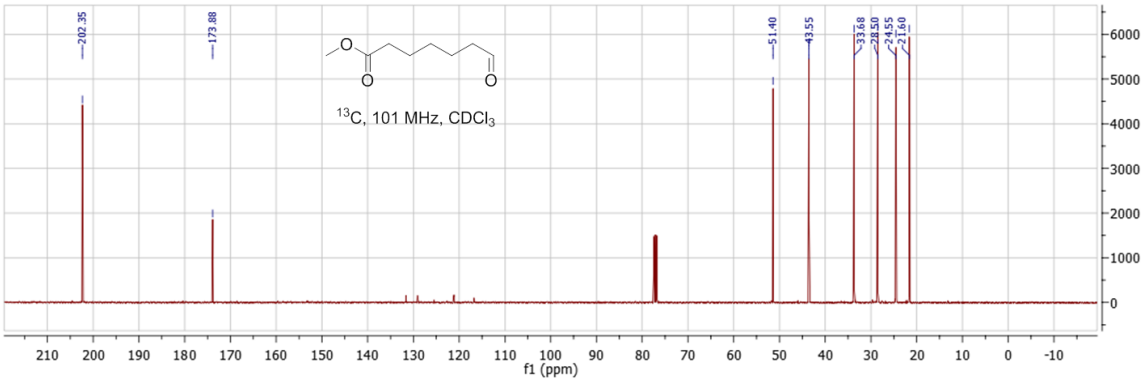

Figure 7.17: ^{13}C-NMR of **I-C7al**.

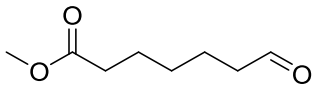

^{1}H NMR (400 MHz, CDCl3) δ 9.69 (t, J = 1.7 Hz, 1H), 3.59 (s, 3H), 2.38 (td, J = 7.3, 1.6 Hz, 2H), 2.25 (t, J = 7.4 Hz, 2H), 1.58 (dt, J = 15.1, 7.4 Hz, 4H), 1.39 – 1.21 (m, 2H).

^{13}C NMR (101 MHz, CDCl3) δ 202.35 (1C), 173.88 (1C), 51.40 (1C), 43.55 (1C), 33.68 (1C), 28.50 (1C), 24.55 (1C), 21.60 (1C).

Quantitative analysis

Quantitative analysis of the reaction mixtures was done by gas chromatography (GC) coupled with a flame ionization detector (FID). An Agilent Technologies 7890B GC System equipped with a Agilent J&W Innowax column (30 m x 0.25 mm x 0.25 μm) was used. Nitrogen as carrier gas with a flow of 1 mL/min and a split ratio of 85/1 were used. Table 7.3 shows the temperature profile of the GC, an exemplary chromatogram is shown in Figure 7.18. Method of external standard was used for quantification.

Table 7.3: GC temperature profile for analysis of isomerizing hydroformylation of 2 and 3.

	rate [°C/min]	temperature [°C]	hold time [min]
start	-	50	1
ramp1	7	155	0
ramp2	20	250	5

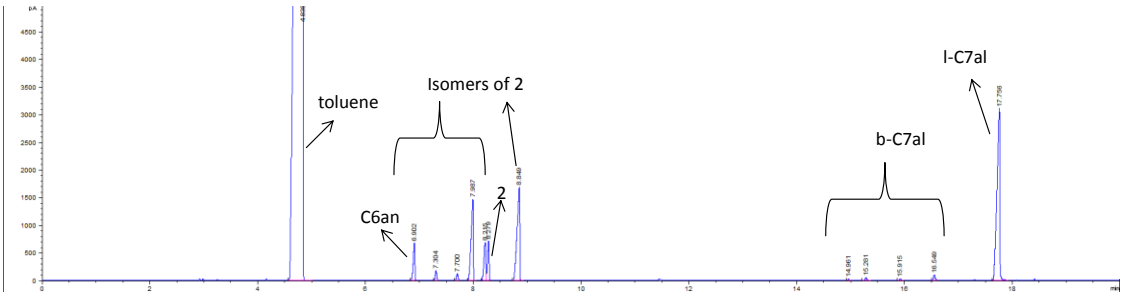

Figure 7.18: Exemplary chromatogram of the isomerizing hydroformylation of **2**.

Analysis branched aldehyde (**b-C7al**) distribution

For identification of the different branched aldehydes **b-C7al** we carried out two non-isomerizing hydroformylation experiments using a Rh/triphenylphosphine (PPh_3) catalyst. Hydroformylation of terminal unsaturated methyl 5-hexenoate leads to addition of the formyl group in position 5 and 6(linear aldehyde, **l-C7al**) of the esters carbon chain (Figure 7.19).

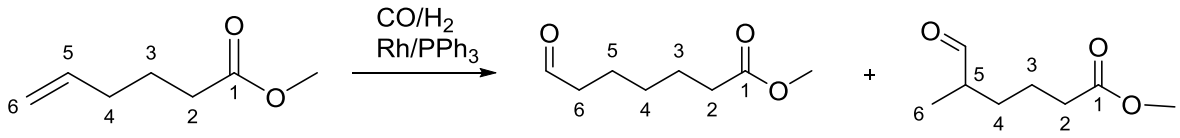

Figure 7.19:Non-isomerizing hydroformylation of methyl 5-hexenoate.

If methyl 3-hexenoate (**2**) is used as substrate, the formyl group is added in position 3 and 4 (Figure 7.20).

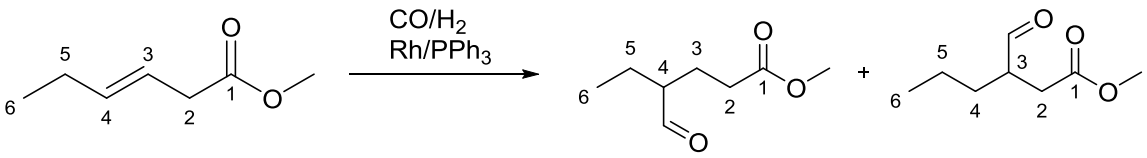

Figure 7.20: Non-isomerizing hydroformylation of methyl 3-hexenoate.

Cut outs from the aldehyde section of the resulting GC-chromatograms are shown Figure 7.21.

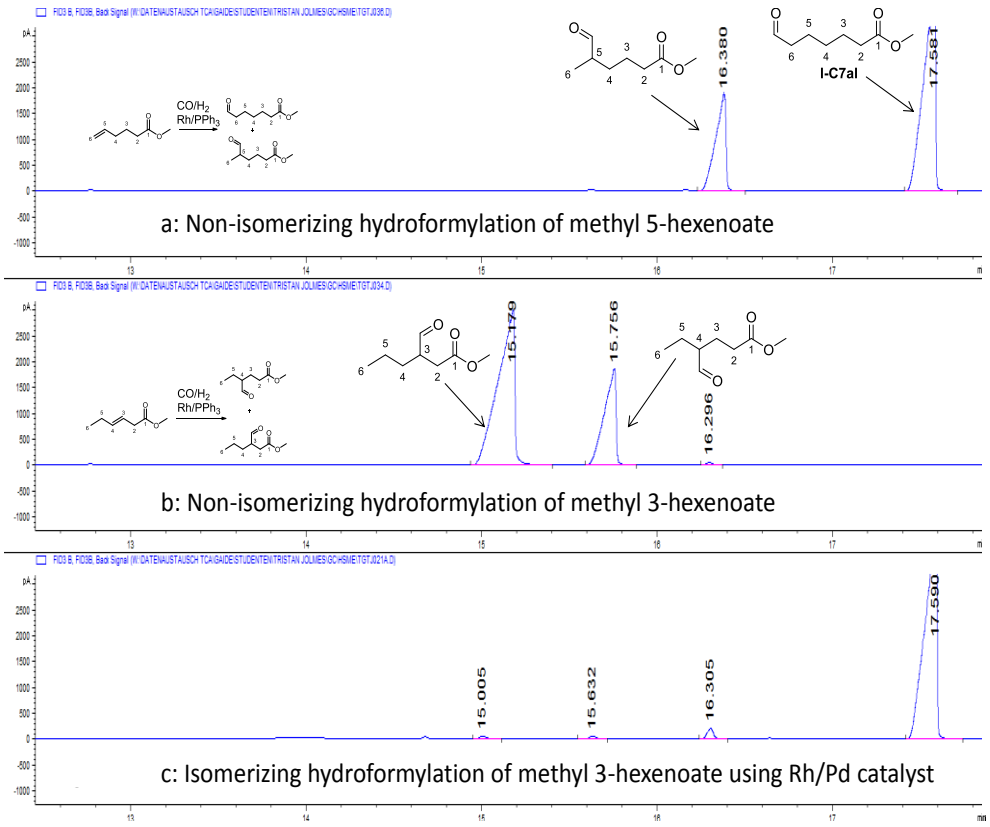

Figure 7.21: Chromatograms of non-isomerizing and isomerizing hydroformylation.
Conditions for non-isomerizing hydroformylation: 2.1 g toluene, 3.5 mmol substrate, 0.5 mol% $Rh(CO)_2acac$, 10 mol% PPh_3, 60 bar synthesis gas (CO/H_2 = 1/1), 3 h, 100 °C, batch reaction in 20 mL autoclave, stirrer speed 500 rpm.

Figure 7.21a shows the resulting chromatogram of the non-isomerizing hydroformylation of methyl 5-hexenoate using a Rh/PPh_3 catalyst. From this reaction, the linear aldehyde **l-C7al** (which was isolated and characterized via NMR spectroscopy, vide supra) and the aldehyde containing the formyl group in position 5 are obtained. Structure of the latter one was further verified by additional GC/MS measurements using an EI mass spectrometer (Figure 7.22a). Characteristic McLafferty fragmentation (m/z 58) confirmed that the formyl group is in position 5 of the carbon chain.

Figure 4.21b shows the resulting chromatogram of the non-isomerizing hydroformylation of methyl 3-hexenoate (**2**) using a Rh/PPh_3 catalyst. From this reaction, aldehydes containing the formyl group in position 3 and 4 of the carbon chain are obtained. Mass spectrometric analysis shows no characteristic McLafferty fragmentation for the branched aldehyde with the formyl group in position 4 (Figure 7.22b). No fragment with m/z 72 was detected and all aldehydes show a fragment with m/z 130.

For the aldehyde bearing the formyl group in position 3 a characteristic McLafferty fragmentation (m/z 116, Figure 7.22c) was observed.

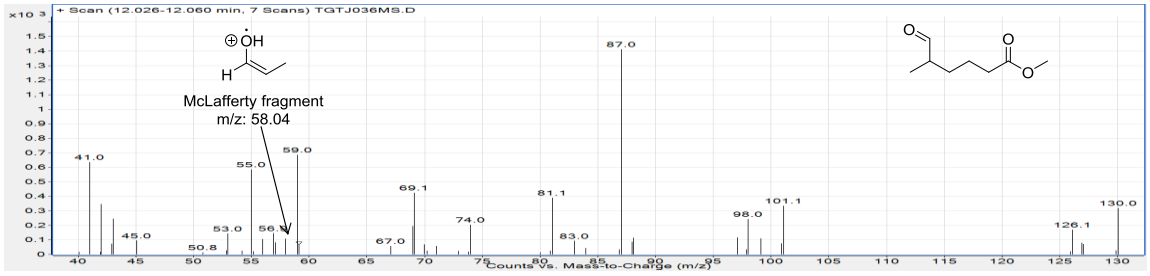

a: Mass spectrum of aldehyde with formyl group in position 5

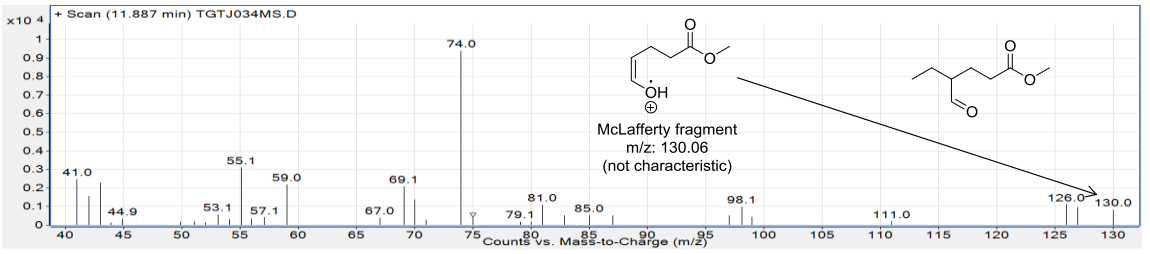

b: Mass spectrum of aldehyde with formyl group in position 4

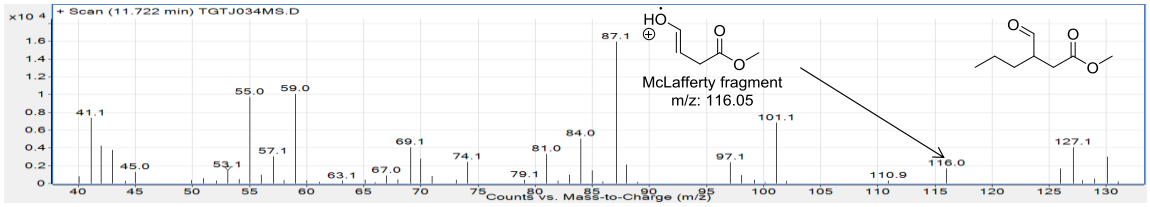

c: Mass spectrum of aldehyde with formyl group in position 3

Figure 7.22: Mass spectra of different branched aldehydes.

ANALYTIC ISOMERZING HYDROFORMYLATION OF ETHYL 4-DECENOATE (**3**)

Product isolation and characterization

Linear aldehyde (**l-C11al**) was isolated from reaction mixture *via* column chromatography using a mixture of cylcohexane/ethyl acettate (10/1 → 5/1). Product **l-C11al** was obtained as slightly yellow colored liquid and analyzed by ^{1}H-NMR (Figure 7.23) and ^{13}C-NMR (Figure 7.24) spectroscopy using a Bruker DRX-400 spectrometer. Branched aldehydes (**b-C11al**), isomers of the substrate (**3**) and the hydrogenated substrate (**C10an**) were identified *via* gas chromatography coupled with mass spectrometry (GC/MS) using an

Agilent Technologies 7890B GC System and a 5977A MSD detector from crude reaction mixture.

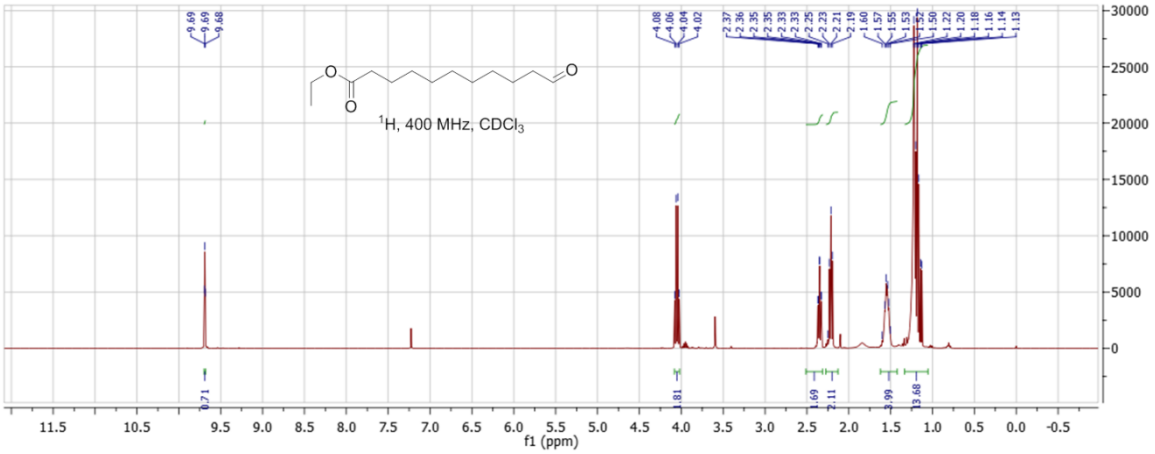

Figure 7.23: ^{1}H-NMR of **I-C11al**.

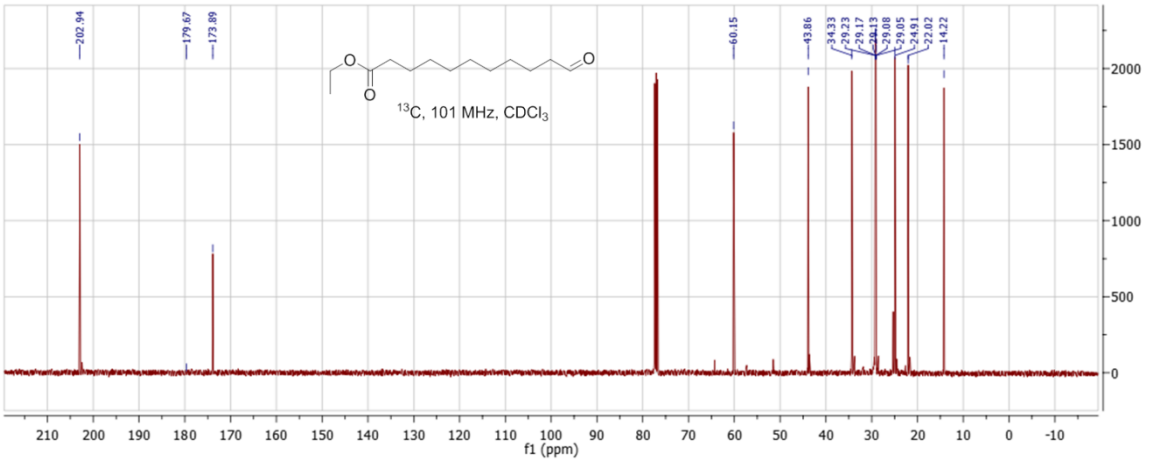

Figure 7.24: ^{13}C-NMR of **I-C11al**.

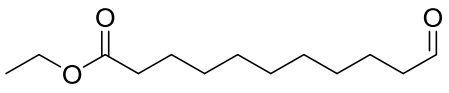

1H NMR (400 MHz, CDCl3) δ 9.69 (t, J = 1.8 Hz, 1H), 4.05 (q, J = 7.1 Hz, 2H), 2.35 (td, J = 7.4, 1.8 Hz, 2H), 2.22 (dd, J = 15.3, 7.8 Hz, 2H), 1.62 – 1.42 (m, 4H), 1.33 – 1.05 (m, 13H).

13C NMR (101 MHz, CDCl3) δ 202.94 (1C), 173.89 (1C), 60.15 (1C), 43.86 (1C), 34.33 (1C), 29.23 (1C), 29.17 (1C), 29.13 (1C), 29.08 (1C), 29.05 (1C), 24.91 (1C), 22.02 (1C), 14.22 (1C).

Quantitative analysis

Quantitative analysis of the reaction mixtures was done by gas chromatography (GC) coupled with a flame ionization detector (FID). An Agilent Technologies 7890B GC System equipped with a Agilent J&W Innowax column (30 m x 0.25 mm x 0.25 μm) was used. Nitrogen as carrier gas with a flow of 1 mL/min and a split ratio of 85/1 Nitrogen as carrier gas with a flow of 1 mL/min and a split ratio of 75/1 were used Table 7.3 shows the temperature profile of the GC, an exemplary chromatogram is shown in Figure 7.25. Method of external standard was used for quantification.

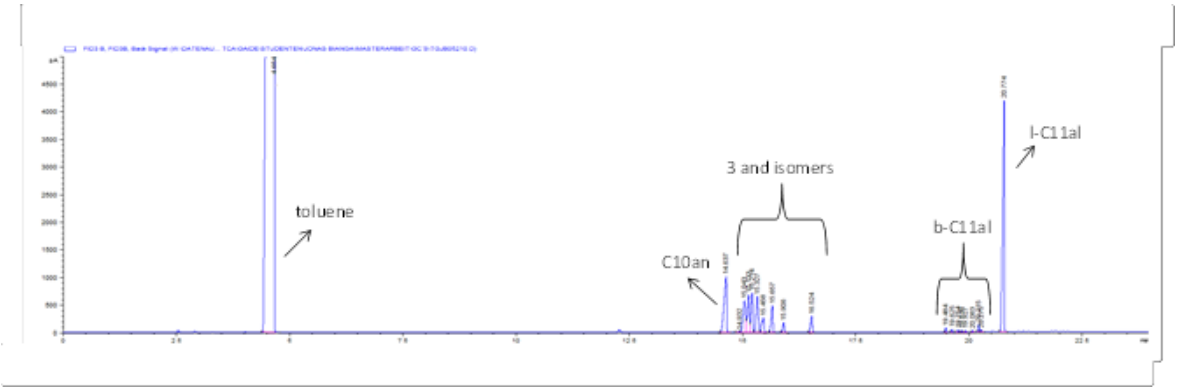

Figure 7.25: Exemplary chromatogram of the isomerizing hydroformylation of **3**.

ANALYTIC ISOMERIZING HYDROFORMYLATION OF METHYL OLEATE (**1**)

Product isolation and characterization

Linear aldehyde (**l-C19al**) was isolated from reaction mixture *via* column chromatography using a mixture of cylcohexane/ethyl acettate (100/1). Product **l-C19al** was obtained as off white solid and analyzed by ^{1}H-NMR (Figure 7.26) and ^{13}C-NMR (Figure 7.27) spectroscopy using a Bruker DRX-400 spectrometer. Branched aldehydes (**b-C19al**), isomers of the substrate (**1**) and the hydrogenated substrate (**C18an**) were identified *via* gas chromatography coupled with mass spectrometry (GC/MS) using an Agilent Technologies 7890B GC System and a 5977A MSD detector from crude reaction mixture.

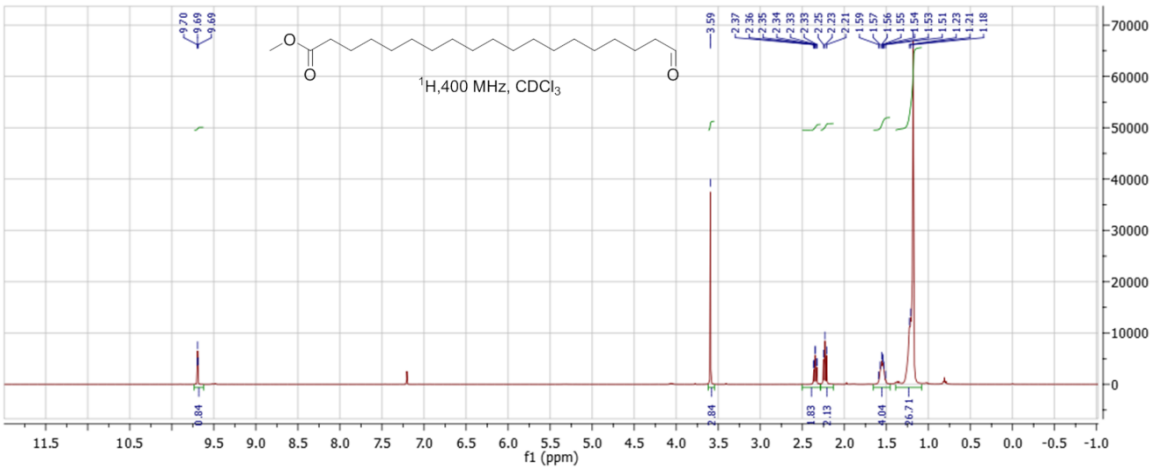

Figure 7.26: ^{1}H-NMR of **I-C19al**.

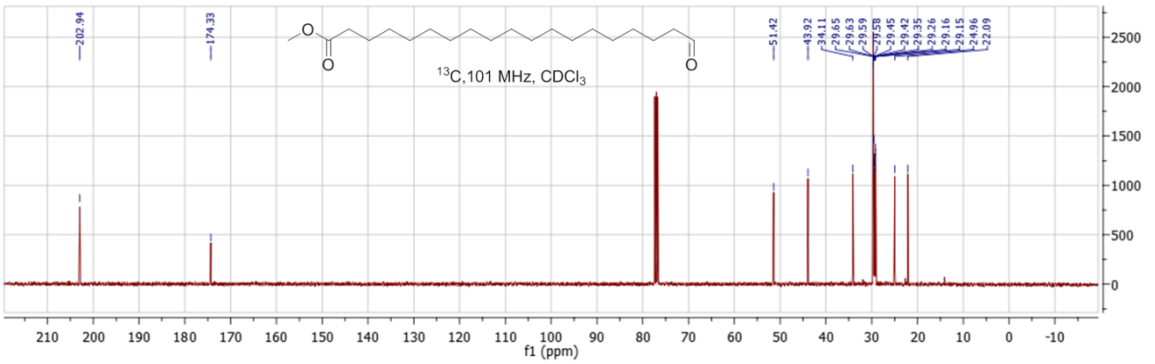

Figure 7.27: ^{13}C-NMR of **I-C19al**.

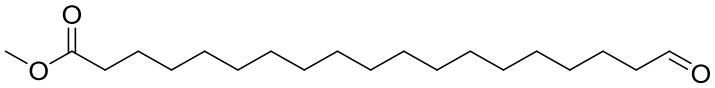

1H NMR (400 MHz, CDCl3) δ 9.69 (t, J = 1.9 Hz, 1H), 3.59 (s, 3H), 2.35 (td, J = 7.4, 1.9 Hz, 2H), 2.23 (t, J = 7.6 Hz, 2H), 1.66 – 1.46 (m, 4H), 1.32 – 1.06 (m, 26H).

13C NMR (101 MHz, CDCl3) δ 202.94 (1C), 174.33 (1C), 51.42 (1C), 43.88 (1C), 34.11 (3C), 29.65 (2C), 29.63 (1C), 29.59 (1C), 29.58 (1C), 29.45 (1C), 29.42 (1C), 29.35 (1C), 29.26 (1C), 29.16 (1C), 29.15 (1C), 24.96 (1C), 22.09 (1C).

Quantitative analysis

Quantitative analysis of the reaction mixtures was done by gas chromatography (GC) coupled with a flame ionization detector (FID). An Agilent Technologies 7890B GC System equipped with an Agilent J&W HP-5 column (30 m x 0.25 mm x 0.25 μm) was used. Nitrogen with a flow of 1 mL/min was used as carrier gas Table 7.4shows the temperature profile of the GC, an exemplary chromatogram is shown in Figure 7.28. Method of internal standard (dodecane) was used for quantification.

Table 7.4: GC temperature profile for analysis of isomerizing hydroformylation of 1.

	rate [°C/min]	temperature [°C]	hold time [min]
start	-	40	3
ramp1	7	100	0
ramp2	20	32	10

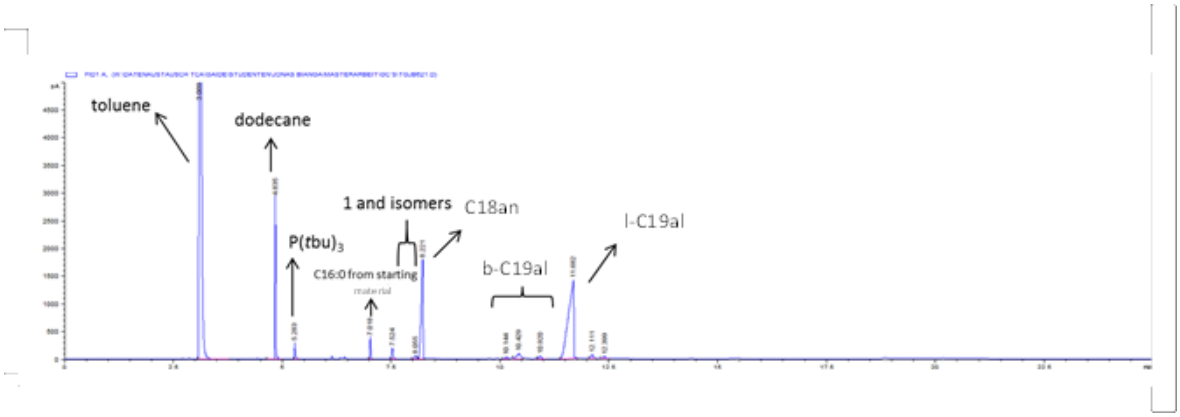

Figure 7.28:Exemplary chromatogram of the isomerizing hydroformylation of **1**.

7.5. List of Figures

Figure 2.1: LLBC principle.....7
Figure 2.2: Principles of *in-situ* (left) and consecutive (right) extraction. 8
Figure 2.3: Principle of temperature-controlled phase transfer catalysis.....9
Figure 2.4: Four states of a temperature-controlled microemulsion system.[23,24,26].....9
Figure 2.5: Principle of temperature-controlled fluorinated solvents. 10
Figure 2.6 Principle of a thermomorphic multicomponent solvent (TMS) system.....11
Figure 2.7**:** Miscibility gap of type I TMS systems at room temperature.[31].....12
Figure 2.8: Ternary diagrams of type II TMS systems at room temperature.[31] 13
Figure 2.9: Isomerising cooligomerisations of linoleic acid with ethene. 15
Figure 2.10: Hydroamination of myrcene with morpholine.....15
Figure 2.11: Hydroformylation of 1-dodecene to tridecanal. 16
Figure 2.12**:** Definition of sequential reactions.[75].....17
Figure 2.13: Hydroformylation of a terminal olefin. 19
Figure 2.14: Mechanism of the cobalt-catalysed hydroformylation (under formation of the linear aldehyde).....20

Figure 2.15: Mechanism of the rhodium-catalysed hydroformylation (under formation of the linear aldeyhde). 21

Figure 2.16: Common side reactions of the hydroformylation. 22

Figure 2.17: Condensation of *n*-butanal. 23

Figure 2.18: Price development of rhodium.[92] 24

Figure 2.19**:** Examples for ligands enabling high linear selectivity in hydroformylations.[109–111] 25

Figure 2.20: Hydroesterification of a terminal olefin. 28

Figure 2.21: Pd-catalysed hydroesterification *via* hydride mechanism. 28

Figure 2.22: Pd-catalysed hydroesterification *via* alkoxy mechanism. 29

Figure 2.23: Tandem isomerisation/hydroesterification of methyl oleate and the 1,2 - DTBPMB ligand. 29

Figure 2.24: Ligands for new hydroesterification catalysts. 30

Figure 4.1: TMS functionality. 36

Figure 4.2: Procedure for TMS design. 38

Figure 4.3: Chemical structure formula of Biphephos (A) and its surface charge in a perfect conductor 39

Figure 4.4: Sigma profile of the Biphephos ligand. 40

Figure 4.5: Hydroformylation and isomerization/hydroformylation tandem reaction. 58

Figure 4.6: Principle of a TMS system.[205] 59

Figure 4.7: Highly selective tandem isomerisation/hydroformylation reactions of internal olefins with subsequent catalyst recycling. 60

Figure 4.8: Product spectrum/BIPHEPHOS ligand. 63

Figure 4.9: Influence of the reaction temperature on the product distribution. 64

Figure 4.10: Reaction Network of the isomerization/hydroformylation tandem reaction. .. 64

Figure 4.11: Influence of TMS system composition on the reaction behaviour. 67

Figure 4.12: Conversion/yield vs. time plot of the isomerization/hydroformylation tandem reaction in a TMS system. 68

Figure 4.13: Catalyst Recycling. 70

Scheme 4.14: Hydroformylation of propylene. 73

Figure 4.15: Ternary diagram of TMS systems. 74

Scheme 4.16: Hydroformylation of 10-undecenoate and observed side reactions. 75

Scheme 4.17: Possible building blocks for the polymer synthesis. 76

Figure 4.18: Product distribution using polar, organic solvents. 76

Figure 4.19: Molecular structure of the applied ligands. 77

Figure 4.20: Temperature screening. 78

Figure 4.21:Hydroformylation of methyl 10-undecenoate and catalyst recycling using a batch autoclave. 79

Figure 4.22: Process flow diagram of the miniplant for the hydroformylation of methyl 10-undecenoate. 80

Figure 4.23: Continuous hydroformylation process in a miniplant. 81

Figure 4.24: Principle of a TMS system. 86

Figure 4.25: Hydroesterification products of methyl 10-undecenoate. 88

Figure 4.26: Examined bidentate ligands in hydroesterification of methyl 10-undecenoate. 89

Figure 4.27: Ternary plots of methanol/dodecane/substrate and methanol/dodecane/product at 25 °C (♦) and 60 °C (▲). 92

Figure 4.28: Catalyst recycling experiments [a]. 97

Figure 4.29: Concept for a continuous hydroesterification process. 98

Figure 4.30: Industrielle Synthesen von Dodecandisäure 102

Figure 4.31: Allgemeine Reaktionsgleichung der Hydroesterifizierung. 102

Figure 4.32: Prinzip eines TMS-Systems [a]. 103

Figure 4.33: Produktspektrum der Hydroesterifizierung von 10-Undecensäuremethylester 104

Figure 4.34: Katalysatorvergleich im Lösungsmittel Methanol. 106

Figure 4.35: Abbildung 6: Recycling-Experimente [a]. 113

Figure 4.36: Shvo's catalyst and applied ligands in the *n*-selective reductive hydroformylation. 118

Figure 4.37: Reductive hydroformylation of castor oil derived substrates 1a-c for the synthesis of linear bifunctional alcohols 3a-**c** via the intermediate linear aldehydes 2a-c. 119

Figure 4.38: Yield vs. time: Reduction of aldehyde 2a to alcohol 3a (with *ex situ* (A) and *in situ* (B) Shvo's catalyst); Reductive hydroformylation of 1a to alcohol 3a (with *ex situ* (C) and *in situ* (D) Shvo's catalyst). 121

Figure 4.39:1: first reaction; 2: first recycling; 3: second recycling. 124

Scheme 4.40: Industrial routes to surfactant-precursors *via* fatty nitriles (top) and *via* hydroaminomethylation of terpenes (bottom). 127

Scheme 4.41: Hydroaminomethylation of an olefin. 128

Figure 4.42: Metal precursor and diphosphine ligand for the catalyst. 128

Figure 4.43: Hydroformylation as the regioselectivity determining step in the hydroaminomethylation of myrcene. 129

Figure 4.44: Yield-time-plot of the hydroaminomethylation of myrcene with diethylamine. 131

Figure 4.45: Substrate scope for the hydroaminomethylation of terpenes. 132

Figure 4.46: Critical micelle concentrations at 20 °C of the synthesized surfactants in comparison to structurally similar, industrially established ones.[315] 133

Scheme 4.47: Isomerization/ω-functionalization of methyl oleate (**1**). 136

Scheme 4.48: Isomerizing hydroformylation and methoxycarbonylation. 137

Scheme 4.49: Isomerizing hydroformylation of methyl oleate: This work compared with literature 138

Scheme 4.50: Approach for development of the isomerizing hydroformylation of FAMEs. 139

Scheme 4.51: Reaction network of the isomerizing hydroformylation of **2**. 140

Scheme 4.52: Synthesis of C1 and likely catalytically active species according to Gooßen et al.[321,322] 141

Figure 4.53: Reaction kinetics of the isomerizing hydroformylation of 2. 146

Figure 4.54: Isomerizing hydroformylation of 4-ethyl decenoate. 147

Figure 5.1: Isomerization/hydroformylation of technical grade decene isomers. 152

Figure 5.2: Hydroformylation of methyl 10-undecenoate. 153

Figure 5.3: Hydroesterification of methyl 10-undecenoate. 154

Figure 5.4: Decision tree for TMS systems. 158

Figure 5.5: Workflow for the systematic development of TMS systems. 159

Figure 5.6: Workflow for process design for TMS systems. 161

Figure 5.7: Future concept of a hybrid separation process for the tandem hydroformylation/hydrogenation of methyl 10-undecenoate. [Rh] = Rh/TPPTS; [Ru] = sulfonated Shvo's catalyst, P1 = ester-aldehyde, P2= ester-alcohol 162

Figure 5.8: Direct surfactant synthesis *via* hydroaminomethylation of myrcene with N-methyl glucamine. 163

Figure 5.9: Follow-up chemistry of α,ω- ester-aldehydes. 164

Figure 7.1: Process chart for the continuously operated hydroformylation miniplant. XI

Figure 7.2: 1-H NMR of the linear hydroformylation product (**2**). XII

Figure 7.3: 13-C NMR of the linear hydroformylation product (**2**). XII

Figure 7.4: Turnover frequencies at different substrate concentrations. XIII

Figure 7.5: Decrease in temperature of the first crude mixture. XIV

Figure 7.6: Decrease in temperature of the first recycled mixture. XV

Figure 7.7: Decrease in temperature of the second recycled mixture. XV

Figure 7.8: Desired and measured temperatures. XVI

Figure 7.9 (left) Hydrogenation of methyl 12-oxododecanoate to methyl 12-hydroxydodecanoate using *in situ* Shvo's catalyst. XVIII

Figure 7.10: (left) Hydroformylation and hydrogenation of methyl 10-undecenoate to methyl 12-hydroxydodecanoate using *in situ* Shvo's catalyst. XIX

Figure 7.11: (right) Hydroformylation and hydrogenation of methyl 10-undecenoate to methyl 12-hydroxydodecanoate using *ex situ* Shvo's catalyst. XIX

Figure 7.12: TEMPERATURE SCREENING. XXVII

Figure 7.13: PRESSURE SCREENING. XXVII

Figure 7.14: SYNGAS COMPOSITION SCREENING. XXVIII

Figure 7.15: GC-CHROMATOGRAMS SHOWING THE PROGRESS OF ISOMERIZATION IN THE ISOMERIZING HYDROFORMYLATION OF **3**. XXIX

Figure 7.16: ^{1}H-NMR of **l-C7al**. XXX

Figure 7.17: ^{13}C-NMR of **l-C7al**. XXX

Figure 7.18: Exemplary chromatogram of the isomerizing hydroformylation of **2**. XXXI

Figure 7.19:Non-isomerizing hydroformylation of methyl 5-hexenoate. XXXI

Figure 7.20: Non-isomerizing hydroformylation of methyl 3-hexenoate. XXXII

Figure 7.21: Chromatograms of non-isomerizing and isomerizing hydroformylation. .. XXXII

Figure 7.22: Mass spectra of different branched aldehydes. XXXIII

Figure 7.23: ^{1}H-NMR of **l-C11al**. XXXIV

Figure 7.24: ^{13}C-NMR of **l-C11al**. XXXIV

Figure 7.25: Exemplary chromatogram of the isomerizing hydroformylation of **3**. XXXV

Figure 7.26: ^{1}H-NMR of **l-C19al**. XXXVI

Figure 7.27: ^{13}C-NMR of **l-C19al**. XXXVI

Figure 7.28:Exemplary chromatogram of the isomerizing hydroformylation of **1**. XXXVII

7.6. List of tables

Table 2.1: Overview over carbonylation reactions.[9] 18

Table 4.1: List of top 5 high (HRSC) and low (LRSC) relative solubility catalyst solvents. 41

Table 4.2: Unfiltered list of top 30 TMS mixtures. 44

Table 4.3: List of top 30 TMS mixtures 46

Table 4.4: List of high relative solubility solvents and decane TMS candidates..... 47

Table 4.5: Comparison of TMS composed of DMF and linear alkanes 47

Table 4.6: Phase Partitioning with Biphephos..... 51

Table 4.7: Hydroformylation results for each selected TMS system. 52

Table 4.8: Optimized reaction conditions for the isomerization/hydroformylation tandem reaction in batch reaction mode. 65

Table 4.9: Component distribution after phase separation. 67

Table 4.10: Distribution of the components between polar and apolar phase [a] 79

Table 4.11: Investigations on the catalyst [a]..... 90

Table 4.12: Investigation on MSA influence in TMS systems [a]..... 93

Table 4.13: Investigations on catalyst stability and activity in TMS systems [a]..... 94

Table 4.14: Investigations on phase behaviour of the TMS system [a]. 96

Table 4.15: Component distribution in methanol/dodecane TMS system. 96

Table 4.16: Einfluss des Pd/MSA-Verhältnisses auf den $Pd_2(dba)_3$/1,2-DTBPMB/MSA-Katalysator [a, b, c]. 107

Table 4.17: Einfluss des Pd/MSA-Verhältnisses auf den $Pd_2(dba)_3$/XANTphos/MSA-Katalysator [a, b, c]..... 108

Table 4.18: Einfluss des Pd/Ligand-Verhältnisses auf den $Pd_2(dba)_3$/1,2-DTBPMB/MSA-Katalysator [a, b, c]. 109

Table 4.19: Einfluss des Pd/Ligand-Verhältnisses auf den $Pd_2(dba)_3$/XANTphos/MSA-Katalysator [a, b, c]..... 109

Table 4.20. Einfluss des CO-Drucks auf den $Pd_2(dba)_3$/1,2-DTBPMB/MSA-Katalysator [a, b, c]..... 110

Table 4.21: Einfluss des CO-Drucks auf den $Pd_2(dba)_3$/XANTphos/MSA-Katalysator [a, b, c]. 111

Table 4.22: Verteilung der Komponenten auf die beiden Phasen nach der Phasentrennung [a]..... 112

Table 4.23:Reductive hydroformylation of 1a-c under optimized reaction conditions. 122

Table 4.24: Trends in reactivity of each catalytic step in the hydroaminomethylation of myrcene with diethylamine, depending on reaction conditions. 130

Table 4.25:Isomerization catalyst screening. 140

Table 4.26: Catalyst development for the isomerizing hydroformylation of methyl 3-hexenoate (**2**). 143

Table 4.27:Double bond isomer distribution of **2** in the equilibrium and distribution of branched aldehydes after reaction. 145

Table 4.28: Catalyst development for the isomerizing hydroformylation of methyl oleate (1). 149

Table 5.1: Inherent advantages and disadvantages of TMS systems. 156

Table 7.1: PALLADIUM-PRECURSORS IN THE ISOMERIZATION OF METHYL 3-HEXENOATE UNDER HYDROFORMYLATION CONDITIONS. XXVI

Table 7.2: DIFFERENT METAL PRECURSORS IN THE ISOMERIZATION OF METHYL 3-HEXENOATE UNDER HYDROFORMYLATION CONDITIONS..... XXVI

Table 7.3: GC temperature profile for analysis of isomerizing hydroformylation of 2 and 3..... XXXI

Table 7.4: GC temperature profile for analysis of isomerizing hydroformylation of 1. XXXVII

7.7. Publications

7.7.1. P. Neubert, I. Meier, T. Gaide, A. Behr, “Additive-Free Palladium-Catalysed Hydroamination of Piperylene with Morpholine”, *Synthesis* **2016**, *48*, 2287–2293.

7.7.2. P. Neubert, I. Meier, T. Gaide, R. Kuhlmann, A. Behr, “First telomerisation of piperylene with morpholine using palladium–carbene catalysts”, *Catal. Commun.* **2016**, *77*, 70–74.

7.7.3. T. Gaide, A. Behr, A. Arns, F. Benski, A. J. Vorholt, “Hydroesterification of methyl 10-undecenoate in thermomorphic multicomponent solvent systems—Process development for the synthesis of sustainable polymer precursors”, *Chem. Eng. Process.* **2016**, *99*, 197–204.

7.7.4. K. McBride, T. Gaide, A. J. Vorholt, A. Behr, K. Sundmacher, “Thermomorphic solvent selection for homogeneous catalyst recovery based on COSMO-RS”, *Chem. Eng. Process.* **2016**, *99*, 97–106.

7.7.5. T. Gaide, A. Behr, M. Terhorst, A. Arns, F. Benski, A. J. Vorholt, „Katalysatorvergleich bei der Hydroesterifizierung von 10-Undecensäuremethylester in thermomorphen Lösungsmittelsystemen“, *Chem. Ing. Tech.* **2016**, *88,*158–167.

7.7.6. T. Gaide, J. M. Dreimann, A. Behr, A. J. Vorholt, “Overcoming Phase-Transfer Limitations in the Conversion of Lipophilic Oleo Compounds in Aqueous Media - A Thermomorphic Approach”, *Angew. Chem., Int. Ed.* **2016**, *55*, 2924–2928.

7.7.7. T. Gaide, J. M. Dreimann, A. Behr, A. J. Vorholt, „Überwindung von Phasentransportlimitierungen in der Umsetzung lipophiler Oleoverbindungen in wässrigen Medien - ein temperaturgesteuerter Ansatz“, *Angew. Chem.* **2016**, *128*, 2977–2981.

7.7.8. T. A. Faßbach, T. Gaide, M. Terhorst, A. Behr, A. J. Vorholt, “Renewable Surfactants via Hydroaminomethylation of Terpenes”, *ChemCatChem* **2017,** *9*, 1359-1362.

7.7.9. T. Gaide, A. Jörke, K. E. Schlipköter, C. Hamel, A. Seidel-Morgenstern, A. Behr, A. J. Vorholt, “Isomerization/hydroformylation tandem reaction of a decene isomeric mixture with subsequent catalyst recycling in thermomorphic solvent systems”, *Appl. Catal., A.* **2017**, *532*, 50–56.

7.7.10. J. M. Dreimann, T. A. Faßbach, S. Fuchs, M. R. L. Fürst, T. Gaide, R. Kuhlmann, K. A. Ostrowski, A. Stadler, T. Seidensticker, D. Vogelsang, H. W. F. Warmeling, A. J. Vorholt, „Vom Laborkuriosum zum kontinuierlichen Prozess. Die Entwicklung thermomorpher Lösungsmittelsysteme“, *Chem. Ing.Tech.* **2017**, *89*, 252-262.

7.7.11. A. Jörke, T. Gaide, A. Behr, A. J. Vorholt, A. Seidel-Morgenstern, C. Hamel, „Hydroformylation and tandem isomerization–hydroformylation of *n*-decenes using a rhodium-BiPhePhos catalyst. Kinetic modeling, reaction network analysis and optimal reaction control”, *Chem. Eng. J.* **2017**, *313*, 382–397.

7.7.12. T. Gaide, J. Bianga, K. E. Schlipköter, A. Behr, A. J. Vorholt, „Linear Selective Isomerization/Hydroformylation of Unsaturated Fatty Acid Methyl Esters: A Bimetallic Approach, *ACS Catal.* **2017***, 7,* 4163-4171.

7.7.13. T. Gaide, A. J. Vorholt, A. Behr, „Hydroformylation" in *Homogeneous Catalysis with Renewables*, Springer-Verlag GmbH, Heidelberg, Germany, **2017**.

7.8. Posters and Lectures

7.8.1. AOCS 106th Annual meeting (Lecture): T. Gaide, A. Behr, A. J. Vorholt, Orlando **2015**, *Hydroesterification of methyl 10-undecenoate in thermomorphic multicomponent solvent systems – Designing new reaction systems in laboratory scale*

7.8.2. 8th Workshop on Fats and Oils as Renewable Feedstock for the Chemical Industry (Poster): T. Gaide, J. Dreimann, A. J. Vorholt, A. Behr, Kalsruhe **2015**, *Process Development for the Hydroformylation of Methyl 10-*

Undecenoate Using Water/Butanol-Solvent Systems – From Laboratory to Miniplant Scale

7.8.3. ACHEMA (Lecture): T. Gaide, A. J. Vorholt, A. Behr, Frankfurt **2015**, *Hydroformylation of long chain olefins and renewables using TMS systems: Design of new reaction systems in laboratory scale*

7.8.4. ACHEMA (Lecture): J. Dreimann, T. Gaide, A. J. Vorholt, A. Behr, Frankfurt **2015**, *Hydroformylation of long chain olefins and renewables using TMS systems: process development in miniplant scale*

7.8.5. DGMK International Conference on Synthesis Gas Chemistry (Poster): T. Gaide, A. Behr, A. J. Vorholt, Dresden **2015**, *Hydroesterification of methyl 10-undecenoate in thermomorphic multicomponent solvent systems – Designing new reaction systems in laboratory scale*

7.8.6. DGMK International Conference on Synthesis Gas Chemistry (Lecture): A. J. Vorholt, T. Gaide, J. Dreimann A. Behr, Dresden **2015**, *Process Development for the Hydroformylation/Hydroesterification of Methyl 10-Undecenoate – from Laboratory to Miniplant Scale*

7.8.7. DGMK International Conference on Synthesis Gas Chemistry (Poster): J. Dreimann, T. Gaide, A. Behr, A. J. Vorholt, Dresden **2015**, *Process Development for the Hydroformylation of Long Chain Olefins and Renewables Using TMS Systems in a Miniplant*

7.8.8. 21st European Conference on Organometallic Chemistry (Poster): A. Behr, T. Gaide, A. J. Vorholt, Bratislava **2015**, *Palladium Catalysed Hydroesterification of Methyl 10-undecenoate Including Catalyst Recycling in Thermomorphic Solvent Systems (TMS) – A Sustainable Route from Renewables to Polymer Precursors*

7.8.9. French Conference on Catalysis (Poster): A. Behr, T. Gaide, A. J. Vorholt, Frejus **2016**, *Development of new homogenous catalyst recycling concepts for fatty compound carbonylation reactions*

7.8.10. 8th Green Solvents Conference (Poster): T. Gaide J. Dreimann, A. J. Vorholt, A. Behr*,* Kiel **2016**,*Tailored Aqueous Solvent Systems for the Immobilization of Homogeneous Transition Metal Catalysts*

7.8.11. 49. Jahrestreffen Deutscher Katalytiker (Poster): T. Gaide, J. Dreimann, A. J. Vorholt, A. Behr, Weimar **2016**, *Catalytic functionalisation of fatty compounds in aqueous thermomorphic solvent systems*

7.8.12. 9. Tag der Chemie (Lecture): T. Gaide, J. Bianga J. Dreimann, A. J. Vorholt, A. Behr, Dortmund **2016**, *Entwicklung neuer Technologien zur homogenkatalytischen Umsetzung nachwachsender Rohstoffe in chemischen Prozessen*

7.8.13. 7. Junges Chemie Symposium Ruhr (Lecture): T. Gaide, J. Bianga J. Dreimann, A. J. Vorholt, A. Behr, Dortmund **2016**, *A temperature controlled approach for the homogeneously catalyzed conversion of renewable resources in aqueous media*

7.8.14. Gordon Research Conference on Green Chemistry (Poster): T. Gaide, J. Dreimann, J. Bianga, A. J. Vorholt, A. Behr, Stowe **2016**, *Process Development for the Carbonylation of Oleocompounds in Aqueous Thermomorphic Solvent Systems*

7.8.15. 20th Green Chemistry & Engineering Conference (Lecture): T. Gaide, J. Dreimann, J. Bianga, A. J. Vorholt, A. Behr, Portland **2016***, A temperature controlled approach for the homogenously catalyzed conversion of oleocompounds in aqueous media*

7.8.16. 50. Jahrestreffen Deutscher Katalytiker (Poster): T. Gaide, J. Bianga, A. J. Vorholt, A. Behr, Weimar **2016**, *ω-Functionalization of fatty acid methyl esters via isomerizing hydroformylation*

7.8.17. 9th Workshop on Fats and Oils as Renewable Feedstock for the Chemical Industry (Lecture): T. Gaide, A. J. Vorholt, A. Behr, Karlsruhe **2017**, *Linear selective isomerization/hydroformylation for ω-functionalization of fatty acid methyl esters*

7.8.18. EuCheMS International Organometallic Conference XXII: A. Behr, A. J. Vorholt, T. Gaide, J. Dreimann, T. Seidensticker, M. Furst, Amsterdam **2017**, *Organometallic Catalysis with Renewables*

7.9. Supervised Thesis

7.9.1. **Benski, Francesco** (BT, 2014): Hydroesterifizierung von 10-Undecensäuremethylester

7.9.2. **Terhorst, Michael** (BT, 2014): Hydroesterifizierung von 10-Undecensäuremethylester in thermomorphen Mehrkomponenten-Lösungsmittelsystemen

7.9.3. **Bianga, Jonas** (BT, 2014): Hydroformylierung von 10-Undecensäuremethylester in thermomorphen Mehrkomponenten-Lösungsmittelsystemen

7.9.4. **Erden, Arnela** (BT, 2014): Hydroformylierung und Oxidation von nachwachsenden Rohstoffen in der homogenen Übergangsmetallkatalyse, eine kritische Betrachtung

7.9.5. **Meier, Christoph** (BT, 2015): Untersuchungen zur intramolekularen Hydroesterifizierung von 10-Undecen-1-ol

7.9.6. **Goclik, Lisa** (BT, 2016): Entwicklung wässriger Lösungsmittelsysteme zur Katalysatorimmobilisierung in homogenkatalytischen Reaktionen

7.9.7. **Wendholt, Sven** (BT, 2016): Untersuchungen verschiedener Katalysator-Recyclingstrategien in der homogenkatalysierten Hydroesterifizierung

7.9.8. **Gilke, Stefan** (BT, 2017): Vergleich verschiedener Katalysator-Recyclingkonzepte in der Methoxycarbonylierung

7.9.9. **Arns, Alexander** (MT, 2015): Thermomorphe Mehrkomponenten-Lösungsmittelsysteme als Recyclingkonzept in Carbonylierungsreaktionen des Undecensäuremethylesters

7.9.10. **Schlipköter, Kim** (MT, 2015): Untersuchungen zur isomerisierenden Hydroformylierung von langkettigen Alkenen und Oleoverbindungen

7.9.11. **Korkmaz, Vedat** (MT, 2016): Tandemkatalyse aus Hydrierung und Hydroformylierung von 10-Undecensäuremethylester sowie die Anwendung der Kristallisation als Recyclingkonzept

7.9.12. **Terhorst, Michael** (MT, 2016): Untersuchungen zur Hydroaminomethylierung nachwachsender 1,3-Diene

7.9.13. **Bianga, Jonas** (MT, 2016): Tandemreaktion aus Isomerisierung und Hydroformylierung ungesättigter Esterverbindungen

7.9.14. **Benski, Francesco** (MT, 2016): Experimentelle Untersuchung und Design eines Prozesses zur Hydroesterifizierung oleochemischer Substrate

7.9.15. **Herrmann, Norman** (MT, 2017): Veredelung von Oleoverbindungen durch Carbonylierungsreaktionen in wässrigen Medien

(BT: Bachelor Thesis; MT: Master Thesis)

8. Curriculum Vitae

Personal Data

Name:	Tom Gaide
Date of Birth:	03.10.1987
Place of Birth:	Mesum, Germany
Nationality:	German

Professional Experience

Since 02/2014	Scientific Assistant at the Laboratory of Technical Chemistry of Prof. Dr. Arno Behr, TU Dortmund University, Dortmund, Germany

Education

Since 02/2014	PhD Student at the Laboratory of Technical Chemistry of Prof. Dr. Arno Behr, TU Dortmund University, Dortmund, Germany
10/2011-01/2014	Master of Science, Chemistry, TU Dortmund, Dortmund, Germany
10/2007-06/2011	Bachelor of Science, Chemistry, TU Dortmund, Dortmund, Germany
08/1998-05/2007	Abitur, Emslandgymnasium, Rheine, Germany